The role of carbohydrate food structure in gastrointestinal digestion, glycaemic response, and appetite regulation

A thesis submitted for the degree of Doctor of Philosophy,

Imperial College London

Mingzhu Cai

2022

Nutrition Section

Department of Metabolism, Digestion and Reproduction

Faculty of Medicine

Imperial College London

Abstract

Dietary fibre has demonstrated benefits against many metabolic diseases such as type 2 diabetes and obesity. Plant cell walls are the primary source of dietary fibre, and the structural integrity largely determines their physiological effects. Intact cell walls encapsulate starch to slow down its digestion and may protect the transport of resistant starch to the large intestine, thereby promoting short-chain fatty acid production and appetite control. However, cell wall structures can be disrupted when plant foods are processed into small particles, which may eliminate health benefits. This thesis aimed to understand the impact of the structural integrity of plant cell walls on human digestion, postprandial glycaemia and appetite using chickpeas as a food model.

Chapter 2 reviewed and meta-analysed 13 randomised crossover trials (RCTs) showing that the large particles of starchy food lowered postprandial glycaemia in healthy subjects. **Chapter 3** designed a two-phase, double-blinded RCT that enabled the examination of digestion and postprandial response in humans. Chickpeas were processed into three structures: broken cells (Broken), intact single cells (Intact-S), and intact cell clusters (Intact-C). **Chapter 4** studied their digestion in the stomach and duodenum and revealed that Intact-S and Intact-C remained their structures largely intact in the upper gastrointestinal tract, thereby lowering the luminal carbohydrate release and attenuating postprandial glycaemia. **Chapter 5** further investigated the digestion behaviours in the terminal ileum and appetite outcomes. Both intact structures delivered more carbohydrate contents to the distal ileum than Broken. Intact-S was more digestible in the ileum whilst Intact-C retained more

carbohydrate for ileal and colonic fermentation. Fermentation levels increased 4-8 hours postprandially, while Intact-C increased ileal acetate, PYY and fullness compared to Broken.

Intact-C presented the greatest benefits in attenuating postprandial glycaemia, promoting fermentation, and suppressing appetite. Our work emphasises the structural integrity of dietary fibre-rich foods in achieving their beneficial effects.

Copyright Declaration

The copyright of the thesis rests with the author. Unless otherwise indicated, its contents are licensed under a Creative Commons Attribution 4.0 International Licence (CC BY-NC). Under this licence, you may copy and redistribute the material in any medium or format. You may also create the distribute modified versions of work, under the condition that you credit the author and do not use it, or any derivative works, for a commercial purpose. When reusing or sharing this work, ensure you make the license terms clear to others by naming the license and linking to the license text. Where a work has been adapted, you should indicate that the work has been changed and describe those changes. Please seek permission from the copyright holder for uses of this work that are not included in this license or permitted under UK Copyright Law.

Declaration of Contributors

This work is original. The majority of the work in this thesis was performed by the author. All collaboration and assistance are declared below.

Chapter 2:

The study was published in the American Journal of Clinical Nutrition under the terms of the Creative Commons CC BY license, which permits unrestricted use, distribution, and reproduction in any medium, provided the original work is properly cited (Appendix 10).

Chapter 3:

Prof Gary Frost designed the study. Study protocol was drafted by the author Mingzhu Cai and was reviewed by Dr Cathrina Edwards (Quadram Institute Bioscience, QIB), Dr Dominic Blunt (Charing Cross Hospital), Dr Martina Tashkova, Dr Katerina Petropoulou and Dr Claire Byrne.

Chapter 4-5:

Study visits were carried out with the assistance of Dr Martina Tashkova, Dr Shilpa Tejpal, and master students Bowen Dou, Claire Ho, Oyinkansola Olotu and Echo Dong. Gastric and duodenal tube placement was performed by Dr Martina Tashkova. Ileal tube placement was performed by Dr Dorminic Blunt (Charing Cross Hospital). Food materials were provided by Dr Cathrina Edwards and prepared by Dr Jennifer Ahn-Jarvis (QIB). Microscopic analysis was performed by Dr Natalia Perez-Moral (QIB). Maltose analysis was performed by Dr Peter Ryden and Dr Shikha Saha (QIB). Radioimmunoassay was performed with the assistance of Prof Kevin Murphy, Dr Gerogia Franco Becker, and Dr Shilpa Tejpal. Glucose and insulin analysis was performed under the guidance of Dr Anna Cherta-murillo and Dr Katerina Petropoulou. Appetite VAS data was collected with the assistance with Bowen Dou and Echo

Dong. Metabolomic profiling was performed under the guidance of Dr Isabel Garcia-Perez and Dr Jose Ivan Serrano Contreras.

Study visits were performed with the help of the research nurses and administration staff at the NIHR Imperial Clinical Research Facility.

Acknowledgements

I would like to thank my primary supervisor **Prof Gary Frost** for offering me the opportunity to study and work under his supervision. I feel extremely lucky to have his advice, mentorship, and encouragement throughout the years. I also appreciate his trust in me and letting me lead on the clinical project presented in this thesis. I would like to thank my second supervisor **Dr Edward Chambers** for his supervision, advice and help whenever I need.

I would like to thank **China Scholarship Council** for funding me over the last four years and providing me the chance to complete my PhD degree. I also feel grateful to have had the support from **Dr Cathrina Edwards, Dr Natalia Perez-Moral, and Dr Peter Ryden** from Quadram Institute Bioscience.

I would like to thank these researchers at Imperial College who have supported and helped me with their time and expertise. These are **Dr Isabel Garcia-Perez, Dr Jose Ivan Serrano Contreras, Prof Kevin Murphy, Dr Anna Cherta, Jennifer Pugh, Dr Hannah Stephen, Dr Gerogia Franco Becker, Agklinta Kiosia, Vally Wu, Dr Aaron Lett, Dr Aygul Dagbasi, Baichen Lu, Monica Hill, Dr Katerina Petropoulou, Dr Claire Byrne, and Dr David Ma.** A special thanks give to the chickpea team. **Dr Martina Tashkova**, thank you for your warmth, kindness, and help from my day 1 at Imperial College and being such a great support throughout my study; **Dr Shilpa Tejpal**, for always standing by me and picking me up at every difficult moment. Thanks Dr Dominic Blunt or helping with the intubation despite all the difficulties. Thank you to my master students **Bowen Dou, Claire Ho, Echo Dong, and Oyinkansola Olotu** who have been great additions to our team. Thanks to my **participants** for their patience and bravery in

enduring seven intestinal tube insertions and for providing us with precious samples. I could not have finished the project without you all.

Finally, I would like to thank my family, who have truly shaped the person I am today. Thank you to **my dad, my mum, and my grandmother** for your unconditional love. I would also like to thank **Bowen**, who has been my companion and my emotional support for the past four years.

Abbreviations

A	Absorbance
AEBSF	4-(2-Aminoethyl) benzenesulfonyl fluoride hydrochloride
AOC	Area over the curve
AP	Area postrema
ARC	Arcuate nucleus
ATP	Adenosine triphosphate
BA	Bile acids
BH	Breath hydrogen
BMI	Body Mass Index
BMRB	Biological Magnetic Resonance Data Bank
BSA	Bovine serum albumin
CA	Glycine/taurine-conjugated cholic acid
cAMP	Cyclic adenosine 3', 5'-monophosphate
CART	Cocaine- and amphetamine- related transcript
CAS	Composite appetite score
CaSR	Calcium-sensing receptor
CCK	Cholecystokinin
CDCA	Glycine/taurine-conjugated chenodeoxycholic acid
CNS	Central nervous system
CRF	Clinical research facility
CV	Coefficient of Variation
DCA	Glycine/taurine-conjugated deoxycholic acid

DF	Dietary fibre
DGM	Dynamic gastric model
DP	Degree of polymerization
DPP-4	Dipeptidyl Peptidase -4
ECGs	Electrocardiograms
EEC	Enteroendocrine cells
ELISA	Enzyme-linked Immunosorbent Assay
FFAR2/3	Free fatty acid receptors 2/3
G-6-P	Glucose-6-phophate
GI tract	Gastrointestinal tract
GIP	Gastric inhibitory peptide
GIPR	Gastric inhibitory peptide receptor
GIT	Gastrointestinal tract
GL	Glycaemic load
GLP-1	Glucagon-like peptide-1
GLP-1R	Glucagon-like peptide-1 receptor
GLUTs	Glucose transporters
GRS	Genetic risk score
HMDB	Human Metabolome Data Base
iAUC	Incremental Area Under the Curve
IPE	Inulin-propionate ester
IQR	Interquartile range
IR	Insulin receptor

Kcal	Kilocalories
LC-MS	Liquid chromatography–mass spectrometry
MARK	Mitogen-activated protein kinase
MCCV	Monte Carlo cross-validation
MCT1	Monocarboxylate transporter 1
MRI	Magnetic resonance imaging
NDC	Non-digestible carbohydrate
NHS	National Health Service
NMR	Nuclear Magnetic Resonance
NPY	Neuropeptide Y
NSP	Non-starch Polysaccharides
OXM	Oxyntomodulin
PBS	Phosphate buffered saline
PIS	Participant information sheet
PKB	Protein kinase B
PLS-DA	Partial-least-squares– discriminant analysis
POMC	Pro-opiomelanocortin
PP	Pancreatic polypeptide
PVN	Paraventricular nucleus
PYY	Peptide YY
RCF	Relative Centrifugal Force
RCTs	Randomized crossover trials
RDS	Rapidly digestible starch

REC	Research Ethics Committee
RIA	Radioimmunoassay
RoB	Risk of bias
RPM	Revolutions per Minute
RS	Resistant starch
RT	Room temperature
SCFAs	Short chain fatty acids
SDS	Slowly digestible starch
SEM	Standard Error of Means
SGLTs	Sodium-glucose symporters
SMCT1	Sodium-coupled monocarboxylate transporter 1
STOCSY	Statistical TOtal Correlation Spectroscopy
STORM	SubseT Optimization by Reference Matching
T2D	Type 2 Diabetes
TGR5(Gpbar1)	G-protein-coupled bile acid receptor
TIM	TNO Gastro-Intestinal Model
TSP	3-(trimethylsilyl)- [2,2,3,3, -2H4]-propionic acid
VAS	Visual analogue scale
VDCCs	Voltage-dependent Ca+ channels
WHO	World Health Organization

Publication, conference, and presentation.

Publications

- Cai M, Dou B, Pugh J E, et al. The impact of starchy food structure on postprandial glycemic response and appetite: a systematic review with meta-analysis of randomized crossover trials[J]. The American journal of clinical nutrition, 2021, 114(2): 472-487.
- Izzi-Engbeaya C, Ma Y, Buckley N W, et al. Effects of corticosterone within the hypothalamic arcuate nucleus on food intake and body weight in male rats[J]. Molecular Metabolism, 2020, 36: 100972.
- Pugh J E, Cai M, Altieri N, et al. A comparison of the effects of resistant starch types on glycaemic response in individuals with type 2 diabetes or prediabetes: A systematic review and meta-analysis. [Accepted by Frontiers in Nutrition]
- Cai M et al., Duodenal carbohydrate digestion and postprandial glycaemia. [Manuscript in preparation]
- Cai M et al., Cell wall structures, gastrointestinal digestion and postprandial metabolism. [Manuscript in preparation]
- Cai M et al., Associations between legume consumption and metabolic risk markers among the UK police force employees: findings from the Airwave Health Monitoring Study. [Manuscript in preparation]

Conference Proceedings

- Cai M et al., "Cell wall matrices in chickpeas and their effects on starch digestion and postprandial metabolism"- accepted for Nutrition Society Winter Conference, January 2023
- Cai M et al., "Digestive behaviours of dietary fibre in the human gastrointestinal tract: a randomised crossover study", Nutrition Future Conference, September 2020

Presentations and Awards

- Poster presentation "Impact of carbohydrate food structure on glycaemic and appetite control" Best poster presentation, Imperial College Food and Nutrition Student Conference, September 2022
- Poster presentation "Understanding how food structure affects gastrointestinal digestion, glycaemic response and appetite". Rising Scientist Day, Imperial College London, March 2021
- Oral presentation "Food structure, glucose and energy homeostasis." Excellent oral presentation, UKCSSA PhD Forum, November 2019

List of Figures

Chapter 1

Figure 1. 1. The interplay between organs and tissue involved in glucose homeostasis. 38

Figure 1. 2 The microstructures of starchy foods.. 64

Figure 1. 3 The changes in starch granules during heating, cooling, and storage.....66

Figure 1. 4 The representative diagram of cell wall structure and organization of its constituents. 68

Figure 1. 5 Human digestive system. 72

Figure 1. 6 Physiology of the duodenum. 76

Figure 1. 7 Carbohydrate digestion and absorption. 78

Figure 1. 8 A diagram to explain the interplay between food structure, gut fermentation, and appetite regulation. 89

Figure 1. 9 The microscopic images of pea single cells and clusters present in duodenal fluids from healthy subjects. Pea single cells (A-C) and cell clusters (D-F).....93

Chapter 2

Figure 2. 1 The diagram of literature search and screening process. 104

Figure 2. 2 The risk of bias (RoB) in included studies. 108

Figure 2. 3 Effects of Intact cell wall structure on (A) postprandial glucose iAUC (mmol/L*min) and (B) insulin iAUC (pmol/L*min) in healthy subjects.. 109

Figure 2. 4 Effects of intact cell wall structures on subjective satiety score (iAUC mm*min) in healthy subjects. 110

Figure 2. 5 Effects of intact cell wall structures on (A) GLP-1 response (iAUC pmol/L*min), (B) PYY response (iAUC pmol/L*min), (C) GIP response (iAUC pmol/L*min), and (D) CCK response (iAUC pmol/L*min) in healthy subjects. 112

Chapter 3

Figure 3. 1 Diagram of the study visits.....119

Figure 3. 2 Diagram of the in-house RIA for plasma GLP-1/PYY concentrations.....130

Figure 3. 3 Types of ELISA. Adapted from theory. labster.com 131

Figure 3. 4 Diagram of sandwich ELISA for insulin detection 132

Figure 3. 5 The structure of CORTRAK system. 134

Figure 3. 6 Methods for ileal tube placement and monitoring. 136

Figure 3. 7 Diagram and analysis plan for human studies. 143

Chapter 4

Figure 4. 1 Schematic diagram of study sampling routine. 153

Figure 4. 2 In vitro digestibility properties of chickpeas with different structures.. 158

Figure 4. 3 Postprandial glycaemia changes following the consumption of chickpea test meals.. 160

Figure 4. 4 Micrographs of chickpea cell structures during gastric and duodenal digestion. 162

Figure 4. 5 Changes in maltose and glucose levels in the stomach and duodenum following the consumption of chickpea test meals. 164

Figure 4. 6 RM-MCCV-PLS-DA score plots of ^{1}H-NMR gastric samples at 15min and duodenal samples at 60 min after consumption of chickpea test meals.. 167

Figure 4. 7 An example of metabolite identification process in skyline significance plot in the comparison between Intact-C vs Broken. 169

Figure 4. 8 Profiles of gastric alanine and duodenal phenylalanine relative concentrations.. 171

Figure 4. 9 Postprandial GIP concentrations following the consumption of chickpea test meals. 173

Figure 4. 10 Postprandial GLP-1 concentrations following the consumption of chickpea test meals.. 175

Figure 4. 11 Postprandial PYY concentrations following the consumption of chickpea test meals. 177

Figure 4. 12 Appetite changes following the consumptions of chickpea test meals.. ..180

Figure 4. 13 Spearman's correlation t tests between gut carbohydrates, glycaemic and appetite markers regardless of food structure. 182

Chapter 5

Figure 5. 1 Outline of the study visit of the ileum study. 201

Figure 5. 2 Composite appetite scores following composition of chickpea test meals.205

Figure 5. 3 The feeling of fullness following composition of chickpea test meals.. 207

Figure 5. 4 The feeling of hunger (A), desire to eat (B), appetite for a meal (C) following composition of chickpea test meals.. 208

Figure 5. 5 The ileal glucose concentrations following composition of chickpea test meals. 210

Figure 5. 6 RM-MCCV-PLS-DA score plots of ^{1}H-NMR ileal samples before and after consumption of chickpea test meals.. 214

Figure 5. 7 The relative amount of ileal acetate over time. 217

Figure 5. 8 Baselines and postprandial changes in breath hydrogen on day 3. 219

Figure 5. 9 Glucose and insulin responses following composition of chickpea test meals..
.....221
Figure 5. 10 Baselines and postprandial changes in GLP-1.....223
Figure 5. 11 Baselines and postprandial changes in PYY. 225
Figure 5. 12 Correlation between ileal metabolites and appetite measurement.. 229

Chapter 6

Figure 6. 1 Overview of results from Chapters 4 and 5. 247
Figure 6. 2 Intraluminal glucose release in the region of the stomach, duodenum, and ileum.. 254

List of Tables

Chapter 1

Table 1. 1 Summary of the main appetite-regulating hormones in gut. 50

Table 1. 2 Classification of carbohydrates based on digestibility.....60

Table 1. 3 The categories of resistant starch (RS).....62

Chapter 2

Table 2. 1 PICOS criteria for inclusion and exclusion of studies 99

Table 2. 2 Search Strategy.....100

Table 2. 3 Study characteristics of included studies (n=13) 105

Chapter 3

Table 3. 1 Nutritional Profile of the Test Meal 121

Table 3. 2 Inclusion and exclusion criteria of the study. 123

Table 3. 3 Methods of sample preparation, processing, and storage 126

Chapter 4

Table 4. 1 Chickpea cell wall structure, *in vitro* starch digestion, and in vivo response. 149

Table 4. 2 Participants Characteristics.....158

Table 4. 3 Metabolites in the stomach associated with food structure. 168

Table 4. 4 Metabolites in duodenum associated with food structure. 170

Chapter 5

Table 5. 1 Participant characteristics.....203

Table 5. 2 Metabolites in the ileum associated with food structure.....215

Table of Contents

Abstract *2*

Copyright Declaration *4*

Declaration of Contributors *5*

Acknowledgements *7*

Abbreviations *9*

Publication, conference, and presentation *13*

List of Figures *15*

List of Tables *19*

Table of Contents *20*

Chapter 1 Introduction *29*

1. 1 Type 2 diabetes (T2D) **29**

1.1.1 Definition 29

1.1.2 Prevalence and economic burden 29

1.1.3 Lifestyle and risk of T2D 30

1.1.4 Lifestyle intervention to prevent T2D development 31

1.2 Obesity **32**

1.2.1 Definition 32

1.2.2 Prevalence and economic burden 32

1.2.3 Cause and treatment 33

1.3 Regulation of glucose homeostasis **36**

1.3.1 The fasting state 36
1.3.2 The postprandial state 37
1.3.3 The role of the Pancreas 38
1.3.4 The role of insulin 39
1.3.5 The role of incretin hormones: GIP and GLP-1 41
1.3.6 Glucose uptake and transport 43
1.3.7 The liver, the adipose, and the skeletal muscle 45
1.3.8 Problem with disrupted glucose homeostasis: insulin resistance 46
1.4 Regulation of appetite 49
1.4.1 The role of the central nervous system (CNS) 49
1.4.2 The role of the GI tract: focus on appetite-regulating hormones 49
1.5 Carbohydrates, T2D, and obesity 54
1.5.1 Carbohydrates and glycaemic index (GI) 54
1.5.2 Glycaemic index and T2D 55
1.5.3 Glycaemic index, appetite, and body weight 56
1.5.4 Summary 57
1.6 Carbohydrate food structure, digestion, and postprandial metabolism 58
1.6.1 Carbohydrate classification. 58
1.6.2 Starch classification 61
1.6.3 Starch structure and digestibility 63
1.6.3.1 The hierarchical structures of starch 63
1.6.3.2 Amylose and amylopectin 64
1.6.3.3 Starch granule morphology 65
1.6.3.4 Gelatinized and retrograded starch 66
1.6.3.5 Cell wall structures 66
1.6.3.6 Food structure affected by processing 70
1.6.4 Carbohydrate food structure and digestion in the human 71
1.6.4.1 Oral digestion 72

1.6.4.2 Gastric digestion 73
1.6.4.3 Small intestinal digestion: the duodenum, jejunum, and ileum 74
1.6.4.4 Large intestinal fermentation 78
1.6.5 short chain fatty acids (SCFAs) 80
1.6.5.1 The production of SCFAs 80
1.6.5.2 The absorption of SCFAs 81
1.6.6 The role of SCFAs in glucose homeostasis 82
1.6.7 The role of SCFAs in appetite regulation 84
1.6.8 Interplay between carbohydrate food structure, gut fermentation, and appetite 86
1.7 Food structure as a tool to lower postprandial glycaemia and suppress appetite 89
1.7.1 Food strategy to modulate starch digestion 89
1.7.2 Cell walls to slow down starch digestion 90
1.7.3 Cell walls to increase type 1 RS amount 91
1.8 Thesis summary and rationale 94
1.9 Thesis hypothesis and aims 95
Chapter 2 Current evidence on how food structure impacts glycaemic response and appetite: systematic review and meta-analysis of randomized crossover trials 97
2.0 Abstract 97
2.1 Introduction 97
2.2 Purposes of this study 98
2.2.1 Hypothesis 98
2.2.2 Aims 98
2.2.3 Outcomes measure 98
2.3. Methods 99
2.3.1 Eligibility 99
2.3.2 Study search and selection 99

2.3.3 Risk of bias assessment 101
2.3.4 Data extraction 102
2.3.5 Data analysis 102
2.4 Results 103
2.4.1 Study characteristics 103
2.4.2 Risk of bias (RoB) in included studies 107
2.4.3 Summary of outcomes: glucose and insulin iAUC 108
2.4.4 Summary of outcomes: satiety scores iAUC 110
2.4.5 Summary of outcomes: gut hormones iAUC 110
2.5 Discussion 113
2.5.1 Overall summary 113
2.5.2 Food structure and glucose and insulin response 113
2.5.3 Food structure and appetite regulation 114
2.5.4 Limitations 115
2.5.5 Future direction 115
2.5.6 Overall conclusion 116
Chapter 3 Experimental methods for human studies 117
3.0 Abstract 117
3.1 Overview 117
3.2 Human study methodology 118
3.2.1 Study Approval 118
3.2.2 Study Design 118
3.2.2.1 Phase 1 study (study visit 1) 119
3.2.2.2 Phase 2 (study visit 2-4) 121
3.2.3 Participant Recruitment 122
3.2.4 Randomizations 124

3.2.5 Sample size 124

3.3 Analysis of blood samples 125

3.3.1 Blood samples collection, processing, and storage 125

3.3.2 Blood glucose analysis 126

3.3.3 Radioimmunoassay 127

3.3.3.1 Insulin analysis 127

3.3.3.2 GLP-1 analysis 128

3.3.3.3. PYY analysis 130

3.3.4 Enzyme-linked Immunosorbent Assay (ELISA) 131

3.3.4.1 Insulin analysis 131

3.3.4.2 GIP analysis 133

3.4 Analysis of gut samples 133

3.4.1 Gut sample collection, processing, and storage 133

3.4.1.1 Method to collect human gastric and duodenal samples 133

3.4.1.2 Method to collect human ileal samples 134

3.4.2 Gut glucose analysis 136

3.4.3 Gastric and duodenal maltose analysis 137

3.4.4 Metabolic profiling 137

3.4.4.1 Metabolites extraction 137

3.4.4.2 ^{1}H NMR Spectroscopy 138

3.4.4.3 NMR data processing 139

3.4.4.4 Metabolites identification 139

3.4.5. Microscopic analysis 140

3.5 Analysis of appetite and food intake 140

3.5.1 Visual Analogue Scales (VAS) 140

3.5.2 Ad libitum food intake 141

3.6 Breath hydrogen: a marker of intestinal fermentation 141

3.7 Overview of analysis plan 142

3.8 Summary..... 143

Chapter 4 The impact of food structure on postprandial glycaemia and starch digestion in the stomach and duodenum 144

4.0 Abstract 144

4.1 Introduction 145

4.1.1 Current methods to study starch digestion 145

4.1.2 Current understanding of the effects of chickpea cell wall structure: in vitro and in vivo findings .147

4.1.3 Physiological role of food structure in metabolic responses 150

4.1.4 Summary.....151

4.2 Purposes of this study 152

4.2.1 Hypothesis 152

4.2.2 Aims 152

4.2.3 Outcome measures 152

4.3. Materials and Methods 153

4.3.1 Study Design 153

4.3.2 Participants recruitments 153

4.3.3 Randomizations 153

4.3.4 Dietary Intervention and test meal preparation 153

4.3.5 Sample collection, processing and analysis.....155

4.3.6 In vitro digestibility Assay.....155

4.3.7 Statistical analysis.....156

4.4 Results 157

4.4.1 *in vitro* starch digestibility assay.....157

4.4.2 Participants characteristics.....158

4.4.3 Acute glycaemia and insulinaemia 159

4.4.4 Cell wall structures during gastric and duodenal digestion 161
4.4.5 Carbohydrate digestion in the stomach and duodenum 163
4.4.6 Metabolomic analysis of gastric and duodenal samples....166
4.4.7 Gut hormones....172
4.4.7.1 GIP....172
4.4.7.2 GLP-1....174
4.4.7.3 PYY 176
4.4.8 Subjective appetite and *ad libitum* food intake 178
4.4.9 Association between gut carbohydrates, glycaemia and appetite: a correlation matrix....181

4.5 Discussion 183

4.5.1 Summary of findings....183
4.5.2 Detailed discussion....183
4.5.3 Overall conclusion 193

Chapter 5 The impact of food structure on appetite regulation and ileal content 194

5.0 Abstract 194

5.1 Introduction 195

5.1.1 Overview....195
5.1.2 Nutrient sensing in the ileum and appetite regulation....195
5.1.3 Food structure and encapsulated nutrients in the ileum 199
5.1.4 Summary....199

5.2 Purposes of this study 200

5.2.1 Hypothesis 200
5.2.2 Aims 200
5.2.3 Outcome measures 200

5.3 Materials and methods.... 201

5.3.1 Study Design 201

5.3.2 Participant recruitment and eligibility....201
5.3.3 Intervention and test meal preparation....202
5.3.4 Randomization....202
5.3.5 Sample collection, processing, and analysis....202
5.3.6 Data analysis....202
5.4 Results....203
5.4.1 Participant characteristics....203
5.4.2 Visual analogue scales....204
5.4.3 Ileal glucose: concentration and time profile....209
5.4.4 Metabolomic analysis of ileum samples....211
5.4.5 Breath Hydrogen....218
5.4.5 Postprandial glycaemia and insulinaemia....220
5.4.6 GLP-1....222
5.4.7 PYY....224
5.4.9 Association between ileal glucose and acetate with appetite regulation....226
5.5 Discussion....231
5.5.1 Summary of findings....231
5.5.2 Detailed discussion....232
5.5.3 Conclusion....243
Chapter 6: General discussion....245
6.0 Summary of main findings in Chapter 4-5....245
6.1 Introduction....248
6.2 Detailed discussion....249
6.3 Strengths, limitation, and future recommendations....259
6.4 Conclusion....262

Bibliography ***.....263***

Appendices ***.....295***

Chapter 1 Introduction

1. 1 Type 2 diabetes (T2D)

1.1.1 Definition

Type 2 diabetes has become a major global health issue. It is characterized by elevated blood glucose levels, resulting from impaired insulin secretion from pancreatic B-cells, insulin resistance in peripheral tissues, or their combination (DeFronzo et al., 2015).

The definition and diagnostic criteria published by the WHO in 2006 is widely used. This includes a fasting plasma glucose concentration >= 7.0mmol/L; or a random venous plasma glucose concentration>=11.1 mmol/L; or 2-hour plasma glucose concentration >=11.1 mmol/l after an oral glucose tolerance test; or an HbA1c >= 48mmol/mol (6.5%)(World Health and International Diabetes, 2006)

T2D has been linked to several comorbidities and other chronic diseases. The most common comorbidities in T2D patients included overweight/obesity, hypertension, dyslipidaemia, and kidney diseases (Iglay et al., 2016, Jelinek et al., 2017). Furthermore, individuals with T2D are at greater risk for both microvascular complications (e.g., retinopathy and neuropathy) and macrovascular complications such as cardiovascular disease (DeFronzo et al., 2015).

1.1.2 Prevalence and economic burden

Diabetes is approaching the proportions of a global epidemic. The International Diabetes Federation has indicated that 537 million people worldwide have diabetes as of 2021 and estimated that there will be 578 million adults with diabetes by 2030 (International Diabetes

Federation, 2021). T2D accounts for 90% of all causes of diabetes and is the primary source of the rising prevalence. According to Diabetes UK reports, 4.3 million people had T2D in the UK which has more than doubled since 1980. The number is predicted to rise to 5.5 million by 2030 (Diabetes UK, 2019).

The high prevalence of T2D presents a growing challenge to public health. The treatment of T2D has been estimated to contribute to National Health Service spending of GBP 10 billion per year, equivalent to 10% of its overall budgets (Hex et al., 2013). A recent analysis showed that even a short period of poor glycaemic control could add 197 million over 10 years to the cost of managing diabetes-related complications (Bain et al., 2020).

1.1.3 Lifestyle and risk of T2D

Epidemiological evidence suggested that lifestyle and dietary factors play a major role in the development of T2D. Adherence to an unhealthy lifestyle including smoking, physical inactivity, and excessive alcohol consumption increased the risk of T2D (Hu et al., 2001, Shi et al., 2013, Shan et al., 2018, Schnurr et al., 2020). Rotating night shift work was associated with a higher risk of T2D in large UK and US cohorts (Shan et al., 2018, Vetter et al., 2018) A western pattern diet containing less fibre and polyunsaturated fat and high in saturated fat were significant risk factors for the incidence of T2D (Mann, 2002, van Dam et al., 2002, Fung et al., 2004). This demands an urgent need for changing lifestyles and unhealthy diet patterns among the general population.

1.1.4 Lifestyle intervention to prevent T2D development

Emerging evidence suggests that lifestyle interventions promoting weight loss are effective in delaying or preventing the development of T2D. Several large-scale randomised crossover trials (RCTs) have revealed that a 5-7% weight loss achieved by diet and moderate exercise could largely reduce the risk of T2D by 29-58% (Knowler et al., 2002, Tuomilehto et al., 2001, Crandall et al., 2008). It is found that lifestyle treatments are effective across different ages and ethnic groups (Knowler et al., 2002). The follow-up studies have found a significant reduction in T2D incidence 3-14 years after the completion of the trials (Li et al., 2008, Lindstrom et al., 2006, Diabetes Prevention Program Research et al., 2009). It may suggest that the beneficial effects of lifestyle interventions persist in the long term.

Despite these encouraging results, it has been recognised that adherence to intensive lifestyle interventions is a big challenge (Schmidt et al., 2020). Current recommendations have advised the public to maintain a balanced eating and moderate physical activity while the incidence of T2D continues to rise. There is a certain need for a more effective approach to controlling glucose metabolism and reducing the risk of T2D for those who find it difficult to follow lifestyle therapies.

Given the above evidence, the benefits of weight loss in the prevention of T2D seem robust. On the other hand, being overweight or obese is statistically increasing the risk of T2D. Findings from a National Cohort US Adults suggest the dramatic rise in obesity has triggered a parallel rise in diabetes statistics (Ford et al., 1997). The risk of diabetes increases by 4.5%-9% for every kilogram of body weight gain(Ford et al., 1997). The term “diabesity” has been

coined between diabetes and obesity to illustrate their interdependence (Zimmet et al., 2001). Being obese (BMI>=30 kg/m^2), after adjusted for genetic risk score (GRS), was associated with a >8-fold increase in risk of T2D compared with normal-weight subjects in the same GRS and lifestyle regime (Schnurr et al., 2020).

Clearly, an integrated approach will be needed to prevent both T2D and weight gain. In the next section, we will be talking about the cause and current interventions for obesity.

1.2 Obesity

1.2.1 Definition

The World Health Organisation (WHO) has defined overweight/obesity as "abnormal or excessive fat accumulation" which threats health (WHO, 2016). A body mass index (BMI), which is calculated as the ratio of a person's body weight in kilogram to the square of their height in meters (kg/m^2), is commonly used to classify the weight status of adults. A BMI >= 25 is considered overweight and a BMI >= 30 is obese(WHO, 2016).

1.2.2 Prevalence and economic burden

Obesity has become a global epidemic since 1997. The WHO report in 2016 estimated that 39% of adults worldwide were overweight, numbering 1.9 billion. Of these more than 650 million adults were obese (WHO, 2016). In the UK, it is estimated that the majority of adults, 67% of men and 60% of women, were overweight (NHS, 2020). This included 26% of men and 29% of women who were obese (NHS, 2020). In addition, nearly 20% of children aged 2 to 15

were classified as obese by their BMI (adjusted for age and sex), suggesting younger generations could become obese at earlier ages and remain obese for longer (NHS, 2020).

Obesity has placed a significant financial burden on the healthcare system worldwide. It has been estimated that the direct cost of obesity accounted for between 0.7%-2.8% of a country's total healthcare expenditures (Withrow and Alter, 2011). In England, there were 11,117 hospital admissions directly attributable to obesity in 2017/2018, up 22% from 2014/2015(NHS, 2020). The direct treatments for overweight/obesity cost the UK-wide NHS £6.1 billion in 2014/2015, and the cost is anticipated to rise to £9.7 billion by 2050(NICE, 2017). The cost of obesity to wider society was estimated at £27 billion in 2014/15 and is projected to reach £49.9 billion per year (NICE, 2017).

1.2.3 Cause and treatment

Overweight and obesity are fundamentally caused by energy intake chronically exceeding energy expenditure, a condition known as positive energy balance. It has been suggested that a small amount of positive energy balance i.e. 50-100 kcal/d could result in gradual weight gain (Hill, 2006). This status could be easily achieved with the current western diet, as it contains high-energy dense foods, has low dietary fibre content, and produces lower satiety signals(Byrne et al., 2015, Popkin et al., 2012). Indeed, the regulation of energy balance is complex and influenced by many biological, behavioural, and environmental factors (Hill, 2006, Benton, 2015).

From an energy balance perspective, weight loss is about avoiding a positive energy balance and promoting a negative energy balance. The goal can be achieved by delivering strategies to decrease energy intake and increase energy expenditure. Current treatments have mainly focused on increasing physical activity and dietary restriction and could successfully lead to weight loss (Hassan et al., 2016). However, weight loss in this way is difficult to maintain in a long-term (Norris et al., 2004, Hassan et al., 2016).

Alternatively, anti-obesity agents have been used to ensure successful long-term weight loss maintenance. Current options fall into two classifications: lipase inhibitors, such as orlistat, and appetite suppressors, such as liraglutide and semaglutide. Orlistat works by inhibiting fat absorption in the intestine (Heck et al., 2000) and has been shown to induce a small but significant improvement in weight reduction (3%) compared to diet treatment alone (Drew et al., 2007). However, its effectiveness varied among individuals, and only a small proportion of patients (15-30%) patients achieved >5% weight loss 2-year post-treatment (Drew et al., 2007). On the other hand, liraglutide and semaglutide are glucagon-like peptide-1 receptor agonists (GLP-1 RA) which reduces calorie intake by suppressing appetite. Liraglutide has resulted in a greater weight loss of 4-6 kg when combined with lifestyle counselling for one year (Davies et al., 2015). Semaglutide has a longer half-life compared to liraglutide, with 165 hours versus 13-15 hours, respectively (Rubino et al., 2022). In a 68-week clinical trial, semaglutide administered once-weekly demonstrated superior efficacy to once-daily liraglutide in reducing weight in adults with overweight and obesity (Rubino et al., 2022). Tirzepatide is a dual glucose-dependent insulinotropic peptide and GLP-1 receptor agonist (GIP/GLP-1 RA). It works by enhancing satiety and improving glucose control and has shown promising results in clinical trials for the treatment of obesity (Min and Bain, 2021, Jastreboff

et al., 2022). Nevertheless, the use of anti-obese drugs has been linked to a higher incidence of adverse events such as nausea, vomiting, diarrhoea, and faecal incontinence (O'Meara et al., 2004, Lean et al., 2014, Jastreboff et al., 2022). Challenges exist in improving both the efficacy and safety of developing anti-obesity agents.

The most effective weight loss strategy to date remains gastrointestinal surgery. The most common surgery includes Rous-en-Y gastric bypass, vertical sleeve gastrectomy and gastric banding, which could decrease the BMI by 12-17 in a long term and reduce total mortality rates (Chang et al., 2014). However, gastrointestinal surgery is an invasive procedure and could lead to undesirable side effects such as dumping syndrome, intestinal obstruction and nutritional deficiencies (Ma and Madura, 2015). Currently, in the UK, bariatric surgery is only available for patients who have a BMI >= 40kg/m^2 with significant obesity-related comorbidities (NICE, 2014), which is not applicable to most of the general public.

Besides calorie restriction, the weight-loss results of gastrointestinal surgery have been linked to profound changes in the secretion of gut hormones with effects on appetite and food intakes (De Silva and Bloom, 2012b, Perry and Wang, 2012, Holst et al., 2018). Neural and gut signals regulating appetite have been gaining attention in this area, leading to the development of pharmaceutical (Wilding et al., 2021) and dietary strategies (Poutanen et al., 2017, Boix-Castejón et al., 2018, King et al., 2018) against obesity based on gut hormones' actions.

Summary

The sections so far have reviewed the dietary and lifestyle strategies to prevent T2D. Interventions that promote weight loss can greatly reduce the risk of T2D. Appetite regulation pathways have been highlighted as a target for anti-obesity therapies. In sections 1.3 and 1.4, we will discuss the regulatory mechanisms of blood glucose and appetite.

1.3 Regulation of glucose homeostasis

Control of blood glucose levels in a narrow range is essential for maintaining normal body function. This section will discuss the physiology that how organs and hormones regulate glucose homeostasis and the potential causes of insulin resistance.

1.3.1 The fasting state

The postabsorptive state defines the period of 6-12h following a meal until the next meal. In healthy individuals, blood glucose concentrations are kept at levels 4.0-5.4 mmol/L at this state (Dimitriadis et al., 2021). Insulin secretion is maintained at the basal rate, with a concentration between 7–10 μU/mL(Dimitriadis et al., 2021). There is no net storage of glucose in this state, as the rates of endogenous glucose production (glucose appearance) are comparable to the rates of glucose removal by the tissues (glucose disappearance). Glucose disposal is non-insulin-dependent, with the majority going to the brain (45-60%). The rest flows into red blood cells (5-10%), skeletal muscle (15-20%), kidneys(10-15%), and adipose tissue (2-4%) (Gerich, 1993).

1.3.2 The postprandial state

The postprandial state is the period during which the body absorbs ingested nutrients before returning to pre-prandial conditions. Plasma glucose levels after a meal are determined by the relative changes in rates of delivery and removal of glucose into the systemic circulation. Immediately after a meal, both delivery and removal increase. During the first 60-90 min, glucose delivery exceeds glucose removal, increasing plasma glucose levels. Afterwards, the removal of glucose considerably increases, thereby reversing the situation (Cydulka and Maloney, 2002). The appearance of ingested glucose into the circulation usually reaches peak values 30-60min after a meal and gradually decreases backing to pre-prandial levels at about 4-5h. The glucose removal from the circulation is taken up by muscle (30%), splanchnic tissue (liver and gut, 30%), brain (15%), adipose tissue (10%) and others (10%)(Gerich, 1993, Cydulka and Maloney, 2002).

The magnitude of postprandial glycaemia is dependent on many factors, including the amount and types of carbohydrates, the rate of gastric emptying and intestinal absorption, the action of hormones, and metabolism in liver and peripheral tissues (Gerich, 1993, Woerle et al., 2003). It involves an integrated mechanism via the regulation of the central nervous centre in which different organs and tissues play a role as shown in **Figure 1.1**.

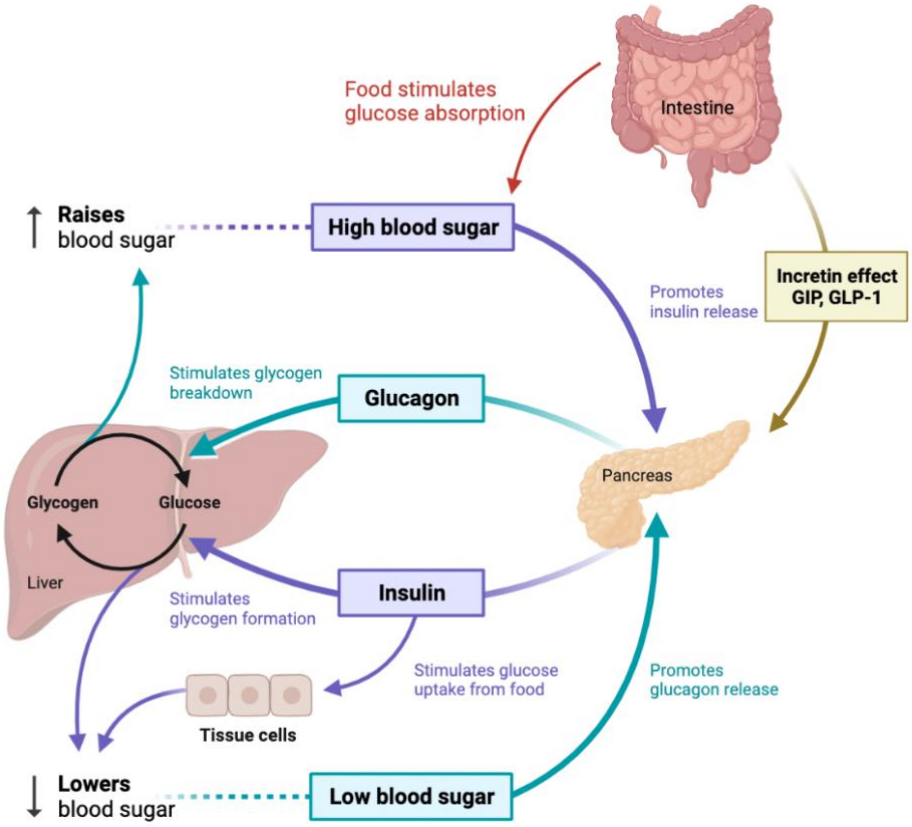


Figure 1. 1. The interplay between organs and tissue involved in glucose homeostasis.

Food ingestion stimulates carbohydrate digestion and absorption in the small intestine which transports to the blood. The pancreas senses the rise in blood glucose and incretin hormones and secretes insulin. Insulin receptors are found in the liver, adipose and skeletal tissues which stimulate the uptake and storage of glucose. When the blood glucose is low in the blood, the pancreas releases glucagon which promotes glycogen breakdown and glucose production in the liver. GIP, gastric inhibitory polypeptide; GLP-1, glucagon-like peptide-1. The figure was adapted and revised from "Regulation of Blood Glucose" by BioRender.com (2022). Retrieved from https://app.biorender.com/biorender-templates

1.3.3 The role of the Pancreas

The pancreas is located posterior to the stomach and is connected to the small intestine, the liver, and the spleen. It plays a key role in glucose homeostasis by regulating the secretion of pancreatic hormones (i.e., insulin and glucagon) and digestive enzymes.

The pancreas is an exocrine and endocrine organ. As an exocrine organ, it secretes the pancreatic juice containing digestive enzymes, including amylase, chymotrypsin, pancreatic lipase, and trypsinogen. These enzymes are secreted into the lumen of acini and directly assist the macronutrient digestion, thus involved in the glucose and energy metabolism (Roder et al., 2016).

In an endocrine manner, the pancreas releases pancreatic hormones into the blood circulation. There are several cell types responsible for secreting hormones with different functions: β-cells, presenting the majority of the islet cells (65-80%), product C-peptide and insulin. α-cells release glucagon, glucagon-like peptide-1 (GLP-1) and gastric inhibitory polypeptide (GIP); γ-cells release pancreatic polypeptide (PP); δ-cells produce somatostatin; and ε-cells produce Ghrelin, which comprises <1% of the total islet cells (Roder et al., 2016). Together, these hormones regulate glucose homeostasis, as discussed in more detail below.

1.3.4 The role of insulin

Insulin is the primary glucose-lowering hormone. It is produced by the cells of the pancreas, in the islets of Langerhans. The secretion of insulin is mainly stimulated by an increase in blood glucose concentrations. On the surface of pancreas β -cells, elevated blood glucose is sensed and taken up by the facilitative glucose transporter (GLUT2). Glucose flows into the cells and

undergoes glycolysis, in the process producing adenosine triphosphate (ATP) and causing the ATP-sensitive K^+ - channels to close. The closure of these channels leads to the depolarization of the membrane and results in the opening of voltage-dependent Ca^+- channels (VDCCs). The increase in intracellular calcium concentrations induces the fusion of insulin-containing granules with the membrane and subsequent release of insulin (Roder et al., 2016, Szablewski, 2011).

The main mechanisms by which insulin lowers blood glucose concentrations are well established. In general, it increases glucose utilization by tissues and organs and promotes glycogen synthesis. It increases the rate of transport of glucose from blood circulation to adipose tissue and muscle; It promotes glycolysis in muscle and adipose tissue; it promotes glycogen synthesis and inhibits glycogen breakdown in the liver, muscle and adipose; it suppresses gluconeogenesis in the liver (Newsholme and Dimitriadis, 2001, Szablewski, 2011).

It is found that insulin secretion is not triggered at the blood glucose concentration of less than 3mmol/L, but it increases when blood glucose rises above this threshold (Gerich, 1993). When blood glucose climbs over 5mmol/L, the beta-cells increase their output (Gerich, 1993). Postprandially, the insulin secretion response to blood glucose occurs in two phases. An initial rapid release of preformed insulin, which usually peaks at 5 min after glucose ingestion. The second phase of secretion is slow and sustained. It is the result of increased insulin synthesis and releases stimulated by increased blood glucose (Aronoff et al., 2004).

It was found that an oral glucose load induces greater insulin secretion than an intravenous glucose load while both ways achieved similar blood glucose levels. This was explained by the

"incretin effect" resulting from two hormones: GIP and GLP-1, which are secreted from the gut during glucose ingestion(Fu et al., 2013). This implies that the signals from the gut are important in the hormonal regulation of glucose metabolism.

1.3.5 The role of incretin hormones: GIP and GLP-1

GIP

GIP is a single 42-amino acid peptide encoded by the *gip* gene. It is synthesized and released from enteroendocrine K cells, which are primarily located in the proximal small intestine (duodenum and jejunum). The circulating levels of GIP are low in the fasted state, and it increases with the ingestion of foods containing carbohydrates and fat. It has been found that GIP-mediated insulin secretion is dependent on glucose levels (Elliott et al., 1993). The ingestion of fat alone, however, stimulated the GIP secretion but not in a sufficient amount to stimulate insulin secretion (Ross and Dupre, 1978).

On the surface of β -cells, circulating GIP can be bound by its specific receptor (GIPR), therefore promoting an increase in intracellular cAMP and Ca^{2+} concentrations. Insulin secretion and release from β -cells is thereby enhanced. GIP also promotes insulin biosynthesis in β -cells through cAMP/MARK/PKB signalling pathways (Trumper et al., 2001, Kim et al., 2005). Human studies have quantified the circulating concentrations of GIP in fasting state at 9-11 pmol/L and these levels increase to a peak of 50-120 pmol/L postprandially (Vilsboll et al., 2001).

A reduction or absence of GIP secretion has been linked to glucose intolerance development. Studies of GIP knockout mice have found that they exhibit mild glucose intolerance associated with reduced levels of glucose-stimulated insulin secretion (Miyawaki et al., 1999). However, these mice did not show significant changes in insulin sensitivity (Pamir et al., 2003). Nasteska *et al.* found that GIP receptor knockout mice exhibit impaired oral glucose tolerance and increased insulin resistance after high-fat feeding. It may suggest a potential therapeutic value of GIP in obesity and diabetes (Nasteska et al., 2014).

GLP-1

The potent role of GIP in insulin secretion is established, although it does not entirely explain the incretin effect observed. In 1983, the successful cloning of the mammalian proglucagon gene resulted in the identification of two new peptides originally from the glucagon sequence, named glucagon-like peptides (GLP-1 and GLP-2) (Bell et al., 1983). Subsequent studies have revealed that the GLP-1, alongside GIP, is more prominent in nutrient-stimulated insulin secretion (Hansotia and Drucker, 2005).

GLP-1 presents in several forms, and the most dominant form in circulating is GLP-1 (7-36) amide. Unlike GIP, GLP-1 is secreted by intestinal L cells which are located mainly in the distal gut. GLP-1 is rapidly released into blood circulation after food ingestion. The increase of plasma GLP-1 is biphasic: an early and rapid peak within 15-20 minutes, followed by a second peak within 60-120 min (Elliott et al., 1993, Rask et al., 2001). It is believed that the first peak of GLP-1 is the result of neural or endocrine signals. The second phase results from a direct action of nutrient interactions with intestinal L cells (Roberge and Brubaker, 1993, Hansotia and Drucker, 2005).

GLP-1 stimulates insulin secretion in a glucose-dependent manner. GLP-1 can increase cAMP levels and activate protein kinase A, thus increasing the transcription activity of the gene that encodes insulin and promoting its biosynthesis. Moreover, GLP-1 also improves β-cell function by increasing the expression of the sulfonylurea receptor, which rectifies the K^+ channel (Drucker, 2007). The physiological importance of GLP-1 has been well-documented. GLP-1 knockout mice were found to be glucose intolerant, with disrupted glucose-stimulated insulin secretion and fasting hyperglycaemia (Scrocchi et al., 1996). In humans, low levels of circulating GLP-1 induced by infusion of exendin(9-39) amide, a specific antagonist of GLP-1, were associated with increased fasting glucose and glucagon levels, suggesting that GLP-1 plays an essential role in fasting glucose homeostasis (Schirra et al., 1998).

GLP-1 has a role in gastric emptying and can affect postprandial glucose response. Gastric emptying is the process by which the contents of the stomach are moved into the duodenum (Jacoby, 2017). Layer et al. demonstrated the "ileal brake mechanism" in humans as they found a strong correlation between the ileal release of GLP-1 and inhibition of gastric acid (Layer et al., 1995). Exogenous GLP-1 slowed gastric emptying and the rates of carbohydrate absorption and consequently reduced the postprandial glucose (Deane et al., 2010) (Marathe et al., 2013).

1.3.6 Glucose uptake and transport

The maintenance of whole-body glycaemia is the result of the regulation of glucose uptake and metabolism by various tissue and organs. The crosstalk between them involves a family

of glucose transporters. There are two major families of glucose transporters: glucose transporters (GLUTs) and Sodium-glucose symporters (SGLTs). Both types comprise a group of subclasses and function in a tissue-specific manner (Navale and Paranjape, 2016).

SGLT family members are 60-80-kDa proteins containing 580-718 amino acids, of which SGLT-1 was the first to be identified and the most extensively studied. SGLT-1 is responsible for glucose absorption in the small intestine (Gorboulev et al., 2012). It is mainly located in the apical membranes of small intestinal cells. SGLT-1 functions as an active transporter, moving glucose up a concentration gradient that results from active sodium extrusion by the basolateral sodium/potassium- ATPase (Chen et al., 2016).

GLUT is a family of proteins comprising 12 membrane-spanning regions. GLUTs transport glucose across the plasma membrane by a facilitated diffusion mechanism. Of which, GLUT 1 is found to present in many fetal and adult tissues and is abundant in human red cells (Mueckler, 1994). GLUT2 is mainly expressed in beta cells of the pancreas, liver and kidney (Mueckler, 1994). In hepatocytes, GLUT2 regulates the entry and exit of glucose from the cells (Navale and Paranjape, 2016). GLUT3 is widely distributed in human tissue and is mainly present in the brain. It has a high affinity for glucose, which facilities its function to transfer glucose into brain cells with greater glucose demands (Navale and Paranjape, 2016). GLUT4 is an insulin-responsive glucose transporter which is located in the heart, skeletal muscle, adipose tissue and brain. The levels of GLUT4-dependent glucose transport could rapidly increase in response to elevated blood insulin, suggesting the importance of GLUT4 in the whole-body glucose disposal (Mueckler, 1994, Bryant et al., 2002).

Besides their role in glucose transport, SGLT1 and GLUT2 could act as glucose sensors in enteroendocrine cells, thus involving the secretion of GIP and GLP-1 stimulated by glucose load (Roder et al., 2014, Cani et al., 2007).

1.3.7 The liver, the adipose, and the skeletal muscle

The whole-body glucose regulation requires normal insulin actions alongside its key target tissues: liver, skeletal muscle, and white adipose tissue.

The role of liver

The liver controls the glucose absorption from the portal vein and endogenous glucose production in the fasted phase. After consuming a meal, carbohydrates are digested and absorbed in the gastrointestinal tract (GI tract), increasing the circulating blood glucose concentrations. Glucose entry into human hepatocytes mainly via transporters GLUT2 (Adeva-Andany et al., 2016). Consequently, it stimulates hepatic glycogen synthesis whilst inhibiting gluconeogenesis (Chadt and Al-Hasani, 2020). It is estimated that nearly half of the ingested glucose is converted to hepatic glycogen (Gerich, 2000). When a carbohydrate-rich diet is consumed, excessive carbohydrates in the liver are converted into fatty acids by lipogenesis (Han et al., 2016).

In the fasting state, the pancreas secrets the peptide hormone glucagon from its alpha cells, stimulating glucose production from glycogen (glycogenolysis), or non-carbohydrate precursors (gluconeogenesis) in the liver. The glucose generated from the liver could provide

essential metabolic fuel for other organs, such as the brain and exercising skeletal muscle (Chadt and Al-Hasani, 2020, Rui, 2014).

Skeletal muscle and adipose tissue

Skeletal muscle is the main tissue controlling postprandial glucose disposal. Glucose uptake in skeletal muscle is mediated by insulin. It occurs when the hormone binds to the insulin receptor (IR) which activates the phosphorylation of the membrane and consequently the translocation of GLUT4 from an intracellular compartment to the cell surface. The presence of GLUT4 on the cell membrane enables the entry of glucose by facilitated diffusion (Pereira et al., 2017). During exercise, circulating insulin levels and muscle contraction act in coordination and enhance GLUT4 expression in muscle (Rodnick et al., 1992). Upon glucose transport into the muscle, it is phosphorylated to glucose 6- phosphate (G-6-P). It will activate glycogen synthase in muscle at resting or enter into the glycolytic or oxidative pathways during exercise (Richter and Hargreaves, 2013).

Similar to skeletal muscle, insulin stimulates glucose uptake in adipose tissue via GLUT4 (Bryant et al., 2002). After a meal, approximately 7-15% of ingested glucose reaching the systemic circulation is taken by adipose tissue (Gerich, 2000). Moreover, insulin has inhibitory effects on lipolysis which lowers the plasma levels of fatty acids, decreasing hepatic glucose production (Gerich, 2000).

1.3.8 Problem with disrupted glucose homeostasis: insulin resistance

Normal insulin actions above are essential for the maintenance of glucose homeostasis. In the conditions that these tissues cannot respond to insulin, disrupted glycaemic metabolism occurs, which is known as insulin resistance. Himsworth et al. were the first to differentiate diabetic patients into two patterns by an “insulin-glucose test”: those who responded quickly to insulin injections (insulin sensitive) and those who responded inadequately (insulin resistance) (Himsworth, 1936).

Insulin resistance is believed to be central to the T2D aetiology (Reed et al., 2021). In this condition, glucose uptake by peripheral tissues decreases which causes hyperglycaemia. At first, β-cells compensate for insulin resistance by increasing insulin secretion to maintain glucose tolerance (Weir and Bonner-Weir, 2004). This leads to hyperinsulinaemia and impairs β-cell functions in a long term. Chronically, the β-cells are unable to produce enough insulin, which leads to hyperglycaemia and the progressive development of prediabetes or T2D (Weir and Bonner-Weir, 2004, Papakonstantinou et al., 2022).

The causes of insulin resistance are not fully understood, while several factors have been associated with its development. These have included genetic abnormalities impairing insulin actions, visceral obesity, sedentary lifestyle, fatty liver, and chronic stress (Papakonstantinou et al., 2022, Lebovitz, 2001). From a dietary perspective, high glycaemic index (GI) and glycaemic load (GL) foods can increase insulin resistance (McKeown et al., 2004). The role of postprandial hyperglycaemia has been highlighted (Tibaldi, 2009, Bell, 2001), and some mechanisms have been proposed by which postprandial hyperglycaemia causes insulin resistance (Agius, 2013, Brynes et al., 2005). When an excessive amount of carbohydrates is consumed, the liver is overpowered which increases the escape of glucose to the peripheral

circulation. This subsequently requires an increase in insulin secretion and plasma insulin levels, which in long term, may lead to the development of insulin resistance (Papakonstantinou et al., 2022).

Dietary interventions to regulate postprandial glycaemia are important to maintain tissue sensitivity to insulin. High-fibre, low-GI foods have shown beneficial effects on insulin secretion (Bodinham et al., 2012), insulin sensitivity (Salmeron et al., 1997, Schulze et al., 2004), and pancreatic functionality (Liese et al., 2005). The mechanisms of these effects are multifactorial and may depend largely on their actions within the GI tract. The presence of fibre content may delay digestion and/or absorption of carbohydrates(Liu et al., 2018) and ameliorate insulin response. The products of bacterial fibre fermentation in the distal gut (e.g, short-chain fatty acids) may have an impact on insulin sensitivity (Sleeth et al., 2013). Investigations are required into the complex physiological effects in the gut and how they may be exploited to improve glycaemic control.

1.4 Regulation of appetite

1.4.1 The role of the central nervous system (CNS)

The physiological regulation of appetite involves a complex interaction between signals from the GI tract, liver and adipose tissue, and signals generated from the central nervous system (CNS) (Alfituri, 2018). The hypothalamus and the brainstem are the main CNS sites for the control of appetite regulation. The arcuate nucleus (ARC) within the hypothalamus senses hormones secreted into the peripheral circulation through a semi-permeable blood-brain barrier (Arora, 2006). There are two types of neurons involved in appetite regulation in the ARC: the orexigenic (appetite-stimulating) neuropeptides Y and the agouti-related peptides, which stimulate appetite, whereas the anorexigenic neuropeptides cocaine- and amphetamine-related transcript (CART) peptide and pro-opiomelanocortin (POMC) which suppress appetite (Chambers et al., 2015a).

When carbohydrates enter the GI tract, the nucleus receives and integrates the signals from stimulation of vagal afferents in the gut and other visceral tissues as well as communicates with neurones in other hypothalamic nuclei and extra-hypothalamic regions of the CNS to regulate energy homeostasis (Chambers et al., 2015a).

1.4.2 The role of the GI tract: focus on appetite-regulating hormones

The GI tract is the largest endocrine organ in the body and can secrete over 100 bioactive peptides (Caron et al., 2016) and more than 30 recognizable gut hormones (Ahlman and

Nilsson, 2001). A various number of gut hormones from different sites of the GI tract have been associated with appetite regulation (**Table 1.1**). Important appetite modulators include leptin, ghrelin, cholecystokinin (CKK), oxyntomodulin (OXM), Peptide YY PYY) , and GLP-1. This section will discuss the hormones that are related to the present work.

Table 1. 1 Summary of the main appetite-regulating hormones in gut.

Hormones	Appetite	Receptor	Secretion site	Other actions
PYY	↓	Y2	L cells in gut	Delays gastric emptying
PP	↓	Y4 Y5	PP cells in pancreas	
GLP-1	↓	GLP-1	L cells in gut	Incretin, lower blood glucose, delays gastric emptying, neurotrophic effect
GLP-2	-	GLP-2	L cells in gut	Intestinal trophic effect
OXM	↓	GLP-1	L cells in gut	
Glucagon	↓	GCGR	Pancreatic α cell	Increases blood glucose/insulin
CCK	↓	CCK 1,2	I cell of small intestine	Gall bladder contraction Pancreatic enzyme secretion
Ghrelin	↑	GHS	Stomach	Growth hormone secretion
Amylin	↓	AMY1-3	Pancreatic β cells	Decreases blood glucose
Leptin	↓	LepR	Stomach	Regulates immune response, glucose, and lipid metabolism

PYY, peptide YY; PP, pancreatic polypeptide; GLP-1, glucagon-like peptide-1; GLP-2, glucagon-like peptide 2; OXM, oxyntomodulin; CCK, cholecystokinin; GCRP, glucagon receptor; LepR, leptin receptor. Adapted and modified from (Suzuki et al., 2010).

PYY

Peptide YY (PYY) belongs to a family of peptides that includes neuropeptide Y (NPY) and pancreatic polypeptide (PP). These peptides are made up of 36 amino acids and have extensive sequences in common (Tatemoto, 1982). PYY is produced by endocrine L cells and is found throughout the small and large intestine, in very low concentrations in the duodenum and jejunum (5-6pmol/g), but in higher concentrations in the terminal ileum (84 pmol/g) and colon (ascending 82pmol/g, sigmoid 196pmol/g) (Adrian et al., 1985).

There are two major forms of PYY in humans: PYY_{1-36} and $PYY_{3-36.}$ PYY_{1-36} is dominant in the fasted state, whereas PYY_{3-36} is the main form produced postprandially, accounting for approximately 63% of the circulating PYY (Grandt et al., 1994). After a meal, plasma PYY increased within 15 minutes and peaked at around 60 minutes and could remain elevated for up to 6 hours (Adrian et al., 1985). It is thought that the first increase occurs before the nutrients have reached the L cells in the distal gut and suggests that a neurohormonal pathway in the proximal gut may be involved. The latter sustained release is the result of the secretion by L cells induced by direct contact with intestinal contents (Imamura, 2002).

Emerging evidence has suggested that PYY_{3-36} has a role in appetite regulation. Battherham *et al.* showed that chronic peripheral administration of PYY_{3-36} decreased food intake and body weight in rodents (Batterham et al., 2002). Some mechanisms have been proposed by a

series of their experiments. Peripheral injection of PYY_{3-36} induced the expression of gene *c-fos* which was associated with the neuronal activation of the arcuate nucleus of the hypothalamus (ARC). Moreover, PYY_{3-36} injection decreased the expression of hypothalamic NPY mRNA. The administration of PYY_{3-36} directly to the ARC decreased food intake. It could act directly on the Y2 receptor in the arcuate nucleus of the hypothalamus (ARC) which is a presynaptic inhibitory autoreceptor (Batterham et al., 2002). Furthermore, PYY_{3-36} could activate POMC neurons in the ARC. These findings appear to suggest that PYY_{3-36} suppresses appetite by acting on the ARC via Y2 receptors, increasing the activity of POMC neurons and suppressing the activity of neuropeptide Y (NPY) neurons (De Silva and Bloom, 2012a). In addition, the anorexigenic effect of PYY_{3-36} may also involve a vagus-brainstem-hypothalamic pathway as evidenced by Koda *et al*. (Koda et al., 2005). Increased levels of PYY delayed gastric emptying and reduced gastrointestinal motivity, which activated ileal brake and decreased food intake (van Avesaat et al., 2015).

Translational research has targeted PYY as a novel treatment for obesity. The oral delivery of peptide hormones has been ineffective due to the difficulty of absorption across the intestinal wall (De Silva and Bloom, 2012a). Oral delivery of PYY with sodium N-caprylate showed an improved absorption of the peptide from the gut, as supraphysiological plasma levels of PYY were observed. Despite this, it failed to result in any significant changes in *ab libitum* food intake (Steinert et al., 2010). Alternatively, designing food to stimulate PYY secretion, via enhancing nutrients that reach the distal parts of the gut, may provide an effective way to regulate appetite (Wilde, 2009).

GLP-1

GLP-1, alongside PYY, is co-expressed and co-secreted in GIT L cells (Eissele et al., 1992). GLP-1 can activate the ileal brake and delay gastric emptying similar to PYY (Schirra et al., 2002, van Avesaat et al., 2015). As previously stated, GLP-1 is an incretin hormone that acts by binding to the GLP-1 receptor (GLP-IR) expressed in pancreatic islets. This facilitates glucose-dependent insulin release after a meal. Besides the pancreas, GLP-1R is also present in CNS areas, which include the ARC and paraventricular nucleus (PVN) in the hypothalamus and the area postrema (AP) in the brainstem(De Silva and Bloom, 2012a). It is believed that the synergistic actions of GLP-1 in the gut and brain, acting on both central and peripheral receptors, contribute to its effects on appetite (Shah and Vella, 2014).

It is well documented that the peripheral administration of GLP-1 can reduce food intake in humans. Gutzwiller et al. were the first to demonstrate that GLP-1 infusions resulted in a dose-dependent reduction in food and calorie intake in healthy human (Gutzwiller et al., 1999). It is further supported by a meta-analysis which reported a similar dose-response relationship in both lean and overweight subjects (Verdich et al., 2001).

The short half-life of GLP-1 presents challenges for its clinical use. It is because endogenous GLP-1 is rapidly broken down by the enzyme dipeptidyl peptidase 4 (DPP4). Therefore, some DPP4 inhibitors and GLP-1R agonists have been developed and used. However, side effects have been commonly reported, such as nausea, vomiting, and diarrhoea, which leads to patients discontinuing with the drug (Cho et al., 2013, Ratner et al., 2006). Instead, the modulation of diet to stimulate GLP-1 rarely results in reported side effects and may be a relevant strategy for appetite regulation (Bodnaruc et al., 2016).

Summary

Sections 1.3 and 1.4 have summarised the regulation of blood glucose and regulation. T2D and obesity are diet-related and multifactorial. Their development can result from several impaired physiological mechanisms in response to diets. The next section will focus on carbohydrates and the possible links to both diseases.

1.5 Carbohydrates, T2D, and obesity

Dietary carbohydrates comprise a significant proportion of the human diet. The type and amount of carbohydrates can largely influence metabolic health outcomes. Glycaemic Index (GI), an important component of carbohydrate quality, has been extensively studied for its relationship with these chronic diseases.

1.5.1 Carbohydrates and glycaemic index (GI)

Carbohydrates are a diverse group of substances formed from carbon, oxygen, and hydrogen atoms in proportions, most of which correspond to the empirical formula $(CH_2O)n$, with n being 3 or more (Coultate, 2009). Dietary carbohydrates are the major energy source in the human diet and have a range of physical and physiological properties (Englyst and Englyst, 2004). The 1998 WHO/FAO proposed that the primary classification of dietary carbohydrates based on their chemical characteristics determined by the degree of polymerization (DP), the type of linkage and individual monomer (Cummings and Stephen, 2007). This chemical approach divides carbohydrates into three groups: sugars (DP1-2), oligosaccharides (DP 3-9), and polysaccharides (DP>=10)(Cummings and Stephen, 2007).

Carbohydrate is the main dietary component affecting postprandial glycaemia(SACN, 2015). Many high-carbohydrate foods common to western diets produce a high glycaemic response which has been implicated in the development of both diseases. It may be attributed to sustained hyperglycaemia and hyperinsulinaemia, and consequently satiety modulation. To describe the postprandial glycaemia in different foods, the glycaemic index (GI) was developed by Jenkins *et al.* and his colleagues (Jenkins et al., 1981). High GI foods refer to those in which carbohydrates are quickly absorbed and show a high glycaemic response, while low GI foods are defined the opposite way (Jenkins et al., 1981). In practice, the GI of a test food corresponds to the incremental area under the blood response curve of 50g available carbohydrates measured over a 2-hour ratio to a standard food containing the same amount of carbohydrates consumed by the same subject (Mann et al., 2007).

1.5.2 Glycaemic index and T2D

To date, several large prospective studies have indicated that the intake of high GI foods increased the risk of T2D (Hodge et al., 2004, Bhupathiraju et al., 2014, Villegas et al., 2007). A large cohort study, during 3,800,618 person-years of follow-up, demonstrated that participants who consumed high GI diets, with high refined cereal and low fibre contents, presented nearly 40% higher risk of T2D compared to those with diets high in cereal fibre and low in GI (Bhupathiraju et al., 2014). Recently, Reynolds and colleagues conducted a series of meta-analyses to understand the role of carbohydrate quality and suggested dietary fibre and whole grains were better predictors of outcomes of non-communicable diseases. This study included 135 million person-years from prospective studies and 58 clinical trials. It showed that a high intake of dietary fibre or whole grains demonstrated a 15-30% reduction in the

risk of mortality and incidence of a wide range of non-communicable diseases such as T2D. GI and GL, however, were suggested to play a relatively less important role as giving non-significant association with the T2D risk (Reynolds et al., 2019). This study raised important considerations that GI as a ranking of postprandial blood glucose cannot fully define the health outcomes of carbohydrates. Dietary fibre and whole grain foods comprise of a broad range of glucose polymers and complex food structure, and their health effects could be through several mechanisms (Chambers et al., 2019a).

1.5.3 Glycaemic index, appetite, and body weight

There have been many theories proposed as to the effect of dietary carbohydrates on appetite. The notion that blood glucose is involved in appetite regulation was originally proposed by Mayer as the "glucostatic hypothesis" (Mayer, 1953). He proposed that low blood concentrations are a key factor in the triggering of hunger and the initiation of food intake (Mayer, 1953). This has been gradually developed into the "GI theory", which proposes that consumption of high GI foods induces rapid high spikes in blood glucose and insulin and a subsequent rapid return to feeling hungry. It has been supported by several acute human studies as evidenced that the GI of diet is related to subjective measures of appetite regulation (Ford and Frost, 2010). Conversely, a number of longer-term interventions have observed no difference between low and high GI foods on appetite and food intake (Ford and Frost, 2010, Poppitt, 2013). Recently, a large-scale study using real-world data suggested postprandial glucose dips 2-3h better predicted the increase of hunger and energy consumption compared to glucose 0-2h incremental area under curve (iAUC) (Wyatt et al., 2021).

Evidence from long-term studies that low GI foods can prevent weight gain and obesity has been controversial. A meta-analysis of 101 randomized control trials found low GI diets resulted in a small but significant reduction in body weight and BMI in adult subjects (Zafar et al., 2019). Reynolds et al. reported that currently available evidence from prospective studies and clinical trials that low GI foods reduced body weight had overall low to very low certainty (Reynolds et al., 2019). Recently, Gaesser and colleagues summarized 30 meta-analyses of RCTs and demonstrated that low-GI foods did not significantly reduce body weight or body fat in adult subjects (Gaesser et al., 2021).

There is growing discussion that whether the effect of GI on appetite and body weight results from postprandial glucose *per se*. In fact, there are many confounding factors that may influence both GI and appetite. Fermentable dietary fibre can affect the ranking of GI and regulate appetite involving hormonal and neural pathways (Pereira and Ludwig, 2001, Wanders et al., 2011). Supporting this, Reynolds *et al.* reported that higher intake of dietary fibre and whole grains had more convincing effects on reduced body weight [effect size: -0.62(-1.19 to -0.05) and -0.37 (-0.63 to -0.11), respectively] compared to intake the low GI foods [effect size -0.29 (-0.62 to 0.03)]. The certainty of the evidence for whole grains and dietary fibre was higher compared to those for low GI foods (Reynolds et al., 2019).

1.5.4 Summary

Epidemiological and clinical studies have associated carbohydrate-based foods with the physiology of both diseases, while the causal mechanism is not fully understood. High GI foods

seem to be a robust risk factor for T2D. However, their effects on appetite and body weight may not be due to the postprandial glucose *per se.* Beyond the GI concept, carbohydrate quality indices, slow-digestible carbohydrates and dietary fibre contents were suggested to better predict metabolic outcomes. The complex food structure and digestion physiology in the human GI tract better explains their health effects (Capuano, 2017b). The next section will describe carbohydrates from the perspective of food structure and discuss their digestion process in the human GI tract.

1.6 Carbohydrate food structure, digestion, and postprandial metabolism

1.6.1 Carbohydrate classification.

As previously mentioned, carbohydrates can be divided into three groups bases on chemical characteristics: sugars (DP1-2), oligosaccharides (DP 3-9), and polysaccharides (DP>=10) (Cummings and Stephen, 2007). The classification based on chemistry is essential, however, it brings challenges when it comes to understanding the effects on health. Indeed, it has been recognized that the classification purely on chemistry does not allow a simple translation into health outcomes, as the physiological effects also depend on their physical properties and complex structures (Cummings and Stephen, 2007). Thus, different carbohydrate classifications shall be used to help address different aspects of health outcomes (Cummings and Stephen, 2007). Glycaemic response, for instance, is strongly correlated to the rate of digestion rather than the chemical properties alone (Jenkins et al., 2004, Jenkins et al., 1982). This necessitates a classification based on digestibility properties to identify foods that are likely to improve glycaemic control.

The digestibility classification lays the foundation on the primary chemistry and is modified based on the rate and extent of small intestine digestibility. Sugars, including monosaccharides and disaccharides, are classified as rapidly digestible carbohydrates. Oligosaccharides such as inulin and oligofructose are classified as in-digestible carbohydrates since they cannot be digested in the small intestine. Polysaccharides include starch and non-starch polysaccharides. As for starch, depending on the rate and extent of the small intestinal digestion it is divided into rapidly digestible starch (RDS), slowly digestible starch (SDS), and resistant starch (RS). Non-starch polysaccharides (NSP), as a major part of dietary fibre, are indigestible carbohydrates as they can escape the small intestine and reach the colon. The digestibility effects are presented in **Table 1.2.** The following literature review will focus on starch, as the major source of dietary carbohydrates, in the concept of their structure and digestion.

Table 1. 2 Classification of carbohydrates based on digestibility

Carbohydrate	Subgroup	Digestibility	Example
Sugars (DP 1-2)	monosaccharides	Rapidly digestible	Fructose Glucose
	disaccharides		Sucrose Lactose
Oligosaccharides (DP 3-10)	/	Indigestible carbohydrate	Inulin Oligofructose
Polysaccharides (DP>10)	Starch	Rapidly digestible starch (RDS)	Processed breads Potato products
		Slowly digestible starch (SDS)	Pasta; Legume Grains
		Resistant starch (RS)	Raw banana Legumes Whole grains
	Non-starch Polysaccharides (NSP)	Indigestible carbohydrate	Cellulose (wheat, peas);hemicellulose (bran, beet root); Gum(oat, carrots); pectin (legumes, citrus fruits)

It was adapted and revised from (Aller et al., 2011)

1.6.2 Starch classification

Starch is the principal carbohydrate reserve in plants and provides essential energy in human diets. The Eatwell guide recommends that starchy foods should account for a third of the food intake for UK adults (Public Health England, 2016). The nutritional and physiological effects of starchy foods are largely dependent on how they are digested and interacted with the GI tract.

Englyst *et al.* developed an *in* vitro method to differentiate starch based on its digestion properties: rapidly digestible starch (RDS), slowly digestible starch (SDS), and resistant starch (RS) (Englyst et al., 1992). RDS is the starch that can be rapidly digested in the small intestine. RDS is found in many starch-based staple foods, such as highly processed bread, potatoes, and boiled white rice. The consumption of RDS-rich foods leads to a rapid rise in blood glucose and insulin levels and over the long term is associated with an increased risk of insulin resistance, metabolic syndrome, and obesity (Ells et al., 2005, Aller et al., 2011).

SDS, in the contrast, induces a slower rate of glucose absorption. It is digested slowly throughout the entire length of the small intestine and therefore induces a sustained and blunt glucose release. Additionally, it leads to lower levels of postprandial insulinaemia and gut hormones (Vinoy et al., 2016). SDS is commonly found in legumes, pasta, and nuts.

RS is defined as the portion of starch that cannot be digested in the small intestine. Thus, it arrives in the distal gut (the distal ileum and colon) where it becomes available for fermentation by gut microbiota. This process generates short chain fatty acids (SCFAs) and stimulates the secretion of gut hormones (Birt et al., 2013). RS is commonly presented in legumes, vegetables, and whole grains. The five common categories of RS are presented in **Table 1.3**

Table 1. 3 The categories of resistant starch (RS)

Type	Description	Food example
RS 1	Physically inaccessible starch	Legumes, whole grains
RS 2	Raw starch granules with the B- or C- polymorph	High amylose maize starch Raw banana
RS 3	Retrograded starch	Cooked and cooled rice
RS 4	Chemically modified starch	Octenyl succinic anhydride modified starch
RS 5	Amylose-lipid complex	Starch-fatty acids Starch-monoglycerides

RS, resistant starch.

A large body of evidence supports that SDS and RS would lead to more favourable metabolism than RDS in glycaemic control and appetite regulation (Miao et al., 2015, Snelson et al., 2019, Rashed et al., 2021, Olagunju and Omoba, 2022). This has derived a critical need for approaches that increase SDS and RS contents in starchy food products. Food structure has

been suggested to act as an useful tool to modulate starch digestion and will be discussed in the next section.

1.6.3 Starch structure and digestibility

It is evident that the digestibility of starch is governed by its food structure. Food structure, as discussed in this thesis, is defined as the arrangement of food constituents at multiple spatial scales. In the context of human digestion, food structure is dynamic due to the changing environment and dictates functionality such as the behaviour of food in the gastrointestinal tract. This section will discuss starch structure at different length scales (nm to cm) and how structural factors influence digestibility.

1.6.3.1 The hierarchical structures of starch

Starchy foods have hierarchical structures as shown in **Figure 1.2**. At the molecular level, starch consists of two forms of glucose polymers: amylose and amylopectin. Amylose is a linear macromolecular with α1–4 glycosidic linkage that forms predominately single-chain helices, whereas amylopectin contains many branched structures with α1–4 as well as α1–6 glycosidic linkages (**Figure 1.2A**) (Whistler et al., 2012). The amylose and amylopectin are organized into a semi-crystalline structure which contains amorphous and crystalline zones. Different organizations can form three types of crystalline starch granules (A, B, and C) and can be differentiated by X-ray diffraction (**Figure 1.2B**) (Zobel, 1988). At the cellular level, starch granules (**Figure 1.2C**), with other structural components like storage proteins and lipids, are embedded inside the cells, protected by cell wall structures (**Figure 1.2D**) (Singh et al., 2013). Cell walls and extra layers of cells act as the physical barriers limiting the access of

digestive enzymes (Rovalino-Cordova et al., 2018). These cellular structures are located in a storage organ like endosperm or cotyledon tissue (**Figure 1.2E**) (Singh et al., 2013).

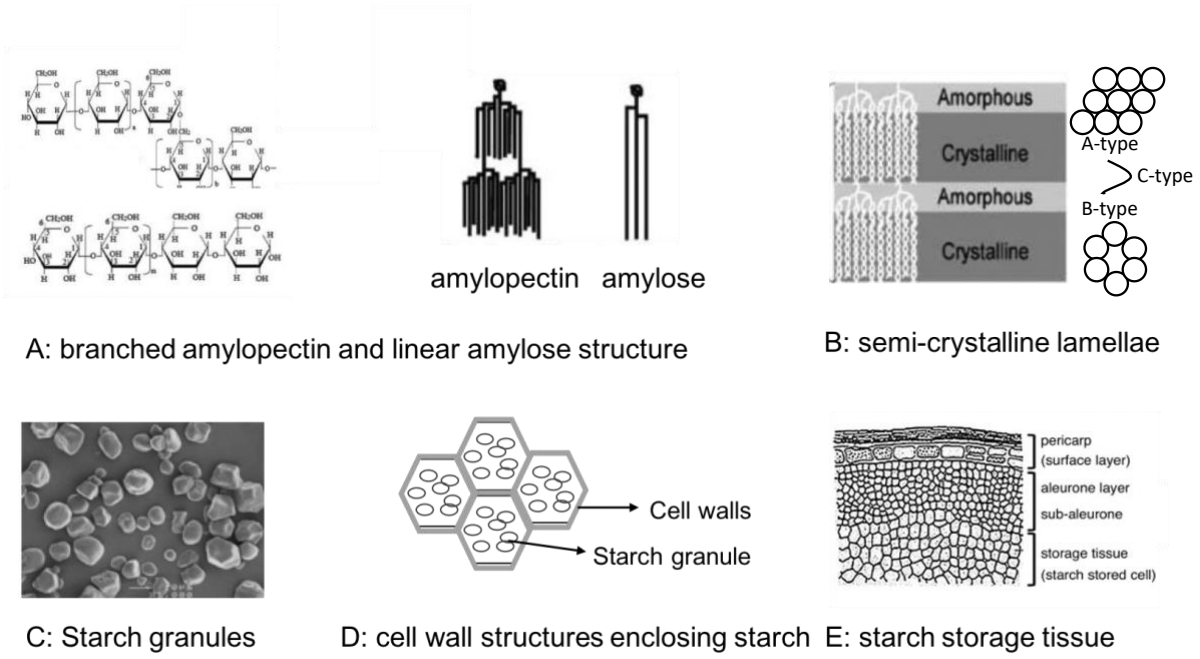


Figure 1. 2 The microstructures of starchy foods. The figure was adapted from (Cai et al., 2021).

1.6.3.2 Amylose and amylopectin

Amylose, due to its predominantly linear structure, is usually packed and arranged tightly in the crystalline regions of starch granules, whereas amylopectin contains mainly short-chain branches and forms a less-dense structure with a larger surface area. Compared to amylose, amylopectin is a more preferable substrate for amylolytic attack and is much easier to digest (Dona et al., 2010). It could explain the differences in digestibility observed in varying amylose contents. Legumes, as an example, generally contain higher amylose contents (30%-50%) compared to other plants such as wheat (20%-30%) (Bajaj et al., 2018). As a result, legumes have shown the lowest *in vitro* digestibility and the highest resistance to digestion in a group of plants (Bajaj et al., 2018, Birt et al., 2013). In another study, the glycaemic index (GI) of rice

noodles decreased as amylose contents increased, suggesting that the rate of digestion inversely correlated with their amylose contents (Srikaeo and Sangkhiaw, 2014).

In addition to the amylose: amylopectin ratio, the fine structure of these glucose polymers also affects digestibility. A higher degree of branching and longer branch lengths could increase *in vitro* digestibility (Syahariza et al., 2013).

1.6.3.3 Starch granule morphology

Starch granules from different botanical sources differ in granule morphology i.e. granule size, size distribution and shape (Lindeboom et al., 2004). The granules vary in size from 1 to 50µm (Cornell et al., 1994). Granule size could also affect digestibility as the surface area and contact per weight between substrate and enzyme decreases when the size of the granule size increases (Svihus et al., 2005). Franco *et al.* have established the relationship that a smaller size of granules resulted in a higher enzymatic susceptibility (Franco et al., 1992).

Granule surface characteristics could also affect starch digestion. The number and size of small openings (pores) on the surface may play an important role in digestion as it controls the water diffusion during food processing and the access of enzymes to the interior of granules during digestion(Tian et al., 2019a). Compared to cereals, raw potato starch granules presented a high level of resistance to *in vitro* digestion due to their smooth and less-pored surface (Garcia-Alonso and Goni, 2000). The hydrolysis in potatoes started from the surface and moved toward the inside of granules as an "outside-in" pattern, whereas the hydrolysis in cereal starches proceeded in an "inside-out" manner with more pores being observed (Warren et al., 2011, Garcia-Alonso and Goni, 2000).

1.6.3.4 Gelatinized and retrograded starch

Most starchy-based foods undergo thermal processing before they are consumed. During processing, starch granules swell and lose their crystallinity, whilst the fine structure of amylose and amylopectin disorders irreversibly. This phenomenon is called gelatinization (Tian et al., 2019a). When cooked starchy foods are stored at low temperatures, gelatinized starch will undergo retrogradation, in which process the starch molecules recrystallize and form into partially ordered structures that differ from their original granules (Tian et al., 2019a). **Figure 1.3** describes the process in which starch granules absorb water and swell at heating and reorder the structures of amylose/ amylopectin at cooling and storage. The relationship between the degree of gelatinization/retrogradation and digestibility has been extensively studied. The degree of gelatinization positively correlated with digestibility, while the level of retrogradation was inversely associated with the digestibility (Pellegrini et al., 2020).

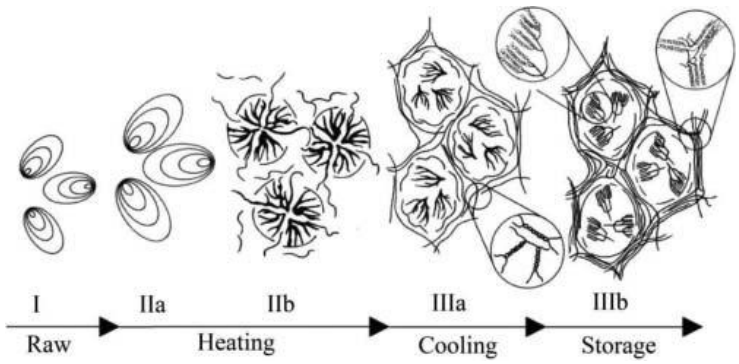


Figure 1. 3 The changes in starch granules during heating, cooling, and storage. Adapted from (Tian et al., 2019a)

1.6.3.5 Cell wall structures

Cell walls are essential and complex structures presented in plants. Cell walls trap starch granules inside cells and play an important role in the control of their digestion. Mechanisms

by which cell walls affect starch digestibility have been proposed based on a series of *in vitro* digestion studies and are summarized below.

The physicochemical properties

Differences in the composition and fine structure of cell walls initiate disparity in the physiochemical properties of different botanicals and consequently affect their digestion (Holland et al., 2020). Literature has reviewed the molecular constituents of a primary cell wall in detail while understanding their organization remains a challenge (Holland et al., 2020). A primary cell wall mainly consists of a network of cellulose microfibrils contained within a gel-like matrix of polysaccharides (hemicelluloses and pectin). This network, as a result, provides its high tensile strength. In addition, some proteins and phenolic compounds are present in the cell walls (**Figure 1.4**). The primary cell walls are classified into the groups: type I cell walls and type II cell walls. Dicotyledonous (e.g., legumes) and non-gramineous monocotyledonous plants have type I cell walls which contain more pectin, while grass/commelinids e.g. wheat and cereal grains have type II cell walls, which have less pectin and a higher amount of phenylpropanoids and/or mixed-linkage (1-3), (1-4)- β-d-glucans (Yokoyama and Nishitani, 2004). This disparity in components and structure can explain the marked differences in digestibility profile between the two types of cell walls (Edwards et al., 2021). Type 1 cell walls (from chickpea tissue) were less permeable to digestive amylase compared to type 2 cell walls (from wheat tissue), resulting in slower and less starch digestion in a dynamic *in vitro* model. This study highlighted the role of cell permeability in the control of starch digestion (Edwards et al., 2021). Other properties such as viscosity, solubility, and water-holding capacity were also shown to influence the digestion process (Holland et al.,

2020). They are involved in the control of gastric emptying, nutrient bioaccessibility and digestion kinetics (Grundy et al., 2016b, Holland et al., 2020).

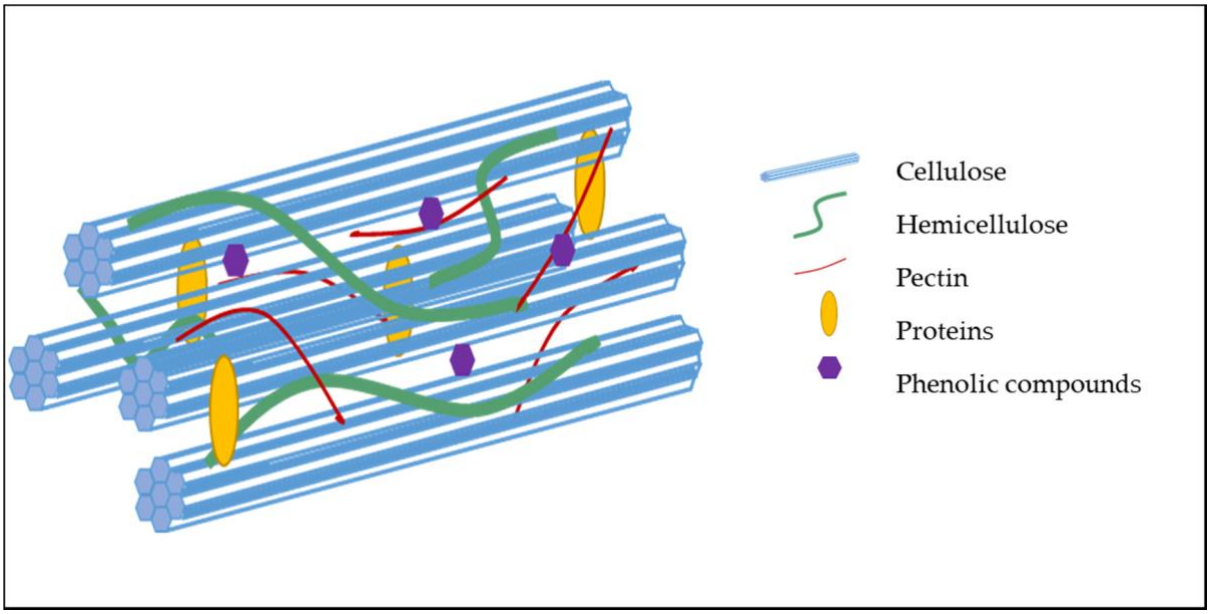


Figure 1. 4 The representative diagram of cell wall structure and organization of its constituents. Adapted from (Holland et al., 2020)

Cell wall barrier mechanism

Starch granules in nature are inside the cells, encapsulated by plant cell wall. The presence of intact cell walls serves as a semi-permeable barrier to limit the interaction between starch and digestive enzymes. The pores on the surface area of cell walls lie in the range 3.5-5.5nm (Brett and Waldron, 1990), which potentially cannot allow the diffusion of amylase which has a diameter of ~8nm (Payan et al., 1980). Porosity largely varied between plant species (Holland et al., 2020). Intact cells separated from plant tissue have been extensively studied and *in vitro* studies confirmed the digestive enzymes cannot diffuse through the cell walls of plant-based foods such as almond(Grundy et al., 2016a), wheat(Bhattarai et al., 2018), chickpea (Bhattarai et al., 2017), peas (Junejo et al., 2021b); whilst other plants seem are

permeable including common beans (Rovalino-Cordova et al., 2018), potato (Li et al., 2019), and bananas (Rongkaumpan et al., 2019).

In addition to porosity, cell wall parameters include thickness, resistance and/or degree of processing affect their permeability to enzyme diffusion (Li et al., 2019, Grundy et al., 2016a, Pallares Pallares et al., 2018). Chickpeas, for instance, have thick and mechanically resistant cell walls and thus could provide effective physical barriers to starch amylolysis during *in vitro* digestion (Edwards et al., 2014b). Same food processing affected differently the cell walls of chickpeas and wheats which subsequently affected their digestion profiles (Edwards et al., 2021). The extent to which cell walls affected the bioaccesibility of starch largely depends on the intactness of cell walls and how much the structural integrity remains after processing, mastication, and digestion in the GI tract (Capuano, 2017b, Holland et al., 2020).

The cell wall barrier mechanism is important to understand the access of enzymes to starch, which has been suggested as the rate-limiting step for starch digestion in cooked legumes (Dhital et al., 2016). The starch that escapes from small intestinal digestion passes into the large intestine and can be fermented by gut microbiota (Birt et al., 2013), providing a potential tool for lowering starch digestion, attenuating blood glucose, and promoting gut fermentation.

Restricted gelatinization mechanism

Besides its function as a physical barrier between starch and enzymes, the cell wall also affects the properties of starch granules during processing. Hydrothermal processing induces starch gelatinization in which process starch granules absorb water and swell. The presence of a cell

wall limits the amount of water that could pass through the cell. Edwards *et al.* observed that the degree of starch gelatinization was inversely related to the intactness of chickpea cell walls (Edwards et al., 2015b). Bhattarai et al. had similar observations in other legume cells, where the preservation of intact cell walls reduced the extent of starch swelling (Bhattarai et al., 2017).

Other mechanisms

Two mechanisms that have recently drawn attention relate to non-specific binding effect and the cytoplasmic matrix effect. The noncatalytic bindings of α-amylase on the cell wall surface (i.e., cellulose) can inhibit the amylase activity and thus reduce starch digestion (Dhital et al., 2015, Li et al., 2018a). The cytoplasmic matrix refers to the starch granules embedded in a protein matrix. In the presence of intact cell walls, starch and protein are tightly packed consequently hindering the access of α-amylase to starch (Rovalino-Cordova et al., 2018).

1.6.3.6 Food structure affected by processing

Most plant-based foods undergo domestic and/or industrial processing, which affects their food structure. Generally, the processing is thought to disrupt their primary structure and establish the secondary structure (Tian et al., 2019a). Understanding how processing affects food structure will help promote foods that have desirable structural properties and deliver metabolic benefits.

Common processing usually includes size reduction and heating. Size reduction treatment, such as milling and blending influences both macro and micro-structures. At the tissue level, starchy food with a smaller particle size could provide a larger surface area available for

enzyme action than those with a larger particle size (Grundy et al., 2016b). At the cellular and starch granule level, smaller food particles are associated with disrupted cell wall structures and increased surface area of starch granule, which makes them more susceptible to enzyme hydrolysis than unprocessed foods (Dhital et al., 2010, Grundy et al., 2016b, Ogawa et al., 2018). Heating with excess water induces gelatinization and structural changes in starch granules. This process destroys the native structure of starch granules and results in an open porous structure which allows internal access to the enzyme and promotes digestion(Alsaffar, 2011, Rewthong et al., 2011).

Summary

This section has summarized the structural constituents of carbohydrates-, particularly starch-based foods, and how structural properties influence starch digestibility. Next, we will discuss how carbohydrate-based foods are digested in humans.

1.6.4 Carbohydrate food structure and digestion in the human

Figure 1.5 presents the anatomy of the human digestive system. The system comprises the oral cavity, the oesophagus, the stomach, the small intestine (duodenum, jejunum, and ileum), and the larger intestine which includes the ascending, transverse, and descending colon, rectum, and anus (Singh and Gallier, 2014). The digestive system works on two levels: mechanical and chemical and it provides enzymes, water and the chemical environment required for digestion and movement (Singh and Gallier, 2014).

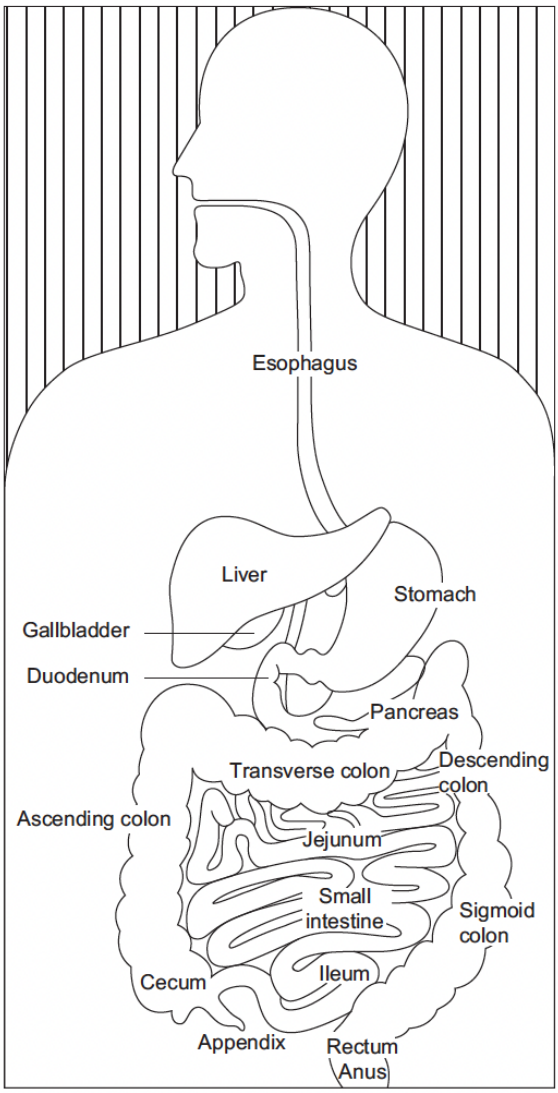


Figure 1. 5 Human digestive system. Adapted from (Singh and Gallier, 2014).

1.6.4.1 Oral digestion

The first stage of digestion occurs in the mouth when the food is processed mechanically and biochemically. The process of mastication (chewing) breaks the food into small pieces and mixes it with saliva to form a bolus (Singh and Gallier, 2014). The mastication reduces the size of food particles until they are small enough to be swallowed and pass through the oesophagus. Solid or semi-solid food is more difficult to manipulate than fluids (Chen, 2009). Saliva releases the glycoprotein mucin which functions as a lubricator to help the bolus

formation and the movement of the food (Chen, 2009). From a nutritional perspective, mastication is a natural way of increasing starch digestibility by disrupting food structure. It reduces particle size and increases the surface area for enzyme interaction. The longer time and exposure of mastication have been associated with a higher starch digestibility and consequently, a higher glycaemic response (Blanquet-Diot et al., 2021, Cai et al., 2021).

Saliva contains digestive enzymes, such as α-amylase generated by salivary glands. When a starchy food enters, salivary amylase hydrolyzes amylose and amylopectin into disaccharide molecules of maltose, decreasing its viscosity (Singh and Gallier, 2014). The enzyme interaction begins almost immediately after food ingestion, as evidenced by the observations that the starch viscosity decreased 10-fold in less than 10 seconds after mixing with the saliva (Vallons et al., 2015, Mandel et al., 2010). However, its contribution to starch full breakdown is relatively minor. The majority of starch digestion occurs in the small intestine (Allison Calabrese, 2022, Chen, 2009).

1.6.4.2 Gastric digestion

The stomach is a J-shaped muscular pouch that processes food with digestive juices. The stomach consists of the cardia, fundus, body, and pylorus. The primary function of the stomach is to prepare ingested food into chyme and regulate its delivery into small intestine, which is measured as the gastric emptying (Goyal et al., 2019). As the ingested food arrives, the stomach induces gastric movement with gastric juice with the effects of mixing, grinding, and sieving, which further reduces the size of food particles (<2mm). This process produces a mixture called chyme (Goyal et al., 2019). In addition to the caloric load, the rate of gastric

emptying also depends on the food form and physical properties. Foods in solid and semi-solid form prolonged gastric emptying compared to fluids. Foods with high viscosity, such as barley and oats containing dietary fibre (β-glucan) slowed the rate of gastric emptying (Wolever et al., 2020, Juvonen et al., 2009, Mackie et al., 2017b).

During fasting, the gastric juice is at a basal pH between 1 and 3. It increases to 5.5-7 after food ingestion and decreases to 4-5 after the half emptying time, returning to the basal value after food leaves the stomach (Singh and Gallier, 2014). When food enters the stomach, the acidic environment inhibits the action of salivary amylase, thus ending salivary digestion (Singh and Gallier, 2014). Nevertheless, some studies have suggested that when a very big meal is consumed, the boluses of foods may remain relatively undisturbed. This could provide barrier protection to salivary amylase and allow it to function in the upper part of the stomach (Frayn, 2009, Rosenblum et al., 1988).

On the other side, the acidic pH ensures the enzyme activity of pepsin and gastric lipase and therefore the degradation of lipids and proteins. The low acidic environment changes food structure such as aggregation of proteins and flocculation of lipids (Singh and Gallier, 2014). Food softening and dissolution happens due to gastric acid hydrolysis (Sensoy, 2021).

1.6.4.3 Small intestinal digestion: the duodenum, jejunum, and ileum

The small intestine is the main site for food digestion, nutrient release, and absorption. The small intestine is the longest part of the GI tract with an approximate length of 6.5 meters (Bowcutt et al., 2014). The small intestine is connected to the stomach by the pylorus and to the colon by the ileocecal valve. It is divided into three sections: duodenum, jejunum, and

ileum. The duodenum is about 20-30cm long and is the location of the ducts where the pancreatic juice and bile enter the intestine. The jejunum (0.8-1.5m) is a coiled middle part followed by the ileum (3-3.5m), which connects to the large intestine through the ileocecal valve (Sensoy, 2021).

Duodenum is U-shaped and divided into four parts: superior, descending, horizontal, and ascending. The superior part is peritoneal, and the rest is retroperitoneal (**Figure 1.6**). Duodenum is the primary region of chemical digestion, in which the secretions of the pancreas (pancreatic juice) and liver (bile salts) play an important role (Knight, 2019). Pancreatic juice mainly contains water, bicarbonate ions, and pancreatic enzymes (Dolenšek et al., 2017). As the chyme enters the duodenum, some gastric secretions arrive and continue the digestive process for a short time. The presence of chyme induces the release of pancreatic juice containing bicarbonate solution that neutralizes the acidic gastric juice (Sensoy, 2021). The arrival of pancreatic juice induces a rapid increase in pH to 5-7 in the duodenum (Humbert et al., 2018, N'Goma et al., 2011). Pancreatic juice contains many enzymes, such as proteases, peptidases, lipases, and pancreatic amylases (Singh and Gallier, 2014). They enter the descending through the hepatopancreatic ampulla (Knight, 2019). Briefly, these digestive enzymes break down proteins, lipids, and carbohydrates into smaller forms. Trypsin, chymotrypsin, and other proteases hydrolyse undigested proteins and peptides from the stomach into amino acids. Lipases break down lipids into fatty acid and glycerol molecules (Goodman, 2010). Bile acids play an important role in lipid digestion. They are produced in the liver and concentrated and stored in the gall bladder. In a healthy person, the liver secretes around 600ml of bile into the duodenum each day (Hundt et al., 2022). During lipid digestion, bile acids lower the surface tension of large fat globules and collapse

them into small droplets, which is called emulsification (Knight, 2019). Carbohydrates are digested by amylase and glucosidase into monosaccharides. Pancreatic amylase attacks the glycosidic bonds between adjacent glucose molecules in polysaccharides, breaking down starch into maltose (Sensoy, 2021). Unlike salivary amylase, pancreatic amylases are efficient over a wide neutral-to -alkaline pH range. Digestion of disaccharides and a few other oligosaccharides is carried out by the enzymes of the small intestinal brush border. Maltase, for instance, cleaves the disaccharide maltose into two molecules of glucose, representing the major source of monosaccharides that can be absorbed (~80%). Other absorbable forms include galactose and fructose (**Figure 1.7**) (Goodman, 2010). Although the chemical breakdown of structures predominates in the small intestine, motor activities (segmenting and peristaltic contractions) have a role in assisting in the mixing and transport of chyme and facilitating its contact with the digestive environment (Sensoy, 2021).

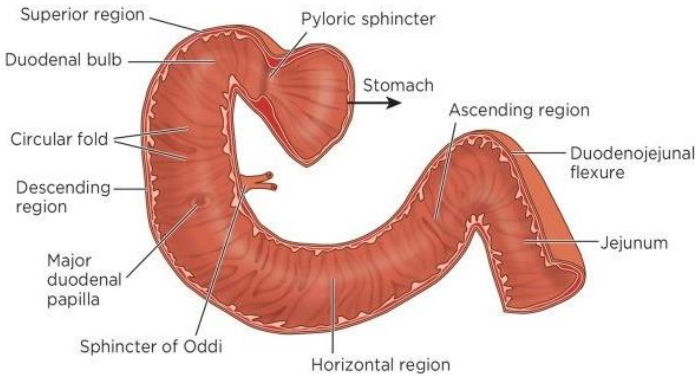


Figure 1. 6 Physiology of the duodenum. Adapted from (Knight, 2019)

The jejunum and ileum continue to finish chemical digestion; besides, they are the main sites for nutrient absorption. Histologically, there is no clear border between the jejunum and the ileum. Whilst the jejunum can be distinguished from the rest of the small intestine by the absence of Brunner's glands (duodenum) and Peter's patches (ileum) (Knight, 2019). The

features of the small intestine allow for optimal absorption of nutrients. The small intestine contains circular folds, villi, and microvilli that increase the surface area of the lumen by 400-600-fold (Welcome, 2019). In addition, they slow down the flow of chyme. Their shape (e.g., finger-like Villi and hair-like microvilli) ensures that the nutrients flow in a spiral rather than moving down the GI tract in a straight line (Welcome, 2019). After carbohydrates have been digested, the products are absorbed and transferred to the circulation via the portal vein in a two-step system. Firstly, glucose enters and concentrates in the enterocyte cells via SGLT-1. Secondly, the intracellular glucose is released into the interstitial space controlled by GLUT2 located in the basolateral membrane (Stümpel et al., 2001). The overview of carbohydrate digestion and absorption in the small intestine has been summarised in **Figure 1.7.** Any undigested foods will reach the large intestine, where they will be fermented by gut bacteria or pass through the faeces.

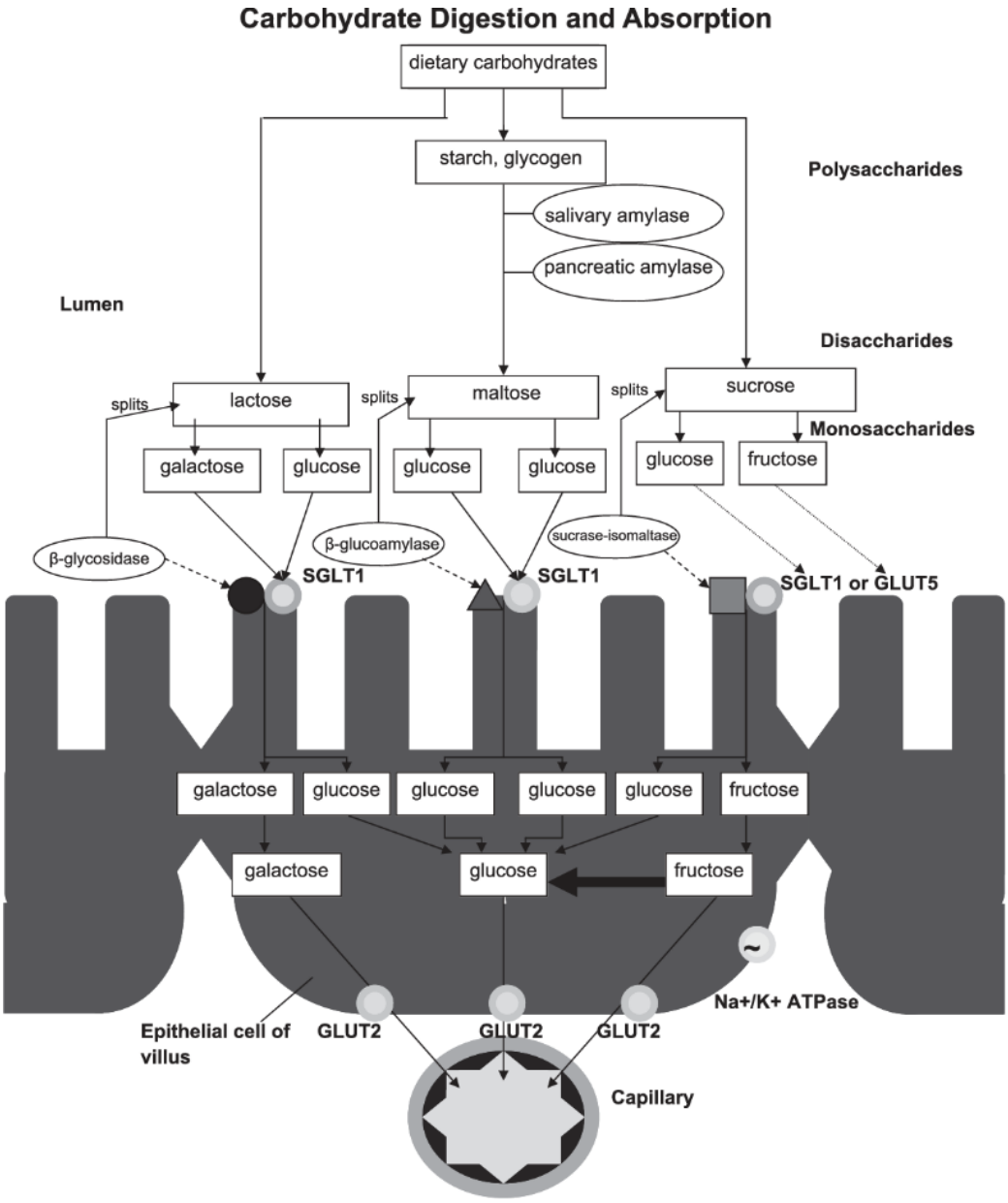


Figure 1. 7 Carbohydrate digestion and absorption. Adapted from (Goodman, 2010)

1.6.4.4 Large intestinal fermentation

Human GIT contains a rich and complex population of microorganisms (>100 trillion). Unlike the upper GIT, the large intestine has a long transit time and a neutral to mildly acidic pH and therefore can support a dense and diverse community of microorganisms (Thursby and Juge, 2017). The vast majority of microorganisms present in the large intestine are bacteria. Six

bacterial phyla are dominated in the human gut: *Bacteroidetes, Firmicutes, Proteobacteria, Verrucomicrobioa, Fusobacterial and Actinobacterial*, with *Firmicutes* and *Bacteroidetes* constituting over 90% of the known community (Arumugam et al., 2011, Qin et al., 2010). Dietary and lifestyle factors can alter the profile of the gut microbiome, and consequently the host physiology (Holscher, 2017).

As mentioned above, resistant starch (RS) and non-starch polysaccharides (NSP, or dietary fibre) undigested from the small bowel can enter the large intestine. Different forms of RS (type 1-5) are fermented into short-chain fatty acids (SCFAs), mainly acetates, propionate and butyrate (Holscher, 2017). Most scientific research has been conducted to investigate the *in vitro* fermentation of various types of RS, with the greatest attention on type 2 RS. Other types remain relatively unclear. NSPs provide the vast majority of carbohydrates entering the colon. The types of NSPs determine the ratios of SCFAs. Pectin yields more acetates, whilst β-glucan produces more acetate and propionates than butyrate (Lovegrove et al., 2017). The physiochemical characteristics and structure of NSPs may influence the degree of gut fermentation (Chung et al., 2019). Some polysaccharides, such as cellulose and psyllium are poorly hydrolysed by the enzymes of microorganisms. In contrast, pectin and β-glucan are highly fermentable due to their high solubility and viscosity (Holscher, 2017, Chung et al., 2019). The metabolism of SCFAs can provide up to 10% of dietary energy (Bergman, 1990). It also provides great benefits to the host metabolism such as glycaemic and energy homeostasis (Lovegrove et al., 2017, Birt et al., 2013). During gut fermentation, gases like H_2 and CH_4 are produced. The measurement of these gases could be served as an indicator of the levels of the fermentation (Parodi et al., 2009).

1.6.5 short chain fatty acids (SCFAs)

The products of microbiota fermentation have key functions in the regulation and glycaemic and energy metabolism via SCFAs pathways. These will be discussed in the next sections.

1.6.5.1 The production of SCFAs

Most SCFAs production occurs in the caecum area (distal ileum, caecum and proximal colon) (Cummings et al., 1987). Besides, the proximal colon has the highest bacterial numbers, fermentation, and proliferation, and is, therefore, the main site for SCFA production. Fermentation is limited in the distal colon due to the depleted carbohydrate and water. (Wong et al., 2006b). A study measured SCFAs from subjects' 3h20min post-mortem and showed that the SCFAs concentration was 13mmol/kg in the ileum and rose by nearly 10-fold in the caecum (131mmol/kg). Furthermore, the concentrations of SCFAs fell along the colon (123mmol/kg for ascending and 80mmol/kg for descending, respectively) (Cummings et al., 1987). Due to the difficulty of accessing the distal gut, SCFAs were mostly measured on faecal samples, which showed a molar ratio of 60:20:20 for acetate: propionate: butyrate respectively (Cummings et al., 1979). This ratio is relatively constant among variable populations, although it could change due to a range of lifestyle and dietary factors (Wong et al., 2006b). RS is one of the principal sources of fermentable carbohydrates. Though most of the research has been done *in vitro* or on animals, a few human studies have observed that the intake of RS could raise faecal SCFAs. The intervention of whole grains, which are rich in RS1 and dietary fibre, resulted in increased butyrate production (Bach Knudsen, 2015). Supplementation of RS2 for 2 weeks increased the concentrations of butyrate and acetate

but not propionate in the faeces (Baxter et al., 2019). Intake of RS3 increased butyrate in the faecal (Schwiertz et al., 2002). Currently, there is very little is known about the gut physiology related to SCFAs production. Indeed, the measurement of SCFAs in the faeces may not adequately represent its production in the gut. Independent of the change in production, the increase of SCFA in faeces could also result from increased faecal bulk or/and shortened transit time (Wong et al., 2006b). Direct measurement of SCFA concentrations in the human gut would be required to gain a better knowledge of SCFAs and their health effects.

1.6.5.2 The absorption of SCFAs

Despite low concentrations, SCFAs are physiologically present in the human upper GI tract. The absorption of SCFAs can happen as early as in the stomach and small intestine. Butyrate and acetate in the protonated form could be absorbed in the human stomach (Saunders, 1991). Acetate, propionate, and butyrate can be readily absorbed in human jejunum at the same rates (Schmitt Jr et al., 1976). The large intestine presents the most abundance of SCFAs. The absorption of SCFAs in the cecum and the colon is efficient and rapid, with only 5-10% being excreted in the faeces (Wong et al., 2006a). Two mechanisms for SCFAs absorption have been proposed: (1) diffusion of protonated SCFAs and (2) anion exchange (Wong et al., 2006a). First, diffusion of protonated SCFAs involves the consumption of luminal CO_2. This process accounts for about 60% of the total SCFA absorption (Ruppin et al., 1980); the rest occurs by cellular uptake of ionized SCFAs involving the diffusion of the Na or K salt of the SCFAs(Fleming et al., 1991). SCFAs can be absorbed in various regions of the caecum and colon, but SCFAs absorbed in the caecum, ascending colon or transverse colon are transported into the superior mesenteric vein, whilst SCFAs absorbed in the descending colon and sigmoid transport into the inferior mesenteric vein. Both further drain into the portal vein

and the liver (Canfora et al., 2015). In addition, it is found that SCFAs absorbed in the sigmoid and rectal region can also enter the liver via the pelvic plexus, draining in this way into the inferior vena cava and reaching the systemic circulation directly (Canfora et al., 2015).

Human peripheral blood concentrations of propionate and butyrate are usually low, and only acetate is present in significant amounts (Robertson et al., 2005, Wolever et al., 1997). Human studies have measured that acetate is absorbed in the highest amount in the liver and reaches the highest peripheral concentrations (19-160 μmol/l), whilst propionate and butyrate are much lower (1-13μmol/l, 1-12μmol/l respectively) (Bloemen et al., 2009, Bloemen et al., 2010).

1.6.6 The role of SCFAs in glucose homeostasis

SCFAs play an important role in the regulation of glucose homeostasis. Some potential mechanisms have been proposed based on rodent models. Firstly, mechanisms can relate to their beneficial effects on islet β-cells. SCFAs can have a protective role in β-cells by reducing levels of oxidative stress and inflammation (Kim et al., 2018). Moreover, SCFAs could improve β-cell function through the inhibition of apoptosis (Pingitore et al., 2017). Secondly, the regulation may be via the metabolism of skeletal muscle and liver tissues. SCFAs can enhance the expression of GLUT4, a primary glucose transporter in skeletal muscle and thus promote glucose uptake (Yamashita et al., 2009). In addition, SCFAs could up-regulate the 5-AMP-activated protein kinase signalling in muscle and liver tissues, consequently having an anti-lipolytic effect in adipocytes and improving insulin sensitivity (Kim et al., 2018, Chambers et al., 2018b). Lastly, SCFAs could modulate the release of gut hormones such as GLP-1 and PYY

through receptors FFAR2/3. GLP-1 could increase insulin secretion and decrease glucagon production in the pancreas (Tolhurst et al., 2012), whereas PYY has been found to increase glucose update in the muscle and adipose tissue (den Besten et al., 2013).

In human subjects, the interventions of SCFAs administration have shown inconsistent findings. The administrations of acetate, propionate, and butyrate had no significant effects on glycaemic measures in human subjects, as reported by a meta-analysis including 43 RCTs. (Cherta-Murillo et al., 2022). A targeted delivery of propionate to the colon has been recently developed (Polyviou et al., 2016). This improved pancreatic β-cell function and insulin sensitivity in adults with overweight and obesity (Chambers et al., 2015b, Pingitore et al., 2017, Chambers et al., 2019b). Altogether the evidence may suggest the source and actions of SCFAs (e.g., how SCFAs are delivered, produced, and absorbed in the gut) are critical to the physiological consequences.

Non-digestible carbohydrates (NDCs) can be substrates for fermentation to produce SCFAs. An increasing number of clinical trials have reported the benefits of dietary fibre and RS intake on glycaemic control such as reduced fasting glucose concentrations and improved insulin sensitivity. Study groups have included healthy, overweight/obese individuals and subjects with metabolic syndrome (Johnston et al., 2010, Xiong et al., 2021). Interventions of whole-grain foods that increased plasma propionate have been associated with a reduction in postprandial insulin as opposed to refined grain foods (Vetrani et al., 2016). A Mediterranean diet consisting of high fibre contents increased butyrate concentrations in plasma and improved insulin sensitivity compared to a low-fibre diet (Vitale et al., 2021). Similarly, Zhao *et al.* treated T2D subjects with a high-fibre diet which caused increased levels of faecal

butyrate concentrations associated with reduced fasting glucose and HbA1c levels. Notably, they found the high-fibre diet promoted a select group of SCFA-producing microbiota in T2D participants. Mice that received transplanted faecal microbiota from participants also showed lower fasting and postprandial blood glucose levels (Zhao et al., 2018). Overall, increasing SCFAs from NDC fermentation may represent a novel strategy to improve glucose homeostasis.

1.6.7 The role of SCFAs in appetite regulation

The role of SCFAs in appetite regulation has been extensively studied. This section will include the discussion of (1) oral ingestion of SCFAs, (2) colonic delivery of SCFAs via interventional supplement i.e. Inulin-propionate ester (IPE) and (3) production of SCFAs from non-digestible carbohydrate intake.

(1) Oral delivered SCFA

Several clinical trials have observed that oral SCFAs may enhance satiety, although others suggested that it could result from its sensory properties (palatability) rather than physiological effects (Darzi et al., 2011, Darzi et al., 2014). Indeed, several studies have reported that incorporating SCFAs into the diet has no effect on food intake in rodents and humans (Darzi et al., 2012, De Vadder et al., 2014). A possible explanation is that some oral SCFAs are absorbed from the upper GI tract and thus may not reach the gut lumen where the intestinal receptors are more densely populated (Chambers et al., 2018a). This is supported by several studies that reported that SCFAs can be absorbed in the stomach and small intestine (Schmitt Jr et al., 1976, Schmitt et al., 1977, Saunders, 1991). Interestingly, a disparity was found between intragastric and intravenous administration of SCFAs. The

intragastric administration of butyrate resulted in a reduction in energy intake while the intravenous administration failed to do so (Li et al., 2018b). This emphasises the importance of gut physiology, as the site and rate of SCFA production in the gut could be critical to the physiological consequences.

(2) Colonic delivered propionate

Targeted delivery of SCFAs to the distal gut has been found to promisingly reduce energy intake. The mechanism has not been yet fully understood, while the anorectic gut hormones releases are thought to be involved. A novel system, inulin-propionate ester (IPE) to deliver propionate to the colon has been recently developed (Polyviou et al., 2016). The acute administration of inulin-propionate ester significantly increased postprandial plasma PYY and GLP-1 and reduced ~14% energy intake in 7 hr at a buffet meal. A 24-week supplementation of inulin-propionate ester reduced weight gain in overweight adults (Chambers et al., 2015b). However, when IPE was added to food products, it reduced *ad libitum* food intake independent of changes in plasma PYY and GLP-1 (Byrne et al., 2019c). The same team found that IPE reduced appetite via slowing reaction time to higher energy foods without changing plasma PYY and GLP-1 (Byrne et al., 2016). The underlying mechanism seems to be multi-factorial and needs to be further investigated.

(3) Non-digestible carbohydrate (NDCs) intake

Growing evidence suggests that NDCs and their fermentation products SCFAs can affect energy homeostasis. Large cohort studies have shown that the intake of dietary fibre and wholegrain is inversely associated with body weight or BMI (Ludwig et al., 1999, Koh-Banerjee et al., 2004, Newby et al., 2007). Animal studies suggested that fibre added to a high-fat diet could decrease energy intake and prevent weight gain (So et al., 2007) (Arora et al., 2012). The mechanisms underlying these observations mainly focused on pathways mediated by PYY

and GLP-1 (Cani et al., 2004). Besides, Frost et al. demonstrated that SCFA acetate can have a direct role in the central appetite regulation (Frost et al., 2014).

When this is applied to human intervention, however, findings have shown inconsistency. Several interventions of NDCs increased appetite-regulating hormones (Johansson et al., 2013, Sandberg et al., 2017), decreased hunger (Willis et al., 2009, Johansson et al., 2013, Sandberg et al., 2017) and energy intake (Bodinham et al., 2010, Johansson et al., 2013), while other studies found no significant effects (Emilien et al., 2017, Al-Mana and Robertson, 2018). The disparity between human and animal studies may be due to the small amount of NDCs in human experimental diets compared to animal studies (1.5% vs. 5% of total energy intake) (Byrne et al., 2015). This is supported by a recent meta-analysis, which has investigated the effects of RS on appetite and observed very high heterogeneity. In the studies that used RS dose >= 25g/d, heterogeneity disappeared and a significant reduction in appetite was observed (Amini et al., 2021). Similarly, it is suggested that a habitual fibre intake in the range of 16-35 g/d (5-10% dry matter intake) is necessary to induce its appetite-suppressing effects (Morrison and Preston, 2016). Clearly, a feasible strategy to increase NDC contents in the human diet is needed.

1.6.8 Interplay between carbohydrate food structure, gut fermentation, and appetite

Carbohydrate food structure has been suggested to affect appetite regulation. A mechanism has been proposed (**Figure 1.8)**, emphasizing the central role of the structural integrity of cell walls. Plant cell walls are the main source of dietary fibre, the non-starch polysaccharides that are indigestible by human enzymes but susceptible to bacterial enzymes (Flint et al., 2012).

The components of cell walls (dietary fibre) per se provide a proportion of substrate for fermentation (Williams et al., 2017); moreover, cell walls control the digestion of intracellular nutrients and thus affect the availability of nutrients that can reach the distal gut for fermentation (Dagbasi et al., 2020b). These can subsequently affect appetite signals through the regulation of SCFAs (Byrne et al., 2015, Chambers et al., 2015a).

This hypothesis has been supported by several *in vitro* digestion studies. Starch within intact cells exhibited much lower digestibility than those within broken cells and isolated pure starch (Rovalino-Cordova et al., 2018, Dhital et al., 2016), indicating RS1 contents may be preserved. Fermentation is still largely unexplored but there is evidence that cell integrity can modulate rates and regions of fermentation, microbiota composition, and production of metabolites (Rovalino-Cordova et al., 2021, Rovalino-Córdova et al., 2020, Bhattarai et al., 2021). Intact-cell kidney bean flour containing high RS1 content promoted SCFAs (butyric acid) production in the distal colon of rats (Henningsson et al., 2001).

Evidence direct from human subjects is scarce. Intact cells could increase entrapped nutrients to the distal gut, but the subsequent effects on appetite remained unclear. Edwards *et al.* collected ileal effluents from healthy ileostomy patients and observed a small proportion of starch entrapped by intact wheat cells in ileal fluids. However, the levels of GLP-1 and PYY were not significantly elevated, which may be due to the lack of colonic function in ileostomy patients (Edwards et al., 2015a). A recent study has provided direct evidence that food structure can influence bacterial fermentation in human subjects (Petropoulou et al., 2020). Small intestinal fluid was collected from healthy human subjects using a nasoduodenal tube after the consumption of two genotypes of peas. Compared to RR wild type peas, rr mutant

peas were more resistant to digestion and preserved more intact cells in the duodenum. This led to more nutrients delivered to the colon for fermentation, as evidenced by the increased levels of ^{13}C SCFAs in urine samples following the consumption of rr peas. However, how this affected appetite was not measured in this study (Petropoulou et al., 2020).

To date, scientific evidence linking food structure, gut fermentation and appetite regulation is still lacking. The hypothesis that food structure can influence the levels of intestinal fermentation rests on the findings that cell wall structure can stay relatively intact in the upper GI tract, which has been supported by several *in vitro* digestion studies and clinical trials on ileostomy patients. However, a complete human digestive system is a more dynamic environment and involves complex physiological feedback, which cannot be represented in these models. There are several questions that remain to be answered. Firstly, how cell wall matrices interact with different sites of the GI tract (e.g., the mastication, gastric grinding, and intestinal passage) and secondly, how much of the intracellular contents can arrive in the large intestine and be utilized for fermentation. Studies on healthy human subjects with direct measurements of gut contents are crucially needed to fill the research gap.

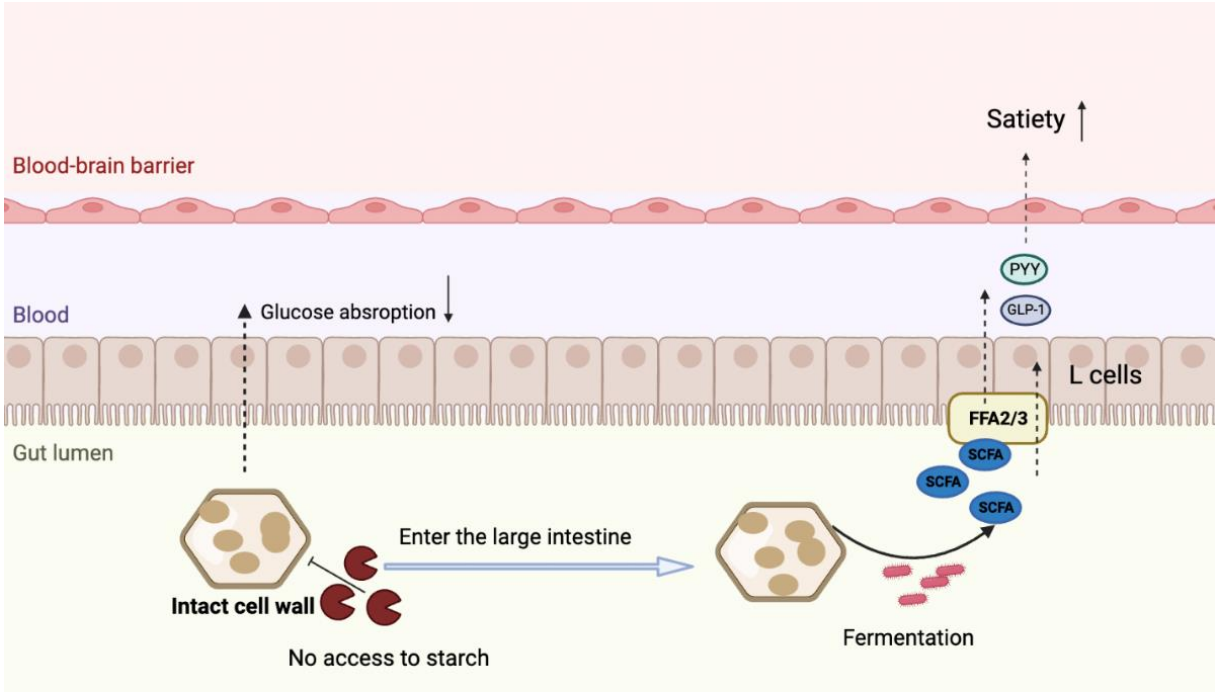


Figure 1. 8 A diagram to explain the interplay between food structure, gut fermentation, and appetite regulation.

1.7 Food structure as a tool to lower postprandial glycaemia and suppress appetite

1.7.1 Food strategy to modulate starch digestion

The literature so far has supported the primary role of starch digestion on metabolic outcomes. The rate and extent of starch digestion in the small intestine determines the glycaemic index (GI) of starchy foods. Starchy foods with a large proportion of rapidly digestible starch (RDS) are associated with a high GI and increase the risk of T2D. Slowly digestible starch (SDS) and resistant starch (RS) have been linked to many metabolic benefits, such as low glycaemic and insulinaemic response and prolonged appetite (Aller et al., 2011). RS, as a major substrate for bacterial fermentation, promotes the production of SCFAs and may benefit both glycaemic and energy homeostasis (Birt et al., 2013, Byrne et al., 2015).

Developing methods to increase SDS and RS contents while decreasing RDS contents has become a growing interest of food industry and research in this area.

Tian *et al.* have proposed two mechanisms to modulate starch digestion: one is to alter the activity of digestive enzymes, which may be less feasible in humans; the other is to hinder the enzyme molecules in contact with starch. The latter has been massively studied, and importantly, the relationship between starch digestibility and its structure has been demonstrated (Tian et al., 2019a). As discussed in Section 1.6.3, several ways to control starch digestion through structural changes at different levels have been demonstrated. Importantly, the control of starch encapsulation by cell wall structure may have the promise to slow down or/and resist starch digestion in the human small intestine.

1.7.2 Cell walls to slow down starch digestion

Intact cell walls separated from plant tissue have been extensively studied in this area. A large number of *in vitro* studies have been done on various foods such as wheat, pea, chickpea, bean, and almond. They have suggested that compared to foods that undergo mechanical processing which caused cell wall ruptures, foods that preserve intact cells had slower rates of digestion of cell contents (Dhital et al., 2016, Grundy et al., 2016a, Han et al., 2008). This has been supported by several human studies. Oatmeal in larger particle size induced a sustained glycaemic response likely attributed to a slower rate of glucose absorption in the upper GI (Mackie et al., 2017b). Coarse wheat porridge slowed down starch digestion as observed in the ileum effluent and lowered glycaemic response than smooth wheat porridge (Edwards et al., 2015a). Whole peas that maintained intact cell walls in the human small

intestine led to slower starch digestion and lower postprandial glycaemia compared to pea flours in which cell walls were disrupted (Petropoulou et al., 2020).

1.7.3 Cell walls to increase type 1 RS amount

The entrapment of starch within intact cell walls provides a possible way to increase type 1 RS. However, this requires their capacity to resist the mechanical regime in the human upper GI tract. Some legume cotyledon cells appear to own this capacity. Peas, chickpeas, mung beans, and red kidney beans, for instance, showed a dramatical decrease in amylase hydrolysis in the form of intact cells compared to broken cells (2-3% vs. 45-50%) (Bhattarai et al., 2017). Similar results were observed in other studies on the same group of legumes (Dhital et al., 2016). Common beans, however, seemed to behave differently: the intact cells reduced the rate but not the extent of starch digestion compared to disrupted cells. After 360 minutes of digestion, comparable hydrolysis was achieved by damaged and intact cell walls. This could be due to the permeability of the cell walls which were insufficient to resist the digestion (Rovalino-Cordova et al., 2018). Altogether the evidence supports the notion that plant foods with certain properties of cell walls (e.g., low permeability) can be tools for increasing RS1 content. However, future investigation is needed to understand their relative integrity during the human GI tract.

Recent work from our research group has brought our attention to cell clusters, which may serve a tool to deliver more RS to the distal gut. Petropoulou *et al.* compared two genetic types of peas and found their distinct structural profiles in the small intestine (Petropoulou, 2019a). As shown in **Figure 1.9**, the cell walls of RR and rr pea both remained relatively intact.

However, the RR pea cells showed a degree of separation, whereas the rr pea cells stuck together to form a cluster. The rr pea was shown to have more starch escaping the small intestinal digestion and reaching the large intestine, leading to elevated levels of SCFAs production and improved glycaemic homeostasis (Petropoulou et al., 2020).

Digestion behaviours of cell clusters have not been studied as widely as isolated intact cells, and the physiological mechanisms have not been understood. “Cell clusters” is sometimes referred as “macroparticles” (Edwards et al., 2021); and from a macrostructural scale, particle size of plant tissue is inversely related to digestion rates (Al-Rabadi et al., 2009, Edwards et al., 2015b, Cassady et al., 2009). Large particles decrease the surface area per weight that allow the enzyme diffusion, which may explain their limited digestibility (Capuano, 2017b). Large and compact cell clusters reduced the release of cellular contents (Netzel et al., 2011), delayed the diffusion of digestive enzymes into the cells (Zahir et al., 2020), and affected the final amount of starch digestion (Edwards et al., 2021). These evidence support the possible impact of cell clusters on the glycaemic response and the amount of RS delivered to the distal intestine, pending validation in clinical trials.

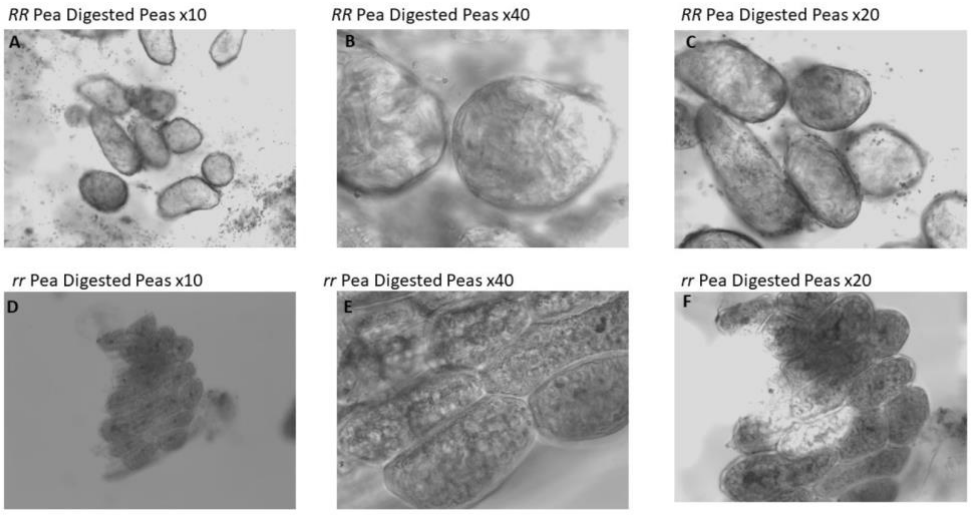


Figure 1. 9 The microscopic images of pea single cells and clusters present in duodenal fluids from healthy subjects. Pea single cells (A-C) and cell clusters (D-F). Adapted from (Petropoulou, 2019a)

1.7.4 Chickpea as the model

As above, the majority of evidence that the cell wall integrity can delay or/and limit starch digestion is from legumes. Indeed, legumes especially chickpeas have thicker and less permeable cell walls and are more resistant to mechanical damage during processing and digestion (Edwards et al., 2015b). The particle size of chickpea tissue was inversely associated with the digestibility of starch, suggesting the intactness of tissue (cell walls) is the key determinant of its digestion (Edwards et al., 2014b). This implied that chickpea cell walls may provide an effective barrier between enzymes and intracellular starch.

The properties of the chickpea cell wall establish the basis on which it can be designed to provide effective SDS and RS sources in humans. As described in section 1.5.3.5, chickpeas

have type 1 cell walls in which the middle lamella is held together largely by non-covalent cross-linked pectic polysaccharides. Cell separation rather than cell damage (from type 2 cell wall) occurs as a result of solubilization and /or heat-catalysed depolymerization of pectin in the middle lamella of contiguous cells during certain processing (Xiong et al., 2022a). A very recent structure-function study demonstrated contrasting digestive behaviours of wheat and chickpea. Hydrothermal processing led to cell damage in wheat tissue while causing cell separation in chickpea tissue. Unlike wheat, chickpea tissue was separated into individual cells with intact cell walls so access to intracellular starch was impeded. A dynamic gastric model (DGM) adding a mechanical effect enhanced the starch digestion in wheat but not chickpea tissue. Notably, this DGM was employed to provide a physiologically relevant stimulation of the human condition (Edwards et al., 2021). The same team have developed PulseOn, a new ingredient made from chickpeas using a unique milling method that preserved cellular structure and increased type 1 RS amount. The results showed that replacing wheat flour with PulseON resulted in a 40% reduced blood glucose response (Bajka et al., 2021).

1.8 Thesis summary and rationale

This thesis aims to determine the impact of carbohydrate food structure on gastrointestinal digestion, postprandial glucose metabolism and appetite regulation. Chickpea is used as the food model due to its cell wall properties and high potential to provide effective RS for bacterial fermentation. Food processing is performed to achieve three tissue structures:

- Chickpea with disrupted cell walls
- Chickpea with intact cell walls (single cells)
- Chickpea with intact cell walls (cell clusters)

The dietary approach has suggested that increasing dietary fibre and RS in the diet may improve glucose and energy homeostasis. However, questions have been raised as their physiological benefits are largely dependent on the intactness of plant cell walls, which can be difficult to preserve during food processing and/ or digestion. Research in this area has been deficient due to the difficulty of assessing the human gut. The present study uses a unique incubation technique that enables real-time sampling from the human GI tract, allowing direct measurements of starch digestion throughout the gut. It will provide an important understanding of how food structure and processing affect the way starch is digested in the small intestine and transported to the large intestine for fermentation. Moreover, this can inform how plant-based food products should be prepared or processed to achieve their favourable metabolic effect. This is particularly important for the design of food products containing RS and dietary fibre toward lowering the risk of T2D and obesity.

1.9 Thesis hypothesis and aims

It is hypothesized that carbohydrate foods with intact structures would delay starch digestion in the small intestine and increase the amount of RS entering the large intestine. This would reduce postprandial glycaemia and prolong satiety.

The aims of the thesis were

- To systematically review the up-to-date evidence on how carbohydrate food structure affects postprandial glycaemic response and appetite.

- To explore the effect of chickpea tissue structure on gastric and duodenal digestion, and acute postprandial metabolism (0-3h) in human subjects.
- To investigate how chickpea tissue structure affects ileal digestion and postprandial metabolism (0-8h) in human subjects.
- To carry out an integrated study on the role of chickpea tissue structure on digestion throughout the gut and postprandial metabolism.

Chapter 2 Current evidence on how food structure impacts glycaemic response and appetite: systematic review and meta-analysis of randomized crossover trials

2.0 Abstract

This Chapter aimed to understand the available evidence about the effects of food structure on metabolic response in vivo. A systematic search identified 13 randomized crossover trials with 191 healthy subjects. Pooled estimates by meta-analyses suggested that intact cell walls of starchy foods can improve postprandial glycaemic and insulinaemic response in healthy subjects. There was insufficient evidence that food structure affects subjective appetite, PYY, CCK, or GLP-1.

2.1 Introduction

Current literature suggests a beneficial role for intact cell walls in postprandial metabolism. Intact cell walls reduce the rate and extent of starch bioaccessibility, observed by in vitro studies (Grundy et al., 2016b, Dhital et al., 2016, Edwards et al., 2021, Junejo et al., 2021b), would be expected to produce an attenuation in glycaemic and insulinaemic responses in vivo. The resistant starch remaining after stimulated digestion would be available for bacterial fermentation and involved in appetite-regulating pathways (Bhattarai et al., 2017, Edwards et al., 2021, Dagbasi et al., 2020b, Holland et al., 2020).

A number of clinical trials and pilot studies have investigated the role of carbohydrate food structure in postprandial metabolism, while a robust conclusion is still difficult to make. One remaining problem is that a pilot clinical trial usually involves a small sample size (e.g., n=10), which may lead to insufficient statistical power (Wittes, 2002, Whitehead et al., 2016). Therefore, a systematic review with meta-analysis would be useful to estimate the effect of interventions and to make defensible conclusions. The present study is the first to summarize the effect of an intact cell wall structure versus a disrupted cell wall structure on postprandial glycaemia and appetite in healthy subjects from published randomized crossover trials (RCTs). This knowledge can aid in providing effective dietary strategies to reduce the risk of T2D and Obesity.

2.2 Purposes of this study

2.2.1 Hypothesis

Carbohydrate food with an intact cell structure would lead to lower postprandial glucose and prolonged satiety compared to carbohydrate food with a disrupted cell wall structure.

2.2.2 Aims

This study aimed to evaluate current evidence from RCTs and to conduct meta-analysis to estimate whether an intact food structure can significantly influence postprandial glucose and appetite compared to a disrupted food structure.

2.2.3 Outcomes measure

- Postprandial glycaemic and insulinaemic responses

- Appetite-regulating gut hormones (PYY and GLP-1)
- Appetite measurement

2.3. Methods

2.3.1 Eligibility

The PICOS (participants, interventions, comparator, outcome, and study design) criteria was applied to establish eligibility (**Table 2.1**).

Table 2. 1 PICOS criteria for inclusion and exclusion of studies

Parameter	Criteria	Exclusion
Population	Healthy adults	Animals
Intervention	Consumption of starchy foods with intact cell wall structures	/
Comparator	Consumption of starchy foods with disrupted cell wall structures	Unmatched energy or macronutrients intake (difference>10%)
Outcome	Acute post-prandial glycaemic response, gut hormone response and appetite	Studies which do not contain these outcomes of interest
Study design	Randomized crossover trials (RCTs)	Not RCTs

2.3.2 Study search and selection

Systematic search was performed on database PubMed, Embase, Ovid Medicine and google scholar for peer-reviewed articles published up to February 2021. The search strategy is

presented in **Table 2.2**. All articles identified by the strategy were firstly imported to Endnote to eliminate duplicated articles and then assessed by 3 reviewers independently. Articles were first screened for their titles and abstracts, and then for full text to determine their suitability for inclusion. Disagreements were resolved through discussion to reach a consensus.

Table 2. 2 Search Strategy

Databases	**Search Terms**
PubMed	blood glucose[MeSH Terms] OR glycaemic index[MeSH Terms] OR insulin[MeSH Terms] OR C-Peptide[MeSH Terms] OR appetite regulation[MeSH Terms] OR appetite regulating hormone[MeSH Terms] OR Peptide YY[MeSH Terms] OR Glucagon-Like Peptide 1[MeSH Terms] OR energy intake OR satiety response[MeSH Terms] AND (human[MeSH Terms] OR adult[MeSH Terms] OR health, women s[MeSH Terms] OR health, men s[MeSH Terms]) AND (starch[MeSH Terms]) OR carbohydrate[MeSH Terms]) AND 'diet') AND trials, randomized clinical[MeSH Terms].
Ovid Medicine	1. Blood Glucose/ or Glycaemic index/ 2. Insulin/ 3. Energy intake/ 4. Appetite/ or Appetite regulation/ or Satiety/ 5. Gastrointestinal Hormones/ or Glucagon-Like Peptide 1/ or Gastric inhibitory Polypeptide/ or Peptide YY/ 6. 1or 2 or 3 or 4 or 5 7. Starch/ and Diet/ 8. 6 and 7 9. Humans / or Male/ or Female/ or Adult/ 10. 8 and 9

Embase	1. Blood Glucose 2. Blood Insulin level/ 3. Satiety response/ or Satiety/ or Food intake/ or Hunger 4. Appetite/ 5. Gastrointestinal Hormones/ 6. Human/ 7. Adult/ 8. Starch/and Diet/ 9. 1or 2 or 3 or 4 or 5 10. 6 or 7 11. 9 and 10 12. 8 and 11
Google Scholar	"food structure" AND ("glycaemia" OR "glucose" OR "food intake" OR "satiety" or "energy intake" OR "gut hormone") AND "randomized crossover"

2.3.3 Risk of bias assessment

The risk of bias within included articles was assessed by three reviewers independently. The assessment was performed using Cochrane RoB2 tool (Sterne et al., 2019) which identified the level or risk of bias (low risk, some concerns, and high risk) on 5 domains: (1) the randomization process, (2) deviations from intended intervention, (3) missing outcome data, (4) measurement of outcomes, and (5) selection of the reported result. Studies were classified

as overall “low risk” if all domains were judged to be low risk. Studies within at least one domain at “high risk” or at least 3 domains at “some concerns” were classified as overall “high risk”. In any other case, studies were classified to be at overall “some concerns”. Any disagreements between reviewers were revolved through discussion to reach a consensus.

2.3.4 Data extraction

Data was collected from journal articles, trial registrations and individual participant data provided by original authors. Data collection table was designed to extract information including reference (first author and year of publication), study design, participant characteristics (population, gender, age, BMI, sample size), intervention and control (test meals, amount of carbohydrates, and duration of sampling), and outcomes of interest.

Demographic data were extracted as mean ± standard deviation. Postprandial glycoaemic response was reflected as blood glucose and insulin incremental AUC (iAUC). Appetite was measured as subjective appetite score iAUC and appetite regulating hormones iAUC. For studies reporting figures instead of numbers, data was extracted from figures using WebPlotDigitizer (https://automeris.io/WebPlotDigitizer/).

2.3.5 Data analysis

Review Manager version 5.3(the Cochrane Collaboration, Software Update, Oxford, UK) was used to perform random effect model meta-analyses. Standard mean differences (SMDs) with 95% confidence intervals (CIs) for iAUC of postprandial glucose, insulin, gut hormones, and

satiety score were calculated. Significant heterogeneity was defined as having I^2 value greater than 50%. A p value of < 0.05 was thought to be statistically significant.

2.4 Results

2.4.1 Study characteristics

The search strategy identified 745 articles in total. Of which, 522 remained after eliminating duplicates. 474 of these articles were not relevant to the topic and were disqualified in the initial screening. Of the remaining 48 articles, 25 were excluded because they included unhealthy subjects (n=3), had mismatched macronutrient consumption (n=7), did not report nutritional profile (n=7), or did not have an RCT design (n=6). A total of 25 studies were eligible, while 13 studies relevant to cell wall structure were included in this thesis Chapter (Anguah et al., 2014, Clegg et al., 2013, O'Donnell et al., 1989, Edwards et al., 2015a, Eelderink et al., 2017, Holt and Miller, 1994, Jenkins et al., 1982, Johansson et al., 2015, Mackie et al., 2017a, Ranawana et al., 2014, Read et al., 1986, Zhu et al., 2013b, Petropoulou et al., 2020). Outcomes of studies investigating molecular structure and starch structure were published elsewhere (Cai et al., 2021). The search and review process were presented in **Figure 2.1**.

A total of 161 participants, aged from 18 to 70 years, were included in the 13 eligible studies. Mean participant BMI ranged from 20.2 to 28.8 kg/m^2. The year of published articles ranged from 1983 to 2020. Details of study characteristics were presented in **Table 2.3**.

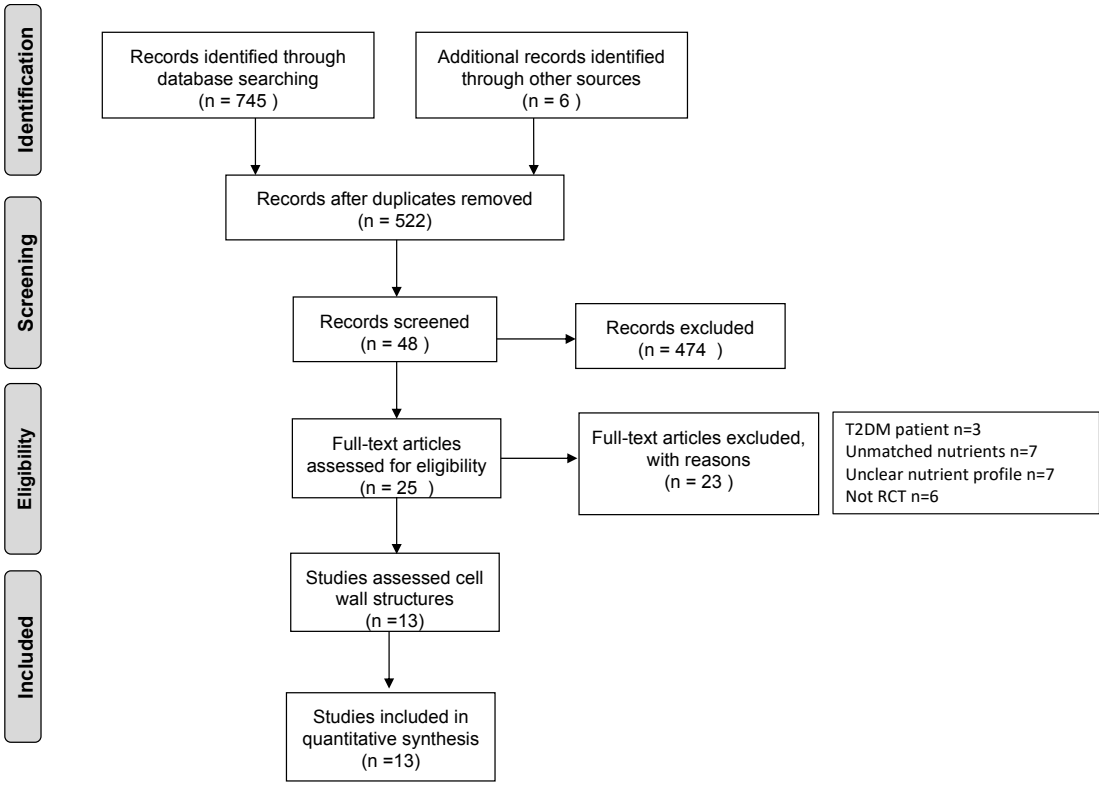


Figure 2. 1 The diagram of literature search and screening process.

Table 2. 3 Study characteristics of included studies (n=13)

Reference	Study Design	Participants (Health status, No. of Participants, Sex, BMI, Age)	Intervention vs. control	Outcomes
Anguah et al 2014 (Anguah et al., 2014)	RCT Double-Blinded	Healthy 4M+8F 23.3 ± 3.1 kg/m2 28± 10 y	CHO 50g whole lentil vs. blended lentil	Glucose ↔ Subjective satiety ↔
Clegg et al 2013(Clegg et al., 2013)	RCT Non-blinded	Healthy 6M+6F M:23.5± 2.9kg/m2 F: 22.1± 2.8kg/m2 M+F: 28.7± 5.9 y	CHO 34g Mixed meal of rice, chicken, carrots, peas, onion, mushroom and celery. Solid mixed meal vs. chunky mixed meal (semi- blended) vs. smooth mixed meal (blended).	solid vs liquid Glucose ↓ Subjective satiety ↓ chunky vs liquid Glucose ↓ Subjective satiety ↔
Donnell et al 1989 (O'Donnell et al., 1989)	RCT BNR	Healthy ileostomy 4M+5F Normal BMI Age 30-69yr	CHO=52.4g Scone made by coarse flour vs. scone made by fine flour	Glucose ↓ Insulin ↓
Edwards et al 2015 (Edwards et al., 2015a)	RCT Single-blinded	Healthy ileostomy 2M+7F 23.9 ± 3.9 kg/m2 47.8 ± 18.0 y	CHO 57.8g Wheat porridge Coarse (>2mm) vs. smooth (<0.2mm)	Glucose ↓ Insulin ↓ GIP ↓ GLP-1 ↔
Eelderink et al 2017 (Eelderink et al., 2017)	RCT BNR	Healthy 10M 22 ± 0.2 kg/m2 24 ± 0.6 y	CHO 50g wheat bread with large particles vs. wheat bread with small particles	Glucose ↔ Insulin ↓ Subjective satiety ↔ GLP-1 ↓ GIP ↔ CCK ↔

Holt et al 1994 (Holt and Miller, 1994)	RCT BNR	Healthy 5M+5F 23.1 ± 0.5 kg/m2 22.3 ± 0.8 y	CHO 57.6g grains served at four degree of milling: whole grain, crack grain (combined as large particles group) vs. coarse flour + fine flour(combined as small particles group).	Glucose ↓ Insulin ↓ Subjective satiety ↑
Jenkins et al 1983 a (Jenkins et al., 1982)	RCT BNR	Healthy 2M+6F 94±5% desirable weight, 29±8 y	CHO 50g whole lentil vs blended lentil	Glucose ↓
Johansson et al 2015(Johansson et al., 2015)	RCT BNR	Healthy 7M+16F 22.8 ± 1.1 kg/m2 59.1 ± 14.7 y	CHO 50g fermented whole grain rye crisp bread vs. unfermented whole grain rye crisp bread	Glucose ↓ Insulin ↓ Subjective satiety ↔
Mackie et al 2017 (Mackie et al., 2017b)	RCT BNR	Healthy 8M 22 ± 0.2 kg/m2 24 ± 0.6 y	CHO 50g Wheat bread with large particles vs. wheat bread with small particles	Glucose↓ Insulin ↓ Subjective satiety ↔ GLP-1 ↓ GIP ↔ CCK ↔
Petropoulou et al 2020 b (Petropoulou et al., 2020)	RCT Double-blinded	Healthy 12 Normal BMI 18-65y	CHO 50g whole peas vs. pea flours	Glucose ↓ Insulin ↓ GIP↓ GLP-1↔
Ranawana et al 2014 (Ranawana et al., 2014)	RCT Non-blinded	Healthy 8M+7F 20.5±4kg/m2 26±6y	CHO 50g rice with15 chews vs. with 30 chews	Glucose ↓

Read et al 1986 (Read et al., 1986)	RCT BNR	Healthy 4M+8F Normal BMI Age 18-2y	CHO=50 Apple, rice, potato and sweetcorn no chews vs. throughout chews	Glucose ↓
Zhu et al 2013 (Zhu et al., 2013a)	RCT BNR	Healthy 21M 24.8±0.6 kg/m2 24± 1 y	CHO 51g pizza 15 chews vs. 40 chews	Glucose ↔ Insulin ↔ GIP ↔ CCK ↔ Ghrelin ↔ Subjective satiety ↔ Energy intake ↔

BNR, blinding not reported, CCK, Cholecystokinin, GIP, gastric inhibitory peptide, GLP-1,Glucagon-like peptide-1,iAUC, incremental AUC; PYY, Peptide YY , RCT, randomized crossover trial, ↔ no significant difference in iAUC between the intervention and control groups, ↓ the iAUC for intervention group is significantly smaller than control group↑ the iAUC for intervention group is significantly bigger than control group.

2.4.2 Risk of bias (RoB) in included studies

After the RoB analysis, 53.8% of included studies had some concern and 46.2% had a low RoB (**Figure 2.2**). The main concerns were arising from the missing output data and ROB due to deviations from the intended intervention.

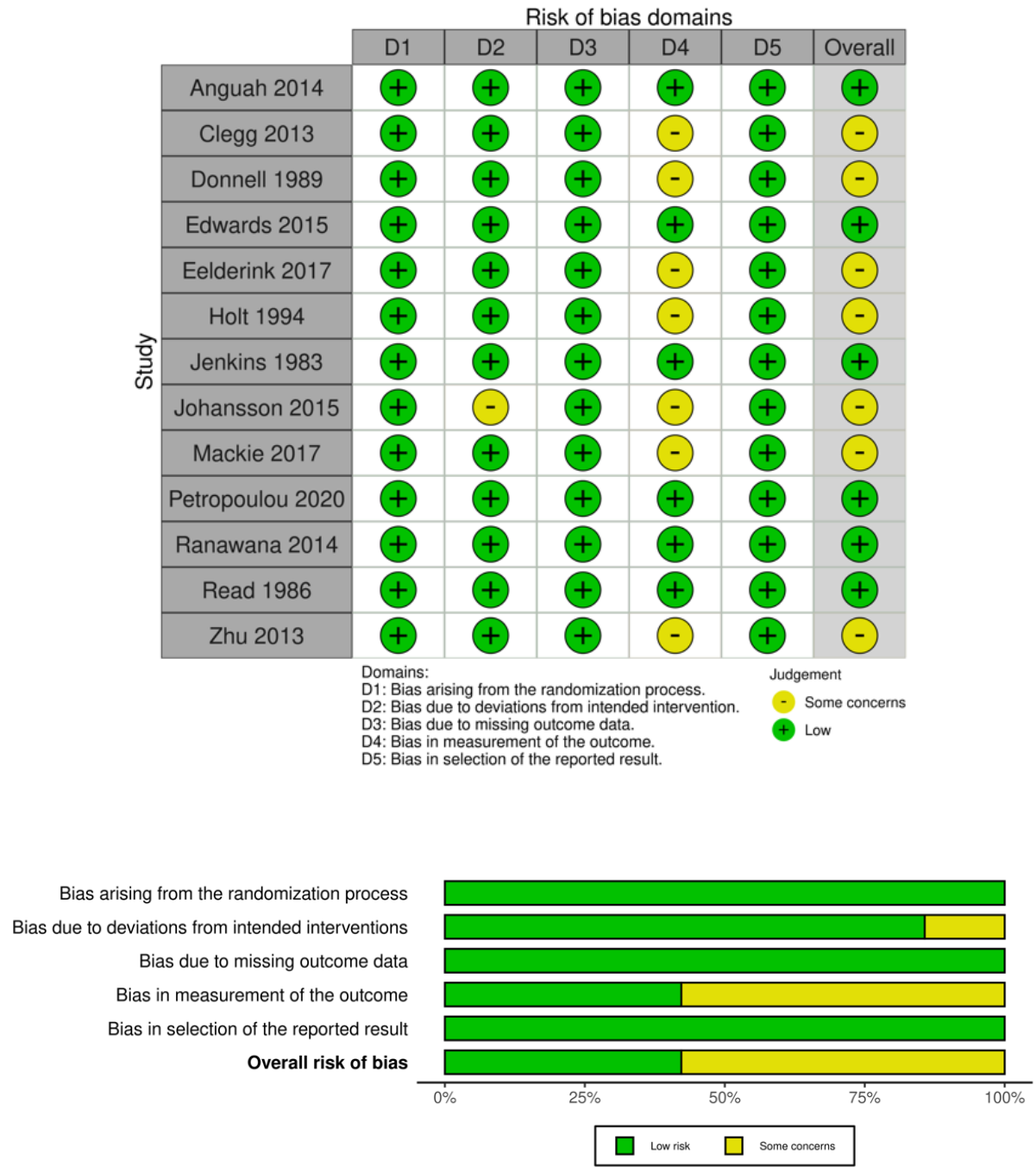


Figure 2. 2 The risk of bias (RoB) in included studies.

2.4.3 Summary of outcomes: glucose and insulin iAUC

Twelve studies examined the effect of intact cell wall structure on glycaemic response in healthy subjects (**Figure 2.3A**). These studies manipulated cell wall structures either by

industrial processing or mastication. An intact cell wall structure was defined as starchy foods having a low degree of milling/ grinding process or bearing less chewing, while the disrupted cell wall was defined in the opposite manner. The meta-analysis (n=192) found that intact cell wall structure resulted in a decreased glucose iAUC (-0.43 mmol/L*min, 95% CI -0.58, -0.28, p<0.001) with a minimal heterogeneity (I^2=1%, p=0.50).

Seven studies evaluated the effects of intact food structure on postprandial insulin iAUC (**Figure 2.3B**). A meta-analysis including 103 subjects showed that intact food structure significantly reduced the insulin iAUC (SMD=-0.63 pmol/L*min, 95% CI -0.86, -0.40, P<0.001). The I^2 statistics suggested insignificant heterogeneity between studies (I^2=33%, p=0.18).

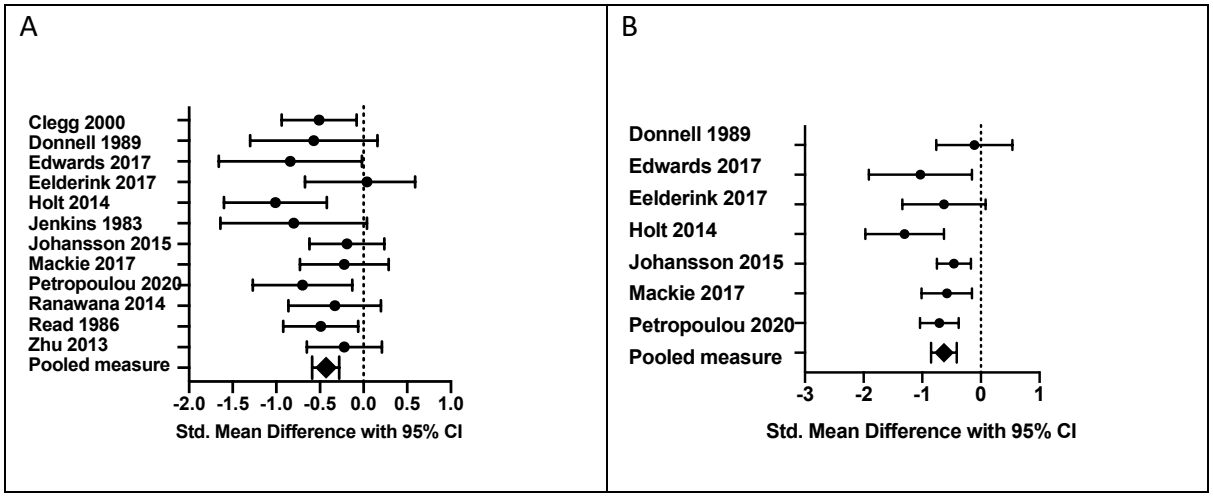


Figure 2. 3 Effects of Intact cell wall structure on (A) postprandial glucose iAUC (mmol/L*min) and (B) insulin iAUC (pmol/L*min) in healthy subjects. Horizontal lines represent 95% CIs. The diamond represents the pooled estimate calculated by the generic inverse-variance method with a random effects model. iAUC, incremental AUC.

2.4.4 Summary of outcomes: satiety scores iAUC

The study identified six RCTs that investigated the effect of intact cell wall structure on satiety score iAUC (mm*min) in healthy subjects (**Figure 2.4**). A meta-analysis (n=98) suggested that there was no significant difference between intact and disrupted cell wall structure (SMD=0.02mm*min; 95% CI -0.19, 0.24, P=0.83). The heterogeneity between these studies was insignificant (I^2=15%, P=0.32).

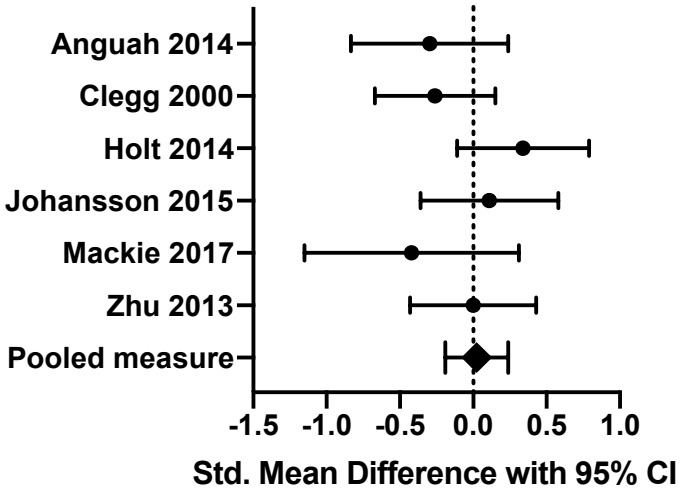


Figure 2. 4 Effects of intact cell wall structures on subjective satiety score (iAUC mm*min) in healthy subjects. Horizontal lines represent 95% CIs. The diamond represents the pooled estimate determined using the generic inverse-variance method with a random effects model. iAUC, incremental AUC.

2.4.5 Summary of outcomes: gut hormones iAUC

Five studies investigated the role of intact cell wall structure in the response of gut hormones including GLP-1, PYY, GIP, and CCK. Four studies measured the GLP-1 iAUC in response to intact or disrupted cell wall structure, and the meta-analysis found no significant difference

between two groups (SMD =-0.25 pmol/L*min, 95% CI -0.85, 0.35, p=0.41) (**Figure 2.5A**). Heterogeneity between studies was significant indicated by I^2 of 65% (p=0.03).

Two studies including 15 participants investigated the PYY response to intact verses disrupted cell wall structure (**Figure 2.5B**). The meta-analysis found no difference between intervention and control groups (SMD=0.09 pmol/L*min, -0.49, 0.66, P=0.77). Heterogeneity was minimal (I^2=0%, P=0.77)

Five studies including 71 subjects investigated the GIP iAUC response (**Figure 2.5C**), and their meta-analysis suggested a significant effect of intact cell wall structure on lowering GIP iAUC (SMD =-0.56 pmol/L*min, CI -1.06, -0.06, p=0.03). Heterogeneity between studies was moderate (I^2=43%, P=0.14).

Two studies including 31 subjects evaluated the effects of intact cell wall structures on CCK iAUC response (**Figure 2.5D**). The meta-analysis found no difference between intact and disrupted cell wall structures (SM-0.14 pmol/L*min, 95% CI -0.49, 0.22, P=0.45). Heterogeneity between two studies was minimal (I^2=0%, P=0.59).

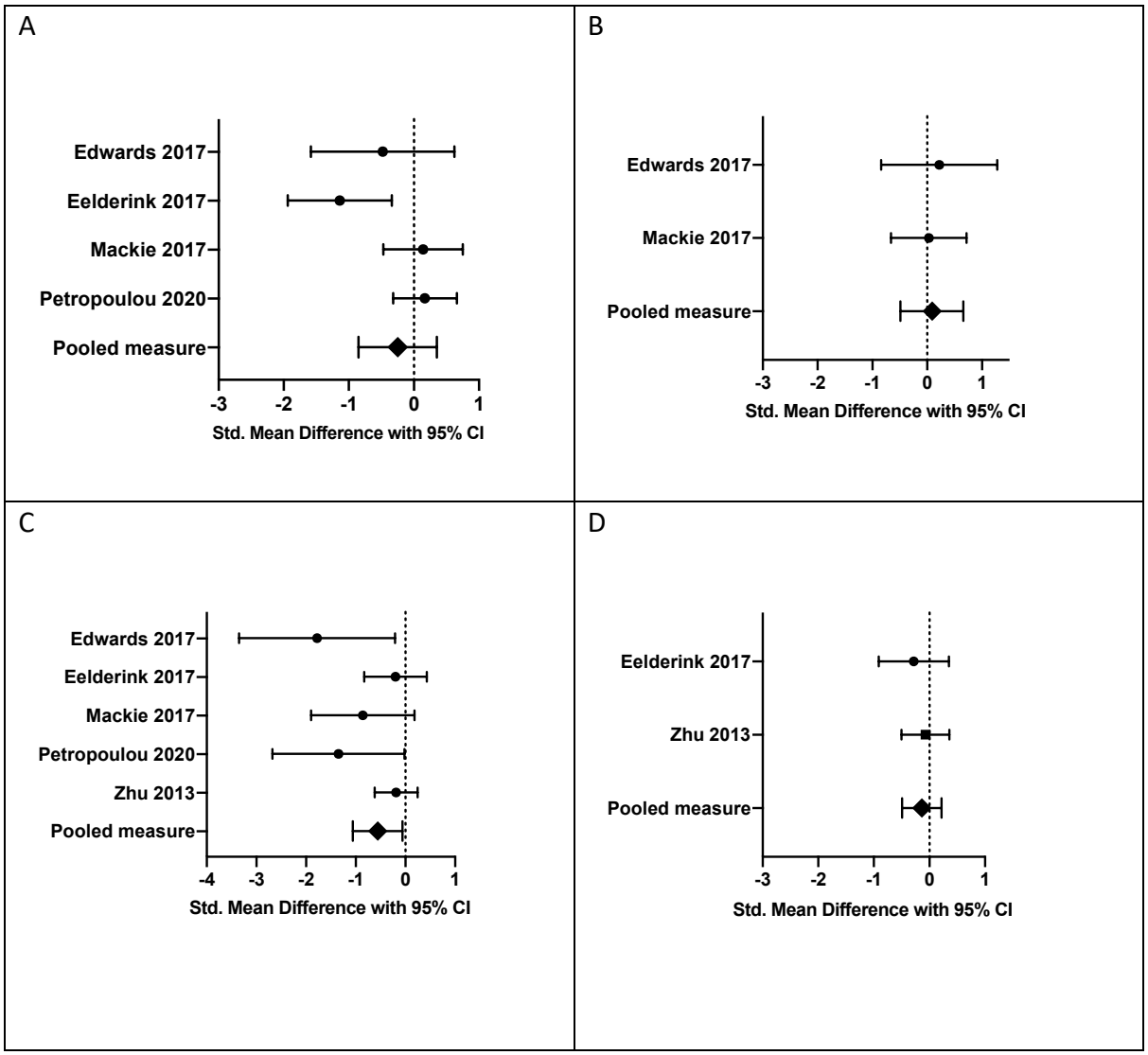


Figure 2. 5 Effects of intact cell wall structures on (A) GLP-1 response (iAUC pmol/L*min), (B) PYY response (iAUC pmol/L*min), (C) GIP response (iAUC pmol/L*min), and (D) CCK response (iAUC pmol/L*min) in healthy subjects. Horizontal lines represent 95% CIs. The diamond represents the pooled estimate determined using the generic inverse-variance method with a random effects model. CCK, Cholecystokinin; GIP, gastric inhibitory peptide; GLP-1, Glucagon-like peptide-1; iAUC, incremental AUC; PYY, Peptide tyrosine–tyrosine.

2.5 Discussion

The present study has systematically reviewed the current evidence in peer reviewed journals about the effects of carbohydrate food structure on glycaemic control and appetite in human subjects.

2.5.1 Overall summary

This study included 13 RCTs and 191 healthy subjects. The meta-analyses suggested that intact cell wall structures of starchy foods reduced postprandial glucose, insulin, and GIP response. Postprandial levels of appetite-regulating hormones GLP-1, PYY and CCK and subjective appetite were not changed by food structure interventions. The summarized outcomes of appetite were from a small number of studies measured over a relatively short period. This needs further validation by a larger cohort with primary outcomes on appetite measurements over a longer time.

2.5.2 Food structure and glucose and insulin response

It is well established that the rate of starch digestion determines postprandial glycaemia. In vitro studies have revealed that intact food structure can delay the rate of starch (Magallanes-Cruz et al., 2017, Pellegrini et al., 2020). For some starchy foods e.g., legumes, cell wall structures control the rate-limiting step of digestion which is the amylase accessing the intracellular starch (Dhital et al., 2016). However, there is limited evidence as to whether the structural changes would be enough to predict an attenuated blood glucose and insulin response *in vivo*. This study provided the first evidence at a systematic review level,

suggesting that intact cell wall structures significantly reduced the magnitudes of glucose, insulin and GIP iAUC postprandially compared to a disrupted cell wall. Intact cell wall structures may cause slow or less glucose production and absorption in the small intestine, causing a reduction in GIP synthesis by K cells and subsequently inhibiting insulin secretion. The results supported the role of food structure in acute glycaemic control in healthy subjects.

2.5.3 Food structure and appetite regulation

It is hypothesized that food structure can influence the amount of nutrients that arrive in the distal gut. As a result, it can affect the levels of intestinal fermentation and gut signals for appetite regulation (Dagbasi et al., 2020b). This study, however, did not seem to support the hypothesis. Intact food structure did not significantly change the subjective appetite scores, CCK, PYY, or GLP-1 in an acute period. The results need to be interpreted with caution, as they were summarized from small sample size trials, some of which assessed appetite but not as the primary outcome. Moreover, the investigation time of included trials was relatively short (2-3 hours) and may not be sufficient to measure the effects of fermentation. Previously, a medium oro-caecal transit time for indigestible, fermentable carbohydrates (inulin and lactulose) was 5 hours measured by breath tests (Schneider et al., 2007). A mean transit time of 6.4 hours was needed for coarse wheat porridge to arrive at terminal ileal effluent in ileostomy patients (Edwards et al., 2015a). Overall, there is currently no sufficient evidence to suggest that food structure can influence appetite and its related hormones. Longer periods of time in future studies would be needed.

2.5.4 Limitations

This study has some limitations. Firstly, the conclusion is based on a small size of studies which may cause low-powered analyses. Furthermore, the number of studies included did not allow for sub-group analysis, for instance, based on participant characteristics, intervention duration, or starchy food types. The sub-group analysis for starchy food types could be important, as type 1 and type 2 cell walls may have contrasting digestion properties and cannot represent the other (Edwards et al., 2021). This study searched and included published data only, which may overestimate the actual magnitude of an effect. Studies report significant effects tend to be published more frequently than those do not (Simundic, 2013).

2.5.5 Future direction

Research gaps remain in existing studies and suggest potential future research. First, the design and identification of food structures should be reported in future studies. Current definitions of food structure have mainly relied on the degree of processing or mastication, however, to what extent these influenced the cell wall or tissue structure was unclear. In fact, some cell walls can be resistant to food processing and stay relatively intact (Do et al., 2019). Measurement of food structure, beyond processing, would add accuracy to interpreting the outcomes. Secondly, the mechanisms by which food structure affects postprandial glycaemia have not been fully understood. The present study found that GIP response was significantly lower in the intact cell wall group, suggesting that intact cell wall can slow down the digestive kinetics and glucose absorption in the small intestine. A broad range of literature has suggested more mechanisms and pathways may be involved. Gastric emptying may play a

role in postprandial glycaemia and can be influenced by food structure (Liu et al., 2021). Moreover, cell wall structures were suggested to influence the efficient amount of dietary fibre and resistant starch that can be delivered to the distal gut (Grundy et al., 2016b, Holland et al., 2020). Overall, the benefits of their effects on glycaemia may result from a complex gut-derived metabolism. Lastly, this review found a limited number of human studies which suggested a non-significant effect on appetite regulation. As mentioned, one of the concerns is that the period of investigation time of included RCTs may be shorter than what it took for food to arrive in the lower part of the gut (Edwards et al., 2015a). Future study design should consider a longer investigation time to capture the effect on fermentation and appetite-regulating signals.

2.5.6 Overall conclusion

In conclusion, manipulating cell wall structures of starchy food provided an effective method to improve glycaemic control in healthy subjects. The mechanisms underpinning these effects are not fully understood and future research should uncover their digestive behaviours in the gut. In addition, there is a need to conduct well-designed investigations over a longer period to validate their role in intestinal fermentation and appetite regulation signals. This Chapter aids with the designing of clinical trials in Chapters 3-5.

Chapter 3 Experimental methods for human studies

3.0 Abstract

Previous Chapters have highlighted the importance of carbohydrate digestion and fermentation within the gut to glycaemic and appetite control. Current techniques, however, are incapable of characterising the gut signalling that mediates these effects. This research involved the design of a study protocol for a randomised crossover trial evaluating the effects of food structure on gut content throughout the GI tract and postprandial responses in healthy subjects, measuring the following outcomes:

- Glycaemic and hormonal profile of blood samples
- Metabolomic profile of gastric, duodenal, and ileal samples
- Carbohydrate concentrations in gastric, duodenal, and ileal samples
- Structural changes occurring in the cell walls of gastric, duodenal, and ileal samples
- Subjective appetite measurements and *ad libitum* food intake
- Breath hydrogen concentrations

3.1 Overview

This research project used several state-of-the-art experimental techniques for collecting, processing, and analysing human samples to provide insights into the physiological effects of carbohydrate food structures on digestion and metabolism. A two-phase, double-blinded, randomized crossover trial was designed and performed on healthy subjects. The first phase

investigated chickpea tissue structure on gastric and duodenal digestion and acute metabolism; the second phase further investigated their effects after 3-day consumption on ileum digestion and metabolism with a focus on appetite regulation. This Chapter will discuss the overall design, and experimental methods used for human studies.

3.2 Human study methodology

3.2.1 Study Approval

This trial was reviewed and approved by the Health Research Authority and London-Camden and King's Cross Research Ethics Committee (REC 19/LO/0962). All the participants received a participants information sheet (PIS) (Appendix 1) and signed informed consent (Appendix 2) before they started the clinical trial. The Principal Investigator maintained participant confidentiality and is registered under the Data Protection Act of 2018. The clinical trial has been registered with the ISRCTN (https://www.isrctn.com/ISRCTN18097249).

3.2.2 Study Design

This study contains one screening and four main study visits (**Figure 3.1**). Study visit 1 was a 4-day inpatient visit; study visit 2,3,4 was a 3-day inpatient visit. A minimum wash-out period of 7 days was required between each main visit to avoid cross-over effects.

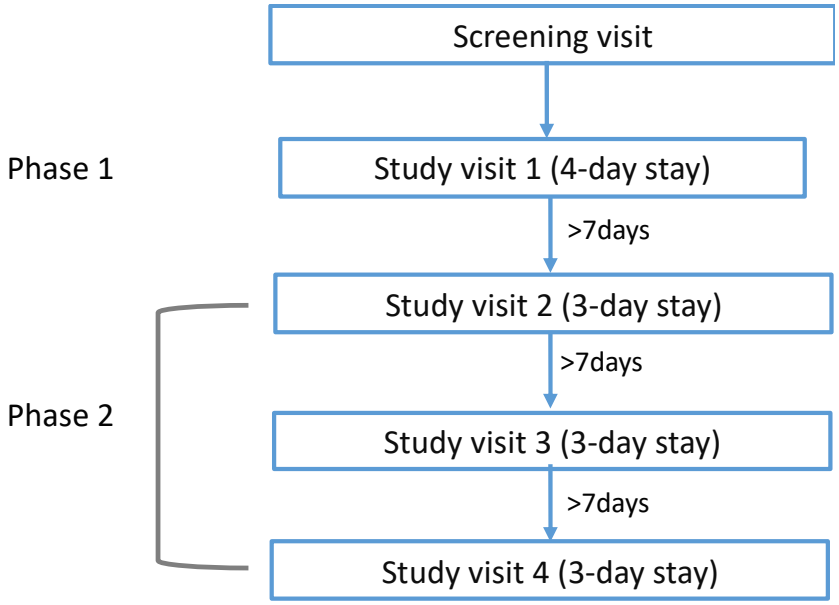


Figure 3. 1 Diagram of the study visits

3.2.2.1 Phase 1 study (study visit 1)

Each participant attended one 4-day inpatient study visit at NIHR Imperial Clinical Research Facility (CRF) at Hammersmith Hospital. The day before the study visit, participants were asked to refrain from caffeine, alcohol, and strenuous exercise. Participants were also requested to fast overnight. On day 1, two enteral feeding tubes were placed in the participants' stomach and small intestine (duodenum) respectively. On days 2,3, and 4, participants received three chickpea test meals in a randomized order. Blood samples and intestinal (gastric and duodenal) samples were taken before and after the test meals for 180min. Blood samples were used for measuring blood glycaemia and hormonal markers. Intestinal samples were used for metabolomic, microscopic and carbohydrate analyses. Visual Analogue Scale (VAS) questionnaire was collected for the same period to measure subjective appetite levels of participants. A lunchtime meal (at 4 h) was provided to measure their *ab*

libitum food intake. On day 4, enteral tubes were removed, and participants were discharged.

Chickpea materials were provided by Quadram Institute Bioscience (Norwich Research Park, Norwich, NR4 7UQ, UK, referred as QIB below). Chickpeas were soaked overnight for 16 hours, before cooked using a Vorwerk Thermomix Version 5. Chickpeas were cooked following a procedure developed by QIB (Appendix 3), to achieve three structures: broken cells, intact single cells, and cell clusters. The cooked chickpeas (60g chickpea materials) were mixed with 15 grams of Stutes no sugar added blackcurrant jam and 115g of Harley's no added-sugar raspberry jelly. Based on the proximate analysis on chickpea materials (performed by accredited food testing provider ALS Laboratories Ltd., Chatteris, UK) and nutritional labels of jam and jelly products, each test meal provided 41.16 g available carbohydrate, 6.58g dietary fiber, 11.02g protein, 3.74g fat for a total 246 kcal (**Table 3.1**). The amount of water served was adjusted (Appendix 3) to achieve the same portion size (760g).

Table 3. 1 Nutritional Profile of the Test Meal

Nutrition per serving[1]			
Energy (KJ)	1022.40	±	3.97
Energy (kcal)	242.70	±	0.76
Avail. CHO (g)	41.16	±	0.40
Starch (g)	29.54	±	0.40
Sugar (g)	2.29	±	0.00
Protein (g)	11.02	±	0.03
Dietary Fibre (g)	6.58	±	0.43
Fat (g)	3.74	±	0.06

[1] Mean of triplicates with SD

3.2.2.2 Phase 2 (study visit 2-4)

Each participant attended three 3-day inpatient visits at NIHR Imperial CRF. On each visit, participants received one of these chickpea-based meals every day for three days in a row. At least 7 days between each study visit for a washout period to avoid the interaction influence of each study visit. The day before each 3-day visit, participants were asked to refrain from caffeine, alcohol, and strenuous exercise. Participants were also requested to fast overnight.

On day 1, a nasoenteric tube was inserted into the participants' terminal ileum as previously described (Byrne et al., 2019a). The tube position was validated with fluoroscopy by

professional radiologists. Day 2 allowed participants to acclimatize to the diet and environment. On day 3, ileal samples and blood samples were collected before breakfast and every hour after it for 8h. Subjective appetite and breath hydrogen concentration were measured by VAS and gastrolyster, respectively for the same period. A professional doctor removed the nasoenteric tube after the last time point on day 3.

Chickpea materials were pre-weighted and packed at QIB. Chickpeas were soaked overnight for 16 hours, rinsed and processed using a Vorwerk Thermomix Version 5. On each study visit day, 160g of chickpea was processed and served in the proportion of 60g, 50g, 50g for breakfast, lunch, and dinner, respectively. Breakfast was served at approximately 9:00 am. Lunch and dinner were served at 240min and 480 min after breakfast accordingly. A low-fibre background diet was served along the chickpea to achieve nutrient balance (46.7% energy from carbohydrate, 19.8% energy from protein, 30.5% energy from fat). The list of foods and nutritional information is in Appendix 4.

3.2.3 Participant Recruitment

Participants were recruited from the Healthy Volunteer Database from NIHR Imperial CRF. Participants who expressed an interest in this study were asked to fill in a pre-screening form and attend a screening visit. During the screening visit, their eligibility was checked based on their health history, anthropometric measurements, ECGs, and blood test results. Inclusion and exclusion criteria were assessed as below (**Table 3.2**).

Table 3. 2 Inclusion and exclusion criteria of the study.

Inclusion Criteria	Exclusion Criteria
Male or female	Abnormal ECG
Age between 18-65 years (inclusive)	Screening blood results outside of normal reference values
Body mass index (BMI) of 18-30 kg/m2	Weight change of ≥ 5kg in the preceding 2 months
Willingness and ability to give written informed consent and willingness and ability to understand, to participate and to comply with the study requirements	Current Smokers
	History of substance abuse and/or excess alcohol intake
	Cancer
	Gastrointestinal disease e.g., inflammatory bowel disease or irritable bowel syndrome, kidney disease, liver disease and pancreatitis
	Pregnancy
	Diabetes or cardiovascular disease

	Participant in a research study or blood donation 12 weeks prior
	Started new medication within the last 3 months likely to interfere with energy metabolism, appetite regulation and hormonal balance, including: anti-inflammatory drugs or steroids, antibiotics, androgens, phenytoin, erythromycin, or thyroid hormones.

3.2.4 Randomizations

Participants who passed the screening were randomized into the study. Randomization was performed using a sealed envelope system (Sealed Envelope Ltd. 2021). The allocation of treatment sequence was blinded to the investigators, technicians performing analysis of blood samples and participants. Investigators and participants remained blinded until the completion of the study and data analysis.

3.2.5 Sample size

This is a pilot study and therefore, sample size calculation was not feasible. A study that investigated the effects of peas structure on human gastric and duodenal digestion found significant differences in gut glucose levels and metabolic profiling in 10 participants

(Petropoulou et al., 2020). Considering a drop-out rate of 20%, a recruitment target of 13 was decided.

3.3 Analysis of blood samples

3.3.1 Blood samples collection, processing, and storage

Human studies collected blood samples to analyse glucose, insulin and gut hormones. Blood samples were collected at pre-determined timepoints by a medical doctor or trained researchers. Blood samples were collected in vacutainers and centrifuged at 2500 g at 4C for 10 minutes. 500ul of supernatant was collected into aliquots and stored at -80 °C for further analysis. For gut hormones analysis, 80ul of aprotinin (20ul/ml blood, Trasylol, Nordic Pharma), 40ul of DPP-4 inhibitor (10ml/ blood) and 40 µl of AEBSF (prefabloc, 1mg/ml blood) was added to lithium heparin tubes before sample collection. Methods for each analysis are presented in **Table 3.3.**

Table 3. 3 Methods of sample preparation, processing, and storage

Analysis	Sample type	Preparation	Collection	Processing	Storage
Glucose	Plasma	/	Sodium fluoride/Potassium Oxalate	Centrifuge immediately	-80°C
Insulin	Serum	/	Clot activator	Clotting for 10 minutes at RT before centrifuge	-80°C
GIP GLP-1 PYY	Plasma	Aprotinin, DPP-4 inhibitors, and AEBSF	Lithium heparin	Centrifuge immediately	-80°C

4-(2-Aminoethyl) benzenesulfonyl fluoride hydrochloride, AEBSF; dipeptidyl peptidase 4DPP-4

3.3.2 Blood glucose analysis

Levels of plasma glucose were measured using GLUC-PAP Kit from Randox (Randox Laboratories Ltd., UK) following the instructions provided. In brief, a volume of 20 µl plasma sample was mixed with 1000 µl buffer containing glucose oxidase and peroxidase. Glucose oxidase can catalyse glucose into gluconate and hydrogen peroxide. Under catalysis of

peroxidase, hydrogen peroxide forms a red violet quinonimine colour as an indicator. The absorbance (A) was measured using a microplate reader (MARS BMG Labtech FLUOstar Omega version 3.42) under 540nm. The concentrations of unknown samples were calculated based on given standards at a concentration of 5.55 mmol/L.

$$\text{Glucose concentration} \quad (mmol/l) \quad = \frac{A_{sample}}{A_{standard}} X\ 5.55$$

Samples and standards were run in duplicates. Within-subject samples from all visits were run in one microplate. A coefficient of variation (CV) <10% was considered acceptable. The average coefficient of variation CV was 3.62% for Chapter 4 and 2.28% for Chapter 5.

3.3.3 Radioimmunoassay

A radioimmunoassay (RIA) is an *in vitro* technique used to measure concentrations of antigens using radioactively labelled molecules. It is based on the principle that a known concentration of a radiolabelled antigen competes with the antigen of interest for the specific binding site of an antibody. The concentration of the antigen in the sample can be calculated by measuring the radioactivity of the antigen-antibody complex and of the unbound antigen following the competitive reaction. The method can be used for any biological molecule in principle and is commonly used for detecting hormonal levels in the blood.

3.3.3.1 Insulin analysis

For Chapter 4 (human study phase 1), serum insulin concentrations were measured using a Human Insulin Specific RIA kit (HI-14K, Merck, UK) with ^{125}I-labelled Human insulin and a

Human insulin antiserum. The kit allows the detection of unknown concentrations of insulin from 3.125 uU/ml to 100uU/ml. It did not cross-react with proinsulin.

The assay was performed following the manufacturer's instructions. On day 1, a volume of 50 µl serum insulin was incubated in a tube with 150 µl of phosphoserine buffer, 50 µl ^{125}I-Insulin and 50 µl antibody for 20 hours at room temperature (20-25 °C). On day 2, separation of the antigen-antibody complexes from free antigen was achieved by adding the secondary antibody. Tubes were drained and the pellets were counted using a gamma counter (LB2111 Multy Crystal Gamma Counter, Berthhold Technologies, Bad Wildbad, Germany) for 1 minute. Insulin concentration was extrapolated from the standard curve generated according to manufacturer instructions using GraphPad Prism version 9. Two quality controls in duplicates were used per assay and used to validate the standard curve. Samples were analysed after all participants had completed the trial to minimise bias. All samples were analysed in duplicates. For Chapter 4, samples were analysed after all participants had completed the study with a CV of 5.34%.

3.3.3.2 GLP-1 analysis

GLP-1 concentrations in human plasma samples were measured by an in-house RIA method (Kreymann et al., 1987). This method used a polyclonal antibody combined completely with amidated GLP-1, but not with GLP 1-37 or GLP 7-37. This antibody did not cross-react with other known gastrointestinal hormones. The limit of detection was 7.5 pmol/L. The radiolabelled I^{125}-GLP-1 was prepared by Professor Kevin Murphy using the iodogen method (Wood et al., 1981). The assay was performed with the assistance of Dr Georgia Franco Becker and Professor Kevin Murphy.

Prior to the assay, 0.06M phosphate buffer (pH=7.34) was prepared to contain 0.3% BSA (1ml/100ml) and TWEEN 20 diluted in 1:10 (2ml/L) (Sigma, Poole, UK). The diagram of the RIA assay is represented in **Figure 3.2**. On day 1, 100ul of plasma sample or standard solution was added to borosilicate glass tube pre-loaded with assay buffer. 50ul of labelled antigen (specific activity: 8 $Bq \cdot fmol^{-1}$) and 50ul rabbit anti-GLP-1 primary antibody were subsequently added. Standard solutions were a set of GLP-1 solutions in volumes of 1,2,3,5,10,15,20,30,50,100 µl at the concentration of 0.125pmol/ml. Tubes were vortexed and incubated for 4 days at 4ºC. On day 5, 250ul of dextrin-coated charcoal (Merck) was added to each tube and samples were immediately centrifuged at 1318 RCF for 30 minutes at 4ºC.After centrifugation, the supernatant and charcoal pellet were separated using Pasteur glass pipettes into new tubes. Their radioactivity was measured using gamma counter (LB2111 Multy Crystal Gamma Counter, Berthhold Technologies, Bad Wildbad, Germany) for 3 minutes. The standard curve was generated using a non-linear two-phase decay plot using GraphPad Prism version 9. Samples were analysed after all participants had completed the study to minimise bias. All samples were analysed in duplicates. The CV was 3.95% for Chapter 4 and 4.87% for Chapter 5.

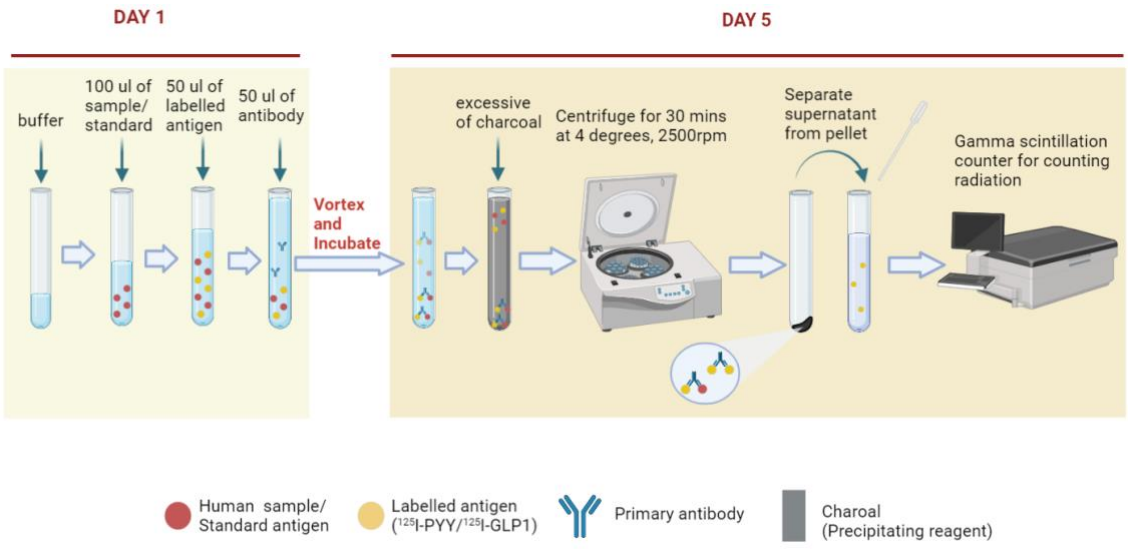


Figure 3. 2 Diagram of the in-house RIA for plasma GLP-1/PYY concentrations

3.3.3.3. PYY analysis

PYY concentrations in human plasma samples were measured by an in-house RIA method (Kreymann et al., 1987). The radiolabelled I^{125}-PYY (specific activity: 54 $Bq \cdot fmol^{-1}$) was prepared by Professor Kevin Murphy using the iodogen method (Wood et al., 1981). Rabbit antiserum (Y21) was synthesised using porcine PYY coupled to bovine serum albumin and employed at a dilution of 1:50,000. The assay was performed with the assistance of Dr Georgia Franco Becker and Professor Kevin Murphy. This assay detected hormones PYY in the form of PYY_{3-36} and PYY_{1-36}. The antibody used did not cross-react with other known gastrointestinal hormones. The limit of detection was 7.5 pmol/L.

Similar to GLP-1, the RIA assay on PYY followed the diagram in **Figure 3.2**. Due to the low concentrations of PYY expected in the samples, 100ul of µl of Bovine Serum Albumin with 0.1% sodium azide (30% w/v solution in PBS) (First Link UK Ltd.) was added to each tube to improve

the accuracy. PYY standard solutions were in volumes of 1,2,3,5,10,15,20,30,50,100 µl at the concentration of 1 pmol/ml. The volume of assay buffer was adjusted accordingly to keep the total volume at 350ul. Samples were analysed after all participants had completed the study to minimise bias. All samples were analysed in duplicates. The CV was 3.34% for Chapter 4 and 3.63% for Chapter 5.

3.3.4 Enzyme-linked Immunosorbent Assay (ELISA)

ELISA is a common laboratory method for detecting and quantifying a protein in a complex mixture. The principle behind this is that the antigen is immobilized on a solid surface (usually a microplate) and then complexed with an antibody that can be linked to a detectable enzyme. The most common ELISA types are direct, indirect, sandwich and competitive as shown in **Figure 3.3**.

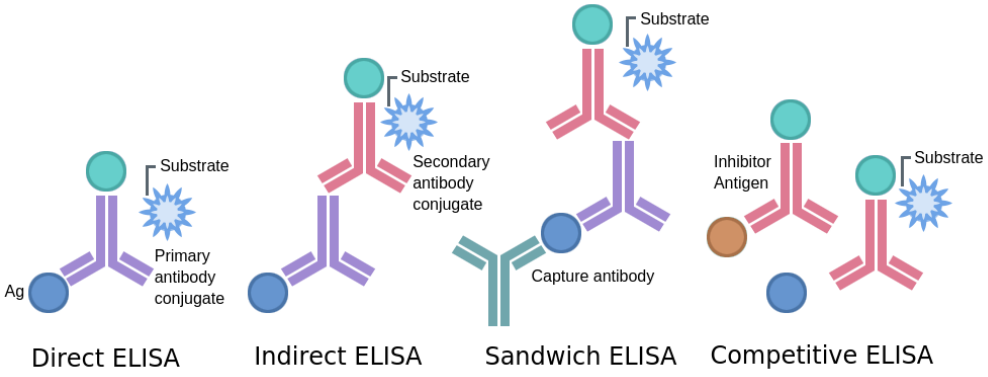


Figure 3. 3 Types of ELISA. Adapted from theory. labster.com

3.3.4.1 Insulin analysis

For Chapter 5 (human study phase 2), insulin analysis was conducted using Human ELISA kits DY8056-05 (from R&D systems, Inc., USA). Assays were performed according to the protocol

provided by the supplier. **Figure 3.4** presents the diagram of sandwich ELISA assays. On day 1, 96-well microplates were coated with capture antibody and incubated at room temperature for 14-16 hours. On day 2, a volume of 100 µl of serum samples or standards was added into each well and was further incubated for 2 hours. Detection antibody label with biotin was added to bind the antigen-antibody complex to form the sandwich. Streptavidin- HRPO was added to bind the biotin and catalyze an enzymatic colour reaction. Stop solution was added after 20 minutes of incubation to end the reaction. The absorbance was measured using a microplate reader (MARS BMG Labtech FLUOstar Omega version 3.42) under 450nm and correlated with the wavelength of 540nm to omit the background. Samples were analysed in duplicates. Samples were measured when all participants finished the trial. The CV was 6.12% for Chapter 5.

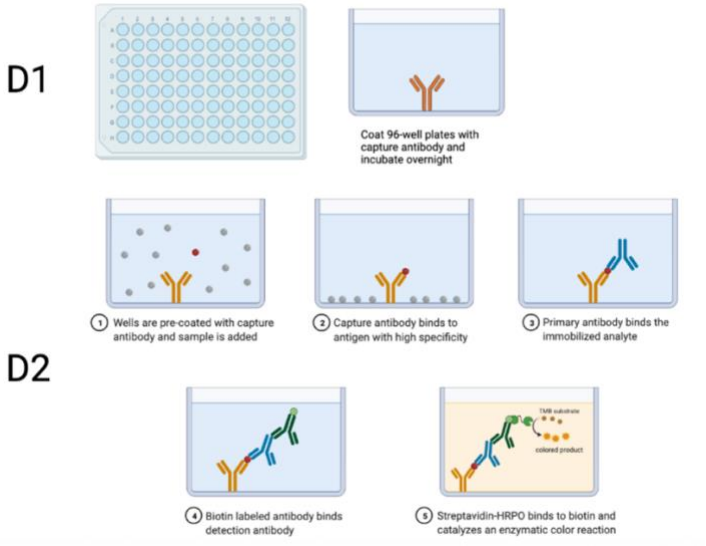


Figure 3. 4 Diagram of sandwich ELISA for insulin detection

3.3.4.2 GIP analysis

Plasma GIP concentrations were measured by Human GIP ELISA kits from (EZHGIP-54K, Merck, UK) based on the specifications. The kit has 100% cross-reactivity to human GIP_{1-42} and GIP_{3-42}. The limit of detection is 8.2 pg/ml.

The protocol followed a sandwich ELISA method. A volume of 20ul of plasma samples or standards was added into of 96-well microplate that was pre-coated with the capture antibody. Microplates were incubated at room temperature for 1.5 hours. Solutions were decanted and the unbound materials were removed by the washed buffer. Detection antibody label with biotin was added to bind the antigen-antibody complex to form the sandwich. Streptavidin- HRPO was added to bind the biotin and catalyze an enzymatic colour reaction. Stop solution was added after 10 minutes of incubation to end the reaction. The absorbance was measured using a microplate reader (MARS BMG Labtech FLUOstar Omega version 3.42) under 450nm and correlated with the wavelength of 590nm to omit the background. Samples were analysed in duplicates. Samples were measured when all participants finished the trial. The CV was 2.42% for Chapter 4.

3.4 Analysis of gut samples

3.4.1 Gut sample collection, processing, and storage.

3.4.1.1 Method to collect human gastric and duodenal samples

A CORTRAK enteral feeding tube system (Avanos Medical UK Limited, UK) was used to collect gastric and duodenal samples in human subjects. The CORTRAK system allowed the

researchers to track the position of the tube without the need for x-rays. The system contains an enteral feeding tube (90cm for the gastric tube, and 140cm for the duodenal use, respectively), a transmitting stylet that emits an electromagnetic signal, a receiver unit that detects the signal, a monitor that displays the location of the gut, and a record system (**Figure 3.5**). Gastric and duodenal tube placements were performed by Dr Martina Tashkova.

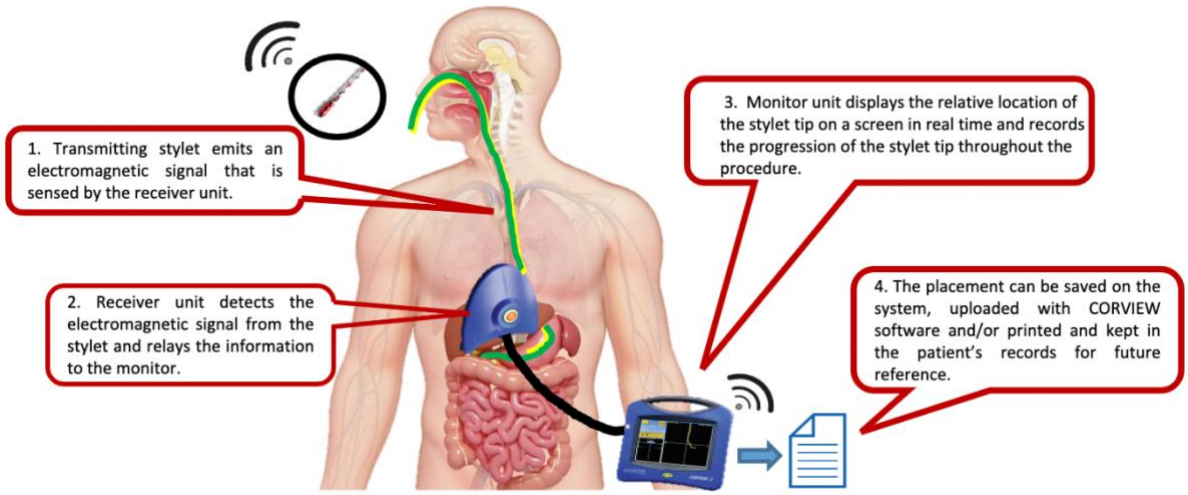


Figure 3. 5 The structure of CORTRAK system. Adapted from (Petropoulou, 2019b)

3.4.1.2 Method to collect human ileal samples

Customized catheters (MUI Scientific, Canada) were designed to collect ileal digesta samples from human subjects, as per the published protocol (Byrne et al., 2019b). Briefly, the catheter is 350cm in length. The Tip End (Left side in **Figure 3.6A**) of the catheter has a balloon with a max volume of 20ml, a detectable tip, and aspiration and air channels. The connector end contains three channels: the aspiration channel to collect digesta, the air channel to connect the pressure, and the balloon channel to control the inflation of the balloon (**Figure 3.6 A**).

Tube placement was performed by Dr Dominic Blunt at the Imaging Department of Charing Cross Hospital (Fulham Palace Rd, London W6 8RF, UK). The dose of fluoroscopy was calculated by Ms. Eugenia Kulama. During tube insertion, the tube was inserted through the nose (**Figure 3.6 B**). Once it passed the stomach and the duodenum, the balloon at the end of the catheter was inflated to 6ml, carrying the tube through the small intestine by peristalsis. The tube position was monitored and validated by fluoroscopy with the administration of dilute barium sulphate. The tips at the end of the catheter gave an indication of tube location (**Figure 3.6 C**). Once the tube arrived at the terminal ileum, the balloon was reduced to approximately 2ml to be restrained from any additional movement for the rest of the 3-day visit. This study observed that a distance of 260 cm usually reached the terminal ileum, in agreement with previous studies (PH van Trijp et al., 2021). The same distance of tube insertion was applied to three occasions within the same participants.

After an overnight stay, the tube position was validated with fluoroscopy at the Imaging Department of Hammersmith Hospital (72 Du Cane Rd, London W12 0HS, UK). During ileal sample collection, tube position was monitored by the pH and colour of digesta samples (**Figure 3.6 D-E**). A pH in the range of 6.5-7.5 indicates an appropriate aspirate from the terminal ileum (Nugent et al., 2001).

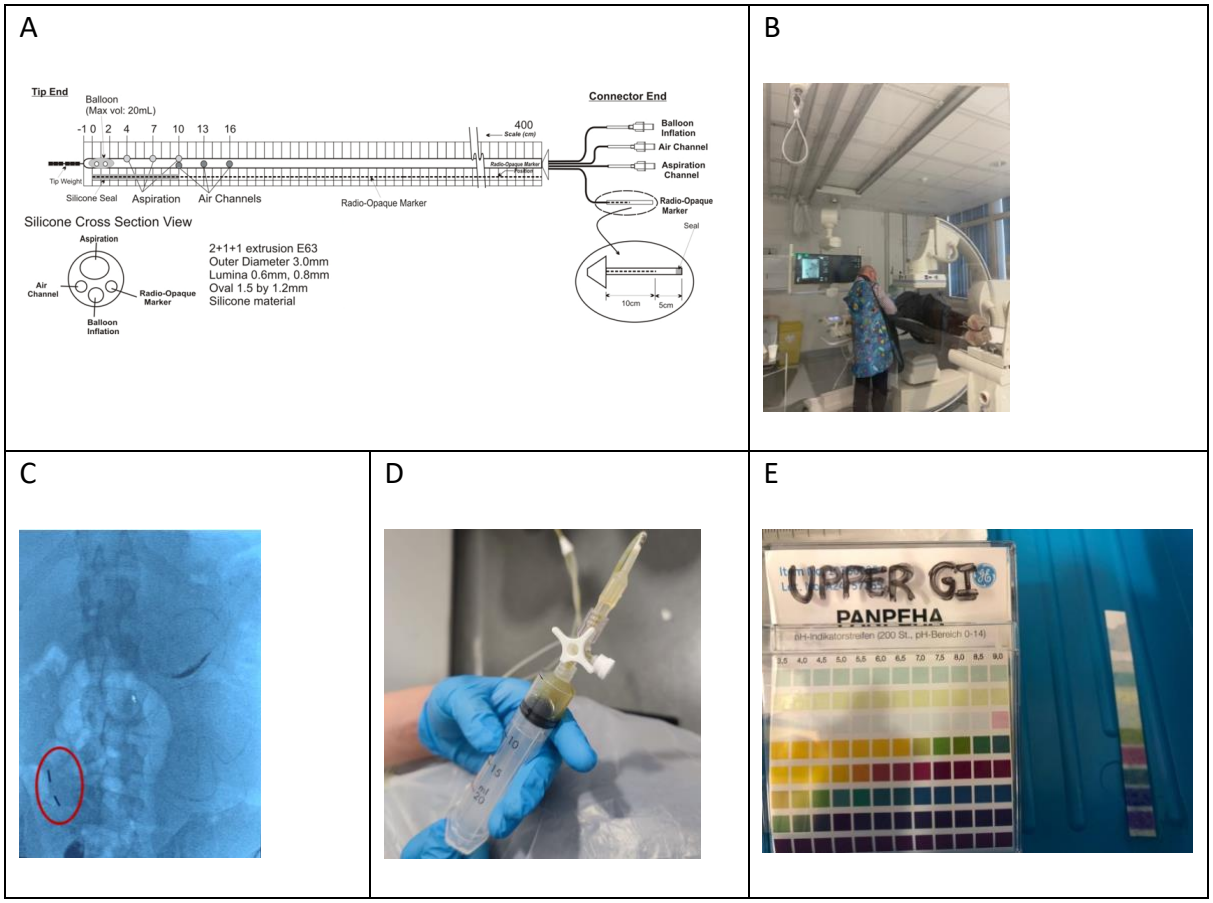


Figure 3. 6 Methods for ileal tube placement and monitoring. The design of nasoenteric tube (A), ileal tube placement (B), tube position monitoring (C), ileal sample collection (D) and pH measurement (E). Figure A was adapted from (Byrne et al., 2019b). The red circle in Figure C indicated the tips at the end of the tube.

3.4.2 Gut glucose analysis

Concentrations of glucose in the stomach, duodenal, and ileal samples were measured by GLUC-PAP Kit from Randox (Randox Laboratories Ltd., UK). The same protocol was followed as described in section 3.3.2, except for an additional step at the beginning. Defrosted

samples were first centrifuged at room temperature for 10 minutes at 13,000 RPM. A volume of 20ul from the supernatant was used for the following steps. Samples were analysed in duplicates. Samples were measured when all participants finished the trial. The CV was 4.2%, 4.8%, and 4.3% for gastric, duodenal (Chapter 4) and ileal samples (Chapter 5), respectively.

3.4.3 Gastric and duodenal maltose analysis

Maltose in the gastric and duodenal samples was measured by LC-MS method at QIB. 45ul of the samples were transferred into HPLC vials. After 5ul of internal standard D-glucose-$^{13}C_6$, 0.1 mg/mL) was added and vortexed for LC-MS analysis run by Agilent 6490 mass spectroscopy.

3.4.4 Metabolic profiling

3.4.4.1 Metabolites extraction

Gastric, duodenal, and ileal samples were centrifuged at room temperature for 15 minutes at 3000g. 450 µl of samples from the supernatant were separated into 5ml vials (Shimadzu™ 5mL Vial, Supelco-27324). Metabolites were extracted from the samples following a published procedure (Garcia-Perez et al., 2020). Briefly, 1 ml methanol, 2 ml of chloroform, and 1 ml water (ratio 1:2:1) were added to each sample. Samples were vortexed for 1 minute and centrifuged at room temperature for 20 minutes at 3000g. After centrifugation, samples were separated into two phases: the aqueous and the organic phase. The aqueous phase

samples were evaporated by a speed vacuum concentrator (Eppendorf Concentrator Plus) to dryness and stored at -80 °C for further analysis.

3.4.4.2 ^{1}H NMR Spectroscopy

The aqueous phase of gut samples was re-constituted in 640 µl of H_2O and sonicated for 10 minutes. Samples were checked after sonication and there was no visible precipitation. 60ul of NMR buffer [a 1.5M phosphate buffer, pH 7.4, 80% D_2O, with 1mM internal standard, 3-(trimethylsilyl)- [2,2,3,3, -2H4]-propionic acid (TSP)] was mixed with 540ul of samples and the mixture was further transferred to 5mm NMR tubes. Quality controls were prepared by pooling 100ul of each sample, independently for gastric, duodenal, and ileal samples.

NMR spectroscopy was performed by Dr. Isabel Garcia-Perez and Dr. Jose Ivan Serrano-Contreras. ^{1}H-NMR spectroscopy was performed at 300K on a Bruker 600 MHz spectrometer (Bruker Biospin, Karsruhe, Germany), as per the programme described by Petropoulou et al. (Petropoulou et al., 2020). It followed a standard one-dimensional pulse sequence with saturation of the water resonance RD – gz,1 – 90° – t – 90° – tm – gz,2 – 90° – ACQ (noesygppr1d) where RD is the relaxation delay, 90° represents the applied 90° radio frequency (rf) pulse, t1 is an interpulse delay set to a fixed interval of 4µs, RD was 2 s and tm (mixing time) was 100 ms. Water suppression was achieved through irradiation on the water signal during RD and tm. Each 21 spectrum was acquired using 4 dummy scans followed by 32 scans and collected into 64 K data points. A spectral width of 20,000 Hz was used for all the samples. Prior to Fourier transformation, the free induction decay values (FIDs) were multiplied by an exponential function corresponding to a line broadening of 0.3 Hz.

023

3.4.4.3 NMR data processing

Multivariable statistical analysis was performed on spectra data. Each spectrum (~24K spectral variables) was automatically phased, baseline corrected, digitized over δ -0.5 to 10 and imported into MatLab (R2021a, Mathworks, Inc.; Natwick, USA), using in-house scripts. Spectral regions corresponding to the internal standard (δ -0.5 to 0.5) and water (δ 4.7 to 4.9) were excluded. All spectra were normalised using median fold change normalisation using in-house scripts.

Data were centred and scaled to account for the repeated measures design and then modelled using partial-least-squares– discriminant analysis (PLS-DA) with Monte Carlo cross-validation (MCCV) (Posma et al., 2018, Garcia-Perez et al., 2017). The fit and predictability of the models were determined by R^2Y and Q^2Y values, respectively.

3.4.4.4 Metabolites identification

Following a published protocol (Garcia-Perez et al., 2020), statistical spectroscopic tools such as Statistical Total Correlation Spectroscopy (STOCSY) and Subset optimization by reference matching (STORM) were used to identify spectra signals. Internal and external databases such as the human Metabolome Data Base (HMDB, Human Metabolome Data Base (HMDB; http://hmdb.ca/), the Biological Magnetic Resonance Data Bank (BMRB; http://www.bmrb.wisc.edu) and the Chenomx metabolites library for 600 MHz (Chenomx, https://www.chenomx.com/libraries/) were used for confirmation of assignments.

3.4.5. Microscopic analysis

Food structures present in gastric and intestinal samples were examined by microscopic analysis, performed by Dr Natalia Perez-Moral at QIB. The aspirated samples were fixed in formalin at the time of collection and transferred to QIB for analysis. A small amount of sample was added to the slide and placed under a light microscope (Olympus BX60 microscope with Jenoptik ProgRes camera). Images were taken at x4, x10 and x20 magnification. To prepare the staining solution, 1% stock solution of toluidine blue was diluted with water at a ratio of 1:80. The staining solution was added to the sample at least 5 minutes prior to imaging.

3.5 Analysis of appetite and food intake

3.5.1 Visual Analogue Scales (VAS)

Visual analogue scales (VAS) are reliable tools to evaluate appetite sensations in human studies (Flint et al., 2000). Chapters 4 and 5 used VAS to assess the pre and postprandial subjective appetite feelings during study visits. VAS consisted of a set of questions which were:

- Hunger (“how hungry do you feel right now?”)
- Fullness (“How full do you feel right now?”)
- Prospective food intake (“How strong is your appetite for a meal?”)
- Desire to eat (“How strong is your desire to eat”)

Participants were asked to answer these questions by drawing a vertical line across a 100mm scale ranging from “not at all” (right extreme) and “extremely” (left extreme). The distance

between the left extreme and the vertical line was measured using the same ruler. A composite appetite score (CAS) was calculated by combining the four measurements following the formula: [hunger+(100-fullness) +desire to eat + appetite for a meal]/4. The fullness was reversed due to its opposing direction to the other three questions (Stubbs et al., 2000).

3.5.2 Ad libitum food intake

Ad libitum food intake refers to the intake of food when it is served without restriction. It is a reproducible measurement of appetite despite individual variations. *Ad libitum* meal is recommended to be used along with VAS for measuring appetite (Gregersen et al., 2008).

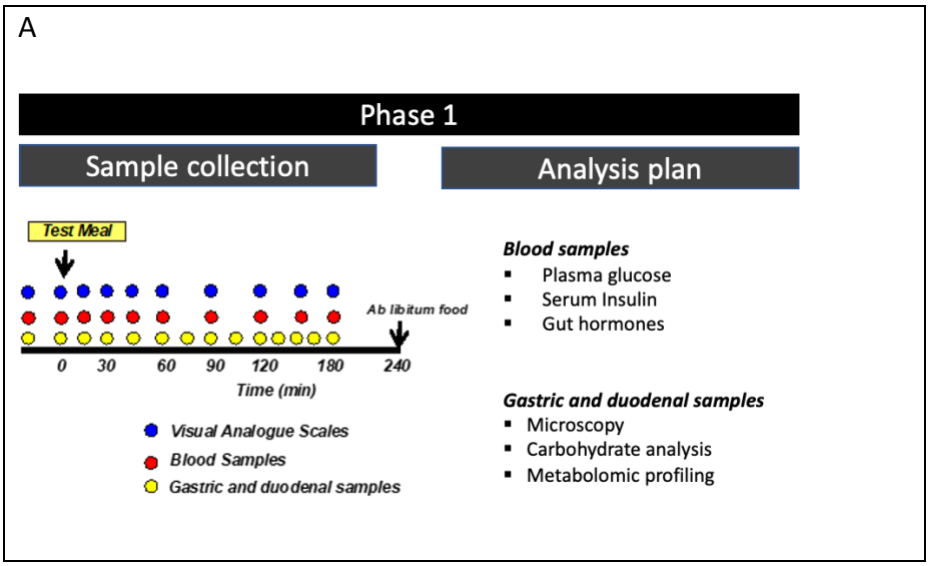
Chapter 4 measured a*d libitum* food intake by providing participants with an excessive, homogenous pasta meal. The meal consisted of 3kg boiled white pasta, mixed thoroughly with 2 pots of tomato sauce (Hearty Food CO. Tomato Herb Pasta Sauce 440g) and 50g of vegetable oil (Flora sunflower oil) to provide approximately 2500 kcal. The pasta meal was cooked following a standard procedure (Appendix 5). Participants had the pasta meal in an isolated room to avoid disturbance from external food smells and noises during food intake. A small amount of water (250ml) was provided along with the pasta meal. Food intake was measured by weighing the grams of food before and after consumption and calculating the difference.

3.6 Breath hydrogen: a marker of intestinal fermentation

Breath hydrogen was used as an indicator of intestinal fermentation in Chapter 5. The rationale is that upon the arrival of fermentable carbohydrates to the lower GI tract, intestinal fermentation activity would increase and produce H_2, which can be excreted through respiration (Rumessen, 1992). In Chapter 5, breath hydrogen concentrations were measured using a gastrolyser (Bedfont Scientific Ltd, UK). Participants were instructed to inhale deeply, hold their breath for 15 seconds and exhale through a mouthpiece connected to the gastrolyser.

3.7 Overview of analysis plan

To summarize, blood samples collected from phase 1 and phase 2 studies were analysed for glucose, insulin, and gut hormones. Gastric, duodenal, and ileal samples were collected for microscopic, carbohydrate and metabolomic profiling analysis. **Figure 3.7** shows the analysis that has been completed and included in the thesis.



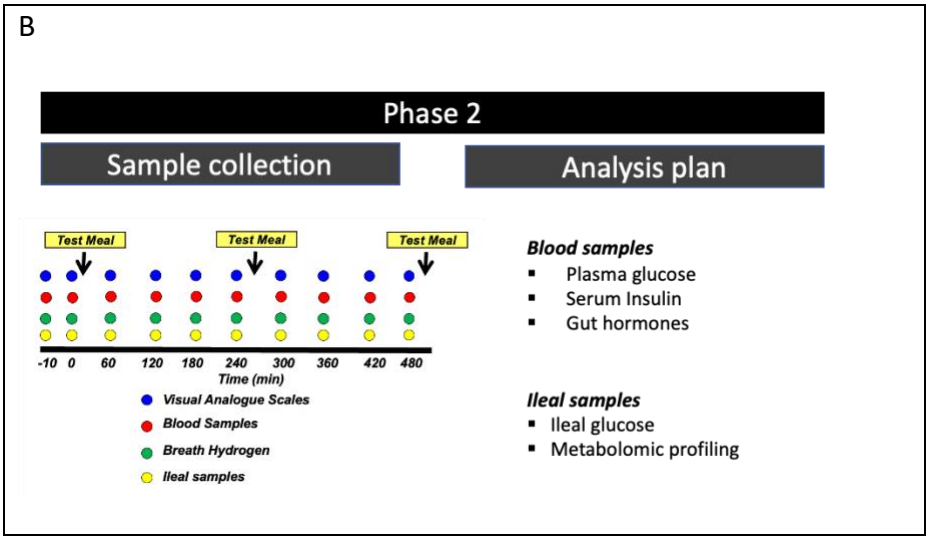


Figure 3. 7 Diagram and analysis plan for human studies. Phase 1 (A) and phase 2 (B) study diagram and completed analysis in this thesis.

3.8 Summary

This Chapter has summarized the experimental methods used for human studies, including clinical study design, and techniques for human sample collection and analysis. These allowed us to gain a deeper understanding of how gut content changes in response to carbohydrate foods differing in structures, and their subsequent effects on glycaemic response and appetite.

Chapter 4 The impact of food structure on postprandial glycaemia and starch digestion in the stomach and duodenum

4.0 Abstract

Understanding of the digestion behaviours of plant cell walls in human GI tract has been limited. This study included 13 subjects in whom intestinal and blood samples were collected before and after their consumption of chickpea broken cells (Broken), intact single cells (Intact-S), and intact cell clusters (Intact-C) for 180 min, for following measurements.

- Microscopic examination of cell wall structure in the gastric and duodenal samples
- Maltose and glucose concentrations in the gastric and duodenal samples
- ^{1}H-NMR metabolic profiling of the gastric and duodenal samples
- Blood glucose and gut hormonal profiles
- Subjective appetite and *ad libitum* food intake

Broken leached out free starch, leading to a high rate and extent of starch digestion which explained its higher postprandial glucose. In Intact-S, most cells remained largely intact whilst some open cells were observed with starch leaching and reduced cell contents in the duodenal aspirations. Intact-C released less starch compared to Intact-S, indicating its stronger barrier effect. Intact-S and Intact-C reduced the release rate of luminal glucose and maltose and the magnitude of blood glucose, insulin, and GIP responses compared to Broken. Intact-S increased satiety, PYY and GLP-1 responses compared to Broken, but did not affect food intake at the subsequent meal.

4.1 Introduction

The upper gastrointestinal tract is the main site for starch digestion. In addition to chemical and mechanical breakdown, it involves complex physiology and is regulated by many neuronal and hormonal factors that can interact with carbohydrate food structure. Studying digestion in humans has been technically difficult, and data directly derived from human subjects are very limited. This section will summarize current methods and understanding of effects of food structure on starch digestion and physiological mechanisms to be addressed.

4.1.1 Current methods to study starch digestion

In vitro static models

In the past decades, many attempts have been made to model human digestion in laboratory conditions. Static digestion models replicate the biochemical conditions in humans such as temperature, enzymes, electrolytes, and pH. Commonly, the gastric phase is reproduced by pepsin hydrolysis of food under a fixed pH and temperature setting (pH 1-2, 37 °C) over a set period (1-3h). This step is followed by an intestinal phase that includes pancreatic enzymes under a pH of 6-7(Guerra et al., 2012). The INFOGEST network of over 35 countries has developed a harmonized procedure for static *in vitro* digestion. The method involves three successive phases: oral, gastric, and intestinal. It stands out for the easy-to-follow procedure and minimal requirement for lab equipment (Brodkorb et al., 2019). The INFOGEST method has been suggested to produce a good intra-lab reproducibility (Egger et al., 2016). It has been

increasingly used in the research of starch, protein, and lipid digestion (Mat et al., 2016, Fernandes et al., 2020) (Junejo et al., 2021a).

In vitro dynamic models

One of the limitations of static models is that they cannot reproduce the mechanical effects, a key factor interacting with food structure during digestion. Such limitations can be vastly improved by dynamic models, which can add more parameters like changes in pH, transit time, and mechanical effects. The Dynamic Gastric Model (DGM) was designed at the Institute of Food Research (Norwich, UK) and addresses the need for stimulating mechanical aspects of gastric digestion (Thuenemann et al., 2015). It adds the region specificity of the stomach: the "body" where gastric secretion and mixed with the food chyme and the "antrum" where the grinding and mixing forces are mainly produced (Thuenemann et al., 2015). The TNO Gastro-Intestinal (TIM-1) Model integrates the stomach and three parts of the small intestine: duodenum, jejunum and ileum. It integrates more parameters of digestion like transit time, peristaltic mixing and transport and intestinal absorption of small molecules through a dialysis system (Minekus, 2015).

Amylase hydrolysis

Starch digestibility can be measured by a single enzyme system based on an enzyme-kinetic approach. Unlike the above models stimulating physiological digestive conditions, Edwards et al., developed a method that uses a single enzyme (porcine pancreatic α-amylase) to provide reasonable predictions of the glycaemic index (Edwards et al., 2019). This method has been

applied to investigate the effect of particle size, cell wall and starch structure on digestion kinetics (Edwards et al., 2014a, Edwards et al., 2018, Patel et al., 2014).

Methods to track digestion in the human

Several methods have been used to track digestion in humans. A variety of methods have been developed to study rates of gastric emptying and gut motility, such as Magnetic resonance imaging (MRI) and 13C-based breath tests (Szarka and Camilleri, 2009). An ingestible wireless motility capsule has been recently designed which enables the measurement of pH, pressure, and the transit time through different regions of the gut (gastric emptying time, small intestinal transit time, colonic transit time and whole gut transit time) (Lee et al., 2014b). These methods can provide some useful information on gut mobility, but they cannot directly address starch digestion kinetics or measure metabolite changes in the gut.

4.1.2 Current understanding of the effects of chickpea cell wall structure: in vitro and in vivo findings

The enzymatic digestion of chickpeas has been studied using *in vitro* models as discussed in Section 1.7.4 . The integrity of cell walls is the key factor affecting starch digestion (Dhital et al., 2016, Rovalino-Cordova et al., 2018). Individual cotyledon cells isolated from chickpeas remained relatively intact in digesta collected from static and dynamic models (Edwards et al., 2021, Palchen et al., 2021, Palchen et al., 2022). Macroparticles (cell clusters, 1.85 µl) of chickpeas limited starch digestibility compared to milled particles (33% vs 83% digested)

(Edwards et al., 2021). Most recently, several studies have compared intact with disrupted cell walls of chickpeas in their *in vitro* digestion and *in vivo* responses, as summarized in **Table 4.1**.

Three studies investigated *in vitro* digestion alongside *in vivo* metabolic responses (two in glycaemic response, and one in appetite, respectively). Edwards et al., developed a novel method that processed chickpeas into flours maintaining intact cells called PulseON. After 90 minutes of stimulated digestion. PulseOn led to less than 40% starch digested, whereas normal chickpea flours were rapidly digested (>80% starch digested) within 30 min. The PulseON had a medium to low GI in human subjects (GI =55 when n=18, GI =48 when n=15, excluding three outliers) (Edwards et al., 2020). Bajka et al., compared chickpea powder made from intact cells and broken cells. Intact cells following 120 min amylolysis assay led to 22% starch digested whilst the number in broken cells was 63%. Drinks made from intact cell powders significantly lowered the glucose $iAUC_{45}$ but not $iAUC_{60}$ and $iAUC_{120}$ in healthy subjects (Bajka et al., 2021). Pälchenet et al., measured starch digestion in chickpeas with intact and open cell walls following INFOGEST static protocol. Chickpeas with open cell wall structure exhibited a rapid and complete starch digestion (>94-99% digested) within 30min; whilst intact cell walls retarded digestion rates and resulted in incomplete starch digestion (22% undigested). Chickpea intact cells increased the feeling of fullness and satiety but did not affect food intake (Palchen et al., 2022). These studies support that chickpea intact cells lowered digestion kinetics whilst final % of starch digested varied largely between studies and/or digestion conditions.

Table 4. 1 Chickpea cell wall structure, *in vitro* starch digestion, and in vivo response.

Reference	Intervention	Comparer	Digestion methods (model, time, enzymes)	In vitro digestion	In vivo responses
(Edwards et al., 2020)	PulseON chickpea powder with intact cells	Normal chickpea flours	In vitro amylolysis 120min pancreatic amylase	PulseON powder decreased starch digestibility than normal flours (<40% vs 80%)	PulseOn had a low to medium GI value
(Edwards et al., 2021)	Chickpeas macroparticles (cell clusters 1.85mm)	Chickpeas broken cells (<1.21 nm)	In vitro amylolysis 220min pancreatic amylase	Chickpea macroparticles had reduced extent of starch digestion (33.0% vs 82.5%)	/
(Bajka et al., 2021)	Intact cell powder (ICP)	Ruptured cell powder (RCP)	In vitro amylolysis 120min Enzymes: pancreatic amylase	ICP decreased starch digestibility than RCP (22% vs 63%)	Glucose $iAUC_{45}$ was 40% higher after RCP than ICP. No differences for glucose $iAUC_{60}$ and $iAUC_{120.}$
(Palchen et al., 2022)	Individual cell flour (PC-I)	Open cell flour (NC-O)	INFOGEST Oral phase: 2 min Gastric phase: 120min	PC-I lowered the digestion kinetics in small intestine [K(min-1): 0.01vs	Fullness and satiety score 0-150min was higher after PC-I

			Intestinal phase: 180min Enzymes: Salivary amylase and pancreatic amylase	0.422] and decreased final % starch digested than NC-O (78% vs 94%)	than NC-O. No differences for food intake.

4.1.3 Physiological role of food structure in metabolic responses

Above studies have linked intact cell walls to favourable responses of glycaemia and appetite. The physiological mechanisms involved have yet to be understood. Indeed, current *in vitro* models are far from representative of the complexity of human digestion physiology. The lack of feedback mechanisms, gut microbiota, and hormonal and nervous control deprives them of the ability to mirror the physiological conditions. There are many feedback mechanisms that are likely to interplay with food structure. During the oral phase, food texture and structure can affect the work of mastication, which can influence satiation and subjective appetite possibly via nervous and hormonal pathways (Robinson et al., 2014, Krop et al., 2018, Slyper, 2021). The taste perception and hydrolysis of starch are linked to CNS that influences salivary and gastric secretion (Brownlee et al., 2018b); in the stomach, particle size plays an important role in gastric motility. Increased particle size and complex food structures tended to delay gastric emptying (Vincent et al., 1995) (Bornhorst and Singh, 2014). In the small intestine, the arrival of food chyme induces the release of bile and enzymes from pancreatic acini. The release of enzymes is regulated by various neural and humoral factors, such as CCK, GLP-1 and PYY (Liddle, 2018, Chandra and Liddle, 2009). These hormones have been previously reported to be affected by food structure (Mackie et al., 2013). Importantly, intact endosperm cells reduced starch bioaccessibility in the small intestine and elicited lower

glucose, insulin and GIP responses compared to disrupted cells (Edwards et al., 2015a). Undigested nutrients have been hypothesized to serve as substrates for intestinal fermentation, stimulating appetite suppression hormones and signals(Dagbasi et al., 2020b). Understanding these pathways would provide further evidence of the nutritional and health benefits.

4.1.4 Summary

Food structure can modulate starch digestion through chemical, mechanical and physiological mechanisms. Current *in vitro* studies have provided a fundamental understanding of chemical enzymatic digestion, and the use of dynamic methods is a great step toward in introducing mechanical aspects that mimic human conditions. These approaches can be useful tools for predicting some in vivo results, e.g., a rank of GI of food products. However, they do not fully mirror the dynamic conditions in humans and are subject to a lack of physiological feedback.

Whether intact cotyledons resist and provide a barrier effect in the human gut remains unclear. This affects the intestinal metabolites, postprandial glucose, and the amount of RS that can be transported to the lower gastrointestinal tract. This use of nasoenteric tube (Petropoulou et al., 2020) would allow researchers to access the digestive fluids from the stomach and duodenum of human subjects, enabling the investigation of metabolic and structural changes during digestion. This opens up the potential for to identify gut metabolites and mechanisms associated with carbohydrate food structure. This Chapter aimed to provide an insight into the digestion and metabolite profile in the stomach and digestion and their role in glycaemic response, subjective appetite and food intake.

4.2 Purposes of this study

4.2.1 Hypothesis

It is hypothesized that compared to chickpeas with broken cell walls, chickpeas with intact cell walls (clusters and separate cells) would retain their structures within the stomach and duodenum, resulting in altered luminal metabolites that can impact circulating glycaemic, gut hormone, and satiety responses.

4.2.2 Aims

The aims of the study were to investigate the cell wall structures and metabolites in the human stomach and duodenum following the consumption of chickpeas meals and to provide mechanistic insights into the postprandial glycaemic and satiety response.

4.2.3 Outcome measures

The primary outcome was the glycaemic response following chickpea-based meals with different structures.

Secondary outcomes included:

(1) Structural changes of chickpeas in the stomach and the duodenum

(2) Maltose and glucose concentrations in the gastric and duodenal samples

(3) Metabolic profiling in the gastric and duodenal samples

(4) Plasma concentrations of GIP, GLP-1, and PYY

(5) Subjective appetite and *ad libitum* food intake

4.3. Materials and Methods

4.3.1 Study Design

Please refers to the phase 1 study as indicated in Section 3.2.2. The diagram of sampling routine is present in **Figure 4.1**.

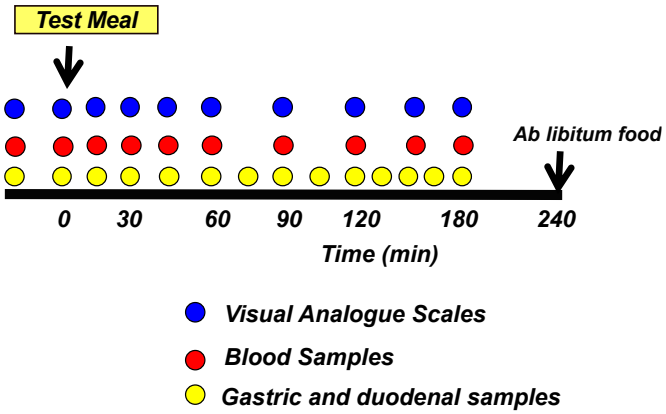


Figure 4. 1 Schematic diagram of study sampling routine.

4.3.2 Participants recruitments

Please refers to Method 3.2.3 for participant recruitment and eligible criterial.

4.3.3 Randomizations

Please refers to Method 3.2.4 for randomizations.

4.3.4 Dietary Intervention and test meal preparation

Tests meals in this study were chickpea-based meals processed to achieve three different structures:

- Chickpea with broken cell walls - Broken
- Chickpea with intact cell walls (separate) -Intact-S
- Chickpea with intact cell walls (clusters)- Intact-C

Preparation of chickpea materials

Whole chickpeas Cicer arietinum L., Kabuli type, Argentine variety (7mm diameter) were supplied by AGT Poortman Ltd. These were dehulled through an abrasive process by holding 200 g batches of dry chickpea (as supplied) in a Steelbrush dehuller (Westrup pre-cleaning debranner, coarse blue roll) for 30s, then sieved on a 3mm grid to exclude fragments of testa. The resulting dehulled chickpea material was weighed out into 75.0 g portions (by a researcher independent to the study at QIB), sealed and labelled. These dehulled chickpea portions were the main ingredient for the 'Broken' and 'Intact-S' chickpea meals, which were freshly prepared on the morning of each study visit using standardised processing protocols to deliver different structures (Appendix 3). For the 'Intact-C' meal, the dehulled chickpeas were further processed by milling to obtain intact tissue particles (1.6-2.0 mm) containing whole cells, before portioning out. These coarse particles were obtained by trickle feeding the dehulled chickpeas through a Buhler miag Vario mill set up with a Roll Gap of 1.8 mm and Roller speed 220:450 rpm on 24.5mm diameter break rolls 5 flutes/cm break rolls in Sharp-Sharp disposition for the first break. Output material was analytically sieved to collect target size fraction (≥ 1.6 and < 2.0 mm), and the oversize material (≥ 2.0 mm) was then re-milled according to the same setting as used for the first break, but with a smaller Roll Gap (0.8 mm), to increase recovery of the target size fraction. This coarsely milled chickpea material (≥1.6

and <2.0 mm) was the main ingredient for the 'Intact-C' meal and was weighed into 75.0 g portions in preparation for the study visits.

Test meal preparation

On the morning of study visit, the pre-weighted chickpea meals were processed by Thermomix tm5 food processor at a fixed programme. Each test meal provided 41.16 g available carbohydrate, 6.58g dietary fiber, 11.02g protein, 3.74g fat for a total 246 kcal. Please refer to **Section 3.2.2.1** for details.

4.3.5 Sample collection, processing and analysis

Please refer to Section 3.3 and 3.4 for details of sample collection, processing and analysis.

4.3.6 In vitro digestibility Assay

90 mg of food materials were weighted into 15ml falcon tubes and suspended in 10ml Phosphate buffered saline (PBS, Oxoid, pH 7.4 at 37 °C). The mixtures were kept in a shaker incubator (E24 Excella, New Brunswick Scientific) set at 37°C for stimulating samples of 3 tubes. *In vitro* digestion was initiated by adding the working solution of porcine pancreatic alpha-amylase (EC 3.2.1.1 A6255, Sigma-Aldrich) with the activity of 89U/ml to each tube. 100 µl of digesta was sampled at 0,10,20,30,40,50,60,75,90, 120min and transferred to a set of Eppendorfs that were pre-loaded with an equal volume of the Stop solution (0.3M Na_2CO_3). The stopped aliquots were centrifuged at 15,000 g for 5min at room temperature. 130 µl of supernatant was collected into the second set of Eppendorfs. The concentrations of reducing

sugar were determined by the PAHBAH assay described previously and expressed as the percentage (%) of starch digested.

4.3.7 Statistical analysis

Please refer to the **Section 3.2.5** for sample size calculation.

Data were checked for normality by the Shapiro-Wilk test ($p>0.01$). Results were presented as means ± standard error of the mean (SEM) or medians (IQR) if data is non-parametric. Logarithmic transformation was conducted for non-parametric data before using parametric statistical tests. Two measurements of baselines before breakfast (T=-10, T=0) were combined as the baseline value. For time-point outcomes, two-way repeated ANOVA was performed to measure the effect of diets, times and their interaction. Mixed effect models were used if there were missing values (e.g., gut carbohydrate analysis). Incremental Area under curve (iAUC) was calculated using the trapezoidal rule, ignoring the area under the baselines. iAUC was compared using a one-way repeated measures ANOVA, followed by post hoc Tukey's Test. Significances were considered $p<0.05$. Statistical analysis was performed using Prism 9.0 (Graphpad Software USA, Biomatters, Ltd). Spearman's correction tests were performed in R studio (Version 2022, Boston, MA, USA).

Peak integration was performed on NMR spectra to calculate the area under peak (Haggart, 2019) and semi-quantify the luminal metabolites (i.e., alanine and phenylalanine) in the gastric and duodenal aspirations.

4.4 Results

4.4.1 *in vitro* starch digestibility assay

Food structure significantly affected *in vitro* starch digestibility **(Figure 4.2)**. Chickpea intact cells and clusters released 30.1% and 54.6 % less starch at the end of the two-hour digestion compared to chickpea broken cells, measured by amounts of reducing sugar (A-B). The microscopic analysis (C-E) revealed that most of the cell wall structures were retained after two-hour of amylase digestion and entrapped a large amount of starch inside the cells. The starch from chickpea broken cells was freely accessible and had almost been digested at the end of digestion.

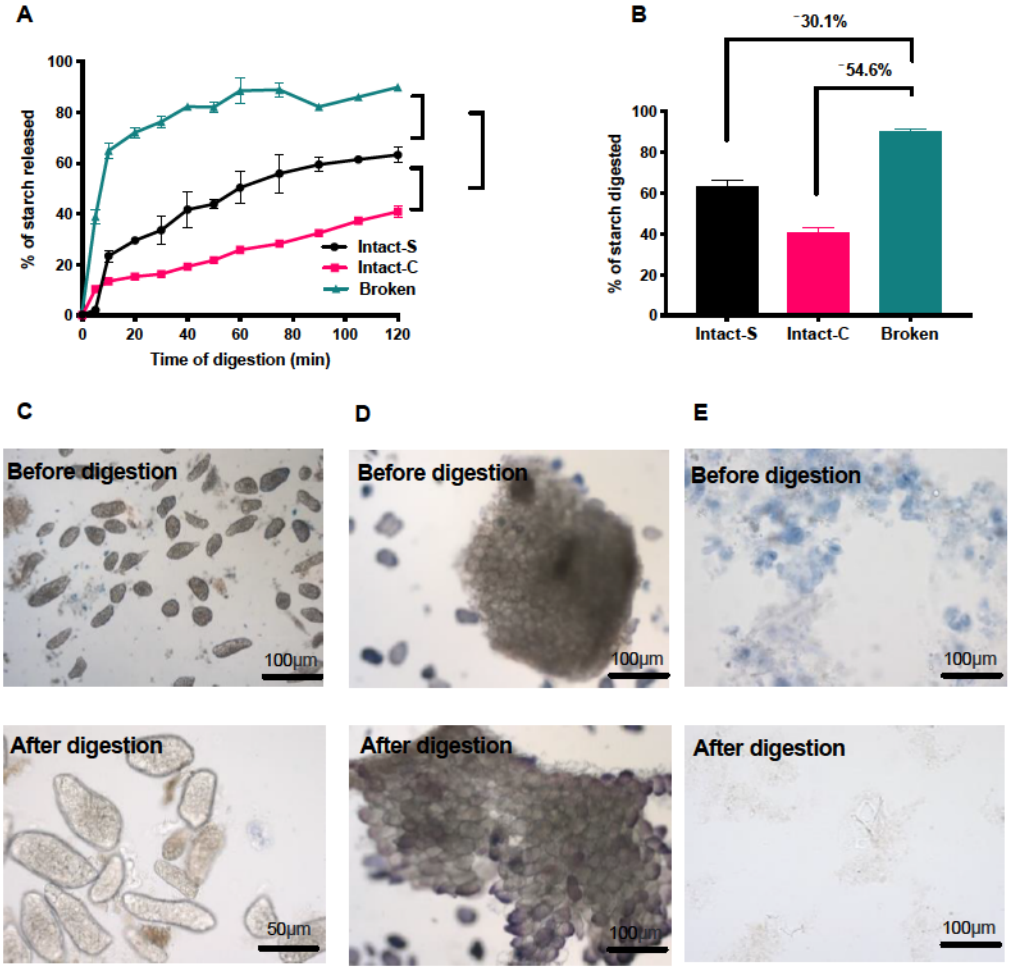


Figure 4. 2 In vitro digestibility properties of chickpeas with different structures. Starch amylolysis curves (A) and percentage of digested starch (B) at end of the digestion show highly significant differences between the Intact-S, Intact-C, and Broken groups. Microscopic images of intact single cells (C), clusters (D), and broken cells (E) of chickpea before and after two-hour in vitro digestion. Two-way ANOVA was performed on time series data. ***p<0.001. Intact-S, intact single cells; Intact-C, intact cell clusters; Broken, Broken cells.

4.4.2 Participants characteristics

13 participants were included in this human study. The characteristics are presented in **Table 4.2**. All subjects completed all three dietary interventions.

Table 4. 2 Participants Characteristics

Variable	Participants
Gender (M: F)	7:6
Age (y)	30.5±2.9[1]
BMI (kg/m^2)	24.3±0.7[1]
Weight (Kg)	70.8±2.8[1]
Fat mass (%)	21.1±1.5[1]

[1] Results presented as Mean ± SEM

4.4.3 Acute glycaemia and insulinaemia

The acute glycaemic response (0-180min) is shown in **Figure 4.3**. The two-way ANOVA suggested that there was a significant effect of food structure on acute glucose response ($p=0.02$). Plasma glucose concentrations were higher in the Broken compared to Intact-C at 15 ($p=0.04$) and 30min ($p<0.001$), and higher than Intact-S at 30,45 and 60min ($p<0.01$, $p<0.01$, and $p=0.03$, respectively). The $iAUC_{0\text{-}180min}$ was significantly higher in the Broken group compared to intact-S and intact-C groups ($p=0.001$, $p<0.001$, respectively).

Postprandial insulin levels were significantly affected by food structure ($p<0.01$). Serum insulin concentrations after the consumption of the Broken were significantly higher at 15min compared to the Intact-S group ($p=0.049$) and were higher than the Intact-C group during 30-90 min ($p=0.023$, $p=0.009$, $p=0.022$, $p=0.031$ respectively). Besides, there was a significant difference between Intact-S and Intact-C groups at 60min ($p=0.040$). The insulin $iAUC_{0\text{-}180min}$ of intact-C was substantially lower than both Intact-S and Broken groups ($p=0.002$, $p<0.001$ respectively).

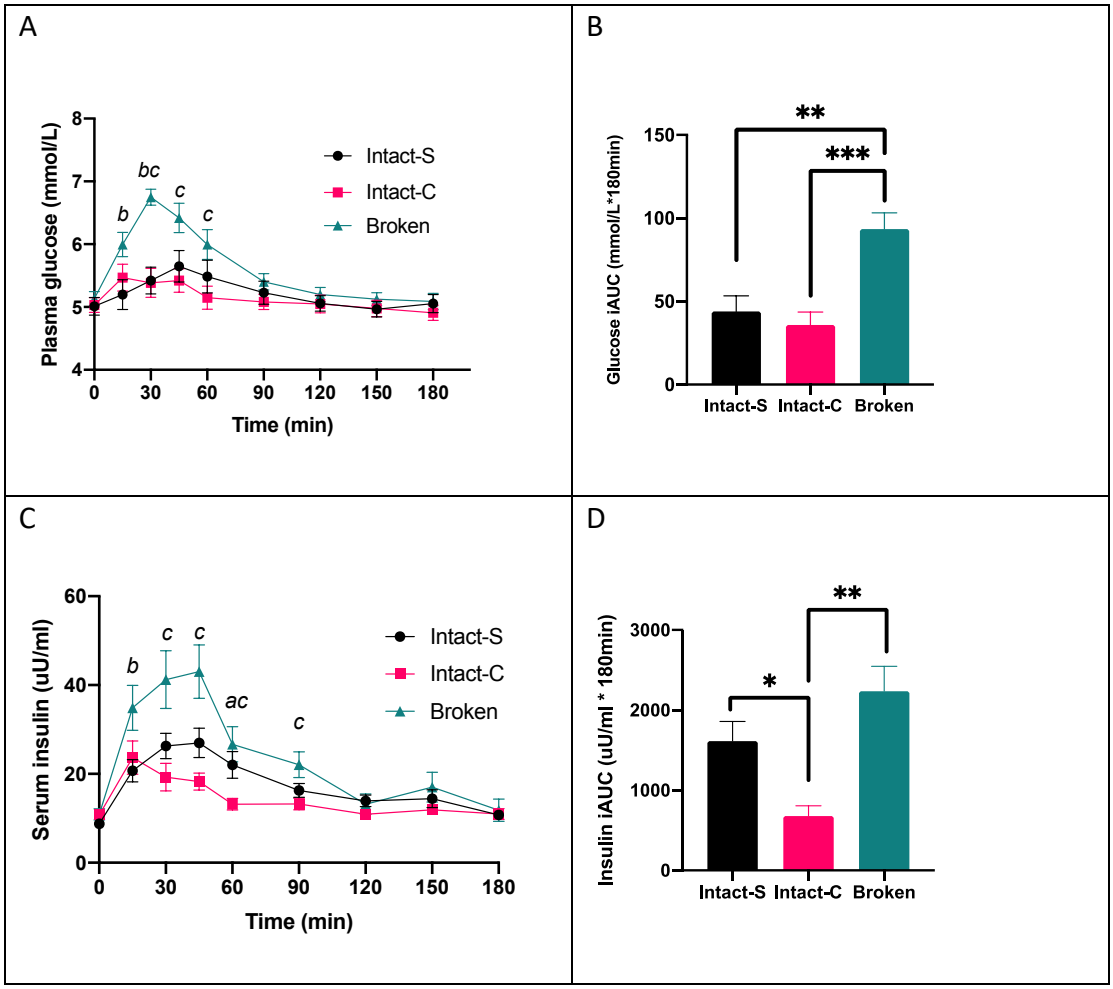


Figure 4. 3 Postprandial glycaemia changes following the consumption of chickpea test meals. Postprandial plasma glucose concentrations (A) and the incremental area under the curve (iAUC) between 0-180min (B). Postprandial serum concentrations (C) and iAUC between 0-180min (D). Data presented as mean ± SEM (n=13). Repeated measures two-way ANOVA with post hoc Tukey's test was performed to test the effect of diets, time points and their interactions. One way ANOVA was performed on iAUC data. Intact-S, intact single cells; Intact-C, intact cell clusters; Broken, Broken cells. Significant differences between interventions annotated: a – Intact-S vs Intact-C; b Intact-S vs Broken and c- Intact-C vs Broken. *p<0.05,**p<0.01,***p<0.001.

4.4.4 Cell wall structures during gastric and duodenal digestion

Figure 4.4 presents micrographs of chickpea cell structures at the stage of Initial Gastric, End Gastric, and End Duodenal digestion (15-180min post ingestion). Chickpea Intact-S (A-C) and Intact-C (D-F) remained relatively intact during 180min of gastric and duodenal digestion. Most of the starch was enclosed within cell matrices that acted as physical barriers. We observed reduced cell contents and starch leakage in some cells in the Intact-S group at the end of duodenal digestion. Comparably, starch leakage was less in Intact-C. Cells in the core of the clusters were largely unchanged. Some cells at the margins separated from the clusters but remained intact (E).

In Broken, the cell contents decreased continuously from the stomach to the duodenum (G-I), with most of the starch disappearing towards the end of duodenal digestion (180min). At a higher magnification (20 x), some cell wall fragments, and undigested starch were observed (I).

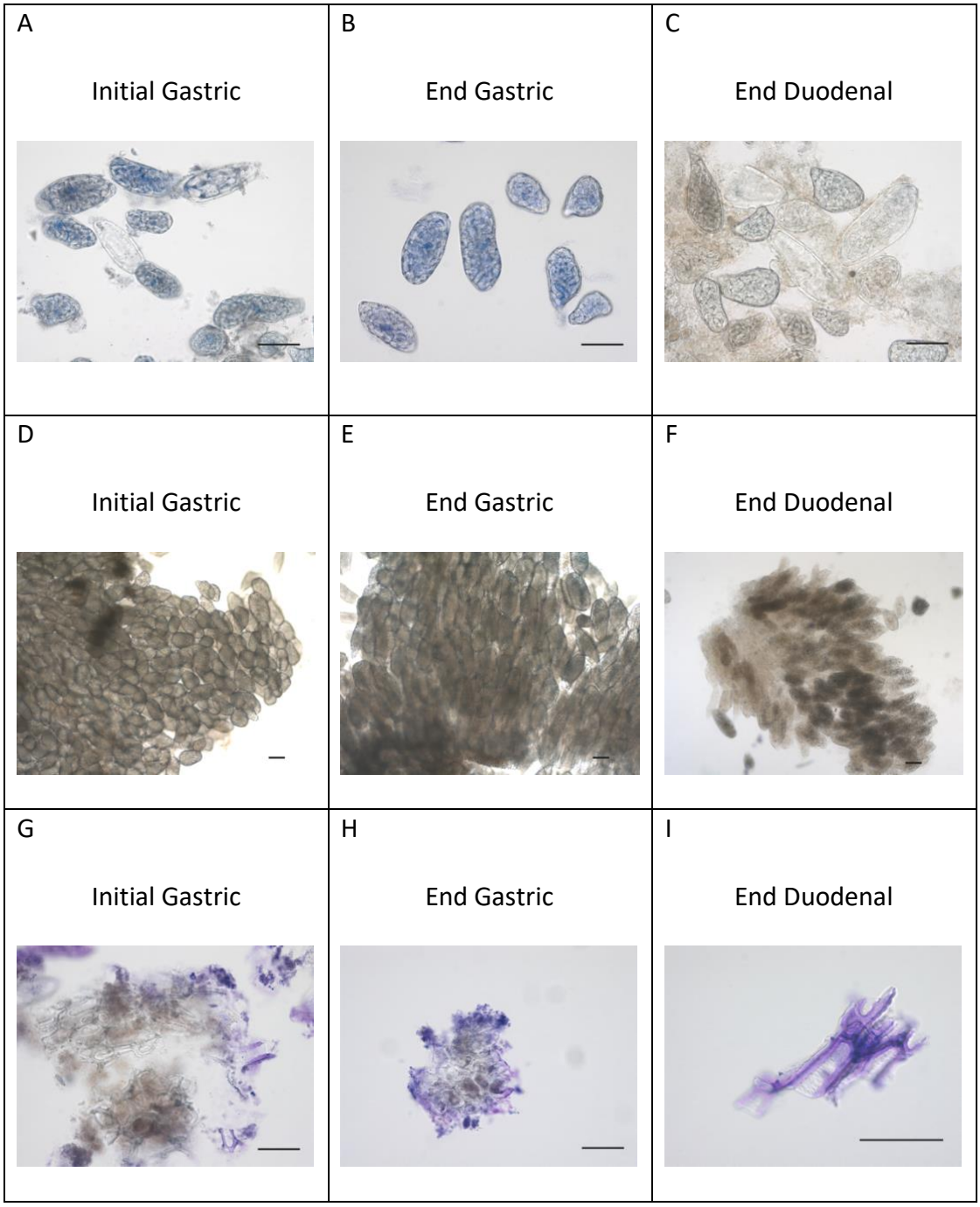


Figure 4. 4 Micrographs of chickpea cell structures during gastric and duodenal digestion.

Chickpea intact single cells at initial gastric (A), end gastric (B), and end duodenal of digestion(C). chickpea clusters at initial gastric (D), end gastric (E), and end duodenal of digestion(F). Chickpea broken cells at initial gastric (G), end gastric (H), and end duodenal of

digestion(I). All panels are light micrographs in which the starch was stained with toluidine blue. Scale bars represent a length scale of 50 μm.

4.4.5 Carbohydrate digestion in the stomach and duodenum

Maltose and glucose were measured in the gastric and duodenal samples (**Figure 4.5**). Luminal glucose matched the trend of luminal maltose over time, and maltose dominated in quantity. Some spikes were observed in duodenal curves which were not present in gastric glucose and maltose profiles, likely indicating the presence of gastric emptying.

Mixed-effect models indicated that food structure significantly affected gastric maltose ($p=0.001$), duodenal maltose ($p=0.026$), gastric glucose($p=0.001$) and duodenal glucose ($p=0.044$). In gastric samples (A and C), the concentrations of maltose remained the highest in Broken during 0-180min and the differences reached significance at most of the time points (Broken> Intact-S, T=15-90min and 150min; Broken > Intact-C, T= 15-165min, all $p<0.05$). Gastric maltose was higher in Intact-S than Intact-C at T= 75-90min. For gastric glucose, the difference between Broken and Intact-S was less pronounced and only observed at T=15min ($p=0.017$). Intact-C exhibited significantly lower gastric glucose than Intact-S (T=105-106, all $p<0.05$) and Broken (T=30min, 60-180min, all $p<0.05$).

Broken exhibited higher duodenal maltose (B) during 0-90min (Broken > Intact-S at T=60-75min; Broken>Intact-C at T=60min). Intact-S had higher duodenal maltose than Intact-C at T=30 and 180min. Similarly, duodenal glucose in Broken increased until 90min and declined

afterwards. Broken had higher duodenal glucose than Intact-S (T=45min) and Intact-C (T=90 and 135-150 min).

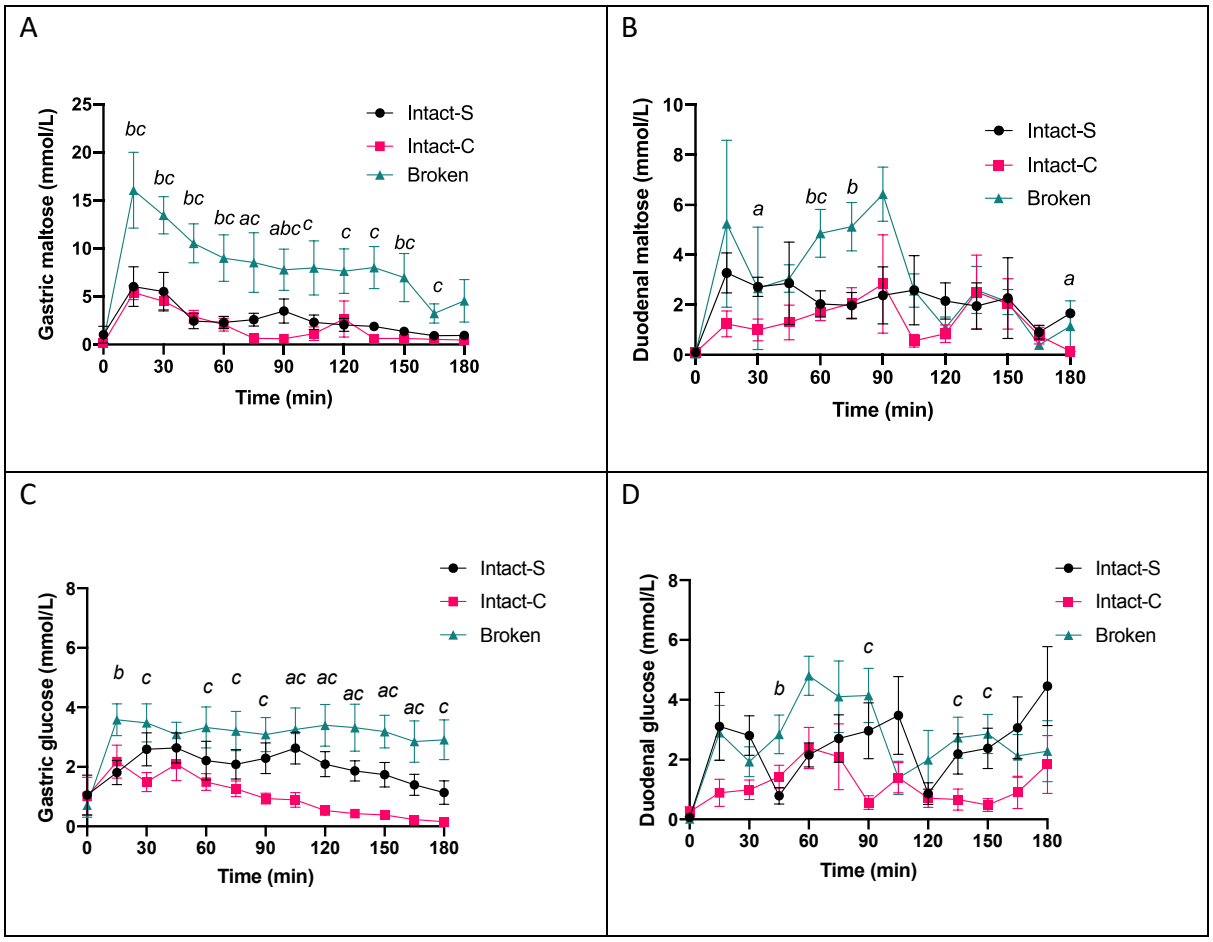


Figure 4. 5 Changes in maltose and glucose levels in the stomach and duodenum following the consumption of chickpea test meals. Gastric maltose (A), duodenal maltose (B), gastric glucose (C), and duodenal glucose (D) levels throughout 0-180min. Analyses were performed in 13 subjects on available samples and data were presented as mean ± SEM. Data did not pass normality distribution test and therefore logarithmic transformation was conducted before using Mixed-effect models. Mixed-effect models were performed to test the effect of diets, time points and their interactions. Intact-S, intact single cells; Intact-C, intact cell clusters; Broken, Broken cells. Significant differences between interventions annotated: a –

Intact-S vs Intact-C; b Intact-S vs Broken and c- Intact-C vs Broken. *p<0.05, **p<0.01, ***p<0.001

4.4.6 Metabolomic analysis of gastric and duodenal samples

The metabolomic profiling was assessed by ^{1}H-NMR followed by PLS-DA analysis (**Figure 4.6)**. Gastric samples at 15 min and duodenal samples at 60 min exhibited significant differences between Intact-S vs Broken (A and D), Intact-S vs. Broken (B and E), and Intact-S and Intact-C (C and F). PLS-DA analysis at all other time points (0-180min) were listed in Appendix 6.

Metabolites that drive the differences were identified. In gastric samples (**Table 4.3**), amylopectin/maltose and glucose were lower in Intact-S and Intact-C compared to Broken. Alanine was higher in Intact-C compared to Broken and Intact-S.

NMR identified dramatic differences in duodenal samples associated with food structure (**Figure 4.7** and **Table 4.4**), Brief, carbohydrates including amylopectin/maltose and glucose were significantly lower in intact structures compared to Broken. Amino acids including valine, leucine, isoleucine, glutamine, phenylalanine, and tryptophan were higher in Intact-C versus Broken. Intact-S and Intact-C had a higher release of taurine-conjugated bile acids compared to Broken.

To exemplify the luminal amino acid release, **Figure 4.8** presented the profiles of gastric alanine and duodenal phenylalanine**.** At T=15min, Intact-C exhibited a higher level of gastric alanine compared to Broken. At T=60 min, Intact-C showed a higher level of duodenal phenylalanine than Broken. These were in line with the results of the PLS-DA analysis above.

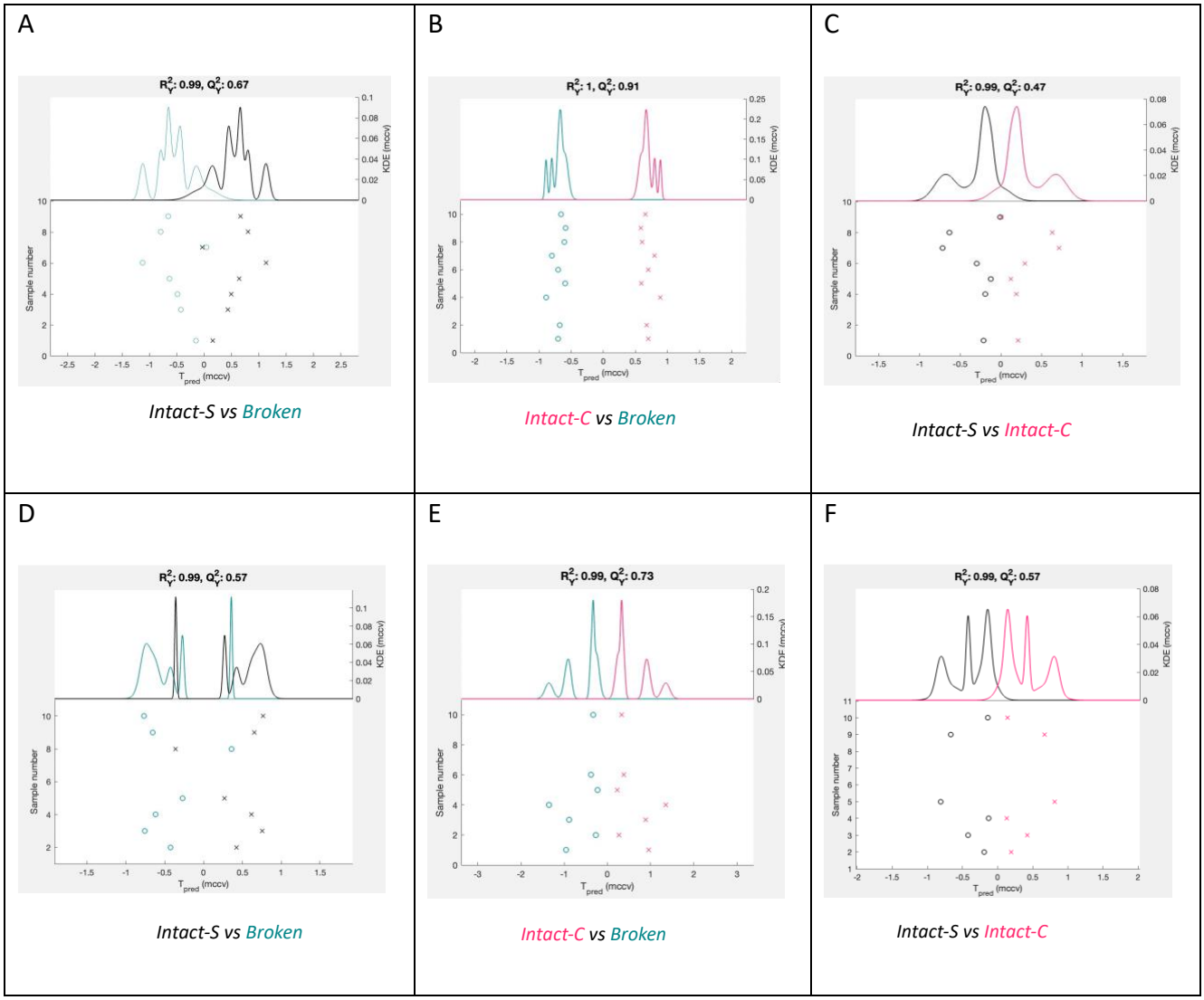


Figure 4. 6 RM-MCCV-PLS-DA score plots of ^{1}H-NMR gastric samples at 15min and duodenal samples at 60 min after consumption of chickpea test meals. The comparisons between Intact-S vs Broken (A), Intact-C vs. Broken (B), and Intact-S and Intact-C (C) in gastric samples at T=15min; and comparisons between Intact-S vs Broken (D), Intact-C vs. Broken €, and Intact-S and Intact-C (F) in duodenal samples at T=60min. Each dot represents the metabolic profile of one subject containing 18,600 spectra variables. The analysis was performed in available paired data. R^2 and Q^2 indicate the fit and predictability of the models. Intact-S, intact single cells; Intact-C, intact cell clusters; Broken, Broken cells.

Table 4. 3 Metabolites in the stomach associated with food structure.

Metabolite	Chemical Shift	Intact-S vs Broken		Intact-C vs Broken		Intact-C vs Intact-S	
		Association	P value	Association	P value	Association	P value
Glucose	4.65(d),5.20(d)	↓	1.45×10^{-8}	↓	6.03×10^{-9}	↓	4.92×10^{-5}
Amylopectin/ maltose	5.42(d), 3.60(d)	↓	1.02×10^{-5}	↓	3.88×10^{-8}	/	>0.05
Alanine	1.48 (d), 3.77(q)	/	>0.05	↑	5.07×10^{-5}	↑	3.25×10^{-5}

The chemical shifts and multiplicities are listed for peaks from significantly associated metabolites. Peaks are only listed if they are in the range of the processed data (9·5–5·5 and 4·5–0·5 ppm). Multiplicity key is as follows: s – singlet, d – doublet, t – triplet, q – quartet, dd – doublet of doublets, dq – doublet of quartets, 2d – two doublets, m – (other) multiplet.

↑ or ↓ indicates a higher or lower release from [X] between [X] vs [Y].

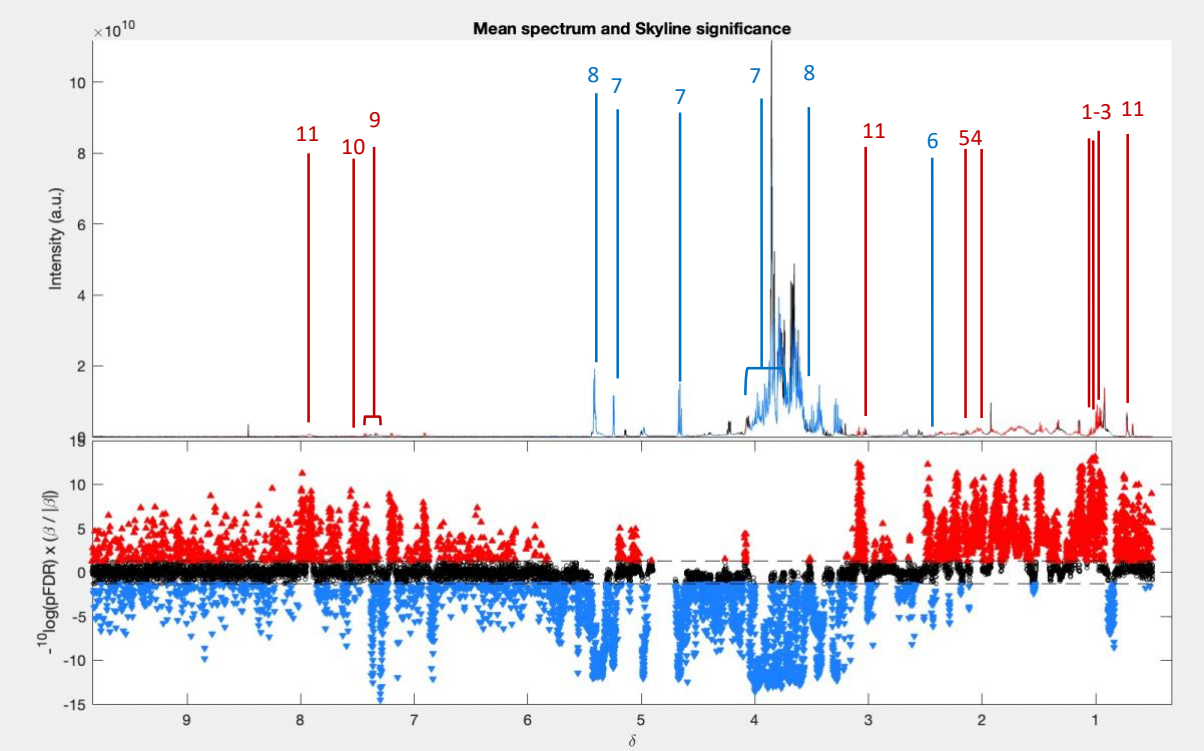


Figure 4. 7 An example of metabolite identification process in skyline significance plot in the comparison between Intact-C vs Broken. Red peaks indicate a higher release following the ingestion of Intact-C compared to Broken. Blue peaks indicate a lower release of Intact-C compared to Broken. Identified metabolites: 1- Valine, 2-Isoleucine, 3-Leucine, 4- Glutamine, 5-Glutamate, 6-Succinate, 7-Glucose, 8-Amylopectin, 9-Phenylalanine,10- Tryptophan, 11-Taurine-conjugated bile acid.

Table 4. 4 Metabolites in duodenum associated with food structure.

Number [a]	Metabolite	Chemical Shift [b]	Intact-S vs Broken		Intact-C vs Broken		Intact-C vs Intact-S	
			Association	P value	Association	P value	Association	P value
1	Valine	0.99(d), 2.46(m)	↑	6.03×10^{-6}	↑	4.04×10^{-6}	/	>0.05
2	Isoleucine	0.92(dd), 1.45(m), 2.01(m)	↑	6.25×10^{-5}	↑	6.20×10^{-5}	/	>0.05
3	Leucine	0.95(t), 1.73(m)	/	>0.05	↑	5.76×10^{-10}	↑	1.90×10^{-9}
4	Glutamate	2.02(m), 2.34(m)	↑	1.01×10^{-8}	↑	0.0003	/	>0.05
5	Glutamine	2.46(m), 6.90(s)	/	>0.05	↑	0.0006	↑	0.0005
6	Succinate	2.41(s)	↓	3.72×10^{-6}	↓	0.0002	/	0.06
7	Glucose	4.65(d),5.20(d)	↓	7.22×10^{-10}	↓	1.57×10^{-11}	↓	9.52×10^{-5}
8	Amylopectin/ Maltose	5.42(d), 3.60(d)	↓	6.78×10^{-6}	↓	1.43×10^{-10}	↓	0.008
9	Phenylalanine	7.35(m),7.38(m), 7.43(m)	/	>0.05	↑	0.0002	/	>0.05
10	Tryptophan	7.5(d), 7.7(d)	↑	0.006	↑	1.83×10^{-6}	↑	8.07×10^{-5}
11	Taurine-conjugated bile acids	7.9-8.0(dd), 3.10(m), 0.7	↑	4.78×10^{-5}	↑	1.78×10^{-8}	/	>0.05

[a] Number is related to the labels in **Figure 4.7**.

[b] The chemical shifts and multiplicities are listed for peaks from significantly associated metabolites. Peaks are only listed if they are in the range of the processed data (9·5–5·5 and 4·5–0·5 ppm). Multiplicity key is as follows: s – singlet, d – doublet, t – triplet, q – quartet, dd – doublet of doublets, dq – doublet of quartets, 2d – two doublets, m – (other) multiplet.

↑ or ↓ indicates a higher or lower release from [X] between [X] vs [Y].

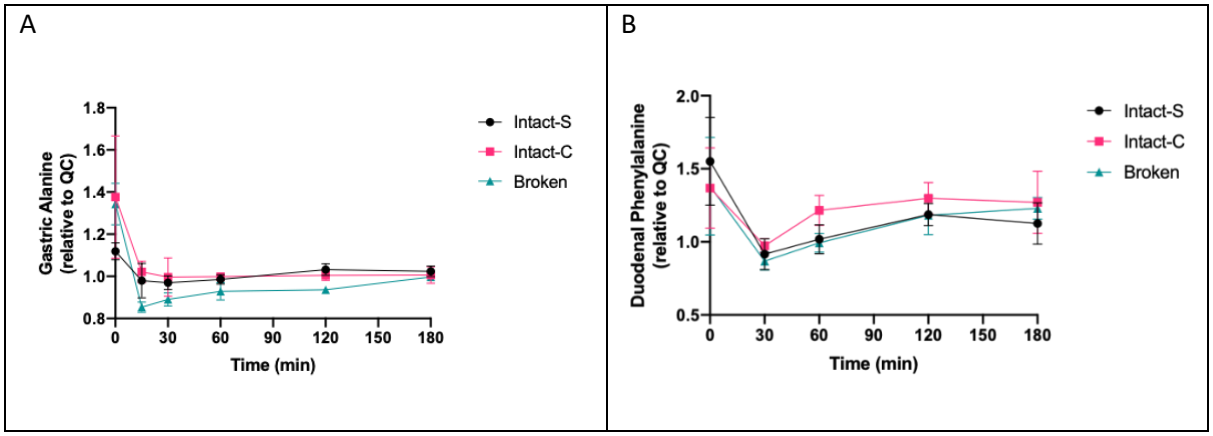


Figure 4. 8 Profiles of gastric alanine and duodenal phenylalanine relative concentrations. The relative amount of gastric alanine (A) and duodenal phenylalanine (B) over time following the consumption of chickpea meals. QC, quality control, a pooled quality control (QC) sample in which a small aliquot of each biological sample in the study was mixed. The relative amount of alanine was calculated by area under peak corresponding to the NMR signal of 1.48 (d) and 7.35(m) ppm, respectively.

4.4.7 Gut hormones

4.4.7.1 GIP

Postprandial response of GIP is shown in **Figure 4.9**. Broken had a rapid increase in GIP during 0-30 min and reduced to the baselines; whilst Intact-S had a slow but prolonged increase in GIP levels. Intact-C had a prolonged but less extent of GIP increase compared to Intact-S. Two-way ANOVA demonstrated that there was a significant interaction effect between diet and time points ($p<0.001$). Broken had higher GIP levels than Intact-S (T=30min, p=0.025) and Intact-C (T=30-90min, p=0.002, 0.012, 0.001, 0.019, respectively). GIP of Intact-S was higher than Intact-C during T=30-120min (p=0.014, 0.014, <0.001, 0.005, and 0.011 respectively). At 180min, GIP levels of Intact-S and Intact-C groups were significantly higher than the Broken group (p=0.002, p=0.024 respectively).

Due to different patterns of GIP increase, iAUC was calculated during 0-60min, 60-180min and 0-180min (B-D). The $iAUC_{0\text{-}60min}$ for GIP ranked as: Broken> Intact-S> Intact-C (Intact-S vs Intact-C, p=0.009; Intact-S vs Broken, p=0.039; Intact-C vs Broken, p=0.003). The $iAUC_{60\text{-}180min}$ and $iAUC_{0\text{-}180min}$ for GIP were higher in Intact-S compared to Intact-C (p=0.015, p=0.008 respectively).

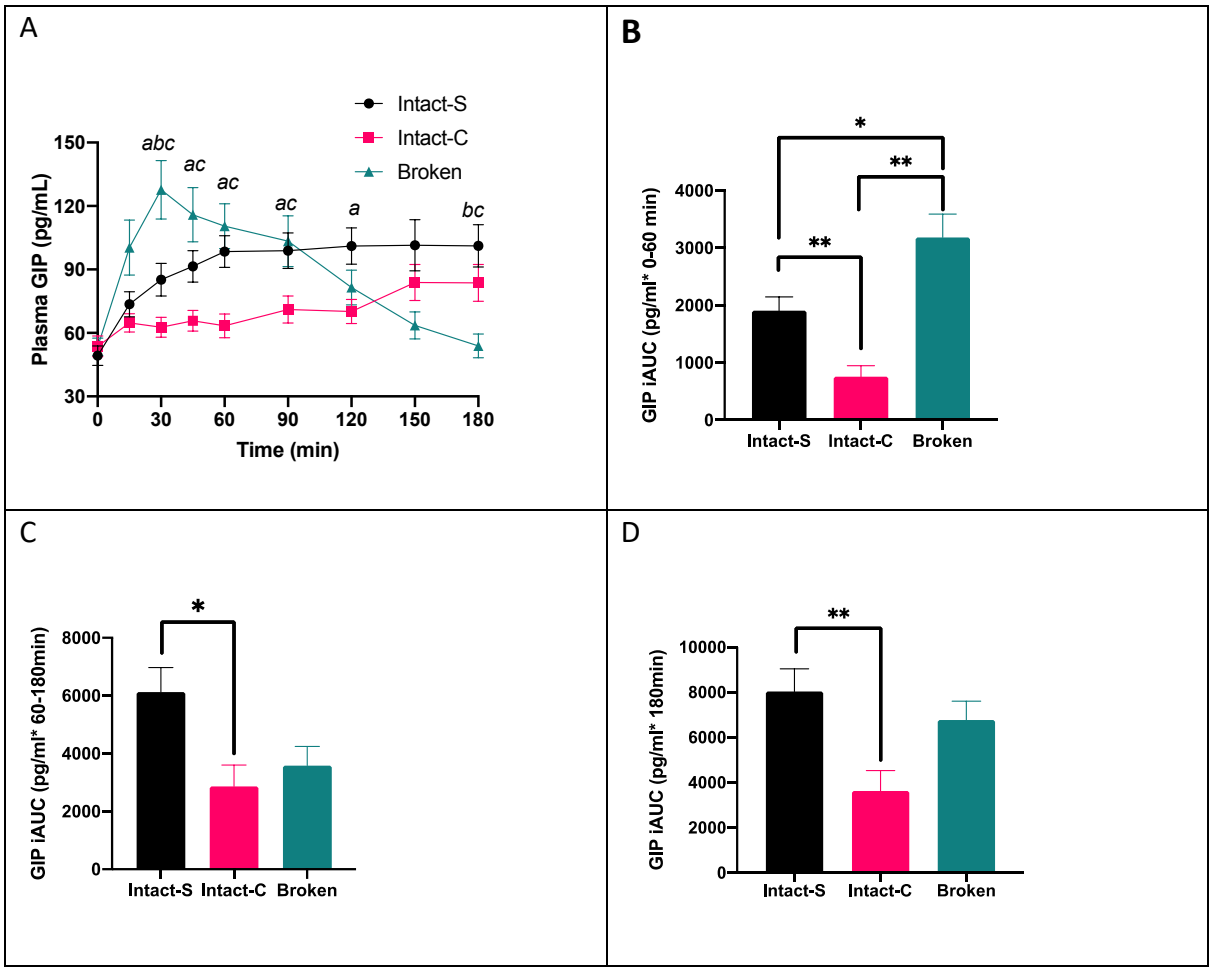


Figure 4. 9 Postprandial GIP concentrations following the consumption of chickpea test meals. GIP concentrations over time (A), the incremental area under the curve (iAUC) between 0-60 (B), 60-180min (C) and 0-180m (D). Data presented as mean ± SEM (n=10). Repeated measures two-way ANOVA with post hoc Tukey's test was performed to test the effect of diets, time points and their interactions. One way ANOVA was performed on iAUC data. Intact-S, intact single cells; Intact-C, intact cell clusters; Broken, Broken cells. Significant differences between interventions annotated: a – Intact-S vs Intact-C; b Intact-S vs Broken and c- Intact-C vs Broken. *p<0.05,**p<0.01,***p<0.001.

4.4.7.2 GLP-1

Time course and iAUC data for the GLP-1 are shown in **Figure 4.10**. There was a significant effect of diet (p=0.002) and the interaction between time points and diets (p=0.034). The post-hoc test found that at 30min, Broken had a higher level of GLP-1 than Intact-C group (p=0.008); GLP-1 of Intact-S group was significantly higher than the group of Broken during 90-180min (p=0.031, p=0.032, p=0.029, and p=0.014, respectively).

The $iAUC_{0\text{-}60min}$ was significantly higher for Broken compared to Intact-C (p=0.007). The $iAUC_{60\text{-}180min}$ was higher for Intact-S compared to Broken (p=0.026). No differences were observed between groups for GLP-1 $iAUC_{0\text{-}180min}$.

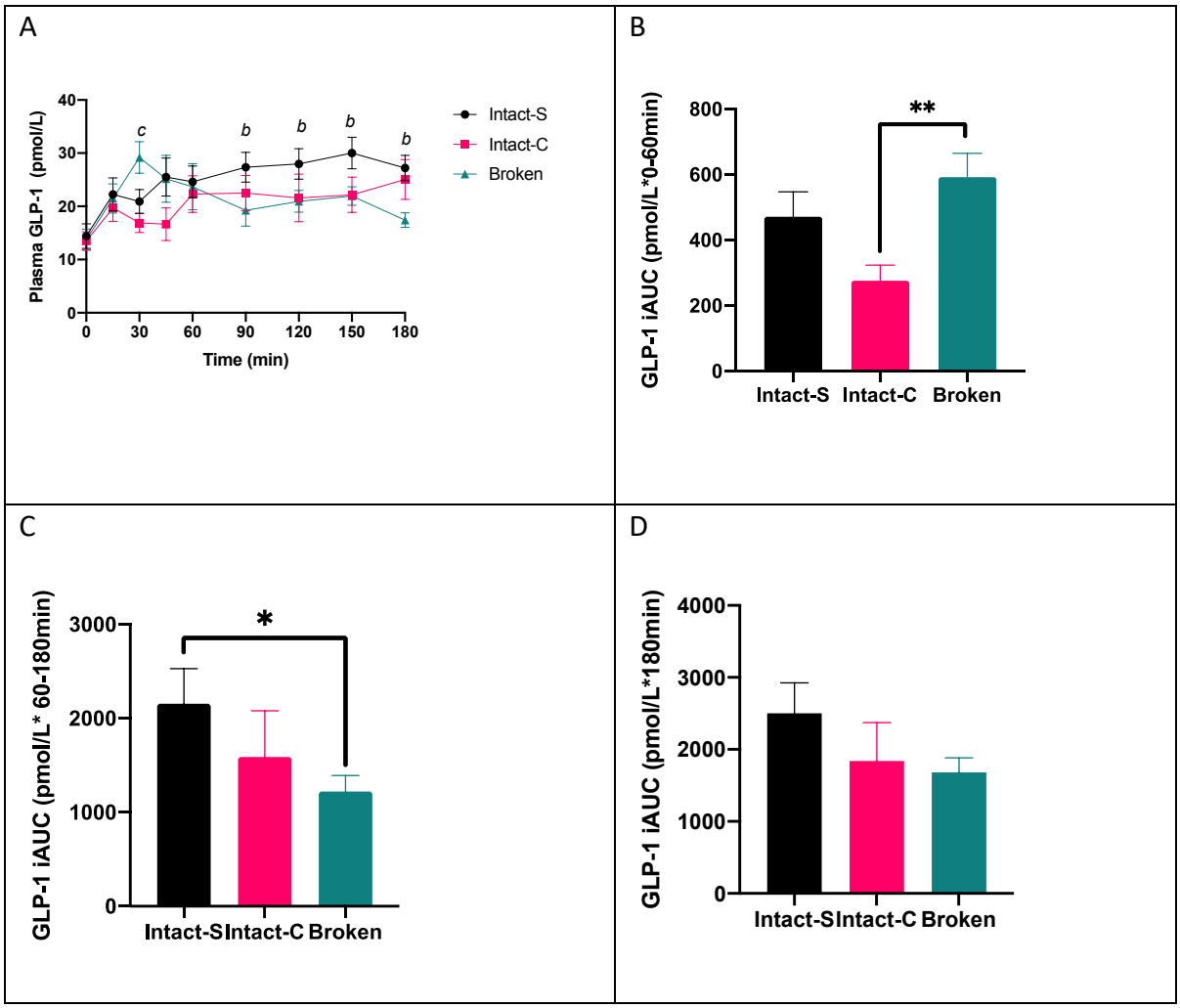


Figure 4. 10 Postprandial GLP-1 concentrations following the consumption of chickpea test meals. GLP-1 concentrations over time (A), the incremental area under the curve (iAUC) between 0-60 min(B), 60-180min (C) and 0-180 min (D). Data presented as mean ± SEM (n=10). Repeated measures two-way ANOVA with post hoc Tukey's test was performed to test the effect of diets, time points and their interactions. One way ANOVA was performed on iAUC data. Intact-S, intact single cells; Intact-C, intact cell clusters; Broken, Broken cells. Significant differences between interventions annotated: a – Intact-S vs Intact-C; b Intact-S vs Broken and c- Intact-C vs Broken. *p<0.05, **p<0.01,***p<0.001.

4.4.7.3 PYY

Postprandial response of PYY is shown in **Figure 4.11**. Two-way ANOVA suggested food structure significantly affected PYY response (p=0.010). Post-hoc test found at 30min, PYY level of Intact-S was significantly higher than Intact-C (p=0.033).

Intact-S had increased PYY $iAUC_{0\text{-}60min}$ than Intact-C and Broken (p=0.041, p=0.009, respectively). There was no significant difference found for PYY $iAUC_{60\text{-}180min}$ or $iAUC_{0\text{-}180min}$, for PYY $iAUC_{0\text{-}180min}$, Intact-S was marginally higher than the Broken (p=0.09).

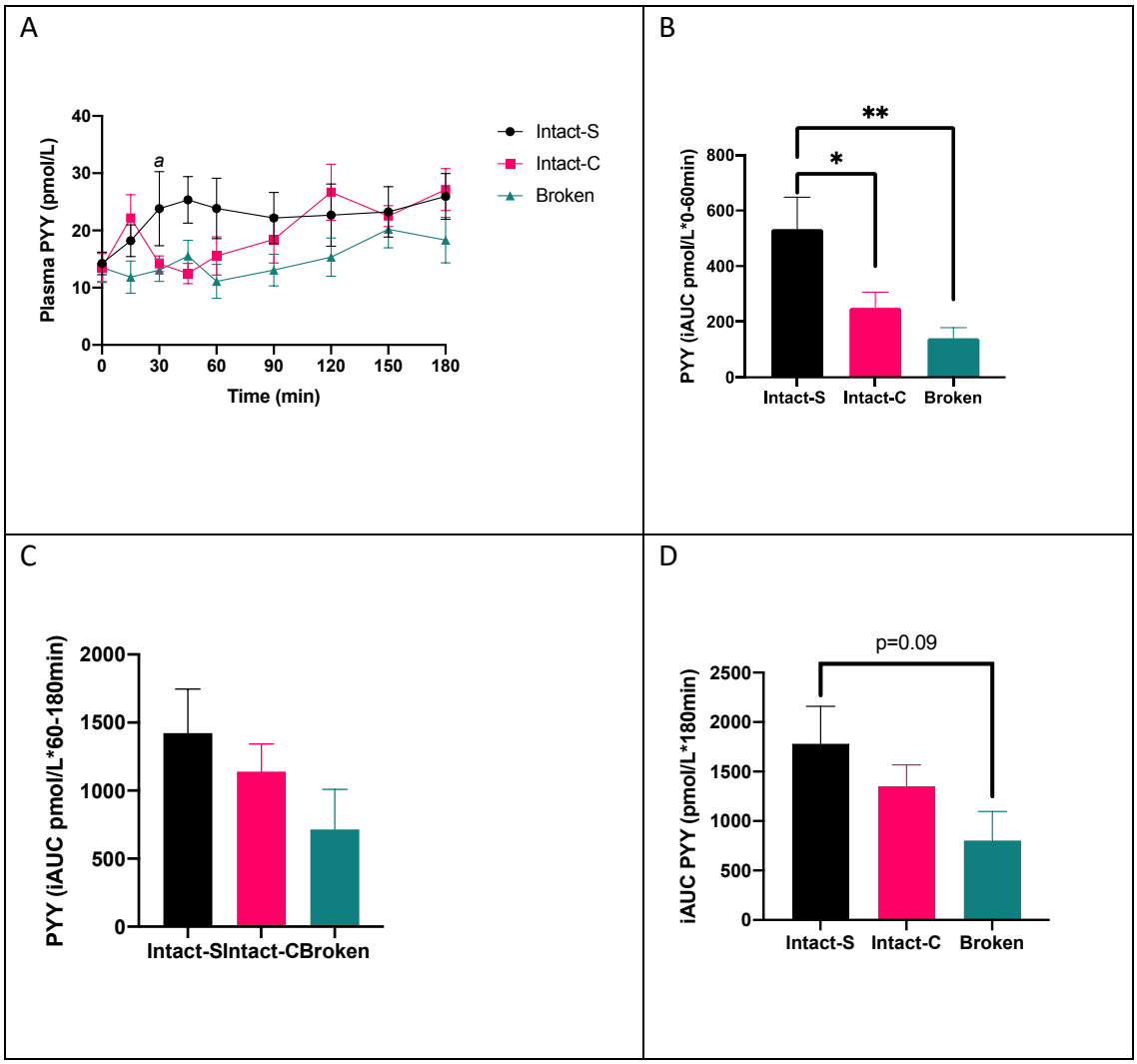


Figure 4. 11 **Postprandial PYY concentrations following the consumption of chickpea test meals.** PYY concentrations over time (A) and the incremental area under the curve (iAUC) between 0-60 min(B), 60-180min (C) and 0-180min (D). Data presented as mean ± SEM (n=10). Repeated measures two-way ANOVA with post hoc Tukey's test was performed to test the effect of diets, time points and their interactions. One way ANOVA was performed on iAUC data. Intact-S, intact single cells; Intact-C, intact cell clusters; Broken, Broken cells. Significant differences between interventions annotated: a – Intact-S vs Intact-C; b Intact-S vs Broken and c- Intact-C vs Broken. *p<0.05, **p<0.01,***p<0.001

4.4.8 Subjective appetite and *ad libitum* food intake

The subjective appetite was measured by the feeling of hunger, fullness, desire to eat, and appetite for a meal, as shown in **Figure 4.12 A-D**. No significant differences were observed in time course data. There was a significant difference in $iAUC_{0\text{-}180min}$ for feeling of fullness between treatments (p=0.005). Fullness $iAUC_{0\text{-}180min}$ of Intact-S was significantly higher than Intact-C (p=0.003) and Broken groups (p=0.030).

Composite appetite score was calculated as ([Feeling of hunger] + [100- feeling of fullness]+ [desire to eat]+ [appetite for a meal])/4. As shown in **Figure 4.12 E**, the iAUC for composite appetite score of Intact-S group was significantly lower than Intact-C (p<0.001) and Broken groups (p=0.030). No difference was found in *ab libitum* food intake between interventions which was measured at 240min postprandially (**Figure 4.12 F**).

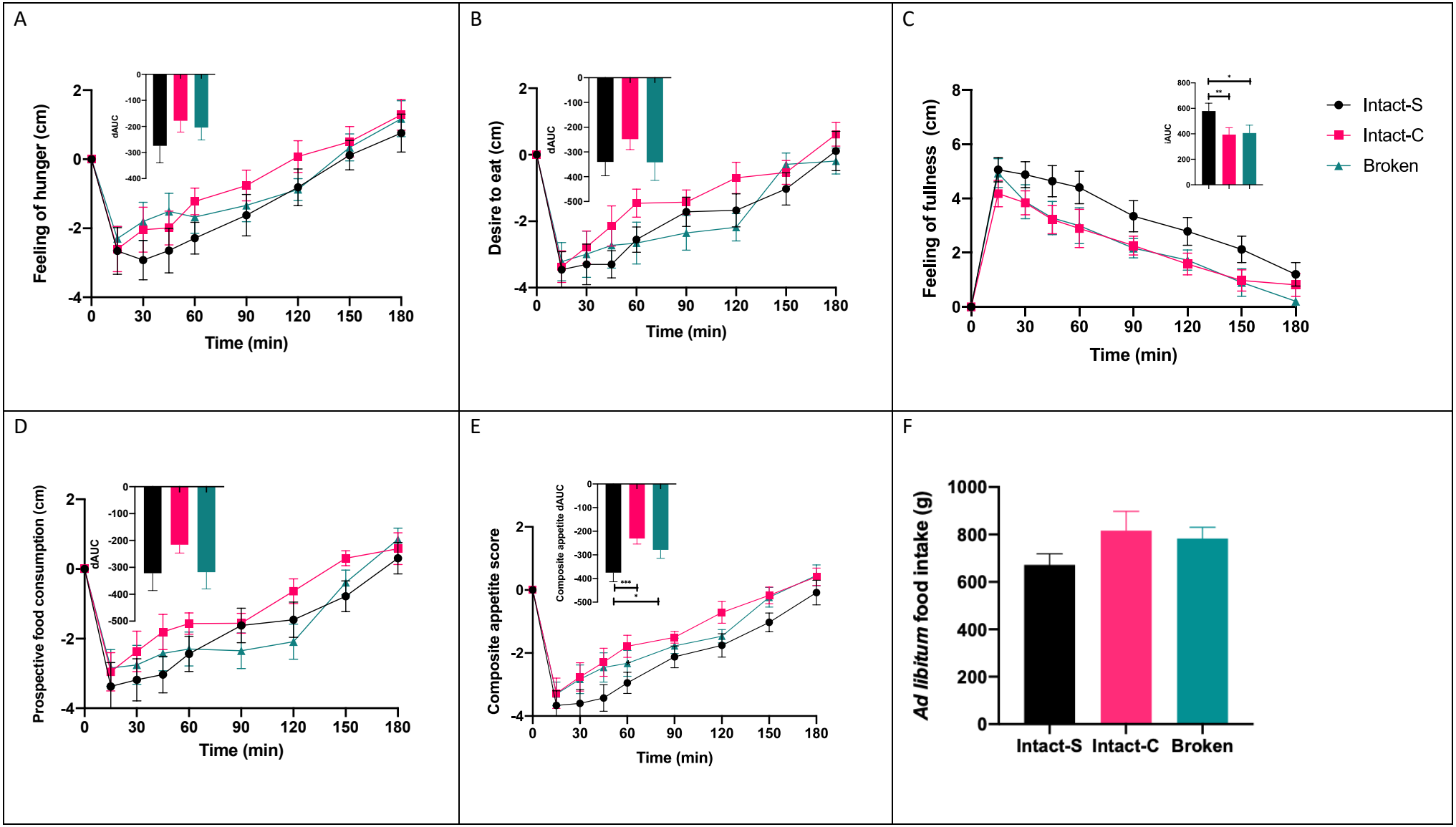

A
Feeling of hunger (cm)
Time (min)
dAUC
B
Desire to eat (cm)
Time (min)
dAUC
C
Feeling of fullness (cm)
Time (min)
iAUC
Intact-S
Intact-C
Broken
D
Prospective food consumption (cm)
Time (min)
dAUC
E
Composite appetite score
Time (min)
Composite appetite dAUC
F
Ad libitum food intake (g)
Intact-S
Intact-C
Broken

Figure 4. 12 Appetite changes following the consumptions of chickpea test meals. Feeling of hunger (A), fullness (B), desire to eat (C), appetite for a meal (D), composite appetite score (E), and ab libitum food intake at 4h postprandially (F). Data presented as mean ± SEM (n=13). Repeated measures two-way ANOVA with post hoc Tukey's test was performed to test the effect of diets, time points and their interactions. One way ANOVA was performed on iAUC data. Intact-S, intact single cells; Intact-C, intact cell clusters; Broken, Broken cells. Significant differences between interventions annotated: a – Intact-S vs Intact-C; b Intact-S vs Broken and c- Intact-C vs Broken. *$p<0.05$,**$p<0.01$,***$p<0.001$.

4.4.9 Association between gut carbohydrates, glycaemia and appetite: a correlation matrix

Spearman's correlation tests were performed to understand the association between gut carbohydrates, glycaemia and appetite markers, regardless of food structure (**Figure 4.13**).

Association with glycaemic biomarkers

Gastric and duodenal maltose and glucose established moderate and significant correlations with blood glucose, insulin and GIP ($0.25 \leq r \leq 0.41$, all $p<0.05$). Gastric maltose was the most significant correlator to plasma glucose ($r=0.41$, $p<0.001$); duodenal maltose demonstrated the strongest correlation with insulin and GIP levels ($r=0.47$, $p=<0.001$; $r=0.42$, $p<0.001$). GIP and GLP-1, as incretin hormones, were correlators to insulin ($r=0.53$, $r=0.40$ respectively).

Association with PYY and GLP-1

No significant correlation was found between gastric and duodenal carbohydrates with PYY or GLP-1, except for the association between duodenal maltose and GLP-1 ($r=0.23$, $p<0.05$). There was a positive correlation between PYY and GLP-1 ($r=0.23$, $p<0.01$).

Association with appetite VAS measurements

Composite appetite was negatively correlated with starch digestion products in the stomach and duodenum, with gastric glucose being the strongest predictor ($r=-0.39$, $p<0.001$).

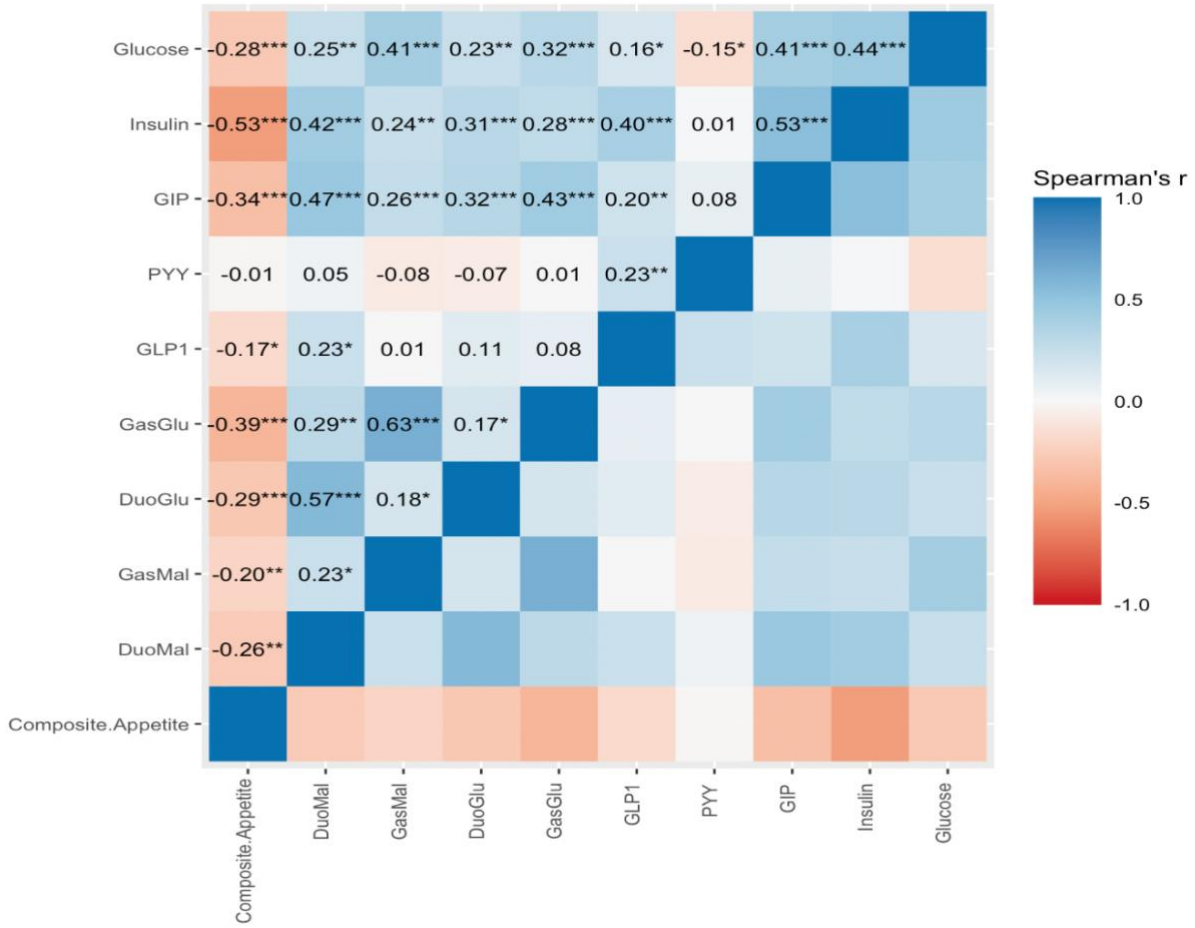


Figure 4. 13 Spearman's correlation t tests between gut carbohydrates, glycaemic and appetite markers regardless of food structure. GasGlu, gastric glucose; DuoGlu, duodenal glucose; GasMal, gastric maltose; DuoMal, duodenal maltose. The colour and number represent the direction and strength of the correlations. *p<0.05,**p<0.01,***p<0.001.

4.5 Discussion

4.5.1 Summary of findings

- Microscopic analyses revealed that Intact-S and Intact-C maintained largely intact in the stomach and duodenum. Intact-C had less starch leakage suggesting its stronger barrier effect.
- Intact-S and Intact-C led to slower rates of glucose and maltose release compared to Broken and incomplete digestion in human stomach and duodenum.
- Intact-S and Intact-C attenuated postprandial responses of blood glucose, insulin and GIP response compared to Broken. Intact-S exhibited higher GIP and insulin response than Intact-C reflecting its higher glucose availability in the small intestine.
- Intact-S had higher means of PYY and GLP-1, increased feeling of fullness and reduced composite appetite scores compared to Intact-C and Broken. Intact-S did not significantly affect *ad libitum* food intake at 240min postprandially.
- Moderate and significant correlations were found between gastric and duodenal carbohydrates with glycaemic and appetite markers.
- Metabolic profiling measured by NMR demonstrated significant differences in the gastric and duodenal digesta between food structure. A lower release of carbohydrates, while a higher release of amino acids and bile acids was identified in intact structure groups versus chickpea broken structure.

4.5.2 Detailed discussion

The aim of this study was to investigate structural changes in plant cell walls during gastric and duodenal digestion and subsequent metabolic responses. 13 subjects consumed chickpea meals with broken cells (Broken), individual intact cells (Intact-S) and cell clusters (Intact-C) and provided 180-minute intestinal and blood samples. The current results agreed with our hypothesis and confirmed the key role of cell wall structure in digestive kinetics and postprandial glucose. Digestion and metabolomic profiles in the upper GI tract explained the postprandial response. Without the protection of the cell wall, Broken released 'free' starch, which was then accessible by amylase. As microscopic observation showed, the starch was almost digested at the end of duodenal digestion (180 minutes). Quantitative data and metabolic profile confirmed its higher digestibility. In contrast, the cell walls of Intact-C and Intact-S remained largely intact and provided an effective digestive barrier, thereby reducing the rate of release of luminal maltose and glucose and lowering the glycaemic response. Intact-C appeared to provide a stronger barrier than Intact-S, as evidenced by its lower intraluminal carbohydrate release, higher cell wall integrity and lower starch leakage. Moreover, Intact-S enhanced satiety compared to Intact-C and Broken, potentially due to elevated GLP-1 and PYY levels, particularly with GLP-1 establishing a negative correlation with CAS. In conclusion, these data emphasise the importance of the gastric and duodenal environment for postprandial blood glucose and appetite. Carbohydrate food structure can be modulated to improve acute postprandial glycaemia in healthy subjects.

Structural changes in the stomach and duodenum

Our study compared the structural changes of Broken, Intact-S and Intact-C during digestion in the upper gastrointestinal tract. To the best of our knowledge, such comparison has not

been reported before. Comparing the original meal (Figure 4.2) with the gastric initiation phase (Figure 4.3), the starch content in Broken was significantly reduced, suggesting its early and rapid digestion. For Intact-S, although the majority of the cell walls remained intact, there were some cells where the cell walls were slightly opened, and the starch content was leached out. This suggested that the mechanical effects of mastication and gastric grinding disrupted the single cells to some extent. For Intact-C, the cell clusters did not appear to be affected by mastication and the cells remained tightly and integrally arranged. Comparing before and after gastric digestion (15 min vs. 180 min), the integrity of Intact-S and Intact-C remained relatively unchanged. We noted that the amount of starch leached by Intact-S during the gastric initiation phase was reduced in the sample at T=180. This indicated that salivary amylase, which entered the stomach with the food, may still be active and able to digest starch. For Intact-C, the structure of the clusters remained intact, encasing a large amount of starch. At the end of the duodenal digestion, the starch content in Broken continued to decrease and only a very small amount of starch content and small cell wall fragments could be seen under a high magnification. For Intact-S, a proportion of empty and open cells and starch exudation was observed. In Intact-C, cells at the edges of the cell clusters showed some degree of separation, however they remained intact, as did the inner cells. We observed minimal spreading of starch from the cells in Intact- C. However, it is important to note a limitation of this study, which was the inhomogeneous staining of the samples. The intracellular starch from Intact-C was less stained compared to that of Broken and Intact-S, likely due to the lower permeability of the samples.

To summarize, microscopic analysis suggested that Intact-C provided a stronger digestion barrier compared to Intact-S. This is likely due to their structural features, as the cell clusters

have less contact area with amylase compared to individual cells. Cells that are at the inner core of the cluster preserved higher structural integrity than individual cells, as being protected by the outer cells. Starch digestion in the intact macroparticles of wheat started from the edge and moved toward the inside of clusters as an "outside-in" pattern (Edwards et al., 2015a). Future investigations should measure whether Intact-C can reduce the extent of starch digestion in the small intestine and deliver more RS to the distal gut.

Maltose and glucose release in the stomach and duodenum

The structural analysis above explained the starch digestion in the stomach and duodenum. Starch is converted by salivary and pancreatic amylase into maltose (Chaikomin et al., 2006). Broken resulted in a rapid and dramatic rise in gastric maltose concentrations (peak at T=30 min), which was consistent with microscopic analysis and confirmed its susceptibility to salivary amylase digestion. Intact-S and Intact-C exhibited slower maltose release rates in the stomach from 0-180 min compared to Broken, as they were mostly encapsulated by intact cell walls. The findings regarding the gastric glucose are interesting. Glucose in the stomach followed the same trend as maltose in the stomach, but in smaller amounts. Glucose production and absorption occur in the small intestine, where maltose is hydrolysed by intestinal maltase (Larner and McNickle, 1955, Singh and Gallier, 2014). The glucose we observed in the stomach should have come mainly from free sugars in the diet. However, maltase has been found in human saliva containing oral bacteria (Birkhed et al., 1975). We, therefore, speculated that some bacterial maltase in saliva converted maltose to glucose, thus explaining the elevated gastric glucose.

In the duodenum, the differences were observed mainly between 0-90min when Broken had higher levels of maltose and glucose compared to intact structures. Additionally, we observed that the duodenal maltose and glucose profiles exhibited “up and down” patterns over the 180min period , a phenomenon not seen in the stomach or *in vitro* duodenal models (Bhattarai et al., 2017). The underlying cause of these “spikes” remains unknown, and we speculate that they may be related to complex physiological events in the duodenum. For instance, the occurrences of gastric emptying and/or dilution through endogenous secretions may play a role in the duodenal carbohydrate concentrations.

Postprandial blood glucose, insulin, and GIP

Postprandial glucose and insulin were significantly lower in Intact-S and Intact-C compared to Broken. These agreed with the hypothesis and corroborated the findings of Bajka *et al.,* which reported that PulseOn made from intact chickpea cells lowered glucose $iAUC_{0\text{-}45min}$ compared to disrupted cells (Bajka et al., 2021). Broadly, several RCTs compared starchy foods with intact structures versus processed structures, as summarized in Chapter 2; the present data aligned with the pooled analysis and led to the conclusion that intact cell wall structure can attenuate postprandial levels of glucose and insulin compared to disrupted cells. Our study observed the differences in postprandial glycaemia mainly during 0-90min, corresponding to the time when higher duodenal carbohydrate in Broken was observed. Glucose absorption mainly happens in the small intestine. Broken released increased glucose, crossing the intestinal brush border membrane (BBM) mediated by SGLT1 and entering the blood circulation (Wu et al., 2020). Our study supported the role of intact structure in attenuating glycaemia by reducing the rates of digestion.

GIP is secreted from K cells stimulated by the presence of glucose in the small intestine, and subsequently stimulates insulin secretion (Seino et al., 2016). GIP response reflects the rates of intestinal glucose release and absorption (Chaikomin et al., 2006) and exhibited distinct time profiles between food structures in our study. Intact-S exhibited a slow but sustained increase in GIP levels, compared to Broken, which had a quick increase in GIP within the first 30 minutes before dropping to baseline levels. Compared to Intact-S, Intact-C showed a sustained but smaller GIP rise. We observed that $iAUC_{0\text{-}60min}$ for GIP ranked as: Broken> Intact-S> Intact-C, reflecting the rates of digestion and carbohydrate release during such period. This was aligned with previous RCTs investigating the acute effects of food structure in GIP (Petropoulou et al., 2020, Mackie et al., 2017b). In Edwards et al., intact wheat endosperm cells lowered the rate of starch digestion in the ileal fluids and reduced GIP response compared to disrupted cells (Edwards et al., 2015a). These evidence altogether suggested that intact cell walls limited glucose release and absorption, thereby reducing the magnitude of GIP response.

Previous studies have not compared postprandial glycaemia between single cells and cell clusters. In our study, postprandial glucose did not differ between Intact-C and Intact-S. Intact-C significantly lowered the iAUC of insulin and GIP (0-180min) compared to Intact-S. This may reflect the higher glucose absorption of Intact-S in the proximal intestine. In support of this, quantitative and metabolomic analyses showed that Intact-S released more carbohydrate in the duodenum. Insulin secretion is stimulated by a rise in blood glucose sensed by pancreatic beta cells (Kwon, 2021). Intact-S had more luminal glucose released which entered the bloodstream, increasing the demand for insulin.

Gut luminal carbohydrates and relation to postprandial glucose

Moderate and significant correlations were found between postprandial glycaemia markers (glucose, insulin, and GIP) and gastric and duodenal carbohydrates ($0.25<=r<=0.41$, all $p<0.05$). This provided solid evidence emphasising the central role of luminal digestion in postprandial glycaemia. Interestingly, plasma glucose was more correlated with gastric maltose than duodenal maltose or glucose. It has been commonly thought that starch digestion in the gastric phase is negligible, given that salivary amylase entering the stomach would be inactivated by the acidic pH shortly (Brownlee et al., 2018a). However, it can be argued by the observation that the amylolytic activity of saliva could maintain 50% of the maximal activity at pH 4.0 (Freitas et al., 2018). In the present study, we observed that the pH in the gastric aspirated samples was in a range of 4-5 initially after meal consumption and did not drop below 3.5 until 60minute post-ingestion (Appendix 7). Moreover, a decrease in the starch content of the gastric aspirate was observed during T=15-180 min. These observations support that salivary amylase may play a more significant role in starch digestion and postprandial glycaemia than generally considered.

Duodenal glucose and maltose significantly correlated to GIP and insulin. Physiologically, glucose present in the duodenum stimulates the secretion of GIP by enteroendocrine K cells. GIP functions as an incretin and stimulates insulin release from pancreatic beta cells (Baggio and Drucker, 2007a). Intraduodenal ingestion of glucose was reported to have load-dependent effects on GIP and insulin response (Schirra et al., 1996, Pilichiewicz et al., 2007).

Metabolomic profiling in the stomach and duodenum

At present, little is known about how food structure affects intestinal metabolites in humans. Metabolomics methods are divided into two distinct groups: targeted metabolomics, which quantifies a defined group of metabolites based on existing hypotheses; and untargeted metabolomics, which provides a universal analysis of all measurable metabolites in a sample (Roberts et al., 2012). This study performed untargeted ^{1}H-NMR metabolic profiling in gastric and duodenal samples. ^{1}H-NMR is a reproducible, highly sensitive method that simultaneously measures thousands of molecules in biological fluids. Its non-selective nature makes it a useful tool for screening metabolites associated with food structure and may provide clues to the mechanism of their postprandial responses. In addition to starch digestion products, we also aimed to use NMR to explore non-carbohydrate metabolites, which may create new research hypotheses and discover novel possible biomarkers.

In this study, the metabolic profiling established significant differences in intestinal samples between food structures. Firstly, the analysis identified a lower release of carbohydrate digestion products (overlapping carbohydrates peaks were found in the range of 3-4ppm, including glucose, maltose, amylopectin, and amylose, as shown in **Figure 4.6**) in intact structure groups. Specifically, glucose and maltose/amylopectin were identified in the duodenum and ranked as: intact-C < Intact-S < Broken. This is in line with the targeted carbohydrate analysis and is mirrored in their ranking of blood glycaemia.

Besides carbohydrates, it established remarkable differences in signals corresponding to amino acids in the duodenum. Chickpeas are a good source of proteins. The encapsulation of

intact cell walls was expected to decrease protein digestibility as suggested by current literature (Rovalino-Cordova et al., 2019, Zahir et al., 2020). Surprisingly, the ^{1}H NMR metabolic profiling indicated a set of amino acids including Valine, Leucine, Isoleucine, and glutamine having a higher release in intact cells and clusters than in broken cells in the duodenum. The underlying reason is unknown, however, there is evidence that encapsulated protein from intact chickpea cells can be digestible in the duodenum (Perez-Moral et al., 2022). During INFOGEST digestion, CCP-enriched bread (bread containing 60% chickpea intact cell powders) had 88% protein digested in the duodenal phase. Confocal images found that after 120min of duodenal digestion, the encapsulated protein no longer appeared within the cells. Interestingly, the release of total amino acids was quicker in CCP-enriched bread compared to white bread during first hour of duodenal digestion (Perez-Moral et al., 2022) . Altogether, it may suggest that beyond the barrier effect, there are other mechanisms that interplay with food structure and the release of amino acids. Future studies should measure the serum levels of amino acids and include quantitative analysis of protein digestion in the gut samples to validate the role in amino acid bioaccessibility/ bioavailability. Moreover, whether proteins and peptides present in plant cell walls could be a source of amino acid release in the duodenum should be considered.

Lastly, NMR spectra corresponding to bile acids (likely taurine-conjugated bile acids) were increased in the intact structures in duodenal samples versus the disrupted cells. The duodenum is the main site of the gut to receive pancreatic secretion including bile acids. Currently, there is no evidence to suggest the interplay between food structure and bile acids; while it is known that diet, particularly dietary fibre can interact with bile acids in the gut (Gunness and Gidley, 2010, Gunness et al., 2016) . Taurine-conjugated bile acids have been

suggested to have beneficial effects on regulating glucose metabolism. They can activate TGR5 receptors and consequently bring a series of physiological benefits, including increasing energy expenditure and GLP-1 secretion, improving insulin sensitivity (Thomas et al., 2009).

Gut hormones and appetite regulation

Our data showed that intact single cells of chickpea increased the means of GLP-1 and PYY, enhanced the feeling of fullness and decreased the composite appetite compared to the Broken. The increased GLP-1 and PYY may be the result of the nutrients (e.g., glucose) that escaped from duodenal digestion entering the lower part of the gut and interacting with L cells (Spreckley and Murphy, 2015). The role of PYY and GLP-1 in appetite regulation has been well established. They have been suggested to reduce food intake via delayed gastric emptying, or/ and vagal and CNS effects (De Silva and Bloom, 2012a). In our study, Intact-S significantly reduced appetite but failed to reduce *ab libitum* food intake. There are some possible explanations. Firstly, the biggest differences in appetite changes were observed during 45-90 min (**Figure 4.11**), whereas the food intake was measured at 240min. Secondly, the calorie load for the test meal was relatively small (242 kcal), which may not be sufficient to induce a difference in food intake. Similarly, Palchen *et al.* 2022 reported that the consumption of a single meal (chickpea individual intact cells) increased subjective satiety but did not change energy intake compared to chickpea open cells (Palchen et al., 2022). Whether this can be translated into a benefit of reducing energy intake remains to be seen and possibly should be investigated over longer interventions.

It is worthwhile to mention that glucose dynamics may also play a role in acute appetite regulation. The correlation matrix suggested insulin had the strongest correlation coefficient with composite appetite (r=-0.53), regardless of the effect of food structure. Gastric and duodenal carbohydrates were negatively associated with composite appetite. A slow release of carbohydrate release in pulses has been suggested to prolong satiety in humans (Leathwood and Pollet, 1988, Clark and Duncan, 2017).

4.5.3 Overall conclusion

Intact cell matrices and broken cells led to significant differences in structural and metabolite profiles in the digesta of the human upper GI tract. Intact individual cell and cell clusters reduced starch digestion kinetics in the stomach and duodenum, attenuating blood glucose, Insulin, and GIP responses. Intact individual cells increased fullness alongside decreased composite appetite scores, which may be attributed to increased PYY and GLP-1. Importantly, current data suggested that intact cell matrices had incomplete digestion in the duodenum and may increase the carbohydrates that travelled to the distal gut. The next Chapter will focus on the metabolism in the ileum with a focus on fermentation and appetite regulation.

Chapter 5 The impact of food structure on appetite regulation and ileal content

5.0 Abstract

Chapter 4 has suggested that intact cell wall matrices of chickpeas reduced carbohydrate bioaccessibility in the duodenum and thus would increase the carbohydrates that travel further down the GI tract. The lower GI tract senses food ingestion and sends signals to the brain to mediate appetite. This Chapter aimed to understand the digestion and fermentation events of the carbohydrates that arrived in the distal ileum and the effects on appetite regulation. 8 healthy subjects attended 3 inpatient visits, during which they consumed chickpea meals (Intact-S, Intact-C, Broken) for continuous 3 days. The following outcomes were examined on day 3:

- Subjective appetite measurements
- Breath hydrogen concentrations
- Plasma PYY and GLP-1 concentrations
- Blood glucose and insulin levels
- Ileal glucose concentrations and time profiles
- Metabolic profiling of ileal samples

Broken had the least amount of carbohydrates arriving at the distal ileum. Intact-S released the highest glucose and maltose levels in the ileum indicating that the carbohydrate of Intact-S arrived and was more digestible in the ileum. Intact-C appeared to retain more carbohydrates for fermentation. Intact-C significantly increased fullness and PYY compared to Broken during 4-8hr likely resulting from increased ileal and colonic fermentation.

5.1 Introduction

5.1.1 Overview

Intact food structure has been suggested to increase the delivery of undigested nutrients to the lower GI tract i.e., the ileum and colon. The lower GI tract is abundant in enteroendocrine L cells, which can sense metabolites produced by the host and the bacteria and co-express PYY and GLP-1 to reduce appetite. The terminal ileum has a high density of L cells as observed in humans and can sense dynamic changes in metabolites (e.g., glucose and SCFAs) due to the co-occurrence of carbohydrate digestion and fermentation. The terminal ileum therefore may represent an important part of the gut-brain axis of appetite regulation.

5.1.2 Nutrient sensing in the ileum and appetite regulation

The prevalence of obesity and overweight is increasing globally (Hruby and Hu, 2015), and prevention is needed. A better understanding of energy homeostasis has been gained through research on gut-brain signalling mechanisms that control appetite and food intake (Turton et al., 1996, le Roux et al., 2007, Batterham and Bloom, 2003, Schwartz et al., 2000). Gut hormones such as GLP-1 and PYY have been identified as potential targets for anti-obesity agents. Enhancing nutrient sensing from diets may offer a natural approach to promote GLP-1 and PYY secretion for appetite suppression (Lu et al., 2021).

L cells are specialized cells that express PYY and GLP-1, and they are located along much of the length of the GI tract, starting at the proximal jejunum and increasing along the ileum and colon (Eissele et al., 1992). The early phase plasma response of GLP-1 could arise from the smaller populations of L cells in the duodenum (Theodorakis et al., 2006). The contact of ingested nutrients with L-cells generally increases along the GI tract. Studies have shown the density of L cells is maximum in the colon and rectum (Theodorakis et al., 2006, Suzuki et al., 2018), whilst the ileum and colon have the highest total L cell number (Hansen et al., 2013). The terminal ileum is responsible for a considerable amount of GLP-1 and PYY secretion (Holst, 2007) (Goldspink et al., 2018), and the density of GLP-1 and PYY-positive cells is similar in the ileocecal and colonic biopsy of healthy individuals (Jorsal et al., 2018). The arrival of nutrients in the ileum can be sensed by L cells (Spreckley and Murphy, 2015). Direct stimulation of the human terminal ileum by a food hydrolysate induced ileal secretions and plasma elevations of PYY and GLP-1. The resulting ileal PYY and GLP-1 secretions exceed those of the caecum (Buchwald et al., 2014).

Gut metabolites and appetite regulation

Metabolites from diet and from the host and microbial metabolism interact with G protein-coupled receptors in the gut epithelium, triggering the release of gut hormones GLP-1 and PYY that act on the appetite regulatory centres in the brain to promote satiety. Glucose and SCFAs, the products of carbohydrate digestion and fermentation, have been well recognized as the stimulators of GLP-1 and PYY secretion (Spreckley and Murphy, 2015). In addition, gut microbiota-derived metabolites such as bile acids, amino acids, and succinate, have been

related to appetite control (Han et al., 2021). These are based on *in vitro* and rodent models, pending clinical evidence to confirm.

To the best of our knowledge, there is no direct evidence from humans that metabolites in the ileum interplay with appetite regulation. Our unpublished work has demonstrated ileal metabolites were significantly different between identical high-fibre diets that underwent minimal processing versus domestic processing (Dagbasi et al., 2020a). Future work is required to identify the metabolites that drove these differences which may help better understand the role of the ileum and explore novel biomarkers for appetite control. This section will mainly focus on glucose and SCFAs, the products of carbohydrate digestion and fermentation, and their possible effects on appetite regulation in the ileum.

Carbohydrate digestion and appetite regulation in the ileum

The ileum is the last part of the small intestine where carbohydrate digestion and absorption take place (Section 1.6.4.3). Hydrolysis of carbohydrates produces monosaccharides, such as glucose, which can be directly sensed by ileal L cells. Enteroendocrine L cells are directly glucose-responsive (Reimann et al., 2008). Glucose exposure leads to membrane depolarization and calcium entry through voltage-gated channels, leading to exocytosis of GLP-1-containing vesicles (Reimann et al., 2008). In human subjects, glucose infusion directly into the ileum increased GLP-1 and PYY secretion, suppressed VAS-reported appetite, and decreased ad libitum EI at the subsequent meal (Poppitt et al., 2017).

Carbohydrate fermentation and appetite regulation in the ileum

The current understanding of ileal fermentation has been very limited. Bacterial fermentation is believed to principally happen in the caecum and proximal colon. Plant cell walls polysaccharides are indigestible to humans. Colonic bacteria have enzymes that can break down the cell walls (Chassard et al., 2010, Pereira et al., 2021) and access intracellular nutrients e.g., starch (Walker et al., 2011). The gut microbiota is the main mediator for fermentation. Existing literature about ileal microbiota is scarce, but some have suggested the distal ileum has a similar microbiota community to the colon (Donaldson et al., 2016, Ahmed et al., 2007). There is some evidence that microbial breakdown of carbohydrates also happened in the terminal ileum (Cummings et al., 1987, Cummings and Macfarlane, 1991). SCFAs were identified in the human ileum but at a lower concentration than the colon (13 ± 6, 131 ± 9, 123 ± 12 mmol/kg in the ileum, caecum and ascending colon respectively) (Cummings et al., 1987). MCT1 and SMCT1 that mediate the transport of SCFAs have been detected in the human ileum (Gill et al., 2005, Borthakur et al., 2010).

Carbohydrate fermentation produces gases and SCFAs, mainly in the form of acetate, propionate and butyrate (40:20:20). SCFAs were identified in the human ileum, with acetate as the dominant form (Cummings et al., 1987). Although SCFAs are waste by-products for the microbiota, they bring a series of benefits to the host. SCFAs have been shown to up-regulate the secretion of GLP-1 and PYY and therefore have an appetite-suppressing effect in human subjects (Byrne et al., 2015). Acetate has been found to play a direct role in central appetite regulation (Frost et al., 2014). However, these findings are mainly from colonic models, and it remains unclear whether ileal fermentation contributes to appetite regulation to a considerable extent.

5.1.3 Food structure and encapsulated nutrients in the ileum

The evidence so far suggests complex food structures can increase the encapsulated nutrients that enter the ileum. Noah *et al.* used intubation techniques to collect ileal fluids from healthy humans after the composition of cooked white beans. They found that 16.5% of ingested starch was not digested in the small intestine due to being enclosed by intact cell walls (Noah et al., 1998). Similarly, an ileostomy study found intact endosperm cells presented in the ileal fluids enclosing a proportion of starch (Edwards et al., 2015a). Another team found intracellular components (carotene) remained encapsulated in intact cells but were absent from ruptured cells in ileal fluids (Tydeman et al., 2010). Recent work from our group compared rr and RR genetic types of peas in human digestion. The rr peas reduced starch digested in the stomach and duodenum compared to RR owing to their structural profiles. The rr peas subsequently increased fermentation levels and propionate and butyrate excretion in 24-hour urine samples (Petropoulou et al., 2020). The above studies provide some clues that intact cell walls enclosing intracellular contents may arrive at the terminal ileum; however, there is no investigation into the effects on appetite regulation.

5.1.4 Summary

The terminal ileum may be an important part of gut-brain appetite signalling, but it has been little investigated. Evidence suggests that the terminal ileum has a high density of L cells, which can sense nutrients and respond by signalling to the brain to reduce appetite. Intact food structure may increase the encapsulated nutrients arriving at the terminal ileum,

resulting in considerable changes in ileal metabolites such as glucose and SCFAs. Whether this plays a role in appetite-regulating signals remains unexplored. In this Chapter, we aimed to understand whether the encapsulated starch would increase fermentation activity in the ileum and reduce appetite in human subjects.

5.2 Purposes of this study

5.2.1 Hypothesis

It is hypothesized that chickpea intact cell structures will affect the profiles of ileal metabolites, including glucose and SCFAs, thus promoting the production of GLP-1 and PYY, and reducing appetite compared to Broken.

5.2.2 Aims

This study aimed to investigate the impact of chickpea cellular structures on ileal metabolites profiles, gut hormone response, and subjective appetite, providing new insights into the mechanisms underlying the health benefits of legumes.

5.2.3 Outcome measures

The primary outcome was the VAS measurement of appetite.

Co-secondary outcomes include:

- Metabolite profiling of ileal samples
- Ileal glucose concentrations and time profiles

- Circulating GLP-1 and PYY concentrations
- Breath hydrogen concentrations
- Blood glucose, insulin concentrations

5.3 Materials and methods

5.3.1 Study Design

Participants attended 3 inpatient visits in which they stayed for 3 days (2nights) at NIHR Imperial CRF. The outline of the study visit is presented in **Figure 5.1.** Please refers to Section 3.2.2.2 for details of the study design.

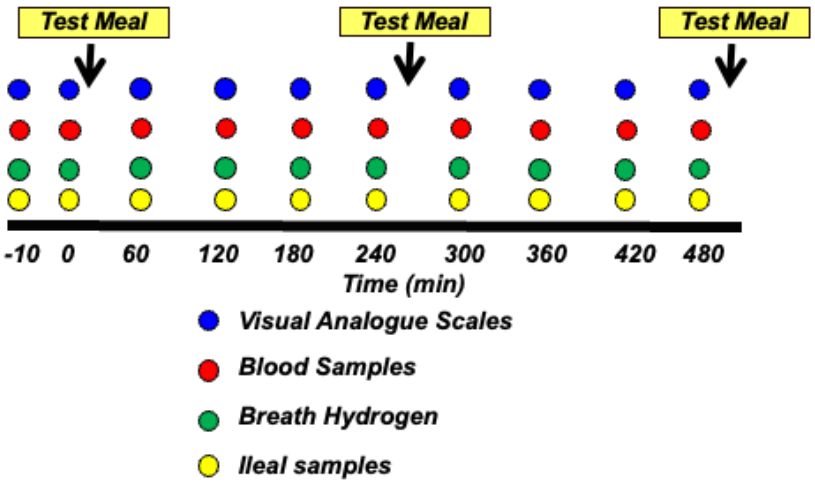


Figure 5. 1 Outline of the study visit of the ileum study.

5.3.2 Participant recruitment and eligibility

Healthy participants were recruited as descripted in Section 3.2.3. Same inclusion and exclusion criteria were applied to establish eligibility as described in **Table 3.2.**

5.3.3 Intervention and test meal preparation

Please refers to Section 3.2.2.2 for dietary intervention.

5.3.4 Randomization

Please refers to Section 3.2.4 for randomization

5.3.5 Sample collection, processing, and analysis

Please refers to Section 3.3 and 3.4 for sample collection, processing and analysis

5.3.6 Data analysis

Data analysis followed the same methods described in Section 4.3.7**.** Peak integration was performed on NMR spectra to calculate the area under peak (Haggart, 2019) and semi-quantify the ileal acetate. Repeated measures correlation was performed using r package 'rmcorr' (Bakdash and Marusich, 2017) to examine the association between ileal metabolites and appetite outcomes.

Five graphic reprehensive parameters (iPeak, iAUC, First X, Peak X, and Last X) were analysed for each participant. Incremental peak (iPeak) was calculated as the maximum rise from

fasted concentrations. Incremental Area under curve (iAUC) refers to the 'peak' area and was calculated using the trapezoidal rule, ignoring the area under the baseline. The 'First X', 'Peak X', and 'Last X' refer to the time to exceed the baseline levels, to reach maximal rise, and to return the baseline levels, respectively. These summary variables were analysed by one-way repeated measure ANOVA, followed by post hoc Tukey's Test.

5.4 Results

5.4.1 Participant characteristics

From thirteen participants from Chapter 4, eight participants (4 female and 4 male) completed the study. The age, weight, BMI and body fat did not differ between each visit (**Table 5.1**).

Table 5. 1 Participant characteristics

	Visit 1	**Visit 2**	**Visit 3**	**P value[1]**
Gender (n, M: F)	4:4			
Age (y)	33.3±4.0	33.3±4.0	33.3±4.0	0.99
Weight (kg)	70.8±4.2	70.2±3.9	71.4±4.3	0.97
BMI (kg/m^2)	24.6±1.1	24.6±1.2	24.8±1.2	0.99
Body fat (%)	22.9±1.9	22.5±1.9	22.4±1.6	0.98

. [1]Values were presented as mean± SEM. Data were analysed by one-way ANOVA.

5.4.2 Visual analogue scales

5.4.2.1 Composite appetite score

A composite appetite score was calculated as stated in Section 3.5.1. Time course and incremental area over curve (iAOC) were presented in **Figure 5.2 A-D**.

Two-way ANOVA suggested that there was no significant difference between treatments for composite appetite score (A). iAOC was calculated for 0-240min (B), 240-480min (C), and 0-480min (D) given the time course of breakfast and lunch. There was no difference in $iAOC_{0\text{-}240min}$ and $iAOC_{0\text{-}480min}$. Intact-C had a trend to decrease composite appetite score $iAOC_{240\text{-}480min}$ than Broken groups, although it did not reach significance (p=0.069).

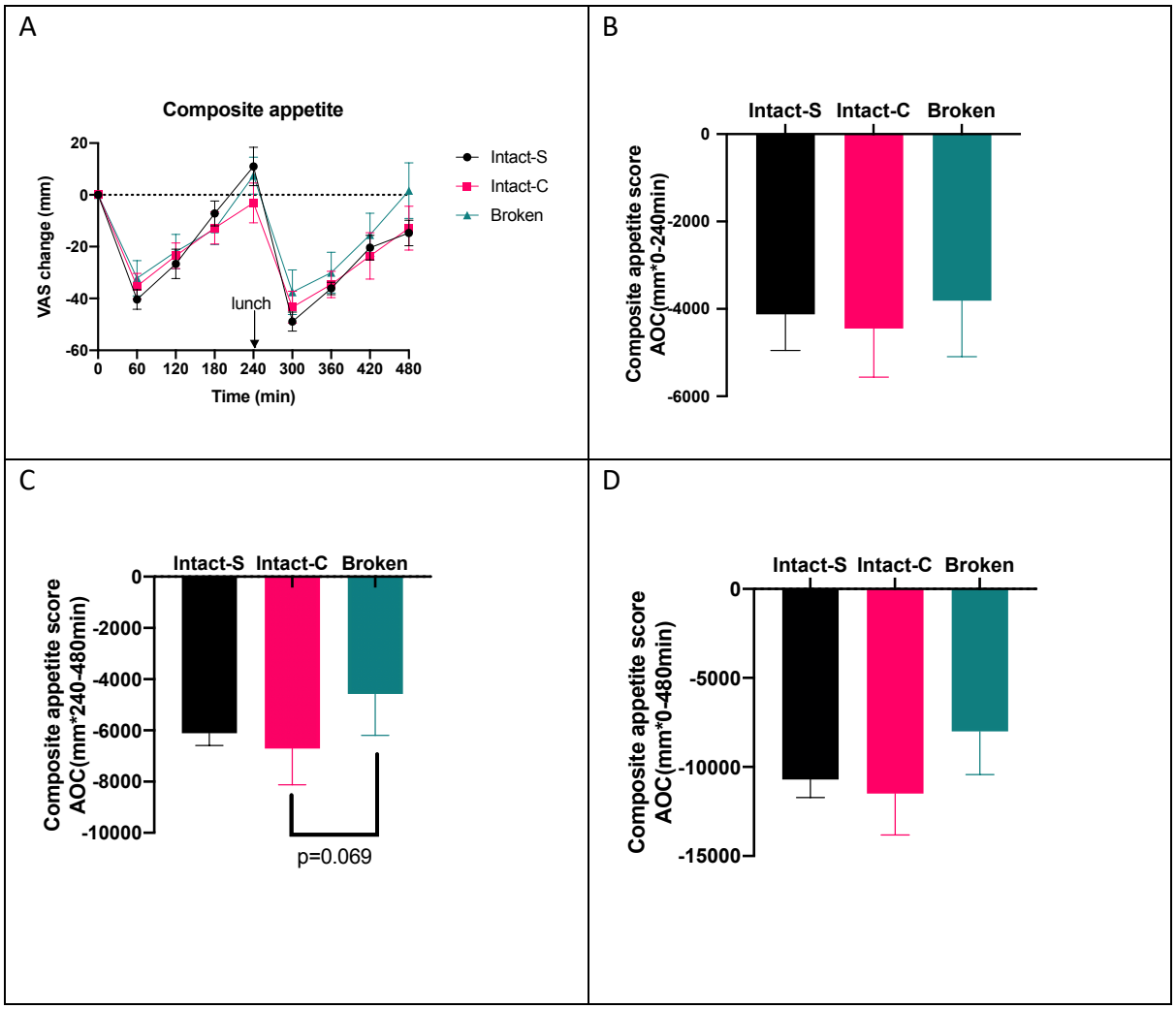


Figure 5. 2 Composite appetite scores following composition of chickpea test meals. Changes to baselines over time (A), and iAOC 0-240min, (B), iAOC 240-480min (C), and iAOC 0-480min (D). Data presented as mean ± SEM (n=8). Repeated measures two-way ANOVA with post hoc Tukey's test was performed to test the effect of diets, time points and their interactions. One-way ANOVA was performed on AOC data. iAOC, incremental Area Over Curve (iAOC); Intact-S, intact single cells; Intact-C, intact cell clusters; Broken, Broken cells. Significant differences between interventions annotated: a – Intact-S vs Intact-C; b Intact-S vs Broken and c- Intact-C vs Broken. *p<0.05, **p<0.01, ***p<0.001.

5.4.2.2 Fullness

Time course and iAUC $_{0\text{-}240min}$, iAUC $_{240\text{-}480min}$, and iAUC $_{0\text{-}480min}$ data were presented in **Figure 5.3**. Two-way ANOVA did not observe any difference in the time course change of fullness between treatments (p=0.16). Differences were observed from fullness iAUC between Intact-C and Broken: the iAUC $_{0\text{-}480min}$ in the Intact-C group was marginally higher than the Broken group (p=0.055), and their difference after lunch (iAUC $_{240\text{-}480min}$) reached a significant level (p=0.027). A linear trend was observed for fullness iAUC$_{240\text{-}480min}$ as Intact-C> Intact-S> Broken (p=0.029).

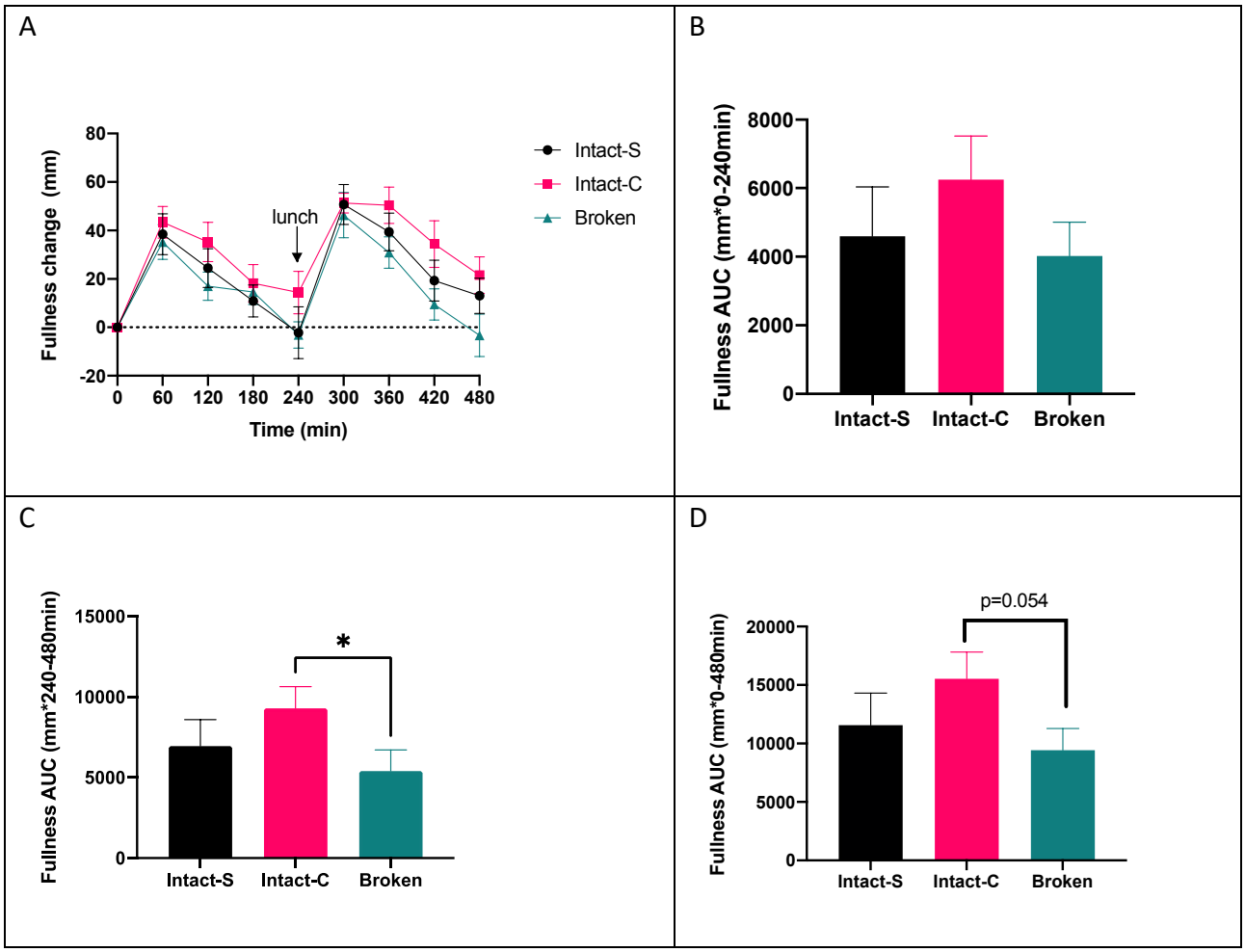


Figure 5. 3 The feeling of fullness following composition of chickpea test meals. Changes to baselines over time (A), and iAUC 0-240min, (B), iAUC 240-480min (C), and iAUC 0-480min (D). Data presented as mean ± SEM (n=8). Repeated measures two-way ANOVA with post hoc Tukey's test was performed to test the effect of diets, time points and their interactions. One-way ANOVA was performed on iAUC data. Intact-S, intact single cells; Intact-C, intact cell clusters; Broken, Broken cells. Significant differences between interventions annotated: a – Intact-S vs Intact-C; b Intact-S vs Broken and c- Intact-C vs Broken. *p<0.05, **p<0.01,***p<0.001.

5.4.2.3 Hunger, desire to eat, and appetite for a meal

Time-course data for other appetite VAS questions hunger, desire to eat, and appetite for a meal were presented in **Figure 5.4 A-C**. There was no significant difference found in the time-course data for hunger, desire to eat or appetite for a meal (p=0.46, p=0.66, p=0.47 respectively). No significant differences were found in any of their iAUC between 0-240min, 240-480min or 0-480min (Appendix 8).

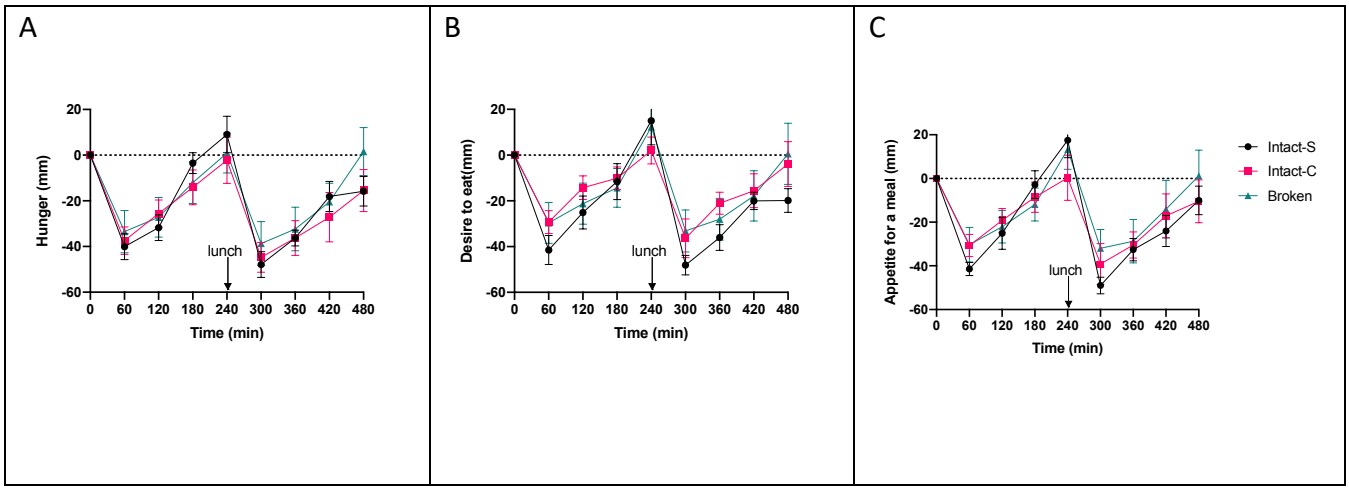


Figure 5. 4 The feeling of hunger (A), desire to eat (B), appetite for a meal (C) following composition of chickpea test meals. Data presented as mean ± SEM (n=8). Repeated measures two-way ANOVA with post hoc Tukey's test was performed to test the effect of diets, time points and their interactions. One way ANOVA was performed on AUC data.

5.4.3 Ileal glucose: concentration and time profile

Figure 5.5 A shows the ileal glucose concentrations during 0-480 min. Mixed effect model suggested a significant difference between food structure interventions ($p<0.001$). Intact-S had higher levels of ileal glucose than Broken throughout most time points after meals (T=120-480min, all $p<0.05$). Intact-S was higher than Intact-C at T=120 min ($p=0.008$). Intact-C had higher levels of ileal glucose than Broken at T=420 min ($p=0.029$). Intact-S had higher $iAUC_{0\text{-}240min}$, $iAUC_{240\text{-}480min}$, and $iAUC_{0\text{-}480min}$ (**B-D**) for ileal glucose than broken ($p=0.022$, $p=0.039$, $p=0.029$). Intact-C had marginally higher $iAUC_{0\text{-}480min}$ than Broken ($p=0.042$).

To estimate when the foods arrived and were retained in the ileum, the time profile of ileal glucose graphs was analysed for each individual as described in Section 5.3.6. Carbohydrates from Intact-S, Intact-C and Broken entered the terminal ileum at 36.3 ± 18.8, 30.6 ± 20.0, and 17.5 ± 7.5 min respectively; then peaked at 157.5 ± 29.9, 247.5 ± 48.7, and 142.5 ± 50.6min; and exited at 343.7 ± 53.6, 451.7 ± 28.3, and 299.3 ± 49.7 min, respectively. There was a significant linear trend ($p=0.031$) for the "exiting time" to delay in the order of Broken< Intact-S<Intact-C. There were no statistically significant differences for the first X and peak X. A significant difference was observed in peak values ($p=0.035$); Intact-S and Intact-C had higher peak values compared to broken (Intact-S: 8.0 ± 2.1 mmol/L vs Broken 0.9 ± 0.2 mmol/L, $p=0.031$; Intact-C: 4.1 ± 0.9 mmol/L vs Broken, $p=0.033$). Graphic reprehensive parameters were summarized in Appendix 9.

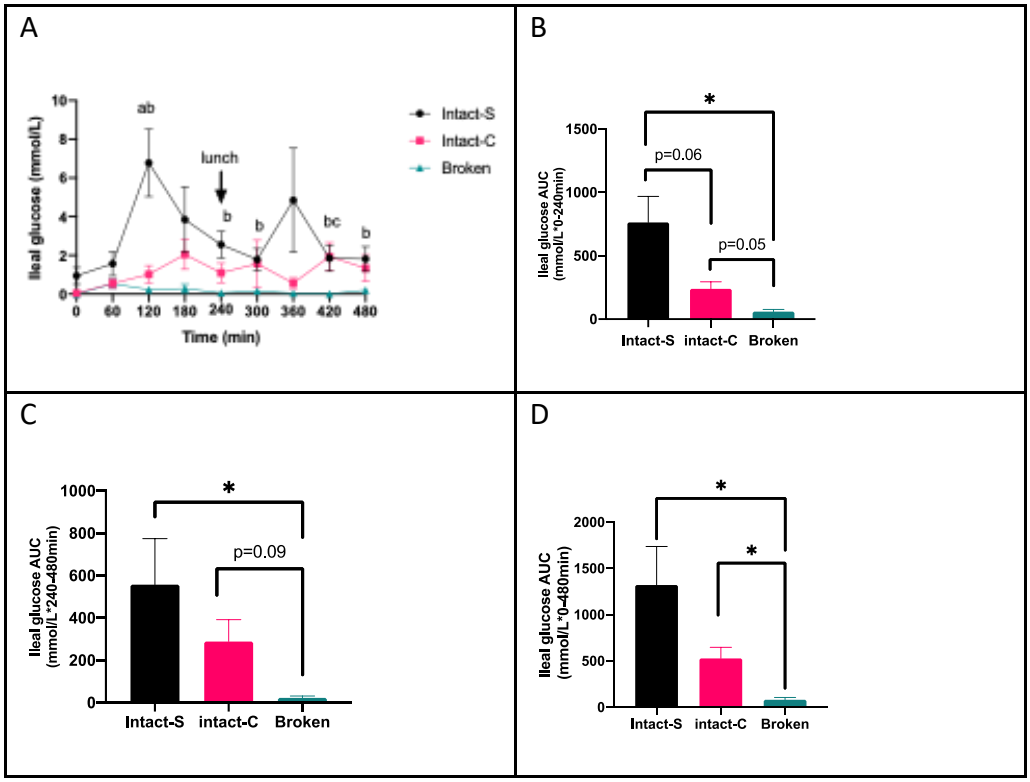


Figure 5. 5 The ileal glucose concentrations following composition of chickpea test meals. Ileal glucose over time (A), and glucose incremental area under curve $iAUC_{0\text{-}240min}$, (B) $iAUC_{240\text{-}480min}$ (C), and the $iAUC_{0\text{-}480min}$ (D). Data presented as mean ± SEM (n=8). Ileal glucose data did not pass normality distribution test and therefore logarithmic transformation was conducted before using mixed-effect model. Mixed- effects model was performed to test the effect of diets, time points and their interactions. One way ANOVA was performed on AUC data. Intact-S, intact single cells; Intact-C, intact cell clusters; Broken, Broken cells. Significant differences between interventions annotated: a – Intact-S vs Intact-C; b Intact-S vs Broken and c- Intact-C vs Broken. *p<0.05, **p<0.01, ***p<0.001.

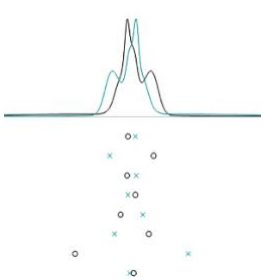
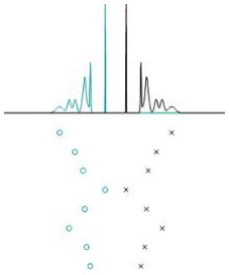
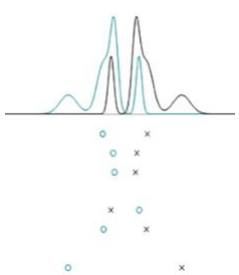
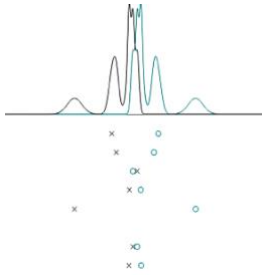
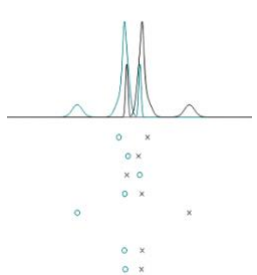
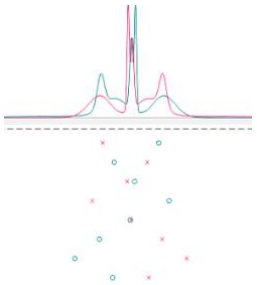
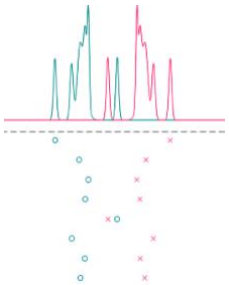
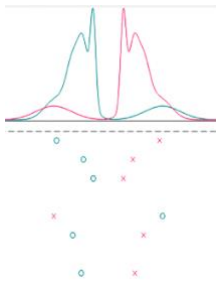
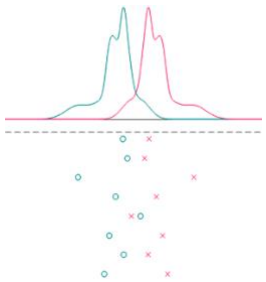
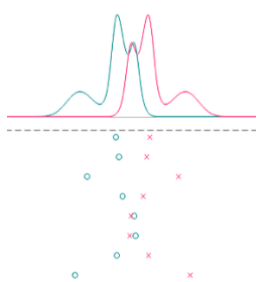
5.4.4 Metabolomic analysis of ileum samples

Figure 5.6 presents the PLS-DA analysis between food structures at T=0, 120, 240, 360, and 480min. The metabolic phenotype between treatments was not different when fasted (T0). Significant differences were observed since T=120min and were preserved until the end of the study visit (T=480min), except for differences between Intact-S and Intact-C were preserved until T=360min.

Metabolic identification was performed at time points when significant differences were observed. Untargeted metabolomic analysis identified 14 small metabolites (full list in **Table 5.2**) that showed significant differences between food structures. These included BCAAs (valine, leucine, and isoleucine), amino acids (alanine, phenylalanine, and tyrosine), secondary bile acids [glycine/taurine-conjugated cholic acid (CA); glycine/taurine-conjugated deoxycholic acid (DCA); glycine/taurine-conjugated chenodeoxycholic acid (CDCA)], carbohydrates (glucose and maltose), and possibly bacterial fermentation products (acetate, succinate, and lactose).

The release of maltose and glucose was the highest in Intact-S, the second highest in Intact-C and the lowest in the Broken during T=120-480min. Intact-C had higher ileal acetate than Broken and Intact-S after lunch (T=360 and T=480min). The relative amount of acetate was quantified by the area under peak corresponding to the signals 1.92 (s), and **Figure 5.7** presents the change of relative amount over time. Ileal acetate was highest in the fasting stage and decreased sharply after the meal. Ileal acetate was elevated in the Intact-S group

at T=240-300 min and in the Intact-C group at T=240-360 min. At T=360-480min, ileal acetate in Intact-C was higher than Broken, coinciding with the results of the PLS-DA analysis.

	T=0 min	T=120 min	T=240 min	T=360 min	T=480 min
Intact-S vs Broken	R^2: 0.81, $Q^{2:}$ -0.19 	R^2: 1, $Q^{2:}$ 0.82 	R^2: 0.98, Q^2 : 0.47 	R^2: 0.99, $Q^{2:}$ 0.45 	R^2: 0.98, Q^2 : 0.40 
Intact-C vs Broken	R^2: 0.95, Q^2 : -0.17 	R^2: 1, Q^2 : 0.78 	R^2: 0.94, Q^2 : 0.12 	R^2: 0.95, Q^2 : 0.50 	R^2: 0.97, Q^2 : 0.48 

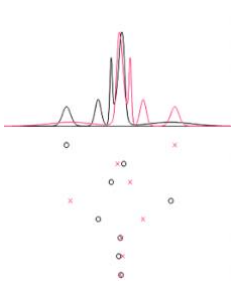
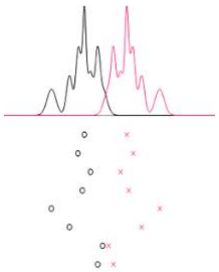
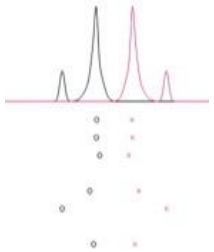
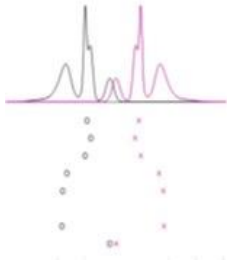
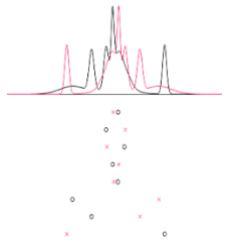
Intact-S vs Intact-C	R^2: 0.88, $Q^{2:}$ -0.67 	R^2: 0.99, $Q^{2:}$ 0.68 	R^2: 1, $Q^{2:}$ 0.71 	R^2: 0.98, $Q^{2:}$ 0.74 	R^2: 0.97, $Q^{2:}$ -0.48 

Figure 5. 6 RM-MCCV-PLS-DA score plots of ^{1}H-NMR ileal samples before and after consumption of chickpea test meals. Each dot represents the metabolic profile of one subject containing 18,600 spectra variables. The analysis was performed in available paired data. R^2 and Q^2 indicate the fit and predictability of the models. Intact-S, intact single cells; Intact-C, intact cell clusters; Broken, Broken cells.

Table 5. 2 Metabolites in the ileum associated with food structure

	Intact-S vs Broken	Intact-C vs Broken	Intact-C vs Intact-S
T=120	CA (0.73) ↑ Valine 0.99(d), 2.46(m) ↑ Leucine 0.95(t), 1.73(m) ↑ Isoleucine 0.92(dd), 1.45(m), 2.01(m) ↑ Lactose 1.32(d) ↓ Alanine 1.48 (d) ↑ Maltose 3.60(d) ↑ Glucose 5.24(d) ↑ Tyrosine 6.91 (d), 7.20(d)↑ Phenylalanine 7.35(m),7.38(m), 7.43(m) ↑	CA (0.73) ↑ Valine 0.99(d), 2.46(m) ↑ Leucine 0.95(t), 1.73(m) ↑ Isoleucine 0.92(dd), 1.45(m), 2.01(m) ↑ Lactose 1.32(d) ↓ Alanine 1.48 (d) ↑ Maltose 3.60(d) ↑ Glucose 5.24(d) ↑ Tyrosine 6.91 (d), 7.20(d)↑ Phenylalanine 7.35(m),7.38(m), 7.43(m) ↑ Taurine-conjugated BAs 7.9 (m) ↑	CDCA (0.67) ↑ Leucine0.95(t), 1.73(m) ↓ Maltose 3.60(d) ↓ Tyrosine 6.91(d),7.20(d) ↑ Phenylalanine 7.35(m),7.38(m), 7.43(m) ↑
T=240	DCA (0.71) ↑ Lactose 1.32(d) ↓ Succinate (2.41) ↓ Maltose 3.60(d) ↑ Glucose 5.24(d) ↑	CA (0.73) ↑ Valine 0.99(d), 2.46(m) ↑ Leucine 0.95(t), 1.73(m) ↑ Isoleucine 0.92(dd), 1.45(m), 2.01(m) ↑ Maltose 3.60(d) ↑ Glucose 5.24(d) ↑ Taurine-conjugated BAs 7.9 (m) ↑	DCA (0.71) ↓ Maltose 3.60(d) ↓ Glucose 5.24(d) ↓
T=360	DCA (0.71) ↑	DCA (0.71) ↑	DCA (0.71) ↓

	Maltose 3.60(d) ↑ Glucose 5.24(d) ↑	Alanine 1.48 (d) ↓ Acetate 1.92(s) ↑ Maltose 3.60(d) ↑ Glucose 5.24(d) ↑	Acetate 1.92(s) ↑ Alanine 1.48 (d) ↑ Maltose 3.60(d) ↓ Glucose 5.24(d) ↓ Tyrosine 6.91 (d), 7.20(d) ↑ Phenylalanine 7.35(m),7.38(m), 7.43(m) ↑
T=480	Maltose 3.60(d) ↑ Glucose 5.24(d) ↑	Acetate 1.92(s) ↑ Maltose 3.60(d) ↑ Glucose 5.24(d) ↑	/

The chemical shifts and multiplicities are listed for peaks from significantly associated metabolites. Peaks are only listed if they are in the range of the processed data (9·5–5·5 and 4·5–0·5 ppm). Multiplicity key is as follows: s – singlet, d – doublet, t – triplet, q – quartet, dd – doublet of doublets, dq – doublet of quartets, 2d – two doublets, m – (other) multiplet. ↑ and ↓ indicated a higher or lower release from [X] in the comparison between [X] and [Y]. BAs, bile acids; CA, glycine/taurine-conjugated cholic acid; DCA, glycine/taurine-conjugated deoxycholic acid; CDCA, glycine/taurine-conjugated chenodeoxycholic acid; Intact-S, intact single cells; Intact-C, intact cell clusters; Broken, Broken cells.

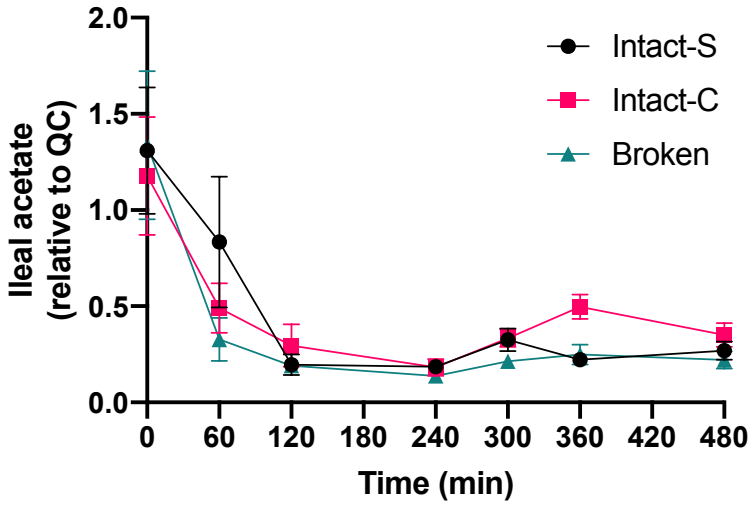


Figure 5. 7 The relative amount of ileal acetate over time. QC, quality control, a pooled quality control (QC) sample in which a small aliquot of each biological sample in the study was mixed. Relative amount was calculated by area under peak corresponding to the NMR signal of 1.92 (s) ppm.

5.4.5 Breath Hydrogen

Day 3 baseline levels (A) and the postprandial response (B) of breath hydrogen (BH) are presented in **Figure 5.8**. There was a significant difference between food structures at the baseline (p= 0.012). The post-hoc test indicated that Intact-C had higher BH than the Broken (p=0.032). There was a trend for significant differences between Intact-S and Intact-C (p=0.09), and between Intact-S and Broken (p=0.05).

The postprandial changes of BH showed a different pattern for food structures. BH in the Broken group increased quickly and peaked at 240 min, it declined after lunch until 480min. Whilst in Intact-S and Intact-C, BH increased slowly but substantially throughout the 480 minutes. Two-way ANOVA demonstrated significant effects from treatments (p=0.025), time (p<0.005), and their interaction (p=0.001). The BH of Broken was higher than Intact-S and/or Intact-C during 120-300 min (all p<0.05). Intact-C was higher than Broken at T =420-480 min (p=0.032, p=0.048).

The time profile of BH was examined as described in Section 5.3.6. The onset of hydrogen excretion was determined by the time when postprandial BH exceeded the baselines, which occurred at 272.6 ± 54.2, 195.7 ± 50.7, and 90.7 ± 38.5 min for intact-S, Intact-C and Broken, respectively. The onset time of BH was significantly delayed in Intact-S and Intact-C compared to Broken (average of Intact-S and Intact-C 234.2± 64.40 min vs Intact-C, one-way ANOVA p= 0.046). As these times were within the retention times of ileal glucose, this suggested that fermentation initiated when carbohydrates remained at the terminal ileum and therefore,

hydrogen excretion should be used as an indicator of intestinal fermentation instead of colonic fermentation.

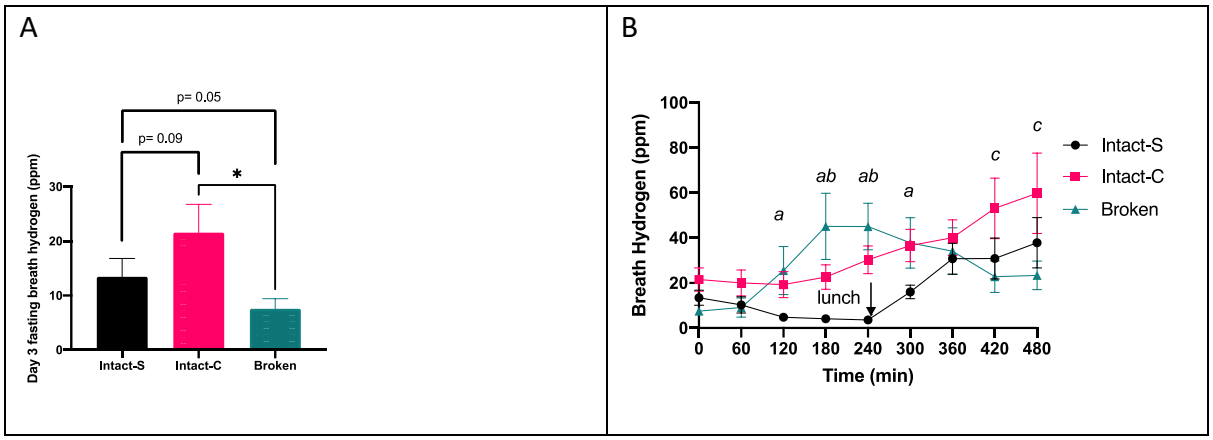


Figure 5. 8 Baselines and postprandial changes in breath hydrogen on day 3. Breath hydrogen at day 3 baseline levels (A) and postprandial concentrations over time (B) during 0-480min. Repeated measures two-way ANOVA with post hoc Tukey's test was performed to test the effect of diets, time points and their interactions. Breath hydrogen did not pass normality distribution test and therefore logarithmic transformation was conducted before using two-way ANOVA analysis. Data presented as mean ± SEM (n=8). Intact-S, intact single cells; Intact-C, intact cell clusters; Broken, Broken cells. Significant differences between interventions annotated: a – Intact-S vs Intact-C; b Intact-S vs Broken and c- Intact-C vs Broken. *p<0.05, **p<0.01,***p<0.001.

5.4.5 Postprandial glycaemia and insulinaemia

The glycaemic and insulinaemic responses are present in **Figure 5.9**. Two-way ANOVA suggested that there was a significant interaction effect between diet and timepoint ($p<0.001$) on plasma glucose response. The post-hoc test showed that Intact-S and Intact-C had lower concentrations of plasma glucose versus Broken at T= 60 min ($p=0.043$, $p=0.033$) and T=300 min ($p=0.030$, $p=0.023$). The glucose $iAUC_{0\text{-}480min}$ demonstrated significant differences between three groups: Intact-C < Intact-S < Broken (Intact-S vs Intact-C, $p=0.028$; Intact-S vs Broken, $p=0.040$; Intact-C vs Broken, $p=0.008$).

The insulin curve during 0-480 min mirrored the changes in plasma glucose. Significant effects were found from treatments ($p=0.038$) and the interaction between treatments and timepoint ($p<0.001$). Similar to glucose response, Intact-S and Intact-C lowered insulin levels one hour after meals: at T=60min ($p=0.046$, $p=0.029$) and T=300min ($p=0.016$, $p=0.030$). The insulin-lowering effect was more prolonged and was observed two hours post-ingestion. Intact-C and Intact-S lowered insulin levels than Broken at T=120 min ($p=0.027$) and T=300 min ($p=0.048$), respectively. The $iAUC_{0\text{-}480min}$ for insulin was significantly higher in Intact-S and Intact-C than in Broken ($p=0.049$, $p=0.049$).

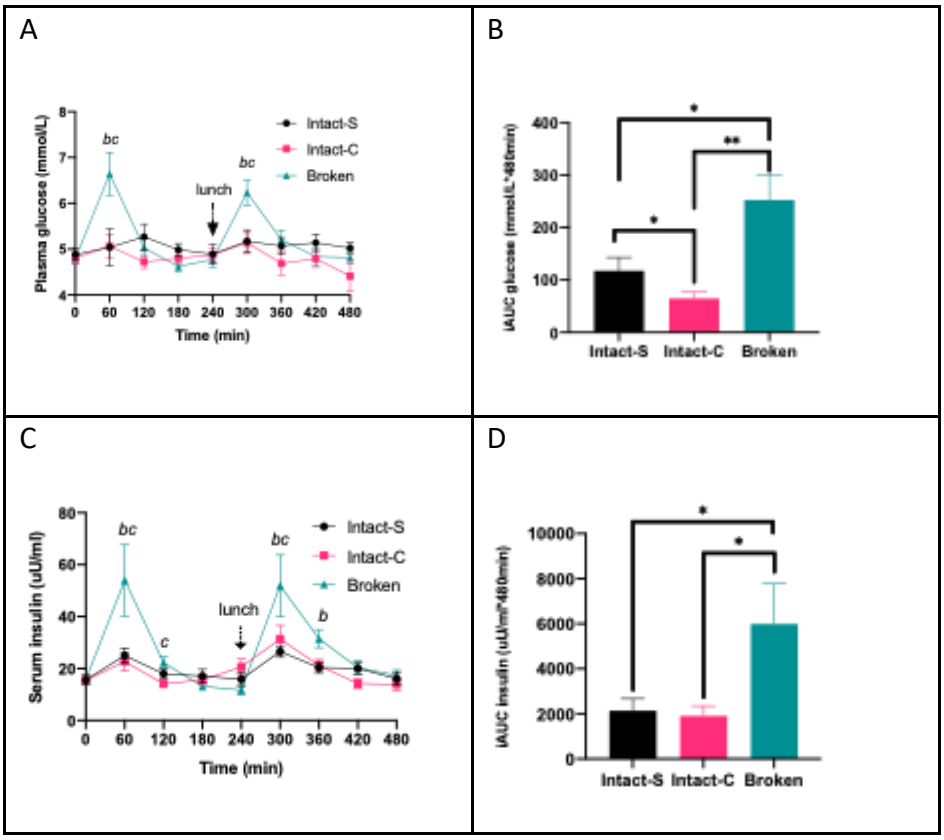


Figure 5. 9 Glucose and insulin responses following composition of chickpea test meals. Plasma glucose over time (A), and glucose incremental area under curve $iAUC_{0\text{-}480min}$, (B), serum insulin over time(C), and the $iAUC_{0\text{-}480min}$ (D). Data presented as mean ± SEM (n=8). Repeated measures two-way ANOVA with post hoc Tukey's test was performed to test the effect of diets, time points and their interactions. One-way ANOVA was performed on AUC data. Intact-S, intact single cells; Intact-C, intact cell clusters; Broken, Broken cells. Significant differences between interventions annotated: a – Intact-S vs Intact-C; b Intact-S vs Broken and c- Intact-C vs Broken. *p<0.05, **p<0.01,***p<0.001.

5.4.6 GLP-1

The baseline and time course data for GLP-1 are shown in **Figure 5.10 A-B**. Intact-C had a higher GLP-1 baseline level compared to Broken ($p=0.038$). No significant difference was found between Intact-S, Intact-C and Broken groups for their post-ingestion data ($p=0.79$, $p<0.001$, $p=0.89$ for the effect of diets, time points and their interactions).

There was no significant difference for GLP-1 iAUC between 0-240 min, 240-480 min or 0-480min, with $p= 0.21, 0.76, 0.47$ respectively (**Figure 5.10 C-E**).

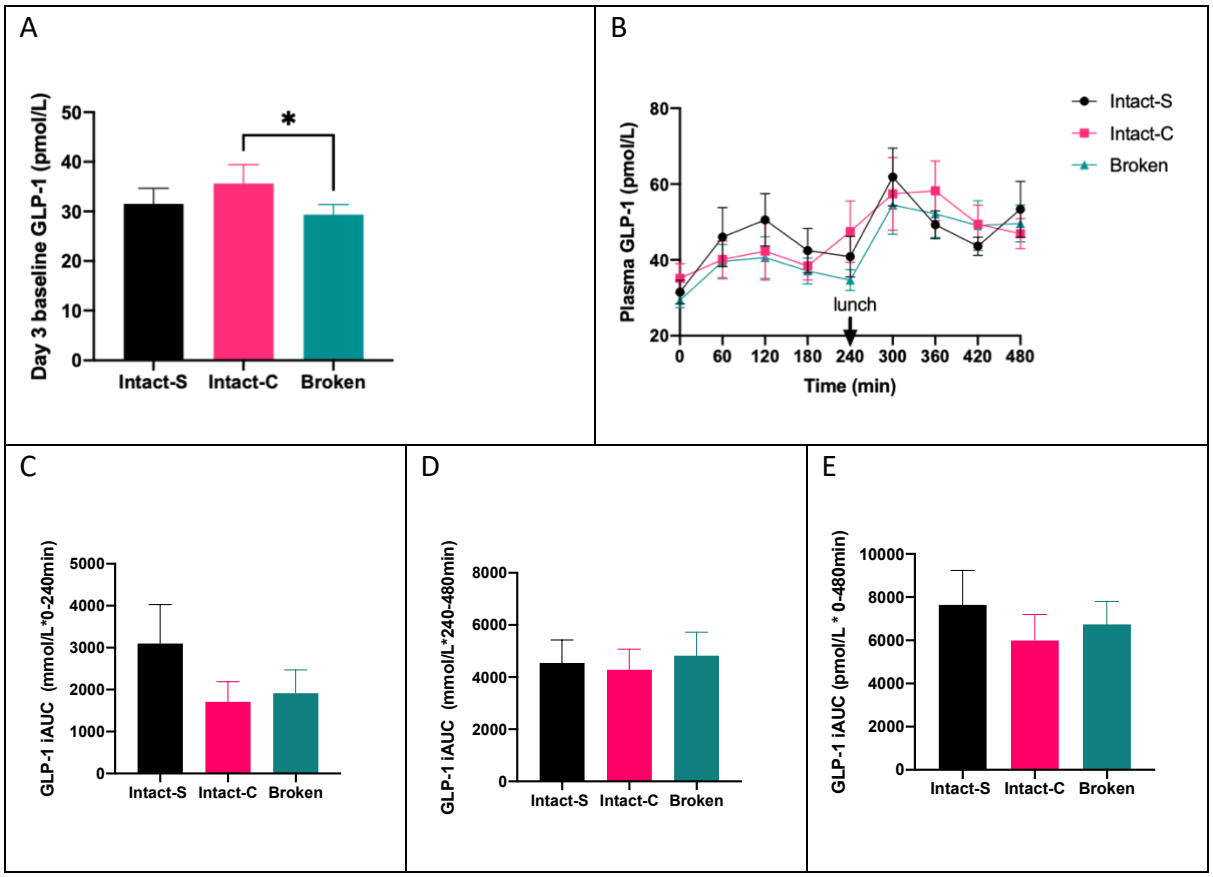


Figure 5. 10 Baselines and postprandial changes in GLP-1. Blood GLP-1 at day 3 baseline levels (A) and postprandial concentrations over time (B), GLP-1 iAUC during 0-240min (C), 240-480min (D) and 0-480min (E). Repeated measures two-way ANOVA with post hoc Tukey's test was performed to test the effect of diets, time points and their interactions. One-way ANOVA was performed on AUC data. Data presented as mean ± SEM (n=8). Intact-S, intact single cells; Intact-C, intact cell clusters; Broken, Broken cells. Significant differences between interventions annotated: a – Intact-S vs Intact-C; b Intact-S vs Broken and c- Intact-C vs Broken. *p<0.05, **p<0.01,***p<0.001.

5.4.7 PYY

The baseline and time course data for PYY are shown in **Figure 5.11 A-B**. There was no significant difference observed at the baseline for PYY (p=0.50). Two-way ANOVA suggested a significant interaction effect between treatments and timepoint on PYY levels (p=0.033). Intact-S had higher PYY than Intact-C and Broken at T= 180 min (p=0.014, p=0.013). Intact-S had higher PYY than Broken at 420 min and 480min (p=0.036, p=0.034).

PYY iAUC $_{0\text{-}480min}$ of Intact-S was significantly higher compared to Broken (p=0.039). $iAUC_{0\text{-}240min}$ or $iAUC_{240\text{-}480min}$ were not significantly different between food structure interventions.

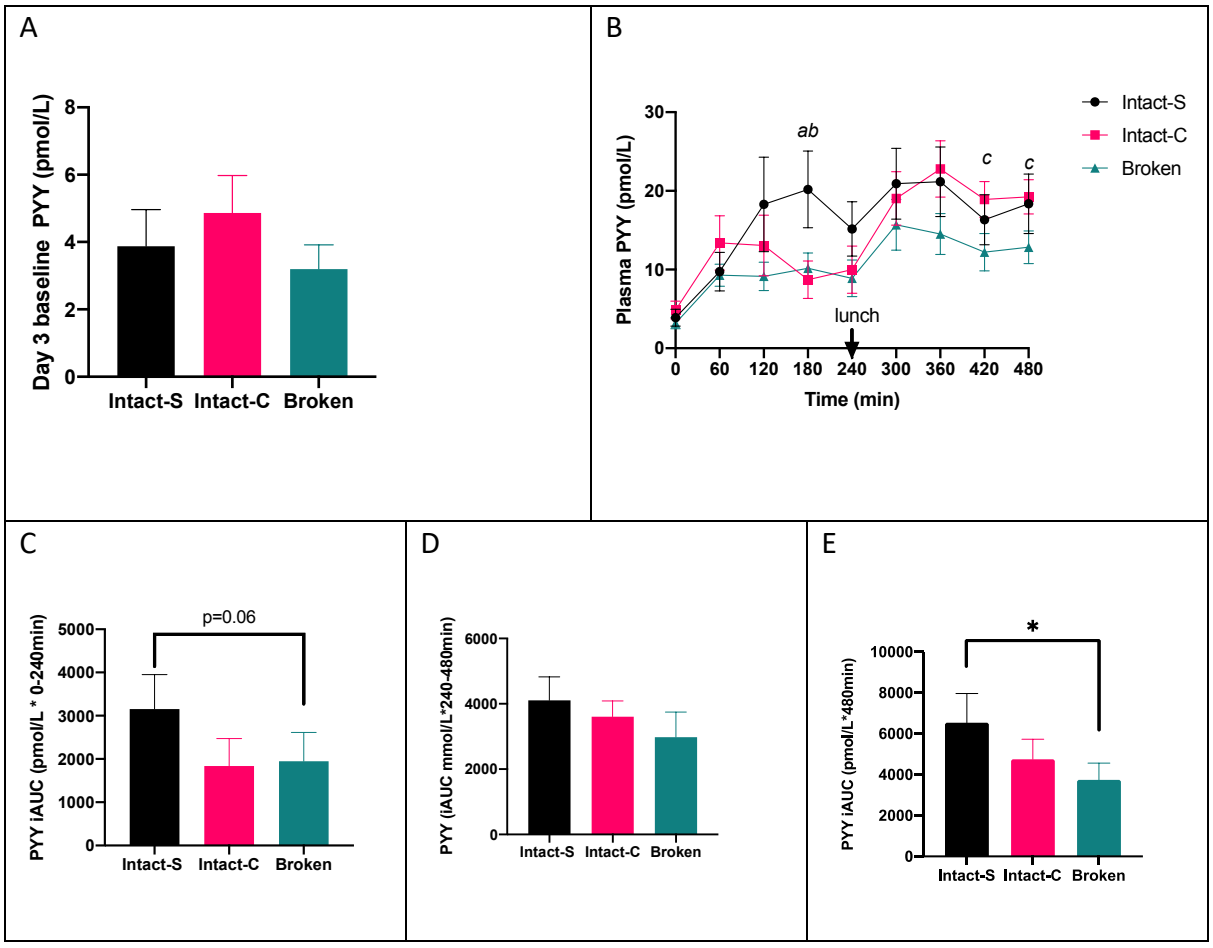


Figure 5. 11 Baselines and postprandial changes in PYY. Blood PYY at day 3 baseline levels (A) and postprandial concentrations over time (B), GLP-1 iAUC during 0-240min (C), 240-480min (D) and 0-480min (E). Repeated measures two-way ANOVA with post hoc Tukey's test was performed to test the effect of diets, time points and their interactions. One-way ANOVA was performed on AUC data. Data presented as mean ± SEM (n=8). Intact-S, intact single cells; Intact-C, intact cell clusters; Broken, Broken cells. Significant differences between interventions annotated: a – Intact-S vs Intact-C; b Intact-S vs Broken and c- Intact-C vs Broken. *p<0.05, **p<0.01,***p<0.001.

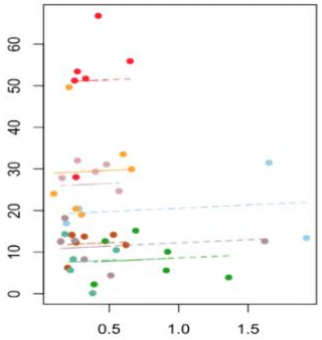
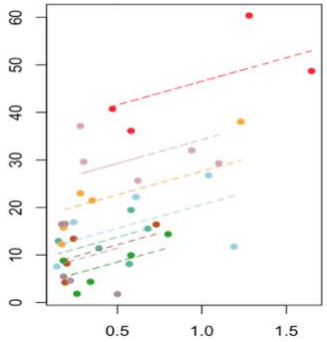
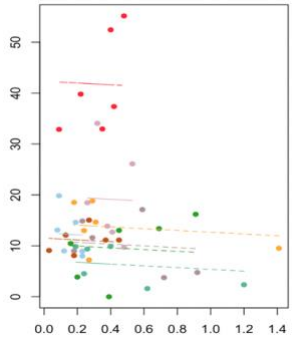
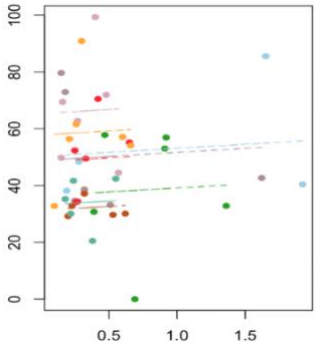
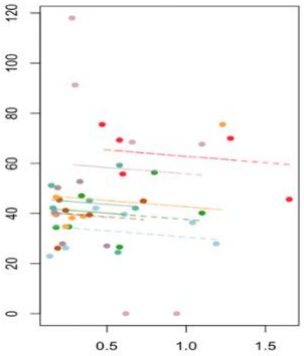
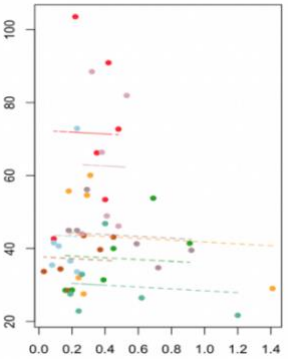
5.4.9 Association between ileal glucose and acetate with appetite regulation

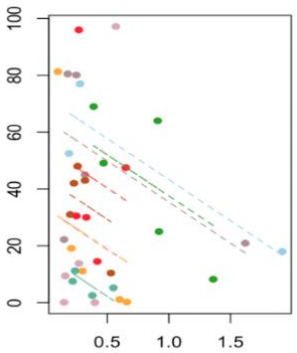
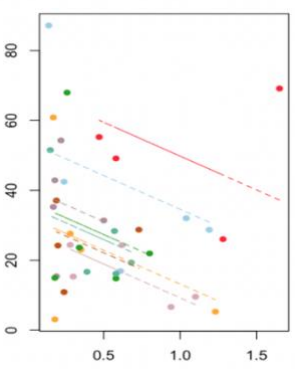
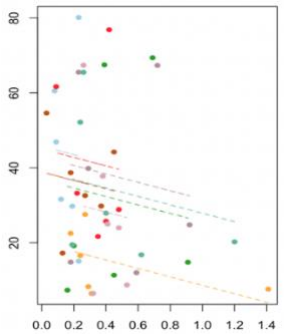
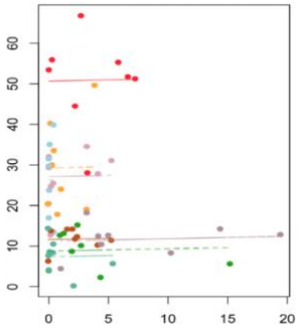
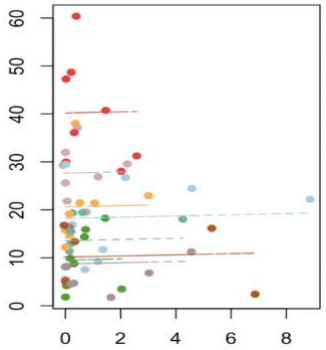
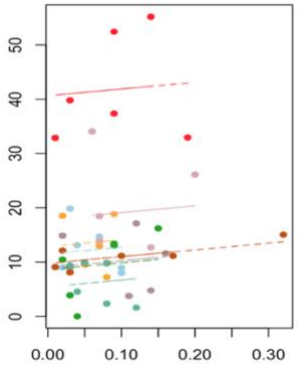
Repeated measure correlation was performed between ileal metabolite: glucose and acetate and PYY, GLP-1, and CAS (**Figure 5.12)** during 60-360min when foods were likely presented in the ileum. The same colour represents measurements within the same subjects.

For Intact-S (the left column), ileal acetate was negatively correlated (p=0.027) with composite appetite score (CAS), with r=-0.40 (-0.67, -0.05). Ileal glucose did not correlate with any appetite measurements.

For Intact-C (the medium column), ileal acetate was positively correlated with circulating PYY levels [r=0.51 (0.18, 0.73), p=0.004] and negatively correlated to CAS [r=-0.37 (-0.64, -0.02), p=0.038]. Ileal acetate did not correlate with GLP-1. Ileal glucose did not correlate with any appetite measurements.

For Broken (right column), ileal glucose and acetate did not correlate with PYY, GLP-1, or CAS

	Intact-S	Intact-C	Broken
Ileal acetate vs PYY (pmol/L)	P =0.84; r=0.03 (-0.30, 0.36) 	**P =0.004; r=0.51 (0.18 0.73) 	P =0.63; r=-0.07(-0.38, 0.25) 
Ileal acetate vs GLP-1 (pmol/L)	P=0.78; r=0.05(-0.28, 0.37) 	P =0.60; r=-0.08(-0.40, 0.24) 	P =0.76; r=-0.05 (-0.36 0.27) 

Ileal acetate vs CAS	*P=0.027; r=-0.40(-0.67 -0.05) 	*P=0.038; r=-0.37 (-0.64, -0.02) 	P=0.36; r=-0.14(-0.44,0.18) 
Ileal glucose (mmol/L) vs PYY (pmol/L)	P=0.85; r=0.03 (-0.24, 0.29) 	P=0.83; r=0.03(-0.24, 0.29) 	P=0.44; r=0.12(-0.20 0.42) 

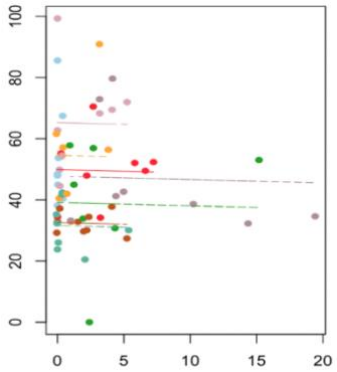
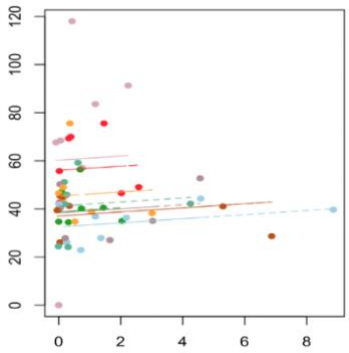
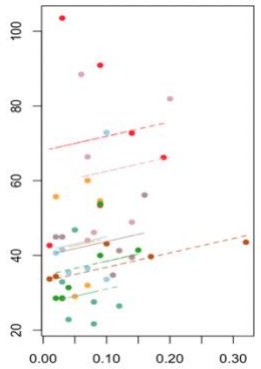
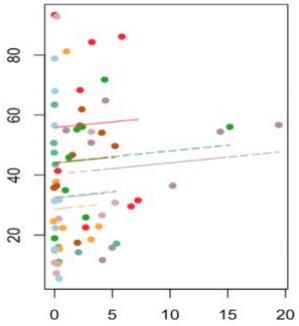
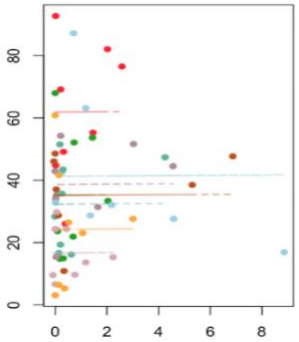
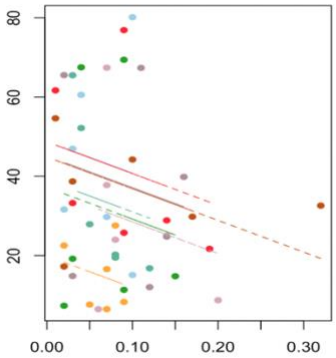
Ileal glucose (mmol/L) vs GLP-1 (pmol/L)	P=0.80; r=-0.02 (-0.28,0.24)  	P=0.53; r=0.09(-0.18, 0.34)  	P=0.29; r=0.17(-0.15, 0.46) 
Ileal glucose (mmol/L) vs CAS	p=0.69; r=0.05 (-0.21, 0.32)  	p=0.97; r=0.01(-0.26, 0.27)  	P=0.14; r=-0.23(-0.51, 0.09) 

Figure 5. 12 Correlation between ileal metabolites and appetite measurement. Repeated measure correlation tests were performed between ileal glucose and acetate, and appetite measurements included PYY, GLP-1, and composite appetite score (n=8). Measurements within the same

subject are in the same colour. Repeated measure correlation is presented with coefficient r with 95% CI. Intact-S, intact single cells; Intact-C, intact cell clusters; Broken, Broken cells; CAS, composite appetite score. *p<0.05, **p<0.01,***p<0.001.

5.5 Discussion

5.5.1 Summary of findings

- At day 3 baselines, fermentation levels of intact-C were increased compared to Broken, as evidenced by elevated levels of breath hydrogen (BH) and GLP-1. Ileal metabolites did not differ between food structures at baselines; the lower region of the gut (i.e., the colon) may have led to this as a prolonged effect from day 2 dinner.
- After meals, Intact-C and Intact-S increased BH from 240min until the end of the measurements (480min). During this period, a trend in fullness iAUC was observed that Intact-C> Intact-S> Broken, where the difference between Intact-C and Broken reached significance. Intact-C increased BH and PYY than Broken at T=420-480min.
- To understand the roles of ileal contents in appetite control, targeted analysis of ileal glucose and metabolic profiling was performed. Ileal glucose release profiles suggested that food arrived at the terminal ileum at 28.1 ±9.4 min and was retained until 343.7 ± 53.6, 451.7 ± 28.3, and 299.3 ± 49.7min for Intact-S, Intact-C and Broken, respectively. Ileal metabolomic profiling demonstrated a distinct difference. Broken had the least carbohydrate arrival and release in the ileum; Intact-S had the highest ileal maltose and glucose release, confirming its digestibility in the ileum; Intact-C remained low digestion in the ileum and thus should have preserved more RS for fermentation.
- Intact-C released higher acetate in the ileum than Intact-S and Broken, which can partly explain its satiety-enhancing effect. Moderate correlations were established between ileal acetate with PYY ($r=0.51$, $p=0.004$) and CAS ($r= - 0.37$,$p=0.038$).

5.5.2 Detailed discussion

This study aimed to understand carbohydrate digestion and fermentation in the distal ileum and the effects on appetite regulation. Eight participants attended inpatient visits during which they consumed chickpea meals for 3 days. Chickpea meals were provided over breakfast, lunch, and dinner containing 60g, 50g, and 50g chickpea materials respectively. They were processed in the same way as Chapter 4 and served with identical low-fibre background diets. Appetite measurement and biological samples were collected on Day 3 over 8 hour-period. A linear trend for fullness iAUC was found between food structure interventions and Intact-C significantly increased fullness during 4-8hr compared to Broken. At the same timeframe, PYY levels increased with a parallel increase in breath hydrogen levels. To understand the role of ileum has played in the appetite change, ileal glucose analysis was performed to provide insights into the amount and time when carbohydrates arrived and left the ileum. Food entered the ileum at 28.1 min (average of three groups), peaked at 182.5 min, and retained until 364.9 min; Broken had the least carbohydrates reaching the ileum. Intact-S had the highest levels of ileal glucose and maltose suggesting carbohydrates of Intact-S arrived and were potent for digestion in the distal ileum. Intact-C compared to Intact-S appeared to preserve more RS for fermentation as evidenced by the elevated BH and ileal acetate and lower rates of ileal glucose release. Ileal acetate significantly correlated to PYY and composite appetite scores in Intact-C which partly explained its satiety-enhancing effect. Our data supported that the intact cell clusters had the greatest benefits for promoting ileal and colonic fermentation and suppressing appetite in the current time frame.

Effects of food structure on subjective appetite measurement

- Fullness

It is hypothesised that carbohydrates with an intact food structure would increase fullness compared to a disrupted structure. The meta-analysis of previous RCTs, however, suggested the effects of intact cell wall structures on appetite were non-significant (Cai et al., 2021). The included studies were mostly wheat-based food which does not necessarily represent legumes due to their distinct cell wall properties (Holland et al., 2020, Edwards et al., 2021). Legumes that preserve intact cell walls matrix present a great possibility to increase RS 1 amounts (Dhital et al., 2016, Edwards et al., 2021, Rovalino-Cordova et al., 2018) and therefore were selected as the food model. This study compared subjective fullness after the consumption of chickpeas in three forms: intact single cells (Intact-S), cell clusters (Intact-C), and broken cells (Broken). Our data found a linear trend between treatments as Intact-C> Intact-S> Broken in the fullness iAUC $_{240\text{-}480min}$ ($p=0.029$). Intact-C significantly increased fullness iAUC $_{240\text{-}480min}$ compared to the Broken. This can be supported by the results of Chapter 4, as Intact-C had the lowest carbohydrate release in the stomach and duodenum and therefore was expected to carry the highest amount of undigested starch to the ileum. An acute effect (0-3hr) on reducing appetite of Intact-S was observed in Chapter 4 but not in the present study, possibly owing to a smaller sample size (n=8). A recent study compared intact cells and open cells of chickpeas in 22 healthy subjects and observed a significant appetite-reducing effect from chickpea intact cells (Palchen et al., 2022). Further investigation should consider including a larger sample size to detect the differences between Intact-S and Broken.

An interesting finding is that the satiety-enhancing effect was observed only after lunch(240-480min). It has been previously reported a preloaded meal with chickpeas reduced appetite and reduce food intake at the next meal (Zafar and Kabir, 2017, Zafar et al., 2011, Mollard et al., 2011). The fermentation of RS is believed to be the major contributor to the subsequent meal effects (Higgins, 2012). Our study observed a delayed and sustained increase in breath hydrogen (BH) in Intact-C and Intact-S after lunch, which corresponded to the timing of the increase in fullness we observed. The oral-caecum transit time based on the ileal glucose release profile was estimated to about 364.9 min. Thus, the enhanced fullness we observed during 240-480min was likely to be attributed to the increased fermentation that occurs around the caecum area (distal ileum, caecum, and proximal colon).

- Desire to eat, hunger, and appetite for a meal

Unlike the fullness, other VAS parameters including the desire to eat, hunger, and appetite for a meal were not affected by food structure in our study. It is uncommon to see discrepancies in VAS appetite measurements (Gibbons et al., 2019). Indeed, the feeling of fullness was the measurement of "satiety" while the others were for measurement of "hungriness." Physiologically they may not be measuring the same thing (Gibbons et al., 2019). Hunger was identified as the best rating replicating the other subjective rating (Sadoul et al., 2014); while others have shown fullness is more closely associated with energy intake (Barkeling et al., 1995). Similar observations were found that only fullness, but no other VAS parameters significantly correlated to subsequent food intake (Parker et al., 2004), especially for young subjects (Flint et al., 2000). To validate the appetite change, future investigations should include objective measurement e.g., food questionnaire or *ad libitum* food intake along with the use of VAS.

Effects of food structure on breath hydrogen

A significant difference was observed in BH at the day 3 baseline. Intact-C had higher BH levels than Broken, which was likely the remaining intervention effects from the previous day. Intake of RS in the evening has been reported to increase the BH levels remaining for 18 hours until the next day (Muir et al., 1995). At baselines, ileal metabolites were not significantly different. This may suggest the elevated levels of BH have resulted from mainly metabolites fin the lower gut (e.g, proximal and/or distal colon).

After breakfast, different timeframe for BH increase was observed for food structures. BH of Intact-S and Intact-C started to increase from 234.2± 64.40 min until the end of the study visit, reflecting a transit time for nutrients to enter the distal ileum where fermentation happening. Previous studies observed a similar period (4-8hr) for raising BH levels after RS interventions (Olesen et al., 1994) (Symonds et al., 2004) (Muir et al., 1995). At 480 min, intact-S and Intact-C reached the highest values which were at 32 (16-56) (ppm) and 42 (17-117) (ppm). These values were comparable to a peak BH value after 7d consumption of 28g RS (van Munster et al., 1994), or after a single ingestion of 60g RS (Robertson et al., 2003). This is likely the result of accumulative RS intake of 3-day intervention. At 420 and 480min, Intact-C was significantly higher than Broken cells.

Different from Intact-S and Intact-C, BH of Broken dramatically increased from 90.7 ± 38.5 min, peaked at 240 min and gradually declined until 480 min. The increase of BH in the Broken group could be because some starch arrived in the distal gut despite its higher digestibility. In

addition, cell wall fragments could be fermented (Day et al., 2012), some studies suggested that broken cell walls could be fermented more quickly than intact cells as bacteria had easier access to intracellular contents (Guan et al., 2020). Moreover, the early increase of BH has previously been reported to be caused by emptying of remnants of previous meal from the ileum into the colon (Read et al., 1985). Interestingly, we identified lactose in the ileal samples at T0 while they were absent in the ileal samples at T60 and T120. The authors speculated whether the increase of BH in the Broken group during 0-2hr was also partly attributed to the ileal lactose travelling down to the colon producing hydrogen. Breath hydrogen tests have been widely used to indicate lactose intolerance based on the principle that undigested lactose reaches the distal gut to produce hydrogen (Rana and Malik, 2014).

Effects of food structure on PYY and GLP-1

A significant linear trend was observed for circulating GLP-1 levels between food structures: (Intact-C: 35.6 ± 3.9 pmol/L; Intact-S: 31.5 ± 3.1 pmol/L ; Broken: 29.4 ± 2.0 pmol/L), with the difference between Intact-C and Broken reaching to a significant level. This agreed with the breath hydrogen results above and together highlighted that Intact-C had increased fermentation activity at the day 3 baseline. On day 1 and 2, participants had been intervened with 105g starch from chickpeas which should provide a considerable amount of RS. Edward et al. suggested only 40% of the starch was digestible in chickpea intact cells which would leave around 60% RS (Edwards et al., 2020); another recent study suggested macroparticles of chickpea that shared similar particle size with Intact-C caused 33.0 ± 0.9% of starch to be digested during a 220min amylolysis assay (Edwards et al., 2021). After meals, GLP-1 levels did not differ between food structures, similar to previous RCTs (Cai et al., 2021), indicating

that intact food structure had non-significant effects on the postprandial GLP-1 during 8-hour postprandially. The reason for a lack of significant change in GLP-1 between food structures is unclear. The fact that we observed a significant change in GLP-1 at baseline may imply that the stimulation of GLP-1 can be delayed and/or prolonged and resulted from a lower region of the gut. Dietary RS has been reported to increase proglucagon in the cecum and colon but not in the ileum compared to a control diet, although the highest noninduced expressions for both groups were detected in the ileum (Zhou et al., 2008). The ileal retention time in Intact-C was estimated to be around 451.7 min and thus current 480min timeframe did not fully capture the GLP-1 secretion derived by the caecum and colon.

PYY did not follow the same pattern as GLP-1. PYY did not differ between food structures at baselines. Significant differences were observed for postprandial PYY: Intact-S had an earlier and higher peak than Broken (T=180min), consistent with the acute response in Chapter 4. Intact-C had higher PYY than Broken at 420 min and 480 min. Notably, the increase in PYY was parallel with the increase in breath hydrogen, possibly suggesting fermentation products stimulated PYY secretion. Two previous RCTs investigated the effects of food structure on PYY response; one studied oatmeal (Mackie et al., 2017b) and the other studied wheat-based porridge (Edwards et al., 2015a). Both reported that intact food structures of starchy foods did not affect PYY iAUC (Mackie et al., 2013, Edwards et al., 2015a). Both studies had a shorter period (180min and 240min); while our data detected differences mainly at 420-480min. Moreover, legume cell walls are thicker than cereals (Stone, 2006); and the same processing treatment differently affected the integrity and digestion kinetics of legume and cereal cell walls (Edwards et al., 2021) and can affect the amount of RS available for fermentation. Edward *et al.,* found that intact endosperm cells did not increase RS amount in the ileal fluids

compared to broken cells (Edwards et al., 2015a); while in our study, Intact-C significantly increased fermentation than Broken evidenced by increased BH levels. Understanding plant cell wall properties and how they interact with the GI tract is essential to interpret their gut hormone responses.

Effects of food structure on glucose and insulin response

This study investigated the glucose and insulin responses following the day 3 interventions. We also aimed to compare the results between Chapters 4 and 5 to understand whether the interventions over 3 days brought additional benefits in attenuating postprandial glycaemia.

Plasma glucose was significantly lower in Intact-C and Intact-S than in Broken. The differences were observed one hour after breakfast and lunch intake (at 60 and 300 min). Broken had the highest peak values which were at 6.52 ± 0.53 mmol/L and 6.15 ± 0.33 mmol/L respectively. The clustered structure had the lowest peak values of 5.21 ± 0.25 mmol/L and 5.14 ± 0.23 mmol/L. These were comparable to the peak values of the acute glucose response to a single meal in Chapter 4. The reduced attenuated glucose response in intact structures was the result of slower rate digestion in the upper GI tract, as discussed in Chapter 4. In addition, a significant difference in glucose iAUC was observed between Intact-C and Intact-S, which was absent in a single meal response. A "second meal" effect may occur in the Intact-C group. A second meal effect is described as an intake of fermentable carbohydrates (e.g., whole grains and legumes) having a prolonged effect and reducing postprandial glycaemia in the subsequent meal. Intake of legumes in the evening decreased the postprandial glycaemia at breakfast the following morning. This effect was lost upon milling or processing which

damaged the structures (Higgins, 2012). Chickpeas have been shown to have a second-meal effect (Mollard et al., 2011). It is believed that intestinal fermentation and the products SCFAs play a role in improving glycaemic metabolism (Higgins, 2012, Wolever et al., 1988, Mollard et al., 2011).

Serum insulin followed a similar response profile to glucose. Intact-C and Intact-S decreased insulin response compared to Broken. The differences were observed 1 and 2 hours after the breakfast and lunch intake (T= 60-120, T=300-360 min). Importantly, the insulin-lowering effects of Intact-S and Intact-C were prolonged compared to the single meal response (differences observed only within 1hr). Some studies found that intake of chickpeas significantly improved medium to long-term glycaemic control, as indicated by fasting blood insulin and glycated protein and insulin sensitivity levels (Rebello et al., 2014). Our data may suggest that day-long intervention of chickpea intact cells and clusters can bring prolonged health outcomes in blood glucose and insulin control than the acute effect of a single meal.

Effects of food structure on ileal glucose

Ileal glucose concentrations were distinct between food structure interventions. Chickpea broken cells resulted in very low concentrations of glucose in the ileum throughout 0-480min (Peak value 0.9 ± 0.2 mmol/L). It is within expectations as Chapter 4 has shown more carbohydrates of Broken were released and digested in the upper GI tract. Existing in vitro studies that mimic human intestinal conditions supported that broken cells of pulses caused a higher starch digestion rate and extent (Xiong et al., 2022b), leading to almost complete starch digestion (94-99%) in the small intestine (Palchen et al., 2022). In contrast to Broken,

Intact-S and Intact-C delivered more carbohydrates to the ileum. Ileal glucose of Intact-S and Intact-C peaked in concentrations at 8.0 ± 2.1 mmol/L and 4.1 ± 0.9mmol/L. This aligned with the findings of Chapter 4 and a series of in vitro studies (Palchen et al., 2022, Rovalino-Cordova et al., 2018), establishing that cell wall integrity improved the delivery of nutrients into the terminal ileum by reducing digestibility in the upper GI tract. We also observed that Intact-S had higher ileal glucose concentrations than Intact-C, likely suggesting that Intact-S was more potent for digestion in the ileum. Intact-C released less glucose in the ileum may be owing to its stronger barrier effects than Intact-S as demonstrated in Chapter 4. The findings led to the conclusion that Intact-C could possess a larger amount of RS that can escape digestion in the distal ileum and enter the colon. Future investigations into cell wall matrices and starch present in the ileal aspirations are required to validate the physiological role of cell clusters.

The time profile of ileal glucose provided some insights into the transit time of food arriving and leaving the ileum (oral-caecum transit time). The results suggested that foods arrived at the terminal ileum and initiated glucose release at 28.1 ± 9.4 min (Mean ± SEM for three groups); peaked at 182.5 ± 26.2 min. There was a significant trend that food structure could delay the time when foods left the ileum (Intact-C: 451.7 ± 28.3min> Intact-S: 343.7 ± 53.6min > Broken: 299.3 ± 49.7 min, p trend = 0.031). Nutrients in the ileum can activate the "ileal brake", a feedback mechanism that results in the inhibition of proximal GI tract motility and secretion (Maljaars et al., 2008). Animal studies have suggested that RS and DF can activate ileal brake (Ratanpaul et al., 2019). Ileal brake can act on PYY and GLP-1 and may serve as a food target for appetite control (Maljaars et al., 2008). The present study showed that Intact-

C and Intact-S enhanced the carbohydrates delivery to the ileum; possibly stimulating the physiological feedback that affected gut mobility and transit time.

The Interplay between food structure, ileal metabolites and appetite regulation

Metabolites present in the ileum can provide critical information about the host and bacterial processes. In our study, ^{1}H-NMR metabolomic profiling was performed in the ileal samples and identified distinct metabolites between food structure interventions. We aimed to understand the interplay between food structure, metabolites from carbohydrate digestion and fermentation (with a focus on glucose and SCFAs), and appetite regulation.

- Ileal glucose

PLS-DA analysis aligned with quantitative analysis confirming the ileal glucose was the highest in Intact-S, the second highest in Intact-C and the lowest in Broken during T=120-360min. Glucose can be directly sensed by L cells and stimulate GLP-1 (Reimann et al., 2008). Ingestion of 30g glucose directly into the ileum increased GLP-1 in ileostomy patients (Zhang et al., 2022); similarly, ingestion of 15 g glucose ingestion into the ileum increased PYY, GLP-1 and reduced appetite in healthy volunteers (Poppitt et al., 2017). In the present study, however, ileal glucose did not relate to PYY, GLP-1, or composite appetite scores in any intervention groups. This may be due to the fact that glucose can be absorbed effectively, and the amount detected in the ileum was relatively lower (e.g. mean peak value 4.1 mmol/L in Intact-C, equivalent to 0.74g/L) than the doses of previous nutrient sensing studies. Therefore, the ileal glucose sensing pathway may not be dominant in appetite regulation seen in our study.

- Ileal acetate and appetite regulation

Acetate is the most abundant form of SCFAs produced from intestinal fermentation. Acetate, propionate and butyrate are present in a ratio of 60:20:20 in the colon and stool (Hijova and Chmelarova, 2007, Cummings et al., 1987). A unique series of measurements in sudden-death bodies found that acetate was present at a concentration of 6.3 ± 0.1 mmol/kg in the human ileum (Cummings et al., 1987). Acetate is mainly the product of the Bacteroidetes phylum (Macfarlane and Macfarlane, 2003), which has been detected in the ileal microbiome community (Villmones et al., 2018). Our study identified acetate as one of the ileal metabolites that drove the differences between food structures. Time course data demonstrated that ileal acetate was the highest at the baselines and reduced after meals. This was aligned with our unpublished data on an ileal intubation study. Food reaching to the ileum caused "flushing effect" and reduced the density of microorganisms, decreasing the levels of microbiota-derived metabolites (Dagbasi, 2022). Ileal acetate was elevated in Intact-C during 240-360 min, and exhibited significantly higher levels compared to Broken and Intact-S evidenced by PLS-DA analysis.

Our study observed an inverse correlation between that ileal acetate and composite appetite score in Intact-S and Intact-C groups. In the Intact-C group where the most significant satiety-enhancing effects were observed, mutual correlations were found between ileal acetate, circulating PYY, and composite appetite score. This reveals the first-time that the arrival of carbohydrates increased ileal fermentation product acetate. Ileal acetate can act as a mediator to reduce appetite possibly via elevating PYY secretion.

Other ileal metabolites

Other possible appetite mediators, including secondary bile acids, BCAAs, amino acids, lactose, and succinate were identified to interplay with food structure interventions. Bile acids and BCAAs were found to have a higher release in the Intact-S and Intact-C than in Broken and the differences were more pronounced in Intact-C. Amino acids (tyrosine and phenylalanine), lactose and succinate were higher in Intact-S than Broken. There is evidence from colonic models and nutrient sensing studies where they have affected gut hormone and appetite regulation. Conjugated bile acids are microbiota-derived metabolites. They can activate the TGR5 signalling that stimulates the PYY and GLP-1 secretions from L cells (Thomas et al., 2009, Christiansen et al., 2019). BCAAs including leucine, isoleucine, and valine are derived from the diet and gut microbiota. The mechanisms by which BCAAs regulate appetite are controversial. BCAAs have provided inconsistent findings on appetite measurements, possibly depending on the ratio of BCAAs: non-BCAAs (Han et al., 2021). BCAAs stimulated CCK secretions via activation of receptor T1R1/T1R3 in porcine gut models (Tian et al., 2019b). L-amino acids e.g, phenylalanine can activate receptor CaSR (Conigrave et al., 2000) and modulate gut hormone release and suppress food intake(Alamshah et al., 2017). Lactose and succinate are intermediate products of carbohydrate fermentation via pyruvate metabolism. They can be further metabolized, producing SCFAs (Oliphant and Allen-Vercoe, 2019, Koh et al., 2016). They were both correlated with ileal acetate ($r=0.44$ and $r=0.73$) but did not correlate with any appetite measurement in this study (data not shown). The role that they have played in this study remains to be elucidated.

5.5.3 Conclusion

Intact-C enhanced fullness compared to the Broken during 240-480min as a result of increased fermentation. Distinct ileal metabolites were observed between food structure interventions during such time which at least partly explained appetite outcomes. Broken had the least carbohydrates that arrived at the ileum; Intact-S and Intact-C increased carbohydrate delivery to the terminal ileum. Intact-S was more digestible and released higher glucose and maltose; whereas Intact-C promoted ileal acetate production which likely played a role in stimulating PYY and increasing fullness. At the end of sampling period (T=420-480min), Intact-C appeared to transport carbohydrates to the colon, during which time it had a significantly higher PYY compared to Broken. Our data confirmed the satiety-enhancing effects of Intact-C.

Chapter 6: General discussion

6.0 Summary of main findings in Chapter 4-5

- Chickpeas with broken and intact cell walls had distinct digestion profiles in the human GI tract. Broken cells released starch into the gut lumen, rendering them rapidly accessible to amylase to produce glucose. Microscopic observation revealed that most empty cells and cell wall fragments after 180min duodenal digestion; quantitative data exhibited a higher release of maltose and glucose from Broken confirming its higher digestibility.
- The structures of intact single cells (Intact-S) and cell clusters (Intact-C) were largely unchanged in the stomach and duodenum and enclosed a large amount of starch at 180min of duodenal digestion. Intact-C had less starch leakage than Intact-S indicating its greater barrier effects.
- Intact-S and Intact-C significantly lowered postprandial response (0-60min) of glucose, and insulin compared to the Broken. Intact-S and Intact-C had a slow but sustained rise in postprandial GIP (0-180min), reflecting their slow luminal glucose release and a widespread release throughout the small intestine.
- Intact-S acutely (0-180min) increased fullness and PYY responses compared to Broken which was independent of fermentation and ileal glucose concentrations.
- Foods began to enter the distal ileum at T=30min and remained there until 360min. During this period, Intact-S and Intact-C delivered more carbohydrates into the terminal ileum compared to broken cells. Intact-S was more digestible in the ileum,

while Intact-C owned the lowest digestibility throughout the gut and thus preserved more carbohydrates for fermentation.

- Intact-C increased fullness (240-480min) compared to broken as a result of elevated ileal and colonic fermentation. During 240-360min, Intact-C promoted SCFA (acetate) production in the terminal ileum, which was positively correlated with PYY and inversely correlated with appetite scores; foods moved to the colon at around 420-480min during which PYY was significantly higher in Intact-C than Broken.
- Chickpea intact and broken cells resulted in significant differences in the metabolomic profiles in the intestinal lumen. Intact-S and Intact-C showed higher levels of conjugated bile acids and amino acids compared to Broken. **Figure 6.1** summarizes the key findings.

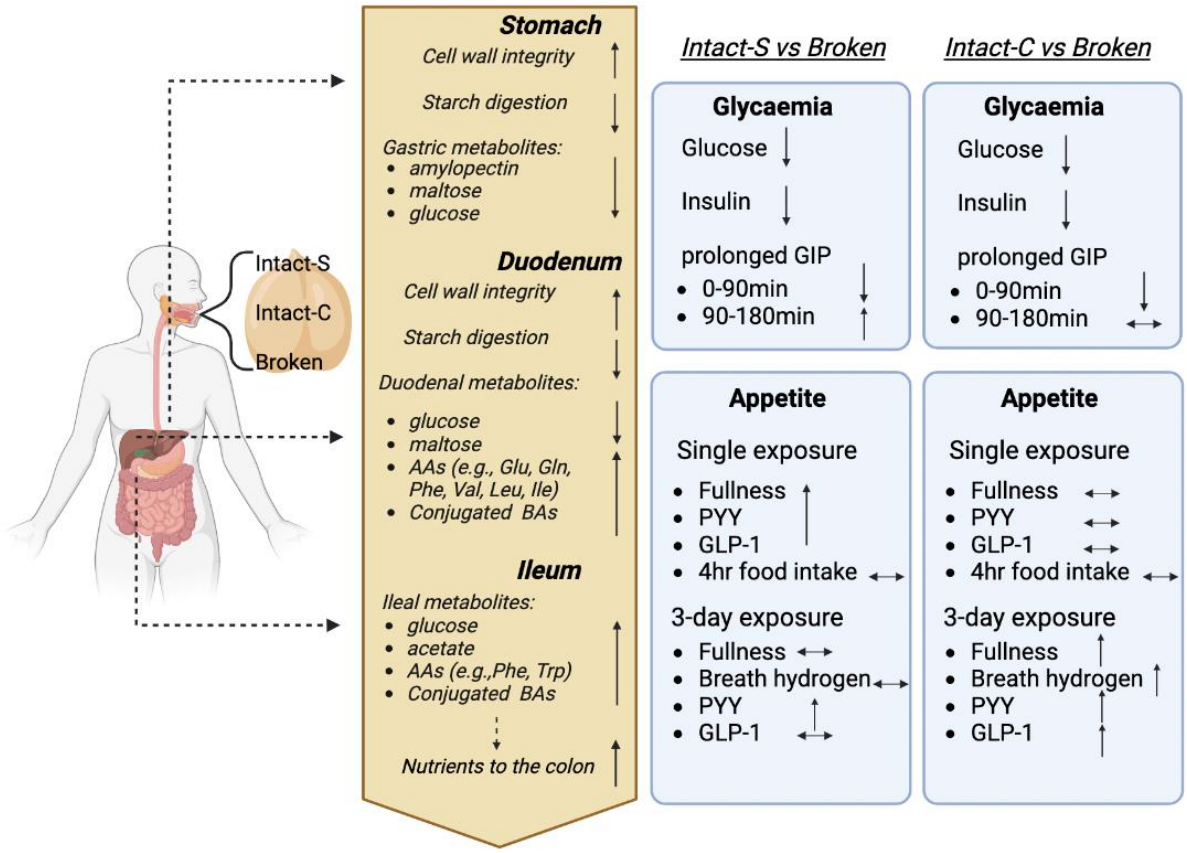


Figure 6. 1 Overview of results from Chapters 4 and 5.

↑ and ↓ indicates significantly higher or lower levels in Intact-S or/and Intact-C compared to Broken. AAs, amino acids; BAs, bile acids; Glu, glutamate; Gln, glutamine; Phe, phenylalanine; Trp, Tryptophan; Val, Valine; Leu, Leucine; Ile, Isoleucine; Intact-S, intact single cells; Intact-C, intact clusters; Broken, broken cells.

6.1 Introduction

There is a broad consensus that a diet rich in dietary fibre (DF) helps prevent a wide range of metabolic diseases (Augustin et al., 2020). The underlying mechanism remains unclear, and its composition alone does not fully characterise the health benefits. DF is mainly part of plant cell walls (Brownlee, 2011), the structure and properties are highly linked to their digestion behaviours in the gut and subsequent metabolism (Capuano, 2017a, Grundy et al., 2016b). Plant cell walls are composed of polysaccharides that do not contain α-glycosidic links and are therefore resistant to pancreatic amylase (Brownlee, 2011, Cummings and Englyst, 1991). Intact cell walls act as a natural digestion barrier, hindering starch hydrolysis in legumes (Brummer et al., 2015), which explains their low glycaemic index (Bajka et al., 2021, Delamare et al., 2020). With macroparticles and cell walls remaining intact through the small intestine, intracellular nutrients may escape digestion (Edwards et al., 2015a, Noah et al., 1998, Petropoulou, 2019b) and can be released in the large intestine upon fermentation of cell walls, promoting SCFAs production.

The beneficial effect of DF largely depends on the structural integrity (e.g. intact cell walls) that modulates the digestion process. However, plant-based foods are mostly milled into fine particles before consumption, causing damage to the cell wall (Edwards et al., 2015b). Without the protection of intact cell structure, carbohydrates are rapidly digested and cause high glycaemic responses (Edwards et al., 2015b, Bajka et al., 2021) . The benefits derived from fermentation and SCFAs can be affected as the transport of cellular structure and contents into the distal gut can be reduced. These have raised concerns about the efficacy of

DF, and underlined the need for a deeper understanding of the interrelations between plant cell wall structures, digestion, and physiological response. This work aimed to understand how cell wall structures affected gastrointestinal digestion, glycaemic and appetite outcomes in human subjects.

6.2 Detailed discussion

Cell wall structure and digestion in the GI tract: the stomach, duodenum, and terminal ileum

Chapter 4, 5 altogether included the same participants and enabled monitoring of the digestion behaviours throughout the GI tract (stomach, duodenum and ileum). Broken cells demonstrated distinct digestion and metabolomic profiles compared to intact cell structures. Microscopy observations showed that in Broken, the majority of starch was leached out of the cells and was therefore freely accessible to pancreatic amylase. In their gastric aspirations, the starch contents were visibly reduced from T=45 min onwards; and by the end of duodenal sampling (180min), most of the starch had disappeared and only cell wall fragments and a small amount of starch can be seen. The quantitative and NMR analysis provided consistent and reliable indications of starch digestion, confirming its higher rates and extent of glucose and maltose release in the upper GI tract. Chapter 5 further examined the digestion in the terminal ileum and showed that the number of carbohydrates from Broken that arrived at the terminal ileum was negligible, confirming the digestion was almost completed in the proximal intestine. This is an important finding as legumes are thought to be good sources of slow-release carbohydrates (Tharanathan and Mahadevamma, 2003, Jenkins et al., 1980); however,

our data suggested that processing-derived disruption to cell walls increased the digestibility in human subjects in a way that could reduce health benefits.

Unlike broken cells, single cells and cell clusters provided a strong physical barrier limiting starch hydrolysis during the gastric and small intestinal passage. Intact single cells after 180min gastric and duodenal digestion remained largely unchanged. Most of the starch was encapsulated by the cell walls despite a small proportion visibly leaking from the cells. Intact cell clusters had shown minimal starch leakage throughout gastric and duodenal digestion. Chickpea cells at the cluster edge and core remained largely intact, although some cells at the edges began to separate. The kinetics of luminal glucose and maltose confirmed their lower rates of digestion compared to Broken. An interesting observation was that the duodenal carbohydrates curve showed spikes (Figure 4.4) whilst these were not observed in gastric curves. The reason is unclear and may indicate a rhythm of gastric emptying. Gastric emptying has been suggested to be delayed by a larger particle size (Vincent et al., 1995, Olausson et al., 2008) and complex carbohydrates (Hasek et al., 2020). In duodenal glucose and maltose curves, Intact-S and Intact-C appeared to slightly delay the rhythms of spikes compared to Broken. Food structure may affect gastric emptying and should be examined further.

The digestion behaviours of cell clusters have not been studied as widely as individual cells. Most of the studies agreed that individual cells benefit from the separation of cell clusters/plant macroparticles, as cell separation weakens the adherence of cells (e.g, pectin in the middle lamella) and facilities the release of cells under mechanical stress, thus avoiding cell wall damage (Dhital et al., 2016, Xiong et al., 2022b). On the other hand, particle size of plant tissue (e.g., almond, carrot, and chickpea) is inversely related to the rate and extent of

digestion (Grundy et al., 2015, Lemmens et al., 2010, Edwards et al., 2015b). Given this, a larger cell cluster (e.g., >500 µm) that maintain structural intactness may limit digestibility compared to intact single cells (e.g., 50 µm). Studies compared intact single cells and cell clusters before were limited and provided conflicting results. Almond samples with the lowest level of lipid digestion were the single almond cells (35 µm diameter) with intact cell wall rather than the biggest macroparticle (1000-2000 µm) (Grundy et al., 2015); whilst one diffusion study found that cell clusters of soybeans delayed the diffusion of the digestive enzyme into cells compared to individual cells suggesting its lower permeability (Zahir et al., 2020). Another study observed that macroparticles of chickpeas (1.85mm fraction) largely limited the extent of starch digestion (only 33.0% digested) (Edwards et al., 2021) . Our study provided the first-ever direct in vivo observations of digestion behaviors of cell clusters compared to single cells and broken cells. The metabolomic profiling confirmed that Intact-C lowered the release of glucose, and maltose /amylopectin compared to Broken and Intact-S in the stomach and duodenum. Microscopic observations revealed that cell clusters initiated cell separation rather than cell rupture and exudated fewer cellular contents compared to Intact-S, revealing it provides a stronger digestion barrier than intact single cells.

So far from Chapter 4, it was concluded that Intact-C lowered the kinetics of digestion compared to Intact-S but whether the digestibility (extent of digestion) could be affected was not clear. Thus, Chapter 5 further investigated the carbohydrate release in the terminal ileum, the ending of the small intestine. Intact-S and Intact-C dramatically increased the proportion of carbohydrates reaching the terminal ileum; with ileal glucose peaks 10 and 5 times higher than those observed following the ingestion of Broken, respectively. An average time of 28min and 365min has been observed when postprandial ileal glucose exceeded and returned

to the baselines; indicating an approximate time when food entering and leaving the ileum. This is in accordance with the literature that biomarkers appeared in ileum samples 30min after ingestion and were retained until 6-7h (Stephen et al., 1983). Intact-S had a higher ileal glucose iAUC than Intact-C, indicating that intact single cells were more susceptible to digestion in the ileum and released more ileal glucose. Maltose as identified from metabolomic profiling supported this which showed a higher release in Intact-S compared to Intact-C during T=60-360min. Intact-C, on the other hand, maintained lower carbohydrate release throughout the intestine; and given the matched macronutrients, more carbohydrates (e.g. RS) should be preserved that escaped small intestinal digestion and entered the colon. In support of this, iAUC of breath hydrogen as the indicator of intestinal fermentation was significantly in Intact-C compared to Intact-S throughout 0-480min. The ileum and colon could have contributed to hydrogen excretion, and we aimed to distinguish their effects by the time profiles. Based on the profiles of breath hydrogen and ileal glucose, it was speculated the timeframe of 240-360min was mainly attributed to the ileum, while the later increase was more predominantly caused by colonic fermentation. Importantly, metabolomic profiling revealed that ileal acetate release was higher in Intact-C than in Broken and Intact-S at T=360min. This confirmed the increased fermentation levels in the ileum for the Intact-C group. In the following time points (420-480min), BH increased rapidly in the Intact-S, probably because foods reached the colon. BH was also increased in Intact-C, but not significantly higher than in Intact-S. It may be due to the longer retention time of Intact-C in the ileum (451.7 ± 28.3 min) and therefore, the current timeframe did not fully capture the colonic fermentation from Intact-C. The fact that Intact-C had the highest fasting BH levels provided some clues that during the overnight period it had the highest fermentation levels, likely resulting from colonic effects.

Altogether, the distribution of intraluminal glucose shown in **Figure 6.2** provides direct evidence that food structure affects the rate, extent, and region of starch digestion in the human GI tract. Broken cells were dominantly and readily digested in the upper GI tract; intact-S had delayed and prolonged starch digestion throughout the small intestine; Intact-C maintained low rates of digestion at the gastric, duodenal, and ileal stage; and due to their matching macronutrients, could provide a considerable amount of RS1 for ileal and colonic fermentation. These novel results reveal the potential of cell clusters of legumes as high RS ingredients, contrasting to what has been observed in wheat-based foods. Studies conducted in individuals with ileotomies found that intact endosperm cells reduced the rate but not the extent of starch digestion (Edwards et al., 2015a). The amount of RS retrieved in the ileum was unaffected by the particle size of white bread and cornflakes (Englyst and Cummings, 1985). A structural function study comparing wheat and chickpeas have revealed that wheat endosperms are more permeable to amylase than chickpea cells (Edwards et al., 2021), which may explain the difference between the two types of plant cell walls. Overall, evidence suggests that cell wall permeability is a determinant factor for its capacity of delivering RS to the distal gut. Cell clusters of legumes pose the greatest potential for promoting fermentation and related benefits.

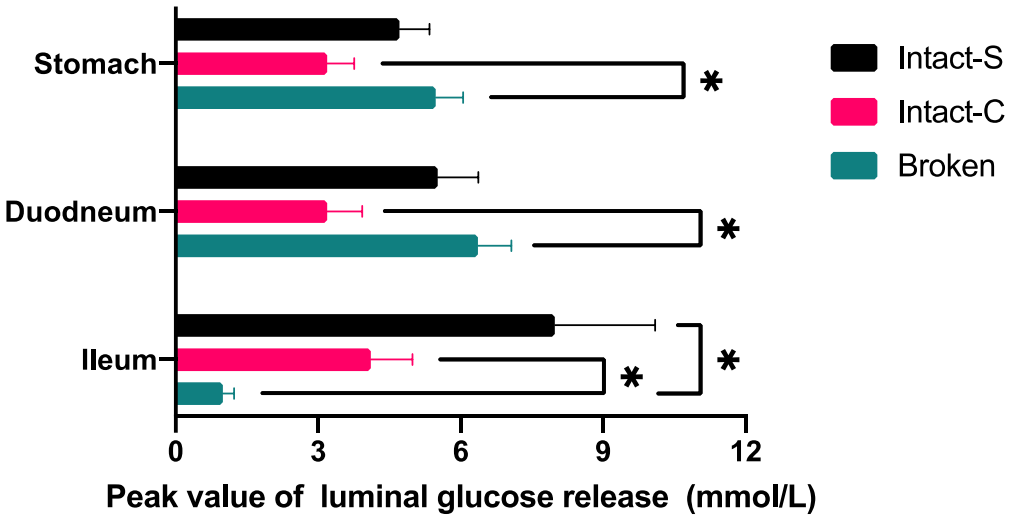


Figure 6. 2 Intraluminal glucose release in the region of the stomach, duodenum, and ileum. Repeated measures one-way ANOVA with post hoc Tukey's test was performed on intraluminal glucose data. Data presented as mean ± SEM (n=13 for the stomach and duodenum, n=8 for the ileum). Intact-S, intact single cells; Intact-C, intact cell clusters; Broken, Broken cells. *p<0.05, **p<0.01, ***p<0.001.

Postprandial glycaemia and small intestinal digestion

Understanding digestion facilitates the interpretation of postprandial glycaemia. It is not surprising to see glucose and insulin responses were significantly higher in Broken compared to intact structures. The rapidly elevated luminal glucose in Broken was absorbed primarily by SGLT1 in the small intestine (Chen et al., 2016), leading to a rapid rise in glucose response. Elevated blood glucose increased insulin requirements; luminal glucose absorption drove GIP secretion by intestinal K cells mainly in the duodenum and proximal jejunum, GIP acts on pancreatic β-cell to promote insulin secretion (Baggio and Drucker, 2007b). Insulin mirrored

the response of glucose in which we observed the biggest differences during 0-60min, with Intact-C and Intact-S showing smaller peaks than Broken. In addition, Intact-C significantly lowered insulin iAUC compared to Intact-S. This can be due to its lowered luminal and blood glucose response that reduced the need for insulin. The GIP response demonstrated different profiles between food structures. GIP in Broken increased dramatically during 0-30 min and gradually declined to baselines, replicating its glycaemic response. Intact-S and Intact-C had a slower but more sustained GIP increase during 0-180 min. Intact-S had higher GIP $iAUC_{0\text{-}180min}$ compared to Intact-C which reflected its higher intestinal glucose release and more widespread release throughout the small intestine.

The mutual correlation between blood glucose, insulin, GIP and luminal carbohydrates confirmed that the kinetics of luminal carbohydrate digestion determined acute glycaemia as we proposed above. These led to the conclusion that intact food structure limited the rates of luminal glucose release; thus, lowering the rise of blood glucose and reducing the requirement for insulin. It was noted that gastric maltose had the most significant correlation with plasma glucose, possibly emphasizing the importance of the early stage of starch digestion (salivary amylase digestion) in postprandial glycaemia. We observed that gastric aspiration could remain at a pH of 4-5 until 60 min post-ingestion supporting that salivary amylase may play a more important role than generally thought. Overall comparing groups, it is confirmed that cellular integrity is a critical factor underpinning the low glycaemic index of DF-rich foods.

Chapter 5 further investigated the glucose and insulin response after repeated and prolonged interventions over 3 days. Fasting values were not affected by intact food structure, as would

be expected given the relatively young (30.5 ± 2.9 y) and healthy subjects included. Intact-S and Intact-C reduced the peak values of glucose and insulin, comparable to the acute response above; timewise, the insulin-lowering effect of Intact-S and Intact-C appeared to be more pronounced. In Chapter 4, insulin differences between food structures persisted until 60 min, whereas in Chapter 5, Intact-S and Intact-C remained lower than Broken until 120 min postprandially. Furthermore, cell clusters exhibited lowered blood glucose compared to single cells, an effect which was not present in the acute response. The amplification of glycaemic benefits can be the result of accumulative RS intake and increased fermentation, which is generally described as the "second meal effect" and has been reported in legume take (Higgins, 2012, Brighenti et al., 2006, Venn and Mann, 2004). Throughout 3-day interventions, subjects consumed 320 g chickpea which provided 160 g starch. Chickpea macroparticles that shared a similar particle size (1.85mm) with Intact-C showed 67 % of starch being indigestible (Edwards et al., 2021). Based on this, the intervention of Intact-C would have provided around 107g RS over 3 days. The realistic dose would be lower than this as the estimation was based on a single enzyme digestion method which did not account for dynamic effects. Nevertheless, a considerable amount of RS should have been provided to promote fermentation. In support of this, we observed increased fermentation levels indicated by breath hydrogen levels and increased fermentation products in the ileum (e.g., acetate). These data suggest that longer consumption of Intact-C may bring additional benefits in glycaemic control possibly owing to its effective RS dose.

Acute appetite and luminal metabolites

In Chapter 4, acute appetite (0-3h) was impacted by food structure, although later Chapter 5 showed that intestinal fermentation appeared to play a lesser role in this period. Intact-S showed an acute effect of reduced appetite and elevated levels of PYY and GLP-1 levels during 0-3 hr. Despite this, food intake did not differ between food structure interventions. The biggest difference in fullness was observed at T=45min while food intake was measured at 240 min post-ingestion, possibly explaining its non-significance. The elevated levels of hormones were hypothesized to be the result of L cells of the distal gut interacting with nutrients e.g, glucose or SCFAs; although our data do not seem to support this as ileal glucose or acetate did not correlate with GLP-1 and PYY in Intact-S. Other metabolites or regions of the gut would be more responsible for these hormonal responses. Indeed, mechanisms that control the gut hormones are highly complex and can be modulated by neuronal (Rudnicki et al., 1992), humoral factors (Martin et al., 2019), and luminal nutrient ingestion(Ueno et al., 2008) (Poppitt et al., 2017). In metabolomic profiling, we identified several metabolites that were up-regulated by Intact-S in the duodenum and ileum that may favour appetite control. These included bile acids, tyrosine, tryptophan, and phenylalanine. Bile acids robustly stimulated PYY secretion via activation of TGR5 receptors in vivo (Kuhre et al., 2018). L amino acids e.g., tryptophan and phenylalanine could activate the amino acids sensor CaSR (Conigrave et al., 2000) ; Oral or duodenal administration of phenylalanine increased PYY secretion in rodent animals (Acar et al., 2020, Alamshah et al., 2017). Particularly, we observed that bile acids and phenylalanine were constantly higher in the duodenum and ileum during 60-120min, corresponding to the time when PYY was evaluated. This led to the

question that whether any of them may have contributed to the increase of PYY in Intact-S and should be examined further.

Appetite regulation and fermentation

Intact food structure may increase fermentation to prolong appetite (Dagbasi et al., 2020a). SCFAs production has been hardly measured in humans due to the difficulty of accessing gut content; rodent models suggested intact legume diets or chickpea diets that were high in RS 1 promoted SCFAs content in the distal colon of rats (Henningsson et al., 2001), altered cecal microbiome and promoted SCFAs production (Monk et al., 2017). Our study provides the first-ever evidence to explore the interplay between plant cell walls, intestinal fermentation, and appetite in healthy humans. Our study confirmed that Intact-C and Intact-S increased the carbohydrates that reach the terminal ileum, as evidenced by higher ileal glucose (5- and 10-fold increase) and maltose levels compared to the Broken. Total intestinal fermentation levels were indicated by breath hydrogen, where Intact-S and Intact-C exhibited a blunt curve during 0-4 hr and a sharper increase in BH during 4-8hr. When BH was increased (4-8hr), Intact-C increased fullness and PYY levels compared to Broken. We further investigated metabolites in the terminal ileum which provided explanations for these appetite outcomes. Ileal acetate was elevated in Intact-C at T=240-360 min and exhibited higher levels compared to Broken and Intact-S. We performed within-subject correlations in which Ileal acetate was positively related to circulating PYY levels and inversely related to composite appetite (T=60-360min). These findings are novel and confirm the critical role of the ileum in appetite signalling in humans. Our study reveals a pathway by which intact cell wall matrices reduce appetite by modulating the ileal fermentation products acetate. Colonic fermentation was not directly

measured, but likely to be active in the timeframe of 420-480min, during which Intact-C elevated PYY compared to Broken. GLP-1 did not differ during 8h postprandial but differed at day 3 baselines, which may indicate the secretion was from the distal gut (e.g, proximal or distal colon). Thus, a longer period of investigation may be required to capture the GLP-1 response.

Compared to Intact-C, the satiety-enhancing effects were less pronounced in the intact-S group during 4-8 hr. Despite the BH levels increasing sharply, it did not achieve significantly higher levels than Broken. Additionally, no significant differences were observed for ileal acetate, PYY or GLP-1 between Intact-S and Broken during the same period. There was a trend that intact-S increased satiety compared to Broken but not to a significant level. The weaker satiety-enhancing effects of Intact-S might be explained by the fact that Intact-S was more digestible in the ileum, leaving fewer carbohydrates available for fermentation. Similarly, an ileostomy study found that intact endosperm cells decreased the rates of digestion but did not increase resistant starch amounts compared to broken endosperm cells (Edwards et al., 2015a). These altogether led to the assumption that Intact-S is more likely to be a good source of slowly digestible starch instead of RS. However, this should be validated by examining cell wall intactness and recovering the RS amount in the ileal aspirations.

6.3 Strengths, limitation, and future recommendations

The greatest novelty lies in the state-of-the-art techniques we used to collect and analyze human gut samples, enabling us to understand the changes in gut contents interplay with

food structure interventions. The in-patient study setting ensured the safety and adherence of inventions. The cross-over study design minimized the bias of confounding factors and the inclusion of the same participants throughout the gastric, duodenal and ileal studies enable the examination of the digestion behaviours throughout the gut.

The research limitations and future considerations are listed below.

- Intestinal transit time could be affected by food structure. The oral-caecum transit time and gastric emptying, although not directly measured, showed signs of being delayed by Intact-C compared to Broken. Future studies should consider measuring the full GI and regional gut transit time, by e.g, ingestible wireless motility captures (Tran et al., 2012, Lee et al., 2014a). The time of carbohydrates arriving at the distal ileum (occurrence of "ileal brake") and the time of gastric emptying deserve investigations to see whether there are any correlations/causations.
- Amino acid release in the duodenum was higher in Intact-S/Intact-C compared to Broken which was a surprising result. Whether intact cell walls can limit of diffusion of trypsin into cells remained to be explored. The higher release of bile acids in Intact-S/Intact-C in the duodenum warrants further investigation.
- A closer look at the ileal metabolism is needed to better understand the discrepancies between Intact-S and Intact-C. First, the intactness of cell wall structures should be analysed along with quantifying resistant starch amounts to confirm their digestibility. Secondly, a direct measurement for SCFAs is required. We identified ileal fermentation products acetate from untargeted NMR analysis. Propionate and Butyrate were also identified in some samples, however, were difficult to identify in others due to overlapping with other signals (e.g., BCAAs). Future studies should

quantity SCFAs using targeted methods. Thirdly, ileal microbiota, particularly these families related to SCFAs, amino acids, and bile acids metabolism should be investigated and linked to the metabolite profile.

- The physico-chemical properties of cell clusters compared to intact cells should be further investigated. Cell wall permeability is suggested to be a key factor affecting their barrier effects in the GI tract. A diffusion study can be performed *in vitro* with labelled amylase (Li and Dhital, 2022, Colosimo et al., 2020) to investigate their interaction with cell walls.
- The fermentability of cell walls should be further investigated. Ileal samples may be incubated with *in vitro* colonic models to understand the fermentation profiles (time, rate, and extent) of cell wall components and cellular contents (e.g, RS).
- Some appetite outcomes have not been satisfactorily explained by current intestinal observations. E.g., the elevated PYY in Intact-S during 0-3 hr was not a result of fermentation or ileal glucose sensing. We hypothesized that some gut metabolites (e.g, bile acids/amino acids) may contribute to this and should be investigated further.
- Future studies should include a large sample size with a longer intervention period. Chapter 5 included n=8 and failed to detect a significant difference in appetite between Intact-S and Broken during 0-4hr, likely because of lower statistical power. The 8-hour sampling time did not fully capture the colonic effects on appetite outcomes and should be extended. The fact that we observed the elevated levels of GLP-1 and breath hydrogen at day 3 baselines suggested there was an increased fermentation activity overnight. A 24-hour period measurement should be considered. Energy intake should have been measured by *ad libitum* food intake, and self-reporting food questionnaires with urinary metabolic phenotyping (Posma et al., 2020)

to understand the long-term effect. Whether glycaemic control (e.g insulin sensitivity) could be improved should be measured over a longer intervention.

- Finally, an integrated look at the metabolite changes throughout different regions of the gut is required. Mapping the metabolomic changes via a network analysis may help better understand the underlying pathways and mechanisms that interplay with postprandial glycaemia and appetite outcomes.

6.4 Conclusion

The data presented in this thesis support the hypothesis that plant cell wall structure affects starch digestibility, glycaemic response, and appetite regulation in humans. Intact cell walls act as physical barriers enclosing starch granules, impeding/reducing starch digestion in the small intestine and enhancing the delivery of carbohydrates to the distal ileum. This explained their lower postprandial glycaemia and insulinaemia. Intact single cells and cell clusters both reduced appetite regulation although discrepancies were observed. Intact single cells acutely reduced appetite which seemed to be independent of fermentation; cell clusters remained low digestibility throughout the gut and preserved more carbohydrates for ileal and colonic fermentation. Ileal acetate was suggested to play a role in PYY secretion and appetite suppression. Overall, cell clusters show the greatest benefits in attenuating glycaemia, promoting fermentation and appetite suppression. Our data also emphasizes the importance of structural integrity for dietary fibre-rich foods in achieving their physiological benefits.

Bibliography

ACAR, I., CETINKAYA, A., LAY, I. & ILERI-GUREL, E. 2020. The role of calcium sensing receptors in GLP-1 and PYY secretion after acute intraduodenal administration of L-Tryptophan in rats. *Nutr Neurosci,* 23**,** 481-489.

ADEVA-ANDANY, M. M., PEREZ-FELPETE, N., FERNANDEZ-FERNANDEZ, C., DONAPETRY-GARCIA, C. & PAZOS-GARCIA, C. 2016. Liver glucose metabolism in humans. *Biosci Rep,* 36.

ADRIAN, T. E., FERRI, G. L., BACARESE-HAMILTON, A. J., FUESSL, H. S., POLAK, J. M. & BLOOM, S. R. 1985. Human distribution and release of a putative new gut hormone, peptide YY. *Gastroenterology,* 89**,** 1070-7.

AGIUS, L. 2013. High-carbohydrate diets induce hepatic insulin resistance to protect the liver from substrate overload. *Biochem Pharmacol,* 85**,** 306-12.

AHLMAN, H. & NILSSON, O. 2001. The gut as the largest endocrine organ in the body. *Annals of Oncology,* 12**,** S63-S68.

AHMED, S., MACFARLANE, G. T., FITE, A., MCBAIN, A. J., GILBERT, P. & MACFARLANE, S. 2007. Mucosa-associated bacterial diversity in relation to human terminal ileum and colonic biopsy samples. *Appl Environ Microbiol,* 73**,** 7435-42.

AL-MANA, N. M. & ROBERTSON, M. D. 2018. Acute Effect of Resistant Starch on Food Intake, Appetite and Satiety in Overweight/Obese Males. *Nutrients,* 10.

AL-RABADI, G. J. S., GILBERT, R. G. & GIDLEY, M. J. 2009. Effect of particle size on kinetics of starch digestion in milled barley and sorghum grains by porcine alpha-amylase. *Journal of Cereal Science,* 50**,** 198-204.

ALAMSHAH, A., SPRECKLEY, E., NORTON, M., KINSEY-JONES, J. S., AMIN, A., RAMGULAM, A., CAO, Y., JOHNSON, R., SALEH, K., AKALESTOU, E., MALIK, Z., GONZALEZ-ABUIN, N., JOMARD, A., AMARSI, R., MOOLLA, A., SARGENT, P. R., GRAY, G. W., BLOOM, S. R. & MURPHY, K. G. 2017. l-phenylalanine modulates gut hormone release and glucose tolerance, and suppresses food intake through the calcium-sensing receptor in rodents. *International Journal of Obesity,* 41**,** 1693-1701.

ALFITURI, A. 2018. The Role of Carbohydrate on Appetite Regulation Editorial Corresponding author. *Clinical research,* 3**,** 1-2.

ALLER, E. E., ABETE, I., ASTRUP, A., MARTINEZ, J. A. & VAN BAAK, M. A. 2011. Starches, sugars and obesity. *Nutrients,* 3**,** 341-69.

ALLISON CALABRESE, C. G., BILLY MEINKE, MARIE KAINOA FIALKOWSKI REVILLA, AND ALAN TITCHENAL 2022. Digestion and Absorption of Carbohydrates. University of Hawai'i at Mānoa.

ALSAFFAR, A. A. 2011. Effect of food processing on the resistant starch content of cereals and cereal products–a review. *International Journal of Food Science & Technology,* 46**,** 455-462.

AMINI, S., MANSOORI, A. & MAGHSUMI-NOROUZABAD, L. 2021. The effect of acute consumption of resistant starch on appetite in healthy adults; a systematic review and meta-analysis of the controlled clinical trials. *Clinical Nutrition ESPEN,* 41**,** 42-48.

ANGUAH, K. O. B., WONNELL, B. S., CAMPBELL, W. W., MCCABE, G. P. & MCCRORY, M. A. 2014. A blended- rather than whole-lentil meal with or without α-galactosidase mildly increases healthy adults' appetite but not their glycemic response. *The Journal of nutrition,* 144**,** 1963-1969.

ARONOFF, S. L., BERKOWITZ, K., SHREINER, B. & WANT, L. 2004. Glucose metabolism and regulation: beyond insulin and glucagon. *Diabetes spectrum,* 17**,** 183-190.

ARORA, S. 2006. Role of neuropeptides in appetite regulation and obesity–a review. *Neuropeptides,* 40**,** 375-401.

ARORA, T., LOO, R. L., ANASTASOVSKA, J., GIBSON, G. R., TUOHY, K. M., SHARMA, R. K., SWANN, J. R., DEAVILLE, E. R., SLEETH, M. L., THOMAS, E. L., HOLMES, E., BELL, J. D. & FROST, G. 2012. Differential effects of two fermentable carbohydrates on central appetite regulation and body composition. *PLoS One,* 7**,** e43263.

ARUMUGAM, M., RAES, J., PELLETIER, E., LE PASLIER, D., YAMADA, T., MENDE, D. R., FERNANDES, G. R., TAP, J., BRULS, T., BATTO, J. M., BERTALAN, M., BORRUEL, N., CASELLAS, F., FERNANDEZ, L., GAUTIER, L., HANSEN, T., HATTORI, M., HAYASHI, T., KLEEREBEZEM, M., KUROKAWA, K., LECLERC, M., LEVENEZ, F., MANICHANH, C., NIELSEN, H. B., NIELSEN, T., PONS, N., POULAIN, J., QIN, J., SICHERITZ-PONTEN, T., TIMS, S., TORRENTS, D., UGARTE, E., ZOETENDAL, E. G., WANG, J., GUARNER, F., PEDERSEN, O., DE VOS, W. M., BRUNAK, S., DORE, J., META, H. I. T. C., ANTOLIN, M., ARTIGUENAVE, F., BLOTTIERE, H. M., ALMEIDA, M., BRECHOT, C., CARA, C., CHERVAUX, C., CULTRONE, A., DELORME, C., DENARIAZ, G., DERVYN, R., FOERSTNER, K. U., FRISS, C., VAN DE GUCHTE, M., GUEDON, E., HAIMET, F., HUBER, W., VAN HYLCKAMA-VLIEG, J., JAMET, A., JUSTE, C., KACI, G., KNOL, J., LAKHDARI, O., LAYEC, S., LE ROUX, K., MAGUIN, E., MERIEUX, A., MELO MINARDI, R., M'RINI, C., MULLER, J., OOZEER, R., PARKHILL, J., RENAULT, P., RESCIGNO, M., SANCHEZ, N., SUNAGAWA, S., TORREJON, A., TURNER, K., VANDEMEULEBROUCK, G., VARELA, E., WINOGRADSKY, Y., ZELLER, G., WEISSENBACH, J., EHRLICH, S. D. & BORK, P. 2011. Enterotypes of the human gut microbiome. *Nature,* 473**,** 174-80.

AUGUSTIN, L. S. A., AAS, A. M., ASTRUP, A., ATKINSON, F. S., BAER-SINNOTT, S., BARCLAY, A. W., BRAND-MILLER, J. C., BRIGHENTI, F., BULLO, M., BUYKEN, A. E., CERIELLO, A., ELLIS, P. R., HA, M. A., HENRY, J. C., KENDALL, C. W. C., LA VECCHIA, C., LIU, S., LIVESEY, G., POLI, A., SALAS-SALVADO, J., RICCARDI, G., RISERUS, U., RIZKALLA, S. W., SIEVENPIPER, J. L., TRICHOPOULOU, A., USIC, K., WOLEVER, T. M. S., WILLETT, W. C. & JENKINS, D. J. A. 2020. Dietary Fibre Consensus from the International Carbohydrate Quality Consortium (ICQC). *Nutrients,* 12.

BACH KNUDSEN, K. E. 2015. Microbial degradation of whole-grain complex carbohydrates and impact on short-chain fatty acids and health. *Adv Nutr,* 6**,** 206-13.

BAGGIO, L. L. & DRUCKER, D. J. 2007a. Biology of incretins: GLP-1 and GIP. *Gastroenterology,* 132**,** 2131-2157.

BAGGIO, L. L. & DRUCKER, D. J. 2007b. Biology of incretins: GLP-1 and GIP. *Gastroenterology,* 132**,** 2131-57.

BAIN, S. C., BEKKER HANSEN, B., HUNT, B., CHUBB, B. & VALENTINE, W. J. 2020. Evaluating the burden of poor glycemic control associated with therapeutic inertia in patients with type 2 diabetes in the UK. *J Med Econ,* 23**,** 98-105.

BAJAJ, R., SINGH, N., KAUR, A. & INOUCHI, N. 2018. Structural, morphological, functional and digestibility properties of starches from cereals, tubers and legumes: a comparative study. *J Food Sci Technol,* 55**,** 3799-3808.

BAJKA, B. H., PINTO, A. M., AHN-JARVIS, J., RYDEN, P., PEREZ-MORAL, N., VAN DER SCHOOT, A., STOCCHI, C., BLAND, C., BERRY, S. E., ELLIS, P. R. & EDWARDS, C. H. 2021. The impact of replacing wheat flour with cellular legume powder on starch bioaccessibility, glycaemic response and bread roll quality: A double-blind randomised controlled trial in healthy participants. *Food Hydrocoll,* 114**,** 106565.

BAKDASH, J. & MARUSICH, L. 2017. Repeated Measures Correlation. *Frontiers in Psychology,* 8.

BARKELING, B., ROSSNER, S. & SJOBERG, A. 1995. Methodological studies on single meal food intake characteristics in normal weight and obese men and women. *Int J Obes Relat Metab Disord,* 19**,** 284-90.

BATTERHAM, R. L. & BLOOM, S. R. 2003. The gut hormone peptide YY regulates appetite. *Ann N Y Acad Sci,* 994**,** 162-8.

BATTERHAM, R. L., COWLEY, M. A., SMALL, C. J., HERZOG, H., COHEN, M. A., DAKIN, C. L., WREN, A. M., BRYNES, A. E., LOW, M. J., GHATEI, M. A., CONE, R. D. & BLOOM, S. R. 2002. Gut hormone PYY(3-36) physiologically inhibits food intake. *Nature,* 418**,** 650-4.

BAXTER, N. T., SCHMIDT, A. W., VENKATARAMAN, A., KIM, K. S., WALDRON, C. & SCHMIDT, T. M. 2019. Dynamics of Human Gut Microbiota and Short-Chain Fatty Acids in Response to Dietary Interventions with Three Fermentable Fibers. *mBio,* 10**,** e02566-18.

BELL, D. S. 2001. Importance of postprandial glucose control. *South Med J,* 94**,** 804-9.

BELL, G. I., SANCHEZ-PESCADOR, R., LAYBOURN, P. J. & NAJARIAN, R. C. 1983. Exon duplication and divergence in the human preproglucagon gene. *Nature,* 304**,** 368-71.

BENTON, D. 2015. Portion size: what we know and what we need to know. *Crit Rev Food Sci Nutr,* 55**,** 988-1004.

BERGMAN, E. 1990. Energy contributions of volatile fatty acids from the gastrointestinal tract in various species. *Physiological reviews,* 70**,** 567-590.

BHATTARAI, R. R., DHITAL, S., MENSE, A., GIDLEY, M. J. & SHI, Y.-C. 2018. Intact cellular structure in cereal endosperm limits starch digestion in vitro. *Food hydrocolloids,* 81**,** 139-148.

BHATTARAI, R. R., DHITAL, S., WILLIAMS, B. A., YANG, H. J., MIKKELSEN, D., FLANAGAN, B. M. & GIDLEY, M. J. 2021. In vitro fermentation of legume cells and components: Effects of cell encapsulation and starch/protein interactions. *Food Hydrocolloids,* 113**,** 106538.

BHATTARAI, R. R., DHITAL, S., WU, P., CHEN, X. D. & GIDLEY, M. J. 2017. Digestion of isolated legume cells in a stomach-duodenum model: three mechanisms limit starch and protein hydrolysis. *Food Funct,* 8**,** 2573-2582.

BHUPATHIRAJU, S. N., TOBIAS, D. K., MALIK, V. S., PAN, A., HRUBY, A., MANSON, J. E., WILLETT, W. C. & HU, F. B. 2014. Glycemic index, glycemic load, and risk of type 2 diabetes: results from 3 large US cohorts and an updated meta-analysis. *Am J Clin Nutr,* 100**,** 218-32.

BIRKHED, D., WICKHOLM, K. & FROSTELL, G. 1975. Degradation of maltose and starch by human saliva and by supernatants of dental plaque material. *Odontol Revy,* 26**,** 7-16.

BIRT, D. F., BOYLSTON, T., HENDRICH, S., JANE, J. L., HOLLIS, J., LI, L., MCCLELLAND, J., MOORE, S., PHILLIPS, G. J., ROWLING, M., SCHALINSKE, K., SCOTT, M. P. & WHITLEY, E. M. 2013. Resistant starch: promise for improving human health. *Adv Nutr,* 4**,** 587-601.

BLANQUET-DIOT, S., FRANÇOIS, O., DENIS, S., HENNEQUIN, M. & PEYRON, M. A. 2021. Importance of oral phase in in vitro starch digestibility related to wholegrain versus refined pastas and mastication impairment. *Food Hydrocolloids,* 112**,** 106277.

BLOEMEN, J. G., DAMINK, S. W. O., VENEMA, K., BUURMAN, W. A., JALAN, R. & DEJONG, C. H. 2010. Short chain fatty acids exchange: Is the cirrhotic, dysfunctional liver still able to clear them? *Clinical nutrition,* 29**,** 365-369.

BLOEMEN, J. G., VENEMA, K., VAN DE POLL, M. C., DAMINK, S. W. O., BUURMAN, W. A. & DEJONG, C. H. 2009. Short chain fatty acids exchange across the gut and liver in humans measured at surgery. *Clinical nutrition,* 28**,** 657-661.

BODINHAM, C. L., FROST, G. S. & ROBERTSON, M. D. 2010. Acute ingestion of resistant starch reduces food intake in healthy adults. *Br J Nutr,* 103**,** 917-22.

BODINHAM, C. L., SMITH, L., WRIGHT, J., FROST, G. S. & ROBERTSON, M. D. 2012. Dietary fibre improves first-phase insulin secretion in overweight individuals. *PLoS One,* 7**,** e40834.

BODNARUC, A. M., PRUD'HOMME, D., BLANCHET, R. & GIROUX, I. 2016. Nutritional modulation of endogenous glucagon-like peptide-1 secretion: a review. *Nutr Metab (Lond),* 13**,** 92.

BOIX-CASTEJÓN, M., HERRANZ-LÓPEZ, M., PÉREZ GAGO, A., OLIVARES-VICENTE, M., CATURLA, N., ROCHE, E. & MICOL, V. 2018. Hibiscus and lemon verbena polyphenols modulate appetite-related biomarkers in overweight subjects: a randomized controlled trial. *Food Funct,* 9**,** 3173-3184.

BORNHORST, G. M. & SINGH, R. P. 2014. Gastric Digestion In Vivo and In Vitro: How the Structural Aspects of Food Influence the Digestion Process. *Annual Review of Food Science and Technology,* 5**,** 111-132.

BORTHAKUR, A., ANBAZHAGAN, A. N., KUMAR, A., RAHEJA, G., SINGH, V., RAMASWAMY, K. & DUDEJA, P. K. 2010. The probiotic Lactobacillus plantarum counteracts TNF-alpha-induced downregulation of SMCT1 expression and function. *Am J Physiol Gastrointest Liver Physiol,* 299**,** G928-34.

BOWCUTT, R., FORMAN, R., GLYMENAKI, M., CARDING, S. R., ELSE, K. J. & CRUICKSHANK, S. M. 2014. Heterogeneity across the murine small and large intestine. *World J Gastroenterol,* 20**,** 15216-32.

BRETT, C. & WALDRON, K. 1990. Cell wall structure and the skeletal functions of the wall. *In:* BRETT, C. & WALDRON, K. (eds.) *Physiology and Biochemistry of Plant Cell Walls.* Dordrecht: Springer Netherlands.

BRIGHENTI, F., BENINI, L., DEL RIO, D., CASIRAGHI, C., PELLEGRINI, N., SCAZZINA, F., JENKINS, D. J. & VANTINI, I. 2006. Colonic fermentation of indigestible carbohydrates contributes to the second-meal effect. *The American journal of clinical nutrition,* 83**,** 817-822.

BRODKORB, A., EGGER, L., ALMINGER, M., ALVITO, P., ASSUNCAO, R., BALLANCE, S., BOHN, T., BOURLIEU-LACANAL, C., BOUTROU, R., CARRIERE, F., CLEMENTE, A., CORREDIG, M., DUPONT, D., DUFOUR, C., EDWARDS, C., GOLDING, M., KARAKAYA, S., KIRKHUS, B., LE FEUNTEUN, S., LESMES, U., MACIERZANKA, A., MACKIE, A. R., MARTINS, C., MARZE, S., MCCLEMENTS, D. J., MENARD, O., MINEKUS, M., PORTMANN, R., SANTOS, C. N., SOUCHON, I., SINGH, R. P., VEGARUD, G. E., WICKHAM, M. S. J., WEITSCHIES, W. & RECIO, I. 2019. INFOGEST static in vitro simulation of gastrointestinal food digestion. *Nat Protoc,* 14**,** 991-1014.

BROWNLEE, I. A. 2011. The physiological roles of dietary fibre. *Food Hydrocolloids,* 25**,** 238-250.

BROWNLEE, I. A., GILL, S., WILCOX, M. D., PEARSON, J. P. & CHATER, P. I. 2018a. Starch digestion in the upper gastrointestinal tract of humans. *Starch - Stärke,* 70**,** 1700111.

BROWNLEE, I. A., GILL, S., WILCOX, M. D., PEARSON, J. P. & CHATER, P. I. 2018b. Starch digestion in the upper gastrointestinal tract of humans. *Starch - Stärke,* 70**,** 1700111.

BRUMMER, Y., KAVIANI, M. & TOSH, S. M. 2015. Structural and functional characteristics of dietary fibre in beans, lentils, peas and chickpeas. *Food Research International,* 67**,** 117-125.

BRYANT, N. J., GOVERS, R. & JAMES, D. E. 2002. Regulated transport of the glucose transporter GLUT4. *Nat Rev Mol Cell Biol,* 3**,** 267-77.

BRYNES, A. E., ADAMSON, J., DORNHORST, A. & FROST, G. S. 2005. The beneficial effect of a diet with low glycaemic index on 24 h glucose profiles in healthy young people as assessed by continuous glucose monitoring. *British Journal of Nutrition,* 93**,** 179-182.

BUCHWALD, H., DORMAN, R. B., RASMUS, N. F., MICHALEK, V. N., LANDVIK, N. M. & IKRAMUDDIN, S. 2014. Effects on GLP-1, PYY, and leptin by direct stimulation of terminal ileum and cecum in humans: implications for ileal transposition. *Surg Obes Relat Dis,* 10**,** 780-6.

BYRNE, C. S., BLUNT, D., BURN, J., CHAMBERS, E., DAGBASI, A., BECKER, G. F., GIBSON, G., MENDOZA, L., MURPHY, K. & POVEDA, C. 2019a. A study protocol for a randomised crossover study evaluating the effect of diets differing in carbohydrate quality on ileal content and appetite regulation in healthy humans. *F1000Research,* 8**,** 1-16.

BYRNE, C. S., BLUNT, D., BURN, J., CHAMBERS, E., DAGBASI, A., FRANCO BECKER, G., GIBSON, G., MENDOZA, L., MURPHY, K., POVEDA, C., RAMGULAM, A., TASHKOVA, M., WALTON, G., WASHIRASAKSIRI, C. & FROST, G. 2019b. A study protocol for a randomised crossover study evaluating the effect of diets differing in carbohydrate quality on ileal content and appetite regulation in healthy humans. *F1000Res,* 8**,** 258.

BYRNE, C. S., CHAMBERS, E. S., ALHABEEB, H., CHHINA, N., MORRISON, D. J., PRESTON, T., TEDFORD, C., FITZPATRICK, J., IRANI, C., BUSZA, A., GARCIA-PEREZ, I., FOUNTANA, S., HOLMES, E., GOLDSTONE, A. P. & FROST, G. S. 2016. Increased colonic propionate reduces anticipatory reward responses in the human striatum to high-energy foods. *Am J Clin Nutr,* 104**,** 5-14.

BYRNE, C. S., CHAMBERS, E. S., MORRISON, D. J. & FROST, G. 2015. The role of short chain fatty acids in appetite regulation and energy homeostasis. *Int J Obes (Lond),* 39**,** 1331-8.

BYRNE, C. S., CHAMBERS, E. S., PRESTON, T., TEDFORD, C., BRIGNARDELLO, J., GARCIA-PEREZ, I., HOLMES, E., WALLIS, G. A., MORRISON, D. J. & FROST, G. S. 2019c. Effects of Inulin Propionate Ester Incorporated into Palatable Food Products on Appetite and Resting Energy Expenditure: A Randomised Crossover Study. *Nutrients,* 11**,** 861.

CAI, M., DOU, B., PUGH, J. E., LETT, A. M. & FROST, G. S. 2021. The impact of starchy food structure on postprandial glycemic response and appetite: a systematic review with meta-analysis of randomized crossover trials. *Am J Clin Nutr,* 114**,** 472-487.

CANFORA, E. E., JOCKEN, J. W. & BLAAK, E. E. 2015. Short-chain fatty acids in control of body weight and insulin sensitivity. *Nat Rev Endocrinol,* 11**,** 577-91.

CANI, P. D., DEWEVER, C. & DELZENNE, N. M. 2004. Inulin-type fructans modulate gastrointestinal peptides involved in appetite regulation (glucagon-like peptide-1 and ghrelin) in rats. *Br J Nutr,* 92**,** 521-6.

CANI, P. D., HOLST, J. J., DRUCKER, D. J., DELZENNE, N. M., THORENS, B., BURCELIN, R. & KNAUF, C. 2007. GLUT2 and the incretin receptors are involved in glucose-induced incretin secretion. *Mol Cell Endocrinol,* 276**,** 18-23.

CAPUANO, E. 2017a. The behavior of dietary fiber in the gastrointestinal tract determines its physiological effect. *Critical Reviews in Food Science and Nutrition,* 57**,** 3543-3564.

CAPUANO, E. 2017b. The behavior of dietary fiber in the gastrointestinal tract determines its physiological effect. *Crit Rev Food Sci Nutr,* 57**,** 3543-3564.

CARON, J., CUDENNEC, B., DOMENGER, D., BELGUESMIA, Y., FLAHAUT, C., KOUACH, M., LESAGE, J., GOOSSENS, J. F., DHULSTER, P. & RAVALLEC, R. 2016. Simulated GI digestion of dietary protein: Release of new bioactive peptides involved in gut hormone secretion. *Food Res Int,* 89**,** 382-390.

CASSADY, B. A., HOLLIS, J. H., FULFORD, A. D., CONSIDINE, R. V. & MATTES, R. D. 2009. Mastication of almonds: effects of lipid bioaccessibility, appetite, and hormone response. *Am J Clin Nutr,* 89**,** 794-800.

CHADT, A. & AL-HASANI, H. 2020. Glucose transporters in adipose tissue, liver, and skeletal muscle in metabolic health and disease. *Pflugers Arch,* 472**,** 1273-1298.

CHAIKOMIN, R., RAYNER, C. K., JONES, K. L. & HOROWITZ, M. 2006. Upper gastrointestinal function and glycemic control in diabetes mellitus. *World J Gastroenterol,* 12**,** 5611-21.

CHAMBERS, E. S., BYRNE, C. S. & FROST, G. 2019a. Carbohydrate and human health: is it all about quality? *The Lancet,* 393**,** 384-386.

CHAMBERS, E. S., BYRNE, C. S., MORRISON, D. J., MURPHY, K. G., PRESTON, T., TEDFORD, C., GARCIA-PEREZ, I., FOUNTANA, S., SERRANO-CONTRERAS, J. I., HOLMES, E., REYNOLDS, C. J., ROBERTS, J. F., BOYTON, R. J., ALTMANN, D. M., MCDONALD, J. A. K., MARCHESI, J. R., AKBAR, A. N., RIDDELL, N. E., WALLIS, G. A. & FROST, G. S. 2019b. Dietary supplementation with inulin-propionate ester or inulin improves insulin sensitivity in adults with overweight and obesity with distinct effects on the gut microbiota, plasma metabolome and systemic inflammatory responses: a randomised cross-over trial. *Gut,* 68**,** 1430-1438.

CHAMBERS, E. S., MORRISON, D. J. & FROST, G. 2015a. Control of appetite and energy intake by SCFA: what are the potential underlying mechanisms? *Proceedings of the Nutrition Society,* 74**,** 328-336.

CHAMBERS, E. S., PRESTON, T., FROST, G. & MORRISON, D. J. 2018a. Role of gut microbiota-generated short-chain fatty acids in metabolic and cardiovascular health. *Current nutrition reports,* 7**,** 198-206.

CHAMBERS, E. S., PRESTON, T., FROST, G. & MORRISON, D. J. 2018b. Role of Gut Microbiota-Generated Short-Chain Fatty Acids in Metabolic and Cardiovascular Health. *Curr Nutr Rep,* 7**,** 198-206.

CHAMBERS, E. S., VIARDOT, A., PSICHAS, A., MORRISON, D. J., MURPHY, K. G., ZAC-VARGHESE, S. E., MACDOUGALL, K., PRESTON, T., TEDFORD, C., FINLAYSON, G. S., BLUNDELL, J. E., BELL, J. D., THOMAS, E. L., MT-ISA, S., ASHBY, D., GIBSON, G. R., KOLIDA, S., DHILLO, W. S., BLOOM, S. R., MORLEY, W., CLEGG, S. & FROST, G. 2015b. Effects of targeted delivery of propionate to the human colon on appetite regulation, body weight maintenance and adiposity in overweight adults. *Gut,* 64**,** 1744-54.

CHANDRA, R. & LIDDLE, R. A. 2009. Neural and hormonal regulation of pancreatic secretion. *Curr Opin Gastroenterol,* 25**,** 441-6.

CHANG, S. H., STOLL, C. R., SONG, J., VARELA, J. E., EAGON, C. J. & COLDITZ, G. A. 2014. The effectiveness and risks of bariatric surgery: an updated systematic review and meta-analysis, 2003-2012. *JAMA Surg,* 149**,** 275-87.

CHASSARD, C., DELMAS, E., ROBERT, C. & BERNALIER-DONADILLE, A. 2010. The cellulose-degrading microbial community of the human gut varies according to the presence or absence of methanogens. *FEMS Microbiol Ecol,* 74**,** 205-13.

CHEN, J. 2009. Food oral processing—A review. *Food Hydrocolloids,* 23**,** 1-25.

CHEN, L., TUO, B. & DONG, H. 2016. Regulation of Intestinal Glucose Absorption by Ion Channels and Transporters. *Nutrients,* 8.

CHERTA-MURILLO, A., PUGH, J. E., ALARAJ-ALSHEHHI, S., HAJJAR, D., CHAMBERS, E. S. & FROST, G. S. 2022. The effects of SCFAs on glycemic control in humans: a systematic review and meta-analysis. *Am J Clin Nutr,* 116**,** 335-361.

CHO, Y. M., WIDEMAN, R. D. & KIEFFER, T. J. 2013. Clinical application of glucagon-like Peptide 1 receptor agonists for the treatment of type 2 diabetes mellitus. *Endocrinol Metab (Seoul),* 28**,** 262-74.

CHRISTIANSEN, C. B., TRAMMELL, S. A. J., WEWER ALBRECHTSEN, N. J., SCHOONJANS, K., ALBRECHTSEN, R., GILLUM, M. P., KUHRE, R. E. & HOLST, J. J. 2019. Bile acids drive colonic secretion of glucagon-like-peptide 1 and peptide-YY in rodents. *Am J Physiol Gastrointest Liver Physiol,* 316**,** G574-G584.

CHUNG, W. S. F., WALKER, A. W., VERMEIREN, J., SHERIDAN, P. O., BOSSCHER, D., GARCIA-CAMPAYO, V., PARKHILL, J., FLINT, H. J. & DUNCAN, S. H. 2019. Impact of carbohydrate substrate complexity on the diversity of the human colonic microbiota. *FEMS Microbiol Ecol,* 95.

CLARK, S. & DUNCAN, A. M. 2017. The role of pulses in satiety, food intake and body weight management. *Journal of Functional Foods,* 38**,** 612-623.

CLEGG, M. E., RANAWANA, V., SHAFAT, A. & HENRY, C. J. 2013. Soups increase satiety through delayed gastric emptying yet increased glycaemic response. *European Journal of Clinical Nutrition,* 67**,** 8-11.

COLOSIMO, R., WARREN, F. J., EDWARDS, C. H., FINNIGAN, T. J. A. & WILDE, P. J. 2020. The interaction of α-amylase with mycoprotein: Diffusion through the fungal cell wall, enzyme entrapment, and potential physiological implications. *Food Hydrocolloids,* 108**,** 106018.

CONIGRAVE, A. D., QUINN, S. J. & BROWN, E. M. 2000. L-amino acid sensing by the extracellular Ca2+-sensing receptor. *Proc Natl Acad Sci U S A,* 97**,** 4814-9.

CORNELL, H. J., HOVELING, A. W., CHRYSS, A. & ROGERS, M. 1994. Particle Size Distribution in Wheat Starch and Its Importance in Processing. *Starch - Stärke,* 46**,** 203-207.

COULTATE, T. P. 2009. *Food: the chemistry of its components*, Royal Society of Chemistry.

CRANDALL, J. P., KNOWLER, W. C., KAHN, S. E., MARRERO, D., FLOREZ, J. C., BRAY, G. A., HAFFNER, S. M., HOSKIN, M., NATHAN, D. M. & DIABETES PREVENTION PROGRAM RESEARCH, G. 2008. The prevention of type 2 diabetes. *Nat Clin Pract Endocrinol Metab,* 4**,** 382-93.

CUMMINGS, J. H. & ENGLYST, H. N. 1991. What is dietary fibre? *Trends in Food Science & Technology,* 2**,** 99-103.

CUMMINGS, J. H., HILL, M. J., BONE, E. S., BRANCH, W. J. & JENKINS, D. J. 1979. The effect of meat protein and dietary fiber on colonic function and metabolism. II. Bacterial metabolites in feces and urine. *Am J Clin Nutr,* 32**,** 2094-101.

CUMMINGS, J. H. & MACFARLANE, G. T. 1991. The control and consequences of bacterial fermentation in the human colon. *J Appl Bacteriol,* 70**,** 443-59.

CUMMINGS, J. H., POMARE, E. W., BRANCH, W. J., NAYLOR, C. P. & MACFARLANE, G. T. 1987. Short chain fatty acids in human large intestine, portal, hepatic and venous blood. *Gut,* 28**,** 1221-7.

CUMMINGS, J. H. & STEPHEN, A. M. 2007. Carbohydrate terminology and classification. *Eur J Clin Nutr,* 61 Suppl 1**,** S5-18.

CYDULKA, R. K. & MALONEY, G. E. 2002. Diabetes mellitus and disorders of glucose homeostasis. *Marx JA, Hockberger RS. Emergency Medicine: concepts and clinical practice. 5th ed. St. Louis (MO): Mosby***,** 1744-62.

DAGBASI, A. 2022. *Carbohydrate food structure, ileal digestion and appetite regulation.* Imperial College London.

DAGBASI, A., BYRNE, C., CONTRERAS, I., MURPHY, K. & FROST, G. 2020a. Understanding the Interplay Between Food Structure, Bacterial Fermentation and Appetite Sensing: A Randomized Crossover Human Trial. *Current Developments in Nutrition,* 4**,** 619-619.

DAGBASI, A., LETT, A., MURPHY, K. & FROST, G. 2020b. Understanding the interplay between food structure, intestinal bacterial fermentation and appetite control. *Proceedings of the Nutrition Society,* 79**,** 514-530.

DARZI, J., FROST, G. S., MONTASER, R., YAP, J. & ROBERTSON, M. D. 2014. Influence of the tolerability of vinegar as an oral source of short-chain fatty acids on appetite control and food intake. *International Journal of Obesity,* 38**,** 675-681.

DARZI, J., FROST, G. S. & ROBERTSON, M. D. 2011. Do SCFA have a role in appetite regulation? *Proceedings of the Nutrition Society,* 70**,** 119-128.

DARZI, J., FROST, G. S. & ROBERTSON, M. D. 2012. Effects of a novel propionate-rich sourdough bread on appetite and food intake. *Eur J Clin Nutr,* 66**,** 789-94.

DAVIES, M. J., BERGENSTAL, R., BODE, B., KUSHNER, R. F., LEWIN, A., SKJØTH, T. V., ANDREASEN, A. H., JENSEN, C. B. & DEFRONZO, R. A. 2015. Efficacy of Liraglutide for Weight Loss Among Patients With Type 2 Diabetes: The SCALE Diabetes Randomized Clinical Trial. *Jama,* 314**,** 687-99.

DAY, L., GOMEZ, J., OISETH, S. K., GIDLEY, M. J. & WILLIAMS, B. A. 2012. Faster fermentation of cooked carrot cell clusters compared to cell wall fragments in vitro by porcine feces. *J Agric Food Chem,* 60**,** 3282-90.

DE SILVA, A. & BLOOM, S. R. 2012a. Gut Hormones and Appetite Control: A Focus on PYY and GLP-1 as Therapeutic Targets in Obesity. *Gut and liver,* 6**,** 10-20.

DE SILVA, A. & BLOOM, S. R. 2012b. Gut Hormones and Appetite Control: A Focus on PYY and GLP-1 as Therapeutic Targets in Obesity. *Gut Liver,* 6**,** 10-20.

DE VADDER, F., KOVATCHEVA-DATCHARY, P., GONCALVES, D., VINERA, J., ZITOUN, C., DUCHAMPT, A., BACKHED, F. & MITHIEUX, G. 2014. Microbiota-generated metabolites promote metabolic benefits via gut-brain neural circuits. *Cell,* 156**,** 84-96.

DEANE, A. M., NGUYEN, N. Q., STEVENS, J. E., FRASER, R. J., HOLLOWAY, R. H., BESANKO, L. K., BURGSTAD, C., JONES, K. L., CHAPMAN, M. J., RAYNER, C. K. & HOROWITZ, M. 2010. Endogenous glucagon-like peptide-1 slows gastric emptying in healthy subjects, attenuating postprandial glycemia. *J Clin Endocrinol Metab,* 95**,** 215-21.

DEFRONZO, R. A., FERRANNINI, E., GROOP, L., HENRY, R. R., HERMAN, W. H., HOLST, J. J., HU, F. B., KAHN, C. R., RAZ, I., SHULMAN, G. I., SIMONSON, D. C., TESTA, M. A. & WEISS, R. 2015. Type 2 diabetes mellitus. *Nat Rev Dis Primers,* 1**,** 15019.

DELAMARE, G. Y. F., BUTTERWORTH, P. J., ELLIS, P. R., HILL, S., WARREN, F. J. & EDWARDS, C. H. 2020. Incorporation of a novel leguminous ingredient into savoury biscuits reduces

their starch digestibility: Implications for lowering the Glycaemic Index of cereal products. *Food chemistry: X,* 5**,** 100078-100078.

DEN BESTEN, G., VAN EUNEN, K., GROEN, A. K., VENEMA, K., REIJNGOUD, D.-J. & BAKKER, B. M. 2013. The role of short-chain fatty acids in the interplay between diet, gut microbiota, and host energy metabolism. *Journal of lipid research,* 54**,** 2325-2340.

DHITAL, S., BHATTARAI, R. R., GORHAM, J. & GIDLEY, M. J. 2016. Intactness of cell wall structure controls the in vitro digestion of starch in legumes. *Food Funct,* 7**,** 1367-79.

DHITAL, S., GIDLEY, M. J. & WARREN, F. J. 2015. Inhibition of alpha-amylase activity by cellulose: Kinetic analysis and nutritional implications. *Carbohydr Polym,* 123**,** 305-12.

DHITAL, S., SHRESTHA, A. K. & GIDLEY, M. J. 2010. Effect of cryo-milling on starches: Functionality and digestibility. *Food Hydrocolloids,* 24**,** 152-163.

DIABETES PREVENTION PROGRAM RESEARCH, G., KNOWLER, W. C., FOWLER, S. E., HAMMAN, R. F., CHRISTOPHI, C. A., HOFFMAN, H. J., BRENNEMAN, A. T., BROWN-FRIDAY, J. O., GOLDBERG, R., VENDITTI, E. & NATHAN, D. M. 2009. 10-year follow-up of diabetes incidence and weight loss in the Diabetes Prevention Program Outcomes Study. *Lancet,* 374**,** 1677-86.

DIABETES UK, D. 2019. Tackling the crisis: Transforming diabetes care.

DIMITRIADIS, G. D., MARATOU, E., KOUNTOURI, A., BOARD, M. & LAMBADIARI, V. 2021. Regulation of Postabsorptive and Postprandial Glucose Metabolism by Insulin-Dependent and Insulin-Independent Mechanisms: An Integrative Approach. *Nutrients,* 13.

DO, D. T., SINGH, J., OEY, I. & SINGH, H. 2019. Modulating effect of cotyledon cell microstructure on in vitro digestion of starch in legumes. *Food Hydrocolloids,* 96**,** 112-122.

DOLENŠEK, J., POHOREC, V., RUPNIK, M. S. & STOŽER, A. 2017. Pancreas physiology. *Challenges in Pancreatic Pathology. Rijeka, Croatia: IntechOpen***,** 19-52.

DONA, A. C., PAGES, G., GILBERT, R. G. & KUCHEL, P. W. 2010. Digestion of starch: In vivo and in vitro kinetic models used to characterise oligosaccharide or glucose release. *Carbohydrate Polymers,* 80**,** 599-617.

DONALDSON, G. P., LEE, S. M. & MAZMANIAN, S. K. 2016. Gut biogeography of the bacterial microbiota. *Nat Rev Microbiol,* 14**,** 20-32.

DREW, B. S., DIXON, A. F. & DIXON, J. B. 2007. Obesity management: update on orlistat. *Vasc Health Risk Manag,* 3**,** 817-21.

DRUCKER, D. J. 2007. The role of gut hormones in glucose homeostasis. *J Clin Invest,* 117**,** 24-32.

EDWARDS, C. H., COCHETEL, N., SETTERFIELD, L., PEREZ-MORAL, N. & WARREN, F. J. 2019. A single-enzyme system for starch digestibility screening and its relevance to understanding and predicting the glycaemic index of food products. *Food Funct,* 10**,** 4751-4760.

EDWARDS, C. H., GRUNDY, M. M., GRASSBY, T., VASILOPOULOU, D., FROST, G. S., BUTTERWORTH, P. J., BERRY, S. E., SANDERSON, J. & ELLIS, P. R. 2015a. Manipulation of starch bioaccessibility in wheat endosperm to regulate starch digestion, postprandial glycemia, insulinemia, and gut hormone responses: a randomized controlled trial in healthy ileostomy participants. *Am J Clin Nutr,* 102**,** 791-800.

EDWARDS, C. H., MAILLOT, M., PARKER, R. & WARREN, F. J. 2018. A comparison of the kinetics of in vitro starch digestion in smooth and wrinkled peas by porcine pancreatic alpha-amylase. *Food Chem,* 244**,** 386-393.

EDWARDS, C. H., RYDEN, P., MANDALARI, G., BUTTERWORTH, P. J. & ELLIS, P. R. 2021. Structure–function studies of chickpea and durum wheat uncover mechanisms by which cell wall properties influence starch bioaccessibility. *Nature Food,* 2**,** 118-126.

EDWARDS, C. H., RYDEN, P., PINTO, A. M., VAN DER SCHOOT, A., STOCCHI, C., PEREZ-MORAL, N., BUTTERWORTH, P. J., BAJKA, B., BERRY, S. E., HILL, S. E. & ELLIS, P. R. 2020. Chemical, physical and glycaemic characterisation of PulseON®: A novel legume cell-powder ingredient for use in the design of functional foods. *Journal of Functional Foods,* 68**,** 103918.

EDWARDS, C. H., WARREN, F. J., CAMPBELL, G. M., GAISFORD, S., ROYALL, P. G., BUTTERWORTH, P. J. & ELLIS, P. R. 2015b. A study of starch gelatinisation behaviour in hydrothermally-processed plant food tissues and implications for in vitro digestibility. *Food Funct,* 6**,** 3634-41.

EDWARDS, C. H., WARREN, F. J., MILLIGAN, P. J., BUTTERWORTH, P. J. & ELLIS, P. R. 2014a. A novel method for classifying starch digestion by modelling the amylolysis of plant foods using first-order enzyme kinetic principles. *Food Funct,* 5**,** 2751-8.

EDWARDS, C. H., WARREN, F. J., MILLIGAN, P. J., BUTTERWORTH, P. J. & ELLIS, P. R. 2014b. A novel method for classifying starch digestion by modelling the amylolysis of plant foods using first-order enzyme kinetic principles. *Food & function,* 5**,** 2751-2758.

EELDERINK, C., NOORT, M. W. J., SOZER, N., KOEHORST, M., HOLST, J. J., DEACON, C. F., REHFELD, J. F., POUTANEN, K., VONK, R. J., OUDHUIS, L. & PRIEBE, M. G. 2017. Difference in postprandial GLP-1 response despite similar glucose kinetics after consumption of wheat breads with different particle size in healthy men. *Eur J Nutr,* 56**,** 1063-1076.

EGGER, L., MÉNARD, O., DELGADO-ANDRADE, C., ALVITO, P., ASSUNÇÃO, R., BALANCE, S., BARBERÁ, R., BRODKORB, A., CATTENOZ, T. & CLEMENTE, A. 2016. The harmonized INFOGEST in vitro digestion method: From knowledge to action. *Food Research International,* 88**,** 217-225.

EISSELE, R., GOKE, R., WILLEMER, S., HARTHUS, H. P., VERMEER, H., ARNOLD, R. & GOKE, B. 1992. Glucagon-like peptide-1 cells in the gastrointestinal tract and pancreas of rat, pig and man. *Eur J Clin Invest,* 22**,** 283-91.

ELLIOTT, R. M., MORGAN, L. M., TREDGER, J. A., DEACON, S., WRIGHT, J. & MARKS, V. 1993. Glucagon-like peptide-1 (7-36)amide and glucose-dependent insulinotropic polypeptide secretion in response to nutrient ingestion in man: acute post-prandial and 24-h secretion patterns. *J Endocrinol,* 138**,** 159-66.

ELLS, L. J., SEAL, C. J., KETTLITZ, B., BAL, W. & MATHERS, J. C. 2005. Postprandial glycaemic, lipaemic and haemostatic responses to ingestion of rapidly and slowly digested starches in healthy young women. *Br J Nutr,* 94**,** 948-55.

EMILIEN, C. H., HSU, W. H. & HOLLIS, J. H. 2017. Effect of resistant wheat starch on subjective appetite and food intake in healthy adults. *Nutrition,* 43-44**,** 69-74.

ENGLYST, H. N. & CUMMINGS, J. H. 1985. Digestion of the polysaccharides of some cereal foods in the human small intestine. *Am J Clin Nutr,* 42**,** 778-87.

ENGLYST, H. N., KINGMAN, S. M. & CUMMINGS, J. H. 1992. Classification and measurement of nutritionally important starch fractions. *Eur J Clin Nutr,* 46 Suppl 2**,** S33-50.

ENGLYST, K. & ENGLYST, H. 2004. 19 - Detecting nutritional starch fractions. *In:* ELIASSON, A.-C. (ed.) *Starch in Food.* Woodhead Publishing.

FERNANDES, J. M., MADALENA, D. A., PINHEIRO, A. C. & VICENTE, A. A. 2020. Rice in vitro digestion: application of INFOGEST harmonized protocol for glycemic index determination and starch morphological study. *J Food Sci Technol,* 57**,** 1393-1404.

FLEMING, S. E., CHOI, S. Y. & FITCH, M. D. 1991. Absorption of short-chain fatty acids from the rat cecum in vivo. *J Nutr,* 121**,** 1787-97.

FLINT, A., RABEN, A., BLUNDELL, J. E. & ASTRUP, A. 2000. Reproducibility, power and validity of visual analogue scales in assessment of appetite sensations in single test meal studies. *Int J Obes Relat Metab Disord,* 24**,** 38-48.

FLINT, H. J., SCOTT, K. P., DUNCAN, S. H., LOUIS, P. & FORANO, E. 2012. Microbial degradation of complex carbohydrates in the gut. *Gut Microbes,* 3**,** 289-306.

FORD, E. S., WILLIAMSON, D. F. & LIU, S. 1997. Weight change and diabetes incidence: findings from a national cohort of US adults. *Am J Epidemiol,* 146**,** 214-22.

FORD, H. & FROST, G. 2010. Glycaemic index, appetite and body weight. *Proc Nutr Soc,* 69**,** 199-203.

FRANCO, C. M. L., DO RIO PRETO, S. J. & CIACCO, C. F. 1992. Factors that Affect the Enzymatic Degradation of Natural Starch Granules -Effect of the Size of the Granules. *Starch - Stärke,* 44**,** 422-426.

FRAYN, K. N. 2009. *Metabolic regulation: a human perspective*, John Wiley & Sons.

FREITAS, D., LE FEUNTEUN, S., PANOUILLE, M. & SOUCHON, I. 2018. The important role of salivary alpha-amylase in the gastric digestion of wheat bread starch. *Food Funct,* 9**,** 200-208.

FROST, G., SLEETH, M. L., SAHURI-ARISOYLU, M., LIZARBE, B., CERDAN, S., BRODY, L., ANASTASOVSKA, J., GHOURAB, S., HANKIR, M., ZHANG, S., CARLING, D., SWANN, J. R., GIBSON, G., VIARDOT, A., MORRISON, D., LOUISE THOMAS, E. & BELL, J. D. 2014. The short-chain fatty acid acetate reduces appetite via a central homeostatic mechanism. *Nat Commun,* 5**,** 3611.

FU, Z., GILBERT, E. R. & LIU, D. 2013. Regulation of insulin synthesis and secretion and pancreatic Beta-cell dysfunction in diabetes. *Curr Diabetes Rev,* 9**,** 25-53.

FUNG, T. T., SCHULZE, M., MANSON, J. E., WILLETT, W. C. & HU, F. B. 2004. Dietary patterns, meat intake, and the risk of type 2 diabetes in women. *Arch Intern Med,* 164**,** 2235-40.

GAESSER, G. A., MILLER JONES, J. & ANGADI, S. S. 2021. Perspective: Does Glycemic Index Matter for Weight Loss and Obesity Prevention? Examination of the Evidence on "Fast" Compared with "Slow" Carbs. *Adv Nutr,* 12**,** 2076-2084.

GARCIA-ALONSO, A. & GONI, I. 2000. Effect of processing on potato starch: in vitro availability and glycaemic index. *Nahrung,* 44**,** 19-22.

GARCIA-PEREZ, I., POSMA, J. M., GIBSON, R., CHAMBERS, E. S., HANSEN, T. H., VESTERGAARD, H., HANSEN, T., BECKMANN, M., PEDERSEN, O. & ELLIOTT, P. 2017. Objective assessment of dietary patterns by use of metabolic phenotyping: a randomised, controlled, crossover trial. *The lancet Diabetes & endocrinology,* 5**,** 184-195.

GARCIA-PEREZ, I., POSMA, J. M., SERRANO-CONTRERAS, J. I., BOULANGE, C. L., CHAN, Q., FROST, G., STAMLER, J., ELLIOTT, P., LINDON, J. C., HOLMES, E. & NICHOLSON, J. K. 2020. Identifying unknown metabolites using NMR-based metabolic profiling techniques. *Nat Protoc,* 15**,** 2538-2567.

GERICH, J. E. 1993. Control of glycaemia. *Baillieres Clin Endocrinol Metab,* 7**,** 551-86.

GERICH, J. E. 2000. Physiology of glucose homeostasis. *Diabetes Obes Metab,* 2**,** 345-50.

GIBBONS, C., HOPKINS, M., BEAULIEU, K., OUSTRIC, P. & BLUNDELL, J. E. 2019. Issues in Measuring and Interpreting Human Appetite (Satiety/Satiation) and Its Contribution to Obesity. *Curr Obes Rep,* 8**,** 77-87.

GILL, R. K., SAKSENA, S., ALREFAI, W. A., SARWAR, Z., GOLDSTEIN, J. L., CARROLL, R. E., RAMASWAMY, K. & DUDEJA, P. K. 2005. Expression and membrane localization of MCT isoforms along the length of the human intestine. *Am J Physiol Cell Physiol,* 289**,** C846-52.

GOLDSPINK, D. A., LU, V. B., BILLING, L. J., LARRAUFIE, P., TOLHURST, G., GRIBBLE, F. M. & REIMANN, F. 2018. Mechanistic insights into the detection of free fatty and bile acids by ileal glucagon-like peptide-1 secreting cells. *Molecular Metabolism,* 7**,** 90-101.

GOODMAN, B. E. 2010. Insights into digestion and absorption of major nutrients in humans. *Advances in physiology education,* 34 2**,** 44-53.

GORBOULEV, V., SCHÜRMANN, A., VALLON, V., KIPP, H., JASCHKE, A., KLESSEN, D., FRIEDRICH, A., SCHERNECK, S., RIEG, T., CUNARD, R., VEYHL-WICHMANN, M., SRINIVASAN, A., BALEN, D., BRELJAK, D., REXHEPAJ, R., PARKER, H. E., GRIBBLE, F. M., REIMANN, F., LANG, F., WIESE, S., SABOLIC, I., SENDTNER, M. & KOEPSELL, H. 2012. Na(+)-D-glucose cotransporter SGLT1 is pivotal for intestinal glucose absorption and glucose-dependent incretin secretion. *Diabetes,* 61**,** 187-96.

GOYAL, R. K., GUO, Y. & MASHIMO, H. 2019. Advances in the physiology of gastric emptying. *Neurogastroenterol Motil,* 31**,** e13546.

GRANDT, D., SCHIMICZEK, M., BEGLINGER, C., LAYER, P., GOEBELL, H., EYSSELEIN, V. E. & REEVE, J. R., JR. 1994. Two molecular forms of peptide YY (PYY) are abundant in human blood: characterization of a radioimmunoassay recognizing PYY 1-36 and PYY 3-36. *Regul Pept,* 51**,** 151-9.

GREGERSEN, N. T., FLINT, A., BITZ, C., BLUNDELL, J. E., RABEN, A. & ASTRUP, A. 2008. Reproducibility and power of ad libitum energy intake assessed by repeated single meals. *Am J Clin Nutr,* 87**,** 1277-81.

GRUNDY, M. M., CARRIERE, F., MACKIE, A. R., GRAY, D. A., BUTTERWORTH, P. J. & ELLIS, P. R. 2016a. The role of plant cell wall encapsulation and porosity in regulating lipolysis during the digestion of almond seeds. *Food Funct,* 7**,** 69-78.

GRUNDY, M. M., EDWARDS, C. H., MACKIE, A. R., GIDLEY, M. J., BUTTERWORTH, P. J. & ELLIS, P. R. 2016b. Re-evaluation of the mechanisms of dietary fibre and implications for macronutrient bioaccessibility, digestion and postprandial metabolism. *Br J Nutr,* 116**,** 816-33.

GRUNDY, M. M., WILDE, P. J., BUTTERWORTH, P. J., GRAY, R. & ELLIS, P. R. 2015. Impact of cell wall encapsulation of almonds on in vitro duodenal lipolysis. *Food Chem,* 185**,** 405-12.

GUAN, N., HE, X., WANG, S., LIU, F., HUANG, Q., FU, X., CHEN, T. & ZHANG, B. 2020. Cell Wall Integrity of Pulse Modulates the in Vitro Fecal Fermentation Rate and Microbiota Composition. *J Agric Food Chem,* 68**,** 1091-1100.

GUERRA, A., ETIENNE-MESMIN, L., LIVRELLI, V., DENIS, S., BLANQUET-DIOT, S. & ALRIC, M. 2012. Relevance and challenges in modeling human gastric and small intestinal digestion. *Trends Biotechnol,* 30**,** 591-600.

GUNNESS, P. & GIDLEY, M. J. 2010. Mechanisms underlying the cholesterol-lowering properties of soluble dietary fibre polysaccharides. *Food Funct,* 1**,** 149-55.

GUNNESS, P., MICHIELS, J., VANHAECKE, L., DE SMET, S., KRAVCHUK, O., VAN DE MEENE, A. & GIDLEY, M. J. 2016. Reduction in circulating bile acid and restricted diffusion across

the intestinal epithelium are associated with a decrease in blood cholesterol in the presence of oat beta-glucan. *FASEB J,* 30**,** 4227-4238.
GUTZWILLER, J. P., GOKE, B., DREWE, J., HILDEBRAND, P., KETTERER, S., HANDSCHIN, D., WINTERHALDER, R., CONEN, D. & BEGLINGER, C. 1999. Glucagon-like peptide-1: a potent regulator of food intake in humans. *Gut,* 44**,** 81-6.
HAGGART, G. A. 2019. csmsoftware/IMPaCTS: Version 1.1.1.
HAN, H., YI, B., ZHONG, R., WANG, M., ZHANG, S., MA, J., YIN, Y., YIN, J., CHEN, L. & ZHANG, H. 2021. From gut microbiota to host appetite: gut microbiota-derived metabolites as key regulators. *Microbiome,* 9**,** 162.
HAN, H. S., KANG, G., KIM, J. S., CHOI, B. H. & KOO, S. H. 2016. Regulation of glucose metabolism from a liver-centric perspective. *Exp Mol Med,* 48**,** e218.
HAN, J.-A., JANG, S.-H. & LIM, S.-T. 2008. In vitro digestibility of rice and barley in forms of raw flour and cooked kernels. *Food Science and Biotechnology,* 17**,** 180-183.
HANSEN, C. F., VRANG, N., SANGILD, P. T. & JELSING, J. 2013. Novel insight into the distribution of L-cells in the rat intestinal tract. *Am J Transl Res,* 5**,** 347-58.
HANSOTIA, T. & DRUCKER, D. J. 2005. GIP and GLP-1 as incretin hormones: lessons from single and double incretin receptor knockout mice. *Regul Pept,* 128**,** 125-34.
HASEK, L. Y., PHILLIPS, R. J., HAYES, A. M. R., KINZIG, K., ZHANG, G., POWLEY, T. L. & HAMAKER, B. R. 2020. Carbohydrates designed with different digestion rates modulate gastric emptying response in rats. *Int J Food Sci Nutr,* 71**,** 839-844.
HASSAN, Y., HEAD, V., JACOB, D., BACHMANN, M. O., DIU, S. & FORD, J. 2016. Lifestyle interventions for weight loss in adults with severe obesity: a systematic review. *Clin Obes,* 6**,** 395-403.
HECK, A. M., YANOVSKI, J. A. & CALIS, K. A. 2000. Orlistat, a new lipase inhibitor for the management of obesity. *Pharmacotherapy,* 20**,** 270-9.
HENNINGSSON, A. M., NYMAN, E. M. & BJORCK, I. M. 2001. Content of short-chain fatty acids in the hindgut of rats fed processed bean (Phaseolus vulgaris) flours varying in distribution and content of indigestible carbohydrates. *Br J Nutr,* 86**,** 379-89.
HEX, N., TAYLOR, M. & BARTLETT, C. 2013. Comments on Waldeyer et al. 'Response to Hex et al. Estimating the current and future costs for Type 1 and Type 2 diabetes in the UK, including direct health costs and indirect societal and productivity costs'. *Diabet Med,* 30**,** 503-4.
HIGGINS, J. A. 2012. Whole grains, legumes, and the subsequent meal effect: implications for blood glucose control and the role of fermentation. *J Nutr Metab,* 2012**,** 829238.
HIJOVA, E. & CHMELAROVA, A. 2007. Short chain fatty acids and colonic health. *Bratisl Lek Listy,* 108**,** 354-8.
HILL, J. O. 2006. Understanding and addressing the epidemic of obesity: an energy balance perspective. *Endocr Rev,* 27**,** 750-61.
HIMSWORTH, H. P. 1936. Diabetes mellitus. Its differentiation into insolin-sensitive and insulin-insensitive types. *Lancet,* 230**,** 127-130.
HODGE, A. M., ENGLISH, D. R., O'DEA, K. & GILES, G. G. 2004. Glycemic index and dietary fiber and the risk of type 2 diabetes. *Diabetes Care,* 27**,** 2701-6.
HOLLAND, C., RYDEN, P., EDWARDS, C. H. & GRUNDY, M. M.-L. 2020. Plant cell walls: Impact on nutrient bioaccessibility and digestibility. *Foods,* 9**,** 201.
HOLSCHER, H. D. 2017. Dietary fiber and prebiotics and the gastrointestinal microbiota. *Gut Microbes,* 8**,** 172-184.
HOLST, J. J. 2007. The physiology of glucagon-like peptide 1. *Physiol Rev,* 87**,** 1409-39.

HOLST, J. J., MADSBAD, S., BOJSEN-MOLLER, K. N., SVANE, M. S., JORGENSEN, N. B., DIRKSEN, C. & MARTINUSSEN, C. 2018. Mechanisms in bariatric surgery: Gut hormones, diabetes resolution, and weight loss. *Surg Obes Relat Dis,* 14**,** 708-714.

HOLT, S. H. & MILLER, J. B. 1994. Particle size, satiety and the glycaemic response. *Eur J Clin Nutr,* 48**,** 496-502.

HRUBY, A. & HU, F. B. 2015. The Epidemiology of Obesity: A Big Picture. *Pharmacoeconomics,* 33**,** 673-89.

HU, F. B., LEITZMANN, M. F., STAMPFER, M. J., COLDITZ, G. A., WILLETT, W. C. & RIMM, E. B. 2001. Physical activity and television watching in relation to risk for type 2 diabetes mellitus in men. *Arch Intern Med,* 161**,** 1542-8.

HUMBERT, L., RAINTEAU, D., TUVIGNON, N., WOLF, C., SEKSIK, P., LAUGIER, R. & CARRIERE, F. 2018. Postprandial bile acid levels in intestine and plasma reveal altered biliary circulation in chronic pancreatitis patients. *J Lipid Res,* 59**,** 2202-2213.

HUNDT, M., BASIT, H. & JOHN, S. 2022. Physiology, Bile Secretion. *StatPearls.* Treasure Island (FL).

IGLAY, K., HANNACHI, H., JOSEPH HOWIE, P., XU, J., LI, X., ENGEL, S. S., MOORE, L. M. & RAJPATHAK, S. 2016. Prevalence and co-prevalence of comorbidities among patients with type 2 diabetes mellitus. *Curr Med Res Opin,* 32**,** 1243-52.

IMAMURA, M. 2002. Effects of surgical manipulation of the intestine on peptide YY and its physiology. *Peptides,* 23**,** 403-7.

INTERNATIONAL DIABETES FEDERATION, I. 2021. IDF Diabetes Atlas Tenth edition 2021.

JACOBY, H. I. 2017. Gastric Emptying. *Reference Module in Biomedical Sciences.* Elsevier.

JASTREBOFF, A. M., ARONNE, L. J., AHMAD, N. N., WHARTON, S., CONNERY, L., ALVES, B., KIYOSUE, A., ZHANG, S., LIU, B., BUNCK, M. C., STEFANSKI, A. & INVESTIGATORS, S.-. 2022. Tirzepatide Once Weekly for the Treatment of Obesity. *N Engl J Med,* 387**,** 205-216.

JELINEK, H. F., OSMAN, W. M., KHANDOKER, A. H., KHALAF, K., LEE, S., ALMAHMEED, W. & ALSAFAR, H. S. 2017. Clinical profiles, comorbidities and complications of type 2 diabetes mellitus in patients from United Arab Emirates. *BMJ Open Diabetes Res Care,* 5**,** e000427.

JENKINS, D. J., THORNE, M. J., CAMELON, K., JENKINS, A., RAO, A. V., TAYLOR, R. H., THOMPSON, L. U., KALMUSKY, J., REICHERT, R. & FRANCIS, T. 1982. Effect of processing on digestibility and the blood glucose response: a study of lentils. *Am J Clin Nutr,* 36**,** 1093-101.

JENKINS, D. J., WOLEVER, T. M., TAYLOR, R. H., BARKER, H., FIELDEN, H., BALDWIN, J. M., BOWLING, A. C., NEWMAN, H. C., JENKINS, A. L. & GOFF, D. V. 1981. Glycemic index of foods: a physiological basis for carbohydrate exchange. *Am J Clin Nutr,* 34**,** 362-6.

JENKINS, D. J., WOLEVER, T. M., TAYLOR, R. H., GHAFARI, H., JENKINS, A. L., BARKER, H. & JENKINS, M. J. 1980. Rate of digestion of foods and postprandial glycaemia in normal and diabetic subjects. *Br Med J,* 281**,** 14-7.

JENKINS, D. J. A., GHAFARI, H., WOLEVER, T. M. S., TAYLOR, R. H., JENKINS, A. L., BARKER, H. M., FIELDEN, H. & BOWLING, A. C. 2004. Relationship between rate of digestion of foods and post-prandial glycaemia. *Diabetologia,* 22**,** 450-455.

JOHANSSON, D. P., LEE, I., RISERUS, U., LANGTON, M. & LANDBERG, R. 2015. Effects of unfermented and fermented whole grain rye crisp breads served as part of a standardized breakfast, on appetite and postprandial glucose and insulin responses: a randomized cross-over trial. *PLoS One,* 10**,** e0122241.

JOHANSSON, E. V., NILSSON, A. C., OSTMAN, E. M. & BJORCK, I. M. 2013. Effects of indigestible carbohydrates in barley on glucose metabolism, appetite and voluntary food intake over 16 h in healthy adults. *Nutr J,* 12**,** 46.

JOHNSTON, K. L., THOMAS, E. L., BELL, J. D., FROST, G. S. & ROBERTSON, M. D. 2010. Resistant starch improves insulin sensitivity in metabolic syndrome. *Diabet Med,* 27**,** 391-7.

JORSAL, T., RHEE, N. A., PEDERSEN, J., WAHLGREN, C. D., MORTENSEN, B., JEPSEN, S. L., JELSING, J., DALBOGE, L. S., VILMANN, P., HASSAN, H., HENDEL, J. W., POULSEN, S. S., HOLST, J. J., VILSBOLL, T. & KNOP, F. K. 2018. Enteroendocrine K and L cells in healthy and type 2 diabetic individuals. *Diabetologia,* 61**,** 284-294.

JUNEJO, S. A., DING, L., FU, X., XIONG, W., ZHANG, B. & HUANG, Q. 2021a. Pea cell wall integrity controls the starch and protein digestion properties in the INFOGEST in vitro simulation. *Int J Biol Macromol,* 182**,** 1200-1207.

JUNEJO, S. A., DING, L., FU, X., XIONG, W., ZHANG, B. & HUANG, Q. 2021b. Pea cell wall integrity controls the starch and protein digestion properties in the INFOGEST in vitro simulation. *International Journal of Biological Macromolecules,* 182**,** 1200-1207.

JUVONEN, K. R., PURHONEN, A. K., SALMENKALLIO-MARTTILA, M., LÄHTEENMÄKI, L., LAAKSONEN, D. E., HERZIG, K. H., UUSITUPA, M. I., POUTANEN, K. S. & KARHUNEN, L. J. 2009. Viscosity of oat bran-enriched beverages influences gastrointestinal hormonal responses in healthy humans. *J Nutr,* 139**,** 461-6.

KIM, S. J., WINTER, K., NIAN, C., TSUNEOKA, M., KODA, Y. & MCINTOSH, C. H. 2005. Glucose-dependent insulinotropic polypeptide (GIP) stimulation of pancreatic beta-cell survival is dependent upon phosphatidylinositol 3-kinase (PI3K)/protein kinase B (PKB) signaling, inactivation of the forkhead transcription factor Foxo1, and down-regulation of bax expression. *J Biol Chem,* 280**,** 22297-307.

KIM, Y. A., KEOGH, J. B. & CLIFTON, P. M. 2018. Probiotics, prebiotics, synbiotics and insulin sensitivity. *Nutr Res Rev,* 31**,** 35-51.

KING, D. G., WALKER, M., CAMPBELL, M. D., BREEN, L., STEVENSON, E. J. & WEST, D. J. 2018. A small dose of whey protein co-ingested with mixed-macronutrient breakfast and lunch meals improves postprandial glycemia and suppresses appetite in men with type 2 diabetes: a randomized controlled trial. *Am J Clin Nutr,* 107**,** 550-557.

KNIGHT, J. 2019. Gastrointestinal tract 3: the duodenum, liver and pancreas. Nursing Times.

KNOWLER, W. C., BARRETT-CONNOR, E., FOWLER, S. E., HAMMAN, R. F., LACHIN, J. M., WALKER, E. A., NATHAN, D. M. & DIABETES PREVENTION PROGRAM RESEARCH, G. 2002. Reduction in the incidence of type 2 diabetes with lifestyle intervention or metformin. *N Engl J Med,* 346**,** 393-403.

KODA, S., DATE, Y., MURAKAMI, N., SHIMBARA, T., HANADA, T., TOSHINAI, K., NIIJIMA, A., FURUYA, M., INOMATA, N. & OSUYE, K. 2005. The role of the vagal nerve in peripheral PYY3–36-induced feeding reduction in rats. *Endocrinology,* 146**,** 2369-2375.

KOH, A., DE VADDER, F., KOVATCHEVA-DATCHARY, P. & BÄCKHED, F. 2016. From Dietary Fiber to Host Physiology: Short-Chain Fatty Acids as Key Bacterial Metabolites. *Cell,* 165**,** 1332-1345.

KOH-BANERJEE, P., FRANZ, M., SAMPSON, L., LIU, S., JACOBS, D. R., JR., SPIEGELMAN, D., WILLETT, W. & RIMM, E. 2004. Changes in whole-grain, bran, and cereal fiber consumption in relation to 8-y weight gain among men. *Am J Clin Nutr,* 80**,** 1237-45.

KREYMANN, B., WILLIAMS, G., GHATEI, M. A. & BLOOM, S. R. 1987. Glucagon-like peptide-1 7-36: a physiological incretin in man. *Lancet,* 2**,** 1300-4.

KROP, E. M., HETHERINGTON, M. M., NEKITSING, C., MIQUEL, S., POSTELNICU, L. & SARKAR, A. 2018. Influence of oral processing on appetite and food intake - A systematic review and meta-analysis. *Appetite,* 125**,** 253-269.

KUHRE, R. E., WEWER ALBRECHTSEN, N. J., LARSEN, O., JEPSEN, S. L., BALK-MOLLER, E., ANDERSEN, D. B., DEACON, C. F., SCHOONJANS, K., REIMANN, F., GRIBBLE, F. M., ALBRECHTSEN, R., HARTMANN, B., ROSENKILDE, M. M. & HOLST, J. J. 2018. Bile acids are important direct and indirect regulators of the secretion of appetite- and metabolism-regulating hormones from the gut and pancreas. *Mol Metab,* 11**,** 84-95.

KWON, O. 2021. Glucose Metabolism. *In:* LEE, S.-H. & KANG, D.-W. (eds.) *Stroke Revisited: Diabetes in Stroke.* Singapore: Springer Singapore.

LARNER, J. & MCNICKLE, C. 1955. GASTROINTESTINAL DIGESTION OF STARCH: I. THE ACTION OF OLIGO-1, 6-GLUCOSIDASE ON BRANCHED SACCHARIDES. *Journal of Biological Chemistry,* 215**,** 723-736.

LAYER, P., HOLST, J. J., GRANDT, D. & GOEBELL, H. 1995. Ileal release of glucagon-like peptide-1 (GLP-1). Association with inhibition of gastric acid secretion in humans. *Dig Dis Sci,* 40**,** 1074-82.

LE ROUX, C. W., WELBOURN, R., WERLING, M., OSBORNE, A., KOKKINOS, A., LAURENIUS, A., LÖNROTH, H., FÄNDRIKS, L., GHATEI, M. A., BLOOM, S. R. & OLBERS, T. 2007. Gut hormones as mediators of appetite and weight loss after Roux-en-Y gastric bypass. *Ann Surg,* 246**,** 780-5.

LEAN, M. E., CARRARO, R., FINER, N., HARTVIG, H., LINDEGAARD, M. L., ROSSNER, S., VAN GAAL, L., ASTRUP, A. & INVESTIGATORS, N. N. 2014. Tolerability of nausea and vomiting and associations with weight loss in a randomized trial of liraglutide in obese, non-diabetic adults. *Int J Obes (Lond),* 38**,** 689-97.

LEATHWOOD, P. & POLLET, P. 1988. Effects of slow release carbohydrates in the form of bean flakes on the evolution of hunger and satiety in man. *Appetite,* 10**,** 1-11.

LEBOVITZ, H. E. 2001. Insulin resistance: definition and consequences. *Exp Clin Endocrinol Diabetes,* 109 Suppl 2**,** S135-48.

LEE, Y. Y., ERDOGAN, A. & RAO, S. S. 2014a. How to assess regional and whole gut transit time with wireless motility capsule. *J Neurogastroenterol Motil,* 20**,** 265-70.

LEE, Y. Y., ERDOGAN, A. & RAO, S. S. 2014b. How to assess regional and whole gut transit time with wireless motility capsule. *Journal of neurogastroenterology and motility,* 20**,** 265.

LEMMENS, L., VAN BUGGENHOUT, S., VAN LOEY, A. M. & HENDRICKX, M. E. 2010. Particle Size Reduction Leading to Cell Wall Rupture Is More Important for the β-Carotene Bioaccessibility of Raw Compared to Thermally Processed Carrots. *Journal of Agricultural and Food Chemistry,* 58**,** 12769-12776.

LI, G., ZHANG, P., WANG, J., GREGG, E. W., YANG, W., GONG, Q., LI, H., LI, H., JIANG, Y., AN, Y., SHUAI, Y., ZHANG, B., ZHANG, J., THOMPSON, T. J., GERZOFF, R. B., ROGLIC, G., HU, Y. & BENNETT, P. H. 2008. The long-term effect of lifestyle interventions to prevent diabetes in the China Da Qing Diabetes Prevention Study: a 20-year follow-up study. *Lancet,* 371**,** 1783-9.

LI, H. & DHITAL, S. 2022. α-Amylase interaction with soluble fibre: Insights from diffusion experiment using fluorescence recovery after photobleaching (FRAP) and permeation experiment using ultrafiltration membrane. *Bioactive Carbohydrates and Dietary Fibre,* 28**,** 100319.

LI, H., GIDLEY, M. J. & DHITAL, S. 2019. Wall porosity in isolated cells from food plants: Implications for nutritional functionality. *Food Chem,* 279**,** 416-425.

LI, P., DHITAL, S., ZHANG, B., HE, X., FU, X. & HUANG, Q. 2018a. Surface structural features control in vitro digestion kinetics of bean starches. *Food Hydrocolloids,* 85**,** 343-351.

LI, Z., YI, C. X., KATIRAEI, S., KOOIJMAN, S., ZHOU, E., CHUNG, C. K., GAO, Y., VAN DEN HEUVEL, J. K., MEIJER, O. C., BERBEE, J. F. P., HEIJINK, M., GIERA, M., WILLEMS VAN DIJK, K., GROEN, A. K., RENSEN, P. C. N. & WANG, Y. 2018b. Butyrate reduces appetite and activates brown adipose tissue via the gut-brain neural circuit. *Gut,* 67**,** 1269-1279.

LIDDLE, R. A. 2018. Chapter 40 - Regulation of Pancreatic Secretion. *In:* SAID, H. M. (ed.) *Physiology of the Gastrointestinal Tract (Sixth Edition).* Academic Press.

LIESE, A. D., SCHULZ, M., FANG, F., WOLEVER, T. M., D'AGOSTINO, R. B., JR., SPARKS, K. C. & MAYER-DAVIS, E. J. 2005. Dietary glycemic index and glycemic load, carbohydrate and fiber intake, and measures of insulin sensitivity, secretion, and adiposity in the Insulin Resistance Atherosclerosis Study. *Diabetes Care,* 28**,** 2832-8.

LINDEBOOM, N., CHANG, P. R. & TYLER, R. T. 2004. Analytical, Biochemical and Physicochemical Aspects of Starch Granule Size, with Emphasis on Small Granule Starches: A Review. *Starch - Stärke,* 56**,** 89-99.

LINDSTROM, J., ILANNE-PARIKKA, P., PELTONEN, M., AUNOLA, S., ERIKSSON, J. G., HEMIO, K., HAMALAINEN, H., HARKONEN, P., KEINANEN-KIUKAANNIEMI, S., LAAKSO, M., LOUHERANTA, A., MANNELIN, M., PATURI, M., SUNDVALL, J., VALLE, T. T., UUSITUPA, M., TUOMILEHTO, J. & FINNISH DIABETES PREVENTION STUDY, G. 2006. Sustained reduction in the incidence of type 2 diabetes by lifestyle intervention: follow-up of the Finnish Diabetes Prevention Study. *Lancet,* 368**,** 1673-9.

LIU, L., KERR, W. L., KONG, F., DEE, D. R. & LIN, M. 2018. Influence of nano-fibrillated cellulose (NFC) on starch digestion and glucose absorption. *Carbohydr Polym,* 196**,** 146-153.

LIU, W., JIN, Y., WILDE, P. J., HOU, Y., WANG, Y. & HAN, J. 2021. Mechanisms, physiology, and recent research progress of gastric emptying. *Crit Rev Food Sci Nutr,* 61**,** 2742-2755.

LOVEGROVE, A., EDWARDS, C. H., DE NONI, I., PATEL, H., EL, S. N., GRASSBY, T., ZIELKE, C., ULMIUS, M., NILSSON, L., BUTTERWORTH, P. J., ELLIS, P. R. & SHEWRY, P. R. 2017. Role of polysaccharides in food, digestion, and health. *Crit Rev Food Sci Nutr,* 57**,** 237-253.

LU, V. B., GRIBBLE, F. M. & REIMANN, F. 2021. Nutrient-Induced Cellular Mechanisms of Gut Hormone Secretion. *Nutrients,* 13.

LUDWIG, D. S., PEREIRA, M. A., KROENKE, C. H., HILNER, J. E., VAN HORN, L., SLATTERY, M. L. & JACOBS, D. R., JR. 1999. Dietary fiber, weight gain, and cardiovascular disease risk factors in young adults. *JAMA,* 282**,** 1539-46.

MA, I. T. & MADURA, J. A., 2ND 2015. Gastrointestinal Complications After Bariatric Surgery. *Gastroenterol Hepatol (N Y),* 11**,** 526-35.

MACFARLANE, S. & MACFARLANE, G. T. 2003. Regulation of short-chain fatty acid production. *Proc Nutr Soc,* 62**,** 67-72.

MACKIE, A. R., BAJKA, B. H., RIGBY, N. M., WILDE, P. J., ALVES-PEREIRA, F., MOSLETH, E. F., RIEDER, A., KIRKHUS, B. & SALT, L. J. 2017a. Oatmeal particle size alters glycemic index but not as a function of gastric emptying rate. *Am J Physiol Gastrointest Liver Physiol,* 313**,** G239-G246.

MACKIE, A. R., BAJKA, B. H., RIGBY, N. M., WILDE, P. J., ALVES-PEREIRA, F., MOSLETH, E. F., RIEDER, A., KIRKHUS, B. & SALT, L. J. 2017b. Oatmeal particle size alters glycemic index but not as a function of gastric emptying rate. *American Journal of Physiology-Gastrointestinal and Liver Physiology,* 313**,** G239-G246.

MACKIE, A. R., RAFIEE, H., MALCOLM, P., SALT, L. & VAN AKEN, G. 2013. Specific food structures supress appetite through reduced gastric emptying rate. *American Journal of Physiology-Gastrointestinal and Liver Physiology,* 304**,** G1038-G1043.

MAGALLANES-CRUZ, P. A., FLORES-SILVA, P. C. & BELLO-PEREZ, L. A. 2017. Starch Structure Influences Its Digestibility: A Review. *J Food Sci,* 82**,** 2016-2023.

MALJAARS, P. W., PETERS, H. P., MELA, D. J. & MASCLEE, A. A. 2008. Ileal brake: a sensible food target for appetite control. A review. *Physiol Behav,* 95**,** 271-81.

MANDEL, A. L., PEYROT DES GACHONS, C., PLANK, K. L., ALARCON, S. & BRESLIN, P. A. 2010. Individual differences in AMY1 gene copy number, salivary alpha-amylase levels, and the perception of oral starch. *PLoS One,* 5**,** e13352.

MANN, J., CUMMINGS, J. H., ENGLYST, H. N., KEY, T., LIU, S., RICCARDI, G., SUMMERBELL, C., UAUY, R., VAN DAM, R. M., VENN, B., VORSTER, H. H. & WISEMAN, M. 2007. FAO/WHO scientific update on carbohydrates in human nutrition: conclusions. *Eur J Clin Nutr,* 61 Suppl 1**,** S132-7.

MANN, J. I. 2002. Diet and risk of coronary heart disease and type 2 diabetes. *Lancet,* 360**,** 783-9.

MARATHE, C. S., RAYNER, C. K., JONES, K. L. & HOROWITZ, M. 2013. Relationships between gastric emptying, postprandial glycemia, and incretin hormones. *Diabetes Care,* 36**,** 1396-405.

MARTIN, A. M., SUN, E. W. & KEATING, D. J. 2019. Mechanisms controlling hormone secretion in human gut and its relevance to metabolism. *J Endocrinol,* 244**,** R1-R15.

MAT, D. J. L., LE FEUNTEUN, S., MICHON, C. & SOUCHON, I. 2016. In vitro digestion of foods using pH-stat and the INFOGEST protocol: Impact of matrix structure on digestion kinetics of macronutrients, proteins and lipids. *Food Research International,* 88**,** 226-233.

MAYER, J. 1953. Glucostatic mechanism of regulation of food intake. *N Engl J Med,* 249**,** 13-6.

MCKEOWN, N. M., MEIGS, J. B., LIU, S., SALTZMAN, E., WILSON, P. W. & JACQUES, P. F. 2004. Carbohydrate nutrition, insulin resistance, and the prevalence of the metabolic syndrome in the Framingham Offspring Cohort. *Diabetes Care,* 27**,** 538-46.

MIAO, M., JIANG, B., CUI, S. W., ZHANG, T. & JIN, Z. 2015. Slowly digestible starch--a review. *Crit Rev Food Sci Nutr,* 55**,** 1642-57.

MIN, T. & BAIN, S. C. 2021. The Role of Tirzepatide, Dual GIP and GLP-1 Receptor Agonist, in the Management of Type 2 Diabetes: The SURPASS Clinical Trials. *Diabetes Therapy,* 12**,** 143-157.

MINEKUS, M. 2015. The TNO Gastro-Intestinal Model (TIM). *In:* VERHOECKX, K., COTTER, P., LOPEZ-EXPOSITO, I., KLEIVELAND, C., LEA, T., MACKIE, A., REQUENA, T., SWIATECKA, D. & WICHERS, H. (eds.) *The Impact of Food Bioactives on Health: in vitro and ex vivo models.* Cham (CH).

MIYAWAKI, K., YAMADA, Y., YANO, H., NIWA, H., BAN, N., IHARA, Y., KUBOTA, A., FUJIMOTO, S., KAJIKAWA, M., KUROE, A., TSUDA, K., HASHIMOTO, H., YAMASHITA, T., JOMORI, T., TASHIRO, F., MIYAZAKI, J. & SEINO, Y. 1999. Glucose intolerance caused by a defect in the entero-insular axis: a study in gastric inhibitory polypeptide receptor knockout mice. *Proc Natl Acad Sci U S A,* 96**,** 14843-7.

MOLLARD, R. C., WONG, C. L., LUHOVYY, B. L. & ANDERSON, G. H. 2011. First and second meal effects of pulses on blood glucose, appetite, and food intake at a later meal. *Applied Physiology, Nutrition, and Metabolism,* 36**,** 634-642.

MONK, J. M., LEPP, D., WU, W., GRAF, D., MCGILLIS, L. H., HUSSAIN, A., CAREY, C., ROBINSON, L. E., LIU, R., TSAO, R., BRUMMER, Y., TOSH, S. M. & POWER, K. A. 2017. Chickpea-supplemented diet alters the gut microbiome and enhances gut barrier integrity in C57Bl/6 male mice. *Journal of Functional Foods,* 38**,** 663-674.

MORRISON, D. J. & PRESTON, T. 2016. Formation of short chain fatty acids by the gut microbiota and their impact on human metabolism. *Gut microbes,* 7**,** 189-200.

MUECKLER, M. 1994. Facilitative glucose transporters. *Eur J Biochem,* 219**,** 713-25.

MUIR, J. G., LU, Z. X., YOUNG, G. P., CAMERON-SMITH, D., COLLIER, G. R. & O'DEA, K. 1995. Resistant starch in the diet increases breath hydrogen and serum acetate in human subjects. *Am J Clin Nutr,* 61**,** 792-9.

N'GOMA, J.-C. B., AMARA, S., DRIDI, K., JANNIN, V. & CARRIÈRE, F. 2011. Understanding the lipid-digestion processes in the GI tract before designing lipid-based drug-delivery systems. *Therapeutic Delivery,* 3**,** 105-124.

NASTESKA, D., HARADA, N., SUZUKI, K., YAMANE, S., HAMASAKI, A., JOO, E., IWASAKI, K., SHIBUE, K., HARADA, T. & INAGAKI, N. 2014. Chronic reduction of GIP secretion alleviates obesity and insulin resistance under high-fat diet conditions. *Diabetes,* 63**,** 2332-43.

NAVALE, A. M. & PARANJAPE, A. N. 2016. Glucose transporters: physiological and pathological roles. *Biophys Rev,* 8**,** 5-9.

NETZEL, M., NETZEL, G., ZABARAS, D., LUNDIN, L., DAY, L., ADDEPALLI, R., OSBORNE, S. A. & SEYMOUR, R. 2011. Release and absorption of carotenes from processed carrots (Daucus carota) using in vitro digestion coupled with a Caco-2 cell trans-well culture model. *Food Research International,* 44**,** 868-874.

NEWBY, P. K., MARAS, J., BAKUN, P., MULLER, D., FERRUCCI, L. & TUCKER, K. L. 2007. Intake of whole grains, refined grains, and cereal fiber measured with 7-d diet records and associations with risk factors for chronic disease. *Am J Clin Nutr,* 86**,** 1745-53.

NEWSHOLME, E. A. & DIMITRIADIS, G. 2001. Integration of biochemical and physiologic effects of insulin on glucose metabolism. *Exp Clin Endocrinol Diabetes,* 109 Suppl 2**,** S122-34.

NHS. 2020. *Statistics on Obesity, Physical Activity and Diet* [Online]. Available: https://digital.nhs.uk/data-and-information/publications/statistical/statistics-on-obesity-physical-activity-and-diet/england-2020#summary [Accessed].

NICE. 2014. *Obesity: identification, assessment and management. Clinical Guideline 189.* [Online]. Available: www.nice.org.uk/guidance/cg189 [Accessed].

NICE. 2017. *Health matters: obesity and the food environment* [Online]. Available: **https://www.gov.uk/government/publications/health-matters-obesity-and-the-food-environment/health-matters-obesity-and-the-food-environment--2#resources** [Accessed].

NOAH, L., GUILLON, F., BOUCHET, B., BULEON, A., MOLIS, C., GRATAS, M. & CHAMP, M. 1998. Digestion of carbohydrate from white beans (Phaseolus vulgaris L.) in healthy humans. *J Nutr,* 128**,** 977-85.

NORRIS, S. L., ZHANG, X., AVENELL, A., GREGG, E., BOWMAN, B., SERDULA, M., BROWN, T. J., SCHMID, C. H. & LAU, J. 2004. Long-term effectiveness of lifestyle and behavioral weight loss interventions in adults with type 2 diabetes: a meta-analysis. *Am J Med,* 117**,** 762-74.

NUGENT, S. G., KUMAR, D., RAMPTON, D. S. & EVANS, D. F. 2001. Intestinal luminal pH in inflammatory bowel disease: possible determinants and implications for therapy with aminosalicylates and other drugs. *Gut,* 48**,** 571-7.

O'DONNELL, L. J., EMMETT, P. M. & HEATON, K. W. 1989. Size of flour particles and its relation to glycaemia, insulinaemia, and colonic disease. *BMJ,* 298**,** 1616-7.

O'MEARA, S., RIEMSMA, R., SHIRRAN, L., MATHER, L. & TER RIET, G. 2004. A systematic review of the clinical effectiveness of orlistat used for the management of obesity. *Obes Rev,* 5**,** 51-68.

OGAWA, Y., DONLAO, N., THUENGTUNG, S., TIAN, J., CAI, Y., REGINIO, F. C., KETNAWA, S., YAMAMOTO, N. & TAMURA, M. 2018. Impact of food structure and cell matrix on digestibility of plant-based food. *Current Opinion in Food Science,* 19**,** 36-41.

OLAGUNJU, A. I. & OMOBA, O. S. 2022. Functionality of Resistant and Slowly Digesting Starch in Cereals. *Functional Cereals and Cereal Foods.* Springer.

OLAUSSON, E. A., ALPSTEN, M., LARSSON, A., MATTSSON, H., ANDERSSON, H. & ATTVALL, S. 2008. Small particle size of a solid meal increases gastric emptying and late postprandial glycaemic response in diabetic subjects with gastroparesis. *Diabetes Res Clin Pract,* 80**,** 231-7.

OLESEN, M., RUMESSEN, J. J. & GUDMAND-HOYER, E. 1994. Intestinal transport and fermentation of resistant starch evaluated by the hydrogen breath test. *Eur J Clin Nutr,* 48**,** 692-701.

OLIPHANT, K. & ALLEN-VERCOE, E. 2019. Macronutrient metabolism by the human gut microbiome: major fermentation by-products and their impact on host health. *Microbiome,* 7**,** 91.

PALCHEN, K., BREDIE, W. L. P., DUIJSENS, D., ISAAC ALFIE CASTILLO, A., HENDRICKX, M., VAN LOEY, A., RABEN, A. & GRAUWET, T. 2022. Effect of processing and microstructural properties of chickpea-flours on in vitro digestion and appetite sensations. *Food Res Int,* 157**,** 111245.

PALCHEN, K., MICHELS, D., DUIJSENS, D., GWALA, S., PALLARES PALLARES, A., HENDRICKX, M., VAN LOEY, A. & GRAUWET, T. 2021. In vitro protein and starch digestion kinetics of individual chickpea cells: from static to more complex in vitro digestion approaches. *Food Funct,* 12**,** 7787-7804.

PALLARES PALLARES, A., ALVAREZ MIRANDA, B., TRUONG, N. Q. A., KYOMUGASHO, C., CHIGWEDERE, C. M., HENDRICKX, M. & GRAUWET, T. 2018. Process-induced cell wall permeability modulates the in vitro starch digestion kinetics of common bean cotyledon cells. *Food Funct,* 9**,** 6544-6554.

PAMIR, N., LYNN, F. C., BUCHAN, A. M., EHSES, J., HINKE, S. A., POSPISILIK, J. A., MIYAWAKI, K., YAMADA, Y., SEINO, Y., MCINTOSH, C. H. & PEDERSON, R. A. 2003. Glucose-dependent insulinotropic polypeptide receptor null mice exhibit compensatory changes in the enteroinsular axis. *Am J Physiol Endocrinol Metab,* 284**,** E931-9.

PAPAKONSTANTINOU, E., OIKONOMOU, C., NYCHAS, G. & DIMITRIADIS, G. D. 2022. Effects of Diet, Lifestyle, Chrononutrition and Alternative Dietary Interventions on Postprandial Glycemia and Insulin Resistance. *Nutrients,* 14.

PARKER, B. A., STURM, K., MACINTOSH, C. G., FEINLE, C., HOROWITZ, M. & CHAPMAN, I. M. 2004. Relation between food intake and visual analogue scale ratings of appetite and other sensations in healthy older and young subjects. *European Journal of Clinical Nutrition,* 58**,** 212-218.

PARODI, A., COLECCHIA, A., ORSOLA-MALPIGHI, P. S., FESTI, D. & PERRI, F. 2009. Methodology and indications of H2-breath testing in gastrointestinal diseases: the Rome Consensus Conference. *Aliment pharmacol ther,* 29**,** 1-49.

PATEL, H., DAY, R., BUTTERWORTH, P. J. & ELLIS, P. R. 2014. A mechanistic approach to studies of the possible digestion of retrograded starch by alpha-amylase revealed using a log of slope (LOS) plot. *Carbohydr Polym,* 113**,** 182-8.

PAYAN, F., HASER, R., PIERROT, M., FREY, M., ASTIER, J., ABADIE, B., DUÉE, B. & BUISSON, G. 1980. The three-dimensional structure of α-amylase from porcine pancreas at 5 Å resolution–the active-site location. *Acta Crystallographica Section B: Structural Crystallography and Crystal Chemistry,* 36**,** 416-421.

PELLEGRINI, N., VITTADINI, E. & FOGLIANO, V. 2020. Designing food structure to slow down digestion in starch-rich products. *Current Opinion in Food Science,* 32**,** 50-57.

PEREIRA, G. V., ABDEL-HAMID, A. M., DUTTA, S., D'ALESSANDRO-GABAZZA, C. N., WEFERS, D., FARRIS, J. A., BAJAJ, S., WAWRZAK, Z., ATOMI, H., MACKIE, R. I., GABAZZA, E. C., SHUKLA, D., KOROPATKIN, N. M. & CANN, I. 2021. Degradation of complex arabinoxylans by human colonic Bacteroidetes. *Nat Commun,* 12**,** 459.

PEREIRA, M. A. & LUDWIG, D. S. 2001. Dietary fiber and body-weight regulation. Observations and mechanisms. *Pediatr Clin North Am,* 48**,** 969-80.

PEREIRA, R. M., MOURA, L. P. D., MUÑOZ, V. R., SILVA, A. S. R. D., GASPAR, R. S., ROPELLE, E. R. & PAULI, J. R. 2017. Molecular mechanisms of glucose uptake in skeletal muscle at rest and in response to exercise. *Motriz: revista de educação física,* 23.

PEREZ-MORAL, N., SAHA, S., PINTO, A. M., BAJKA, B. H. & EDWARDS, C. H. 2022. In vitro protein bioaccessibility and human serum amino acid responses to white bread enriched with intact plant cells. *Food Chem,* 404**,** 134538.

PERRY, B. & WANG, Y. 2012. Appetite regulation and weight control: the role of gut hormones. *Nutr Diabetes,* 2**,** e26.

PETROPOULOU, A. 2019a. *The role of plant-based food structures on gastrointestinal digestion, colonic fermentation and glucose homeostasis.* PhD, Imperial College London.

PETROPOULOU, A. 2019b. The role of plant-based food structures on gastrointestinal digestion, colonic fermentation and glucose homeostasis. PhD thesis.Imperial College London.

PETROPOULOU, K., SALT, L. J., EDWARDS, C. H., WARREN, F. J., GARCIA-PEREZ, I., CHAMBERS, E. S., ALSHAALAN, R., KHATIB, M., PEREZ-MORAL, N., CROSS, K. L., KELLINGRAY, L., STANLEY, R., KOEV, T., KHIMYAK, Y. Z., NARBAD, A., PENNEY, N., SERRANO-CONTRERAS, J. I., CHARALAMBIDES, M. N., MIGUENS BLANCO, J., CASTRO SEOANE, R., MCDONALD, J. A. K., MARCHESI, J. R., HOLMES, E., GODSLAND, I. F., MORRISON, D. J., PRESTON, T., DOMONEY, C., WILDE, P. J. & FROST, G. S. 2020. A natural mutation in Pisum sativum L. (pea) alters starch assembly and improves glucose homeostasis in humans. *Nature Food,* 1**,** 693-704.

PH VAN TRIJP, M., WILMS, E., RÍOS-MORALES, M., MASCLEE, A. A., BRUMMER, R. J., WITTEMAN, B. J., TROOST, F. J. & HOOIVELD, G. J. 2021. Using naso- and oro-intestinal catheters in physiological research for intestinal delivery and sampling in vivo: practical and technical aspects to be considered. *The American Journal of Clinical Nutrition,* 114**,** 843-861.

PILICHIEWICZ, A. N., CHAIKOMIN, R., BRENNAN, I. M., WISHART, J. M., RAYNER, C. K., JONES, K. L., SMOUT, A. J., HOROWITZ, M. & FEINLE-BISSET, C. 2007. Load-dependent effects

of duodenal glucose on glycemia, gastrointestinal hormones, antropyloroduodenal motility, and energy intake in healthy men. *Am J Physiol Endocrinol Metab,* 293**,** E743-53.

PINGITORE, A., CHAMBERS, E. S., HILL, T., MALDONADO, I. R., LIU, B., BEWICK, G., MORRISON, D. J., PRESTON, T., WALLIS, G. A., TEDFORD, C., CASTANERA GONZALEZ, R., HUANG, G. C., CHOUDHARY, P., FROST, G. & PERSAUD, S. J. 2017. The diet-derived short chain fatty acid propionate improves beta-cell function in humans and stimulates insulin secretion from human islets in vitro. *Diabetes Obes Metab,* 19**,** 257-265.

POLYVIOU, T., MACDOUGALL, K., CHAMBERS, E. S., VIARDOT, A., PSICHAS, A., JAWAID, S., HARRIS, H. C., EDWARDS, C. A., SIMPSON, L., MURPHY, K. G., ZAC-VARGHESE, S. E., BLUNDELL, J. E., DHILLO, W. S., BLOOM, S. R., FROST, G. S., PRESTON, T., TEDFORD, M. C. & MORRISON, D. J. 2016. Randomised clinical study: inulin short-chain fatty acid esters for targeted delivery of short-chain fatty acids to the human colon. *Aliment Pharmacol Ther,* 44**,** 662-72.

POPKIN, B. M., ADAIR, L. S. & NG, S. W. 2012. Global nutrition transition and the pandemic of obesity in developing countries. *Nutr Rev,* 70**,** 3-21.

POPPITT, S. D. 2013. 9 - Carbohydrates and satiety*. *In:* BLUNDELL, J. E. & BELLISLE, F. (eds.) *Satiation, Satiety and the Control of Food Intake.* Woodhead Publishing.

POPPITT, S. D., SHIN, H. S., MCGILL, A. T., BUDGETT, S. C., LO, K., PAHL, M., DUXFIELD, J., LANE, M. & INGRAM, J. R. 2017. Duodenal and ileal glucose infusions differentially alter gastrointestinal peptides, appetite response, and food intake: a tube feeding study. *Am J Clin Nutr,* 106**,** 725-735.

POSMA, J. M., GARCIA-PEREZ, I., EBBELS, T. M. D., LINDON, J. C., STAMLER, J., ELLIOTT, P., HOLMES, E. & NICHOLSON, J. K. 2018. Optimized Phenotypic Biomarker Discovery and Confounder Elimination via Covariate-Adjusted Projection to Latent Structures from Metabolic Spectroscopy Data. *J Proteome Res,* 17**,** 1586-1595.

POSMA, J. M., GARCIA-PEREZ, I., FROST, G., ALJURAIBAN, G. S., CHAN, Q., VAN HORN, L., DAVIGLUS, M., STAMLER, J., HOLMES, E., ELLIOTT, P. & NICHOLSON, J. K. 2020. Nutriome–metabolome relationships provide insights into dietary intake and metabolism. *Nature Food,* 1**,** 426-436.

POUTANEN, K. S., DUSSORT, P., ERKNER, A., FISZMAN, S., KARNIK, K., KRISTENSEN, M., MARSAUX, C. F., MIQUEL-KERGOAT, S., PENTIKÄINEN, S. P., PUTZ, P., SLAVIN, J. L., STEINERT, R. E. & MELA, D. J. 2017. A review of the characteristics of dietary fibers relevant to appetite and energy intake outcomes in human intervention trials. *The American Journal of Clinical Nutrition,* 106**,** 747-754.

PUBLIC HEALTH ENGLAND, P. 2016. The Eatwell Guide.

QIN, J., LI, R., RAES, J., ARUMUGAM, M., BURGDORF, K. S., MANICHANH, C., NIELSEN, T., PONS, N., LEVENEZ, F., YAMADA, T., MENDE, D. R., LI, J., XU, J., LI, S., LI, D., CAO, J., WANG, B., LIANG, H., ZHENG, H., XIE, Y., TAP, J., LEPAGE, P., BERTALAN, M., BATTO, J. M., HANSEN, T., LE PASLIER, D., LINNEBERG, A., NIELSEN, H. B., PELLETIER, E., RENAULT, P., SICHERITZ-PONTEN, T., TURNER, K., ZHU, H., YU, C., LI, S., JIAN, M., ZHOU, Y., LI, Y., ZHANG, X., LI, S., QIN, N., YANG, H., WANG, J., BRUNAK, S., DORE, J., GUARNER, F., KRISTIANSEN, K., PEDERSEN, O., PARKHILL, J., WEISSENBACH, J., META, H. I. T. C., BORK, P., EHRLICH, S. D. & WANG, J. 2010. A human gut microbial gene catalogue established by metagenomic sequencing. *Nature,* 464**,** 59-65.

RANA, S. V. & MALIK, A. 2014. Hydrogen breath tests in gastrointestinal diseases. *Indian J Clin Biochem,* 29**,** 398-405.

RANAWANA, V., LEOW, M. K. & HENRY, C. J. 2014. Mastication effects on the glycaemic index: impact on variability and practical implications. *Eur J Clin Nutr,* 68**,** 137-9.

RASHED, A. A., SAPARUDDIN, F., RATHI, D. G., NASIR, N. N. M. & LOKMAN, E. F. 2021. Effects of Resistant Starch Interventions on Metabolic Biomarkers in Pre-Diabetes and Diabetes Adults. *Front Nutr,* 8**,** 793414.

RASK, E., OLSSON, T., SODERBERG, S., JOHNSON, O., SECKL, J., HOLST, J. J., AHREN, B., NORTHERN SWEDEN MONITORING OF, T. & DETERMINANTS IN CARDIOVASCULAR, D. 2001. Impaired incretin response after a mixed meal is associated with insulin resistance in nondiabetic men. *Diabetes Care,* 24**,** 1640-5.

RATANPAUL, V., WILLIAMS, B. A., BLACK, J. L. & GIDLEY, M. J. 2019. Review: Effects of fibre, grain starch digestion rate and the ileal brake on voluntary feed intake in pigs. *Animal,* 13**,** 2745-2754.

RATNER, R. E., MAGGS, D., NIELSEN, L. L., STONEHOUSE, A. H., POON, T., ZHANG, B., BICSAK, T. A., BRODOWS, R. G. & KIM, D. D. 2006. Long-term effects of exenatide therapy over 82 weeks on glycaemic control and weight in over-weight metformin-treated patients with type 2 diabetes mellitus. *Diabetes Obes Metab,* 8**,** 419-28.

READ, N., AL-JANABI, M., BATES, T., HOLGATE, A., CANN, P., KINSMAN, R., MCFARLANE, A. & BROWN, C. 1985. Interpretation of the breath hydrogen profile obtained after ingesting a solid meal containing unabsorbable carbohydrate. *Gut,* 26**,** 834-842.

READ, N. W., WELCH, I. M., AUSTEN, C. J., BARNISH, C., BARTLETT, C. E., BAXTER, A. J., BROWN, G., COMPTON, M. E., HUME, K. E., STORIE, I. & ET AL. 1986. Swallowing food without chewing; a simple way to reduce postprandial glycaemia. *Br J Nutr,* 55**,** 43-7.

REBELLO, C. J., GREENWAY, F. L. & FINLEY, J. W. 2014. A review of the nutritional value of legumes and their effects on obesity and its related co-morbidities. *Obesity Reviews,* 15**,** 392-407.

REED, J., BAIN, S. & KANAMARLAPUDI, V. 2021. A Review of Current Trends with Type 2 Diabetes Epidemiology, Aetiology, Pathogenesis, Treatments and Future Perspectives. *Diabetes Metab Syndr Obes,* 14**,** 3567-3602.

REIMANN, F., HABIB, A. M., TOLHURST, G., PARKER, H. E., ROGERS, G. J. & GRIBBLE, F. M. 2008. Glucose sensing in L cells: a primary cell study. *Cell Metab,* 8**,** 532-9.

REWTHONG, O., SOPONRONNARIT, S., TAECHAPAIROJ, C., TUNGTRAKUL, P. & PRACHAYAWARAKORN, S. 2011. Effects of cooking, drying and pretreatment methods on texture and starch digestibility of instant rice. *Journal of Food Engineering,* 103**,** 258-264.

REYNOLDS, A., MANN, J., CUMMINGS, J., WINTER, N., METE, E. & TE MORENGA, L. 2019. Carbohydrate quality and human health: a series of systematic reviews and meta-analyses. *Lancet,* 393**,** 434-445.

RICHTER, E. A. & HARGREAVES, M. 2013. Exercise, GLUT4, and skeletal muscle glucose uptake. *Physiol Rev,* 93**,** 993-1017.

ROBERGE, J. N. & BRUBAKER, P. L. 1993. Regulation of intestinal proglucagon-derived peptide secretion by glucose-dependent insulinotropic peptide in a novel enteroendocrine loop. *Endocrinology,* 133**,** 233-40.

ROBERTS, L. D., SOUZA, A. L., GERSZTEN, R. E. & CLISH, C. B. 2012. Targeted metabolomics. *Curr Protoc Mol Biol,* Chapter 30**,** Unit 30.2.1-24.

ROBERTSON, M. D., BICKERTON, A. S., DENNIS, A. L., VIDAL, H. & FRAYN, K. N. 2005. Insulin-sensitizing effects of dietary resistant starch and effects on skeletal muscle and adipose tissue metabolism. *Am J Clin Nutr,* 82**,** 559-67.

ROBERTSON, M. D., CURRIE, J. M., MORGAN, L. M., JEWELL, D. P. & FRAYN, K. N. 2003. Prior short-term consumption of resistant starch enhances postprandial insulin sensitivity in healthy subjects. *Diabetologia,* 46**,** 659-65.

ROBINSON, E., ALMIRON-ROIG, E., RUTTERS, F., DE GRAAF, C., FORDE, C. G., TUDUR SMITH, C., NOLAN, S. J. & JEBB, S. A. 2014. A systematic review and meta-analysis examining the effect of eating rate on energy intake and hunger. *Am J Clin Nutr,* 100**,** 123-51.

RODER, P. V., GEILLINGER, K. E., ZIETEK, T. S., THORENS, B., KOEPSELL, H. & DANIEL, H. 2014. The role of SGLT1 and GLUT2 in intestinal glucose transport and sensing. *PLoS One,* 9**,** e89977.

RODER, P. V., WU, B., LIU, Y. & HAN, W. 2016. Pancreatic regulation of glucose homeostasis. *Exp Mol Med,* 48**,** e219.

RODNICK, K. J., PIPER, R. C., SLOT, J. W. & JAMES, D. E. 1992. Interaction of insulin and exercise on glucose transport in muscle. *Diabetes Care,* 15**,** 1679-89.

RONGKAUMPAN, G., AMSBURY, S., ANDABLO-REYES, E., LINFORD, H., CONNELL, S., KNOX, J. P., SARKAR, A., BENITEZ-ALFONSO, Y. & ORFILA, C. 2019. Cell Wall Polymer Composition and Spatial Distribution in Ripe Banana and Mango Fruit: Implications for Cell Adhesion and Texture Perception. *Front Plant Sci,* 10**,** 858.

ROSENBLUM, J. L., IRWIN, C. L. & ALPERS, D. H. 1988. Starch and glucose oligosaccharides protect salivary-type amylase activity at acid pH. *Am J Physiol,* 254**,** G775-80.

ROSS, S. A. & DUPRE, J. 1978. Effects of ingestion of triglyceride or galactose on secretion of gastric inhibitory polypeptide and on responses to intravenous glucose in normal and diabetic subjects. *Diabetes,* 27**,** 327-33.

ROVALINO-CORDOVA, A. M., FOGLIANO, V. & CAPUANO, E. 2018. A closer look to cell structural barriers affecting starch digestibility in beans. *Carbohydr Polym,* 181**,** 994-1002.

ROVALINO-CORDOVA, A. M., FOGLIANO, V. & CAPUANO, E. 2019. The effect of cell wall encapsulation on macronutrients digestion: A case study in kidney beans. *Food Chem,* 286**,** 557-566.

ROVALINO-CORDOVA, A. M., FOGLIANO, V. & CAPUANO, E. 2021. In vitro colonic fermentation of red kidney beans depends on cotyledon cells integrity and microbiota adaptation. *Food Funct,* 12**,** 4983-4994.

ROVALINO-CÓRDOVA, A. M., FOGLIANO, V. & CAPUANO, E. 2020. Effect of bean structure on microbiota utilization of plant nutrients: An in-vitro study using the simulator of the human intestinal microbial ecosystem (SHIME®). *Journal of Functional Foods,* 73**,** 104087.

RUBINO, D. M., GREENWAY, F. L., KHALID, U., O'NEIL, P. M., ROSENSTOCK, J., SØRRIG, R., WADDEN, T. A., WIZERT, A., GARVEY, W. T., ARAUZ-PACHECO, C., CANNON, K., DOWNEY, H. J., FITZ-PATRICK, D., GEOHAS, J., GERETY, G., GILBERT, J., HOLLANDER, P., KLEIN, E., LAUFER, K., O'DONNELL, P., ROSENBLIT, P. & TOTH, P. 2022. Effect of Weekly Subcutaneous Semaglutide vs Daily Liraglutide on Body Weight in Adults With Overweight or Obesity Without Diabetes. *JAMA,* 327**,** 138.

RUDNICKI, M., KUVSHINOFF, B. W. & MCFADDEN, D. W. 1992. Extrinsic neural contribution to ileal peptide YY (PYY) release. *J Surg Res,* 52**,** 591-5.

RUI, L. 2014. Energy metabolism in the liver. *Compr Physiol,* 4**,** 177-97.

RUMESSEN, J. J. 1992. Hydrogen and methane breath tests for evaluation of resistant carbohydrates. *Eur J Clin Nutr,* 46 Suppl 2**,** S77-90.

RUPPIN, H., BAR-MEIR, S., SOERGEL, K. H., WOOD, C. M. & SCHMITT, M. G., JR. 1980. Absorption of short-chain fatty acids by the colon. *Gastroenterology,* 78**,** 1500-7.

SACN. 2015. *Carbohydrates and Health* [Online]. . Available: https://assets.publishing.service.gov.uk/government/uploads/system/uploads/attachment_data/file/445503/SACN_Carbohydrates_and_Health.pdf [Accessed 2022].

SADOUL, B. C., SCHURING, E. A., MELA, D. J. & PETERS, H. P. 2014. The relationship between appetite scores and subsequent energy intake: an analysis based on 23 randomized controlled studies. *Appetite,* 83**,** 153-159.

SALMERON, J., ASCHERIO, A., RIMM, E. B., COLDITZ, G. A., SPIEGELMAN, D., JENKINS, D. J., STAMPFER, M. J., WING, A. L. & WILLETT, W. C. 1997. Dietary fiber, glycemic load, and risk of NIDDM in men. *Diabetes Care,* 20**,** 545-50.

SANDBERG, J. C., BJÖRCK, I. M. E. & NILSSON, A. C. 2017. Effects of whole grain rye, with and without resistant starch type 2 supplementation, on glucose tolerance, gut hormones, inflammation and appetite regulation in an 11–14.5 hour perspective; a randomized controlled study in healthy subjects. *Nutrition Journal,* 16**,** 25.

SAUNDERS, D. R. 1991. Absorption of short-chain fatty acids in human stomach and rectum. *Nutrition research,* 11**,** 841-847.

SCHIRRA, J., KATSCHINSKI, M., WEIDMANN, C., SCHAFER, T., WANK, U., ARNOLD, R. & GOKE, B. 1996. Gastric emptying and release of incretin hormones after glucose ingestion in humans. *J Clin Invest,* 97**,** 92-103.

SCHIRRA, J., STURM, K., LEICHT, P., ARNOLD, R., GÖKE, B. & KATSCHINSKI, M. 1998. Exendin (9-39) amide is an antagonist of glucagon-like peptide-1 (7-36) amide in humans. *The Journal of clinical investigation,* 101**,** 1421-1430.

SCHIRRA, J., WANK, U., ARNOLD, R., GOKE, B. & KATSCHINSKI, M. 2002. Effects of glucagon-like peptide-1(7-36)amide on motility and sensation of the proximal stomach in humans. *Gut,* 50**,** 341-8.

SCHMIDT, S. K., HEMMESTAD, L., MACDONALD, C. S., LANGBERG, H. & VALENTINER, L. S. 2020. Motivation and Barriers to Maintaining Lifestyle Changes in Patients with Type 2 Diabetes after an Intensive Lifestyle Intervention (The U-TURN Trial): A Longitudinal Qualitative Study. *Int J Environ Res Public Health,* 17.

SCHMITT JR, M. G., SOERGEL, K. H. & WOOD, C. M. 1976. Absorption of short chain fatty acids from the human jejunum. *Gastroenterology,* 70**,** 211-215.

SCHMITT, M. G., JR., SOERGEL, K. H., WOOD, C. M. & STEFF, J. J. 1977. Absorption of short-chain fatty acids from the human ileum. *Am J Dig Dis,* 22**,** 340-7.

SCHNEIDER, A. R., JEPP, K., MURCZYNSKI, L., BINIEK, U. & STEIN, J. 2007. The inulin hydrogen breath test accurately reflects orocaecal transit time. *Eur J Clin Invest,* 37**,** 802-7.

SCHNURR, T. M., JAKUPOVIC, H., CARRASQUILLA, G. D., ANGQUIST, L., GRARUP, N., SORENSEN, T. I. A., TJONNELAND, A., OVERVAD, K., PEDERSEN, O., HANSEN, T. & KILPELAINEN, T. O. 2020. Obesity, unfavourable lifestyle and genetic risk of type 2 diabetes: a case-cohort study. *Diabetologia,* 63**,** 1324-1332.

SCHULZE, M. B., LIU, S., RIMM, E. B., MANSON, J. E., WILLETT, W. C. & HU, F. B. 2004. Glycemic index, glycemic load, and dietary fiber intake and incidence of type 2 diabetes in younger and middle-aged women. *Am J Clin Nutr,* 80**,** 348-56.

SCHWARTZ, M. W., WOODS, S. C., PORTE, D., JR., SEELEY, R. J. & BASKIN, D. G. 2000. Central nervous system control of food intake. *Nature,* 404**,** 661-71.

SCHWIERTZ, A., LEHMANN, U., JACOBASCH, G. & BLAUT, M. 2002. Influence of resistant starch on the SCFA production and cell counts of butyrate-producing Eubacterium spp. in the human intestine. *J Appl Microbiol,* 93**,** 157-62.

SCROCCHI, L. A., BROWN, T. J., MACLUSKY, N., BRUBAKER, P. L., AUERBACH, A. B., JOYNER, A. L. & DRUCKER, D. J. 1996. Glucose intolerance but normal satiety in mice with a null mutation in the glucagon-like peptide 1 receptor gene. *Nat Med,* 2**,** 1254-8.

SEINO, Y., MAEKAWA, R., OGATA, H. & HAYASHI, Y. 2016. Carbohydrate-induced secretion of glucose-dependent insulinotropic polypeptide and glucagon-like peptide-1. *J Diabetes Investig,* 7 Suppl 1**,** 27-32.

SENSOY, I. 2021. A review on the food digestion in the digestive tract and the used in vitro models. *Current research in food science,* 4**,** 308-319.

SHAH, M. & VELLA, A. 2014. Effects of GLP-1 on appetite and weight. *Rev Endocr Metab Disord,* 15**,** 181-7.

SHAN, Z., LI, Y., ZONG, G., GUO, Y., LI, J., MANSON, J. E., HU, F. B., WILLETT, W. C., SCHERNHAMMER, E. S. & BHUPATHIRAJU, S. N. 2018. Rotating night shift work and adherence to unhealthy lifestyle in predicting risk of type 2 diabetes: results from two large US cohorts of female nurses. *BMJ,* 363**,** k4641.

SHI, L., SHU, X. O., LI, H., CAI, H., LIU, Q., ZHENG, W., XIANG, Y. B. & VILLEGAS, R. 2013. Physical activity, smoking, and alcohol consumption in association with incidence of type 2 diabetes among middle-aged and elderly Chinese men. *PLoS One,* 8**,** e77919.

SIMUNDIC, A.-M. 2013. Bias in research. *Biochemia medica,* 23**,** 12-15.

SINGH, H. & GALLIER, S. 2014. Chapter 2 - Processing of Food Structures in the Gastrointestinal Tract and Physiological Responses. *In:* BOLAND, M., GOLDING, M. & SINGH, H. (eds.) *Food Structures, Digestion and Health.* San Diego: Academic Press.

SINGH, J., KAUR, L. & SINGH, H. 2013. Chapter Four - Food Microstructure and Starch Digestion. *In:* HENRY, J. (ed.) *Advances in Food and Nutrition Research.* Academic Press.

SLEETH, M., PSICHAS, A. & FROST, G. 2013. Weight gain and insulin sensitivity: a role for the glycaemic index and dietary fibre? *Br J Nutr,* 109**,** 1539-41.

SLYPER, A. 2021. Oral Processing, Satiation and Obesity: Overview and Hypotheses. *Diabetes Metab Syndr Obes,* 14**,** 3399-3415.

SNELSON, M., JONG, J., MANOLAS, D., KOK, S., LOUISE, A., STERN, R. & KELLOW, N. J. 2019. Metabolic Effects of Resistant Starch Type 2: A Systematic Literature Review and Meta-Analysis of Randomized Controlled Trials. *Nutrients,* 11.

SO, P. W., YU, W. S., KUO, Y. T., WASSERFALL, C., GOLDSTONE, A. P., BELL, J. D. & FROST, G. 2007. Impact of resistant starch on body fat patterning and central appetite regulation. *PLoS One,* 2**,** e1309.

SPRECKLEY, E. & MURPHY, K. G. 2015. The L-Cell in Nutritional Sensing and the Regulation of Appetite. *Front Nutr,* 2**,** 23.

SRIKAEO, K. & SANGKHIAW, J. 2014. Effects of amylose and resistant starch on glycaemic index of rice noodles. *LWT - Food Science and Technology,* 59**,** 1129-1135.

STEINERT, R. E., POLLER, B., CASTELLI, M. C., DREWE, J. & BEGLINGER, C. 2010. Oral administration of glucagon-like peptide 1 or peptide YY 3-36 affects food intake in healthy male subjects. *The American Journal of Clinical Nutrition,* 92**,** 810-817.

STEPHEN, A., HADDAD, A. & PHILLIPS, S. 1983. Passage of carbohydrate into the colon: direct measurements in humans. *Gastroenterology,* 85**,** 589-595.

STERNE, J. A. C., SAVOVIĆ, J., PAGE, M. J., ELBERS, R. G., BLENCOWE, N. S., BOUTRON, I., CATES, C. J., CHENG, H.-Y., CORBETT, M. S., ELDRIDGE, S. M., EMBERSON, J. R., HERNÁN, M. A., HOPEWELL, S., HRÓBJARTSSON, A., JUNQUEIRA, D. R., JÜNI, P., KIRKHAM, J. J., LASSERSON, T., LI, T., MCALEENAN, A., REEVES, B. C., SHEPPERD, S., SHRIER, I., STEWART, L. A., TILLING, K., WHITE, I. R., WHITING, P. F. & HIGGINS, J. P. T. 2019. RoB 2: a revised tool for assessing risk of bias in randomised trials. *BMJ,* 366**,** l4898.

STONE, B. 2006. Cell walls of cereal grains. *Cereal Foods World,* 51**,** 62-65.

STUBBS, R. J., HUGHES, D. A., JOHNSTONE, A. M., ROWLEY, E., REID, C., ELIA, M., STRATTON, R., DELARGY, H., KING, N. & BLUNDELL, J. 2000. The use of visual analogue scales to assess motivation to eat in human subjects: a review of their reliability and validity with an evaluation of new hand-held computerized systems for temporal tracking of appetite ratings. *British Journal of Nutrition,* 84**,** 405-415.

STÜMPEL, F., BURCELIN, R., JUNGERMANN, K. & THORENS, B. 2001. Normal kinetics of intestinal glucose absorption in the absence of GLUT2: Evidence for a transport pathway requiring glucose phosphorylation and transfer into the endoplasmic reticulum. *Proceedings of the National Academy of Sciences,* 98**,** 11330-11335.

SUZUKI, K., IWASAKI, K., MURATA, Y., HARADA, N., YAMANE, S., HAMASAKI, A., SHIBUE, K., JOO, E., SANKODA, A., FUJIWARA, Y., HAYASHI, Y. & INAGAKI, N. 2018. Distribution and hormonal characterization of primary murine L cells throughout the gastrointestinal tract. *Journal of Diabetes Investigation,* 9**,** 25-32.

SUZUKI, K., SIMPSON, K. A., MINNION, J. S., SHILLITO, J. C. & BLOOM, S. R. 2010. The role of gut hormones and the hypothalamus in appetite regulation. *Endocr J,* 57**,** 359-72.

SVIHUS, B., UHLEN, A. K. & HARSTAD, O. M. 2005. Effect of starch granule structure, associated components and processing on nutritive value of cereal starch: A review. *Animal Feed Science and Technology,* 122**,** 303-320.

SYAHARIZA, Z. A., SAR, S., HASJIM, J., TIZZOTTI, M. J. & GILBERT, R. G. 2013. The importance of amylose and amylopectin fine structures for starch digestibility in cooked rice grains. *Food Chem,* 136**,** 742-9.

SYMONDS, E. L., KRITAS, S., OMARI, T. I. & BUTLER, R. N. 2004. A Combined 13CO2/H2 Breath Test Can Be Used to Assess Starch Digestion and Fermentation in Humans. *The Journal of Nutrition,* 134**,** 1193-1196.

SZABLEWSKI, L. 2011. Glucose homeostasis–mechanism and defects. *Diabetes-Damages and Treatments,* 2.

SZARKA, L. A. & CAMILLERI, M. 2009. Methods for measurement of gastric motility. *Am J Physiol Gastrointest Liver Physiol,* 296**,** G461-75.

TATEMOTO, K. 1982. Isolation and characterization of peptide YY (PYY), a candidate gut hormone that inhibits pancreatic exocrine secretion. *Proceedings of the National Academy of Sciences,* 79**,** 2514-2518.

THARANATHAN, R. N. & MAHADEVAMMA, S. 2003. Grain legumes—a boon to human nutrition. *Trends in Food Science & Technology,* 14**,** 507-518.

THEODORAKIS, M. J., CARLSON, O., MICHOPOULOS, S., DOYLE, M. E., JUHASZOVA, M., PETRAKI, K. & EGAN, J. M. 2006. Human duodenal enteroendocrine cells: source of both incretin peptides, GLP-1 and GIP. *Am J Physiol Endocrinol Metab,* 290**,** E550-9.

THOMAS, C., GIOIELLO, A., NORIEGA, L., STREHLE, A., OURY, J., RIZZO, G., MACCHIARULO, A., YAMAMOTO, H., MATAKI, C., PRUZANSKI, M., PELLICCIARI, R., AUWERX, J. & SCHOONJANS, K. 2009. TGR5-mediated bile acid sensing controls glucose homeostasis. *Cell Metab,* 10**,** 167-77.

THUENEMANN, E. C., MANDALARI, G., RICH, G. T. & FAULKS, R. M. 2015. Dynamic Gastric Model (DGM). *In:* VERHOECKX, K., COTTER, P., LÓPEZ-EXPÓSITO, I., KLEIVELAND, C., LEA, T., MACKIE, A., REQUENA, T., SWIATECKA, D. & WICHERS, H. (eds.) *The Impact of Food Bioactives on Health: in vitro and ex vivo models.* Cham: Springer International Publishing.

THURSBY, E. & JUGE, N. 2017. Introduction to the human gut microbiota. *Biochem J,* 474**,** 1823-1836.

TIAN, J., OGAWA, Y., SHI, J., CHEN, S., ZHANG, H., LIU, D. & YE, X. 2019a. The microstructure of starchy food modulates its digestibility. *Crit Rev Food Sci Nutr,* 59**,** 3117-3128.

TIAN, M., HENG, J., SONG, H., ZHANG, Y., CHEN, F., GUAN, W. & ZHANG, S. 2019b. Branched chain amino acids stimulate gut satiety hormone cholecystokinin secretion through activation of the umami taste receptor T1R1/T1R3 using an in vitro porcine jejunum model. *Food Funct,* 10**,** 3356-3367.

TIBALDI, J. 2009. Importance of postprandial glucose levels as a target for glycemic control in type 2 diabetes. *South Med J,* 102**,** 60-6.

TOLHURST, G., HEFFRON, H., LAM, Y. S., PARKER, H. E., HABIB, A. M., DIAKOGIANNAKI, E., CAMERON, J., GROSSE, J., REIMANN, F. & GRIBBLE, F. M. 2012. Short-chain fatty acids stimulate glucagon-like peptide-1 secretion via the G-protein-coupled receptor FFAR2. *Diabetes,* 61**,** 364-71.

TRAN, K., BRUN, R. & KUO, B. 2012. Evaluation of regional and whole gut motility using the wireless motility capsule: relevance in clinical practice. *Therap Adv Gastroenterol,* 5**,** 249-60.

TRUMPER, A., TRUMPER, K., TRUSHEIM, H., ARNOLD, R., GOKE, B. & HORSCH, D. 2001. Glucose-dependent insulinotropic polypeptide is a growth factor for beta (INS-1) cells by pleiotropic signaling. *Mol Endocrinol,* 15**,** 1559-70.

TUOMILEHTO, J., LINDSTROM, J., ERIKSSON, J. G., VALLE, T. T., HAMALAINEN, H., ILANNE-PARIKKA, P., KEINANEN-KIUKAANNIEMI, S., LAAKSO, M., LOUHERANTA, A., RASTAS, M., SALMINEN, V., UUSITUPA, M. & FINNISH DIABETES PREVENTION STUDY, G. 2001. Prevention of type 2 diabetes mellitus by changes in lifestyle among subjects with impaired glucose tolerance. *N Engl J Med,* 344**,** 1343-50.

TURTON, M. D., O'SHEA, D., GUNN, I., BEAK, S. A., EDWARDS, C. M. B., MEERAN, K., CHOI, S. J., TAYLOR, G. M., HEATH, M. M., LAMBERT, P. D., WILDING, J. P. H., SMITH, D. M., GHATEI, M. A., HERBERT, J. & BLOOM, S. R. 1996. A role for glucagon-like peptide-1 in the central regulation of feeding. *Nature,* 379**,** 69-72.

TYDEMAN, E. A., PARKER, M. L., FAULKS, R. M., CROSS, K. L., FILLERY-TRAVIS, A., GIDLEY, M. J., RICH, G. T. & WALDRON, K. W. 2010. Effect of carrot (Daucus carota) microstructure on carotene bioaccessibility in the upper gastrointestinal tract. 2. In vivo digestions. *J Agric Food Chem,* 58**,** 9855-60.

UENO, H., YAMAGUCHI, H., MIZUTA, M. & NAKAZATO, M. 2008. The role of PYY in feeding regulation. *Regul Pept,* 145**,** 12-6.

VALLONS, K. J. R., OUDHUIS, L. A. A. C. M., HELMENS, H. J. & KISTEMAKER, C. 2015. The Effect of Oral Processing on the Viscosity of Thickened Drinks for Patients With Dysphagia. *Annals of rehabilitation medicine,* 39**,** 772-777.

VAN AVESAAT, M., TROOST, F. J., RIPKEN, D., HENDRIKS, H. F. & MASCLEE, A. A. 2015. Ileal brake activation: macronutrient-specific effects on eating behavior? *Int J Obes (Lond),* 39**,** 235-43.

VAN DAM, R. M., RIMM, E. B., WILLETT, W. C., STAMPFER, M. J. & HU, F. B. 2002. Dietary patterns and risk for type 2 diabetes mellitus in U.S. men. *Ann Intern Med,* 136**,** 201-9.

VAN MUNSTER, I. P., DE BOER, H. M., JANSEN, M. C., DE HAAN, A. F., KATAN, M. B., VAN AMELSVOORT, J. M. & NAGENGAST, F. M. 1994. Effect of resistant starch on breath-hydrogen and methane excretion in healthy volunteers. *Am J Clin Nutr,* 59**,** 626-30.

VENN, B. J. & MANN, J. I. 2004. Cereal grains, legumes and diabetes. *Eur J Clin Nutr,* 58**,** 1443-61.

VERDICH, C., FLINT, A., GUTZWILLER, J. P., NASLUND, E., BEGLINGER, C., HELLSTROM, P. M., LONG, S. J., MORGAN, L. M., HOLST, J. J. & ASTRUP, A. 2001. A meta-analysis of the effect of glucagon-like peptide-1 (7-36) amide on ad libitum energy intake in humans. *J Clin Endocrinol Metab,* 86**,** 4382-9.

VETRANI, C., COSTABILE, G., LUONGO, D., NAVIGLIO, D., RIVELLESE, A. A., RICCARDI, G. & GIACCO, R. 2016. Effects of whole-grain cereal foods on plasma short chain fatty acid concentrations in individuals with the metabolic syndrome. *Nutrition,* 32**,** 217-221.

VETTER, C., DASHTI, H. S., LANE, J. M., ANDERSON, S. G., SCHERNHAMMER, E. S., RUTTER, M. K., SAXENA, R. & SCHEER, F. 2018. Night Shift Work, Genetic Risk, and Type 2 Diabetes in the UK Biobank. *Diabetes Care,* 41**,** 762-769.

VILLEGAS, R., LIU, S., GAO, Y. T., YANG, G., LI, H., ZHENG, W. & SHU, X. O. 2007. Prospective study of dietary carbohydrates, glycemic index, glycemic load, and incidence of type 2 diabetes mellitus in middle-aged Chinese women. *Arch Intern Med,* 167**,** 2310-6.

VILLMONES, H. C., HAUG, E. S., ULVESTAD, E., GRUDE, N., STENSTAD, T., HALLAND, A. & KOMMEDAL, O. 2018. Species Level Description of the Human Ileal Bacterial Microbiota. *Sci Rep,* 8**,** 4736.

VILSBOLL, T., KRARUP, T., DEACON, C. F., MADSBAD, S. & HOLST, J. J. 2001. Reduced postprandial concentrations of intact biologically active glucagon-like peptide 1 in type 2 diabetic patients. *Diabetes,* 50**,** 609-13.

VINCENT, R., ROBERTS, A., FRIER, M., PERKINS, A. C., MACDONALD, I. A. & SPILLER, R. C. 1995. Effect of bran particle size on gastric emptying and small bowel transit in humans: a scintigraphic study. *Gut,* 37**,** 216-9.

VINOY, S., LAVILLE, M. & FESKENS, E. J. 2016. Slow-release carbohydrates: growing evidence on metabolic responses and public health interest. Summary of the symposium held at the 12th European Nutrition Conference (FENS 2015). *Food Nutr Res,* 60**,** 31662.

VITALE, M., GIACCO, R., LAIOLA, M., DELLA PEPA, G., LUONGO, D., MANGIONE, A., SALAMONE, D., VITAGLIONE, P., ERCOLINI, D. & RIVELLESE, A. A. 2021. Acute and chronic improvement in postprandial glucose metabolism by a diet resembling the traditional Mediterranean dietary pattern: Can SCFAs play a role? *Clin Nutr,* 40**,** 428-437.

WALKER, A. W., INCE, J., DUNCAN, S. H., WEBSTER, L. M., HOLTROP, G., ZE, X., BROWN, D., STARES, M. D., SCOTT, P., BERGERAT, A., LOUIS, P., MCINTOSH, F., JOHNSTONE, A. M., LOBLEY, G. E., PARKHILL, J. & FLINT, H. J. 2011. Dominant and diet-responsive groups of bacteria within the human colonic microbiota. *The ISME Journal,* 5**,** 220-230.

WANDERS, A. J., VAN DEN BORNE, J. J., DE GRAAF, C., HULSHOF, T., JONATHAN, M. C., KRISTENSEN, M., MARS, M., SCHOLS, H. A. & FESKENS, E. J. 2011. Effects of dietary fibre on subjective appetite, energy intake and body weight: a systematic review of randomized controlled trials. *Obes Rev,* 12**,** 724-39.

WARREN, F. J., ROYALL, P. G., GAISFORD, S., BUTTERWORTH, P. J. & ELLIS, P. R. 2011. Binding interactions of α-amylase with starch granules: The influence of supramolecular structure and surface area. *Carbohydrate polymers,* 86**,** 1038-1047.

WEIR, G. C. & BONNER-WEIR, S. 2004. Five stages of evolving beta-cell dysfunction during progression to diabetes. *Diabetes,* 53 Suppl 3**,** S16-21.

WELCOME, M. O. 2019. Gastrointestinal physiology: development, principles and mechanisms of regulation.

WHISTLER, R. L., BEMILLER, J. N. & PASCHALL, E. F. 2012. *Starch: chemistry and technology*, Academic Press.

WHITEHEAD, A. L., JULIOUS, S. A., COOPER, C. L. & CAMPBELL, M. J. 2016. Estimating the sample size for a pilot randomised trial to minimise the overall trial sample size for the external pilot and main trial for a continuous outcome variable. *Stat Methods Med Res,* 25**,** 1057-73.

WHO. 2016. *Obesity and overweight* [Online]. Available: https://www.who.int/news-room/fact-sheets/detail/obesity-and-overweight [Accessed].

WILDE, P. J. 2009. Eating for life: designing foods for appetite control. *J Diabetes Sci Technol,* 3**,** 366-70.

WILDING, J. P. H., CALANNA, S. & KUSHNER, R. F. 2021. Once-Weekly Semaglutide in Adults with Overweight or Obesity. Reply. *N Engl J Med,* 385**,** e4.

WILLIAMS, B. A., GRANT, L. J., GIDLEY, M. J. & MIKKELSEN, D. 2017. Gut Fermentation of Dietary Fibres: Physico-Chemistry of Plant Cell Walls and Implications for Health. *Int J Mol Sci,* 18.

WILLIS, H. J., ELDRIDGE, A. L., BEISEIGEL, J., THOMAS, W. & SLAVIN, J. L. 2009. Greater satiety response with resistant starch and corn bran in human subjects. *Nutr Res,* 29**,** 100-5.

WITHROW, D. & ALTER, D. A. 2011. The economic burden of obesity worldwide: a systematic review of the direct costs of obesity. *Obes Rev,* 12**,** 131-41.

WITTES, J. 2002. Sample size calculations for randomized controlled trials. *Epidemiol Rev,* 24**,** 39-53.

WOERLE, H. J., MEYER, C., DOSTOU, J. M., GOSMANOV, N. R., ISLAM, N., POPA, E., WITTLIN, S. D., WELLE, S. L. & GERICH, J. E. 2003. Pathways for glucose disposal after meal ingestion in humans. *Am J Physiol Endocrinol Metab,* 284**,** E716-25.

WOLEVER, T., JENKINS, D., OCANA, A. M., RAO, V. A. & COLLIER, G. R. 1988. Second-meal effect: low-glycemic-index foods eaten at dinner improve subsequent breakfast glycemic response. *The American Journal of Clinical Nutrition,* 48**,** 1041-1047.

WOLEVER, T. M., JOSSE, R. G., LEITER, L. A. & CHIASSON, J. L. 1997. Time of day and glucose tolerance status affect serum short-chain fatty acid concentrations in humans. *Metabolism,* 46**,** 805-11.

WOLEVER, T. M. S., TOSH, S. M., SPRUILL, S. E., JENKINS, A. L., EZATAGHA, A., DUSS, R., JOHNSON, J., CHU, Y. & STEINERT, R. E. 2020. Increasing oat β-glucan viscosity in a breakfast meal slows gastric emptying and reduces glycemic and insulinemic responses but has no effect on appetite, food intake, or plasma ghrelin and PYY responses in healthy humans: a randomized, placebo-controlled, crossover trial. *Am J Clin Nutr,* 111**,** 319-328.

WONG, J. M., DE SOUZA, R., KENDALL, C. W., EMAM, A. & JENKINS, D. J. 2006a. Colonic health: fermentation and short chain fatty acids. *J Clin Gastroenterol,* 40**,** 235-43.

WONG, J. M. W., DE SOUZA, R., KENDALL, C. W. C., EMAM, A. & JENKINS, D. J. A. 2006b. Colonic Health: Fermentation and Short Chain Fatty Acids. *Journal of Clinical Gastroenterology,* 40**,** 235-243.

WOOD, W. G., WACHTER, C. & SCRIBA, P. C. 1981. Experiences using chloramine-T and 1, 3, 4, 6-tetrachloro-3 alpha, 6 alpha-diphenylglycoluril (Iodogen) for radioiodination of materials for radioimmunoassay. *J Clin Chem Clin Biochem,* 19**,** 1051-6.

WORLD HEALTH, O. & INTERNATIONAL DIABETES, F. 2006. Definition and diagnosis of diabetes mellitus and intermediate hyperglycaemia : report of a WHO/IDF consultation. Geneva: World Health Organization.

WU, T., RAYNER, C. K., JONES, K. L., XIE, C., MARATHE, C. & HOROWITZ, M. 2020. Role of intestinal glucose absorption in glucose tolerance. *Curr Opin Pharmacol,* 55**,** 116-124.

WYATT, P., BERRY, S. E., FINLAYSON, G., O'DRISCOLL, R., HADJIGEORGIOU, G., DREW, D. A., KHATIB, H. A., NGUYEN, L. H., LINENBERG, I., CHAN, A. T., SPECTOR, T. D., FRANKS, P. W., WOLF, J., BLUNDELL, J. & VALDES, A. M. 2021. Postprandial glycaemic dips predict appetite and energy intake in healthy individuals. *Nat Metab,* 3**,** 523-529.

XIONG, K., WANG, J., KANG, T., XU, F. & MA, A. 2021. Effects of resistant starch on glycaemic control: a systematic review and meta-analysis. *Br J Nutr,* 125**,** 1260-1269.

XIONG, W., DEVKOTA, L., ZHANG, B., MUIR, J. & DHITAL, S. 2022a. Intact cells: "Nutritional capsules" in plant foods. *Compr Rev Food Sci Food Saf,* 21**,** 1198-1217.

XIONG, W., DEVKOTA, L., ZHANG, B., MUIR, J. & DHITAL, S. 2022b. Intact cells: “Nutritional capsules” in plant foods. *Comprehensive Reviews in Food Science and Food Safety,* 21**,** 1198-1217.

YAMASHITA, H., MARUTA, H., JOZUKA, M., KIMURA, R., IWABUCHI, H., YAMATO, M., SAITO, T., FUJISAWA, K., TAKAHASHI, Y., KIMOTO, M., HIEMORI, M. & TSUJI, H. 2009. Effects of acetate on lipid metabolism in muscles and adipose tissues of type 2 diabetic Otsuka Long-Evans Tokushima Fatty (OLETF) rats. *Biosci Biotechnol Biochem,* 73**,** 570-6.

YOKOYAMA, R. & NISHITANI, K. 2004. Genomic basis for cell-wall diversity in plants. A comparative approach to gene families in rice and Arabidopsis. *Plant Cell Physiol,* 45**,** 1111-21.

ZAFAR, M. I., MILLS, K. E., ZHENG, J., PENG, M. M., YE, X. & CHEN, L. L. 2019. Low glycaemic index diets as an intervention for obesity: a systematic review and meta-analysis. *Obesity Reviews,* 20**,** 290-315.

ZAFAR, T. A. & KABIR, Y. 2017. Chickpeas suppress postprandial blood glucose concentration, and appetite and reduce energy intake at the next meal. *J Food Sci Technol,* 54**,** 987-994.

ZAFAR, T. A., KABIR, Y. & GHAZAII, C. 2011. Low glycemic index foods suppress glycemic responses, appetite and food intake in young Kuwaiti females. *Kuwait J Sci Eng,* 38**,** 111-123.

ZAHIR, M., FOGLIANO, V. & CAPUANO, E. 2020. Effect of soybean processing on cell wall porosity and protein digestibility. *Food Funct,* 11**,** 285-296.

ZHANG, X., CHENG, Z., DONG, S., RAYNER, C., WU, T., ZHONG, M., ZHANG, G., WANG, K. & HU, S. 2022. Effects of ileal glucose infusion on enteropancreatic hormone secretion in humans: relationship to glucose absorption. *Metabolism,* 131**,** 155198.

ZHAO, L., ZHANG, F., DING, X., WU, G., LAM, Y. Y., WANG, X., FU, H., XUE, X., LU, C., MA, J., YU, L., XU, C., REN, Z., XU, Y., XU, S., SHEN, H., ZHU, X., SHI, Y., SHEN, Q., DONG, W., LIU, R., LING, Y., ZENG, Y., WANG, X., ZHANG, Q., WANG, J., WANG, L., WU, Y., ZENG, B.,

WEI, H., ZHANG, M., PENG, Y. & ZHANG, C. 2018. Gut bacteria selectively promoted by dietary fibers alleviate type 2 diabetes. *Science,* 359**,** 1151-1156.

ZHOU, J., MARTIN, R. J., TULLEY, R. T., RAGGIO, A. M., MCCUTCHEON, K. L., SHEN, L., DANNA, S. C., TRIPATHY, S., HEGSTED, M. & KEENAN, M. J. 2008. Dietary resistant starch upregulates total GLP-1 and PYY in a sustained day-long manner through fermentation in rodents. *Am J Physiol Endocrinol Metab,* 295**,** E1160-6.

ZHU, Y., HSU, W. H. & HOLLIS, J. H. 2013a. Increasing the number of masticatory cycles is associated with reduced appetite and altered postprandial plasma concentrations of gut hormones, insulin and glucose. *British Journal of Nutrition,* 110**,** 384-390.

ZHU, Y., HSU, W. H. & HOLLIS, J. H. 2013b. Increasing the number of masticatory cycles is associated with reduced appetite and altered postprandial plasma concentrations of gut hormones, insulin and glucose. *Br J Nutr,* 110**,** 384-90.

ZIMMET, P., ALBERTI, K. G. & SHAW, J. 2001. Global and societal implications of the diabetes epidemic. *Nature,* 414**,** 782-7.

ZOBEL, H. 1988. Starch crystal transformations and their industrial importance. *Starch ‐Stärke,* 40**,** 1-7.

Appendices

Appendix 1: Participant Information sheet (PIS)

INFORMATION SHEET FOR RESEARCH PARTICIPANTS

You will be given a copy of this Information Sheet and a signed copy of your consent form to keep, should you decide to participate in the study.

Determining the effect of chickpea tissue-structures on metabolic responses, satiety and gut content along the entire gastrointestinal tract.

Professor Gary Frost

You are being invited to take part in a research study. Before you decide, it is important for you to understand why the research is being done and what it will involve. Please take time to read the following information carefully and discuss it with friends, relatives and your GP if you wish. Ask us if there is anything that is not clear or if you would like more information and it will not affect your future care. Take time to decide whether or not you wish to take part.

If you do decide to take part, please let us know beforehand if you have been involved in any other study during the last year. You are free to withdraw at any time without explanation. Thank you for reading this.

WHAT IS THE PURPOSE OF THIS STUDY?

A number of reports globally demonstrate the rates of obesity and type 2 diabetes continue to increase. It highlights the importance of the maintenance of an energy balance and glucose homeostasis. Chickpeas are high in resistant starches and protein, and these nutrients have been shown to stimulate gut hormone secretion that could regulate glucose homeostasis. Therefore, this study aims to investigate the impact of different chickpea tissue-structures on gut hormone secretion, thus explaining the chickpeas' influences on glucose control and satiety reported in previous studies. This project will improve understanding of the relationship among food structure ranging in processing, nutrient bioavailability and chickpea-induced release of gut hormone.

WHY HAVE I BEEN INVITED?

You have been invited to take part in this study because you meet the following criteria:

- You are aged 18-65 years (inclusive)
- You have a body mass index (BMI) between 18.5-30 kg/m^2
- You have the willingness and ability to give written informed consent and willingness and ability to understand, participate and comply with the study requirements

If any of the following apply to you then unfortunately you are unsuitable to take part in this study:

- Abnormal ECG
- Screening blood results outside of normal reference values
- Weight change of ≥ 5kg in the preceding 2 months

- Current smokers
- History of substance abuse and/or excess alcohol intake • Pregnancy • Diabetes • Cardiovascular disease
- Cancer
- Gastrointestinal disease e.g. inflammatory bowel disease or irritable bowel syndrome
- Kidney disease
- Liver disease
- Pancreatitis
- Started new medication within the last 3 months likely to interfere with energy metabolism, appetite regulation and hormonal balance, including: anti-inflammatory drugs or steroids, antibiotics, androgens, phenytoin, erythromycin or thyroid hormones.
- Participation in a research study in the 12 week period prior to entering this study.
- Any blood donation within the 12 week period prior to entering this study

DO I HAVE TO TAKE PART?

It is up to you to decide whether or not to take part. If you do decide to take part you will be given this information sheet to keep and be asked to sign a consent form. If you decide to take part you are still free to withdraw at any time and without giving a reason.

WHAT WILL HAPPEN TO ME IF I TAKE PART?

Registered at ICHNT:

The participants will be registered as a patient at Imperial College Healthcare NHS Trust, please include in PIS that patients will be register at ICHNT

Health Screening:

If you do decide to participate, you will initially be invited to attend a health screening to confirm your eligibility for the study. You will be asked to attend the NIHR/Wellcome Trust Imperial Clinical Research Facility at Hammersmith Hospital where you will be interviewed and examined by one of the researchers. You will have a blood test (to check your liver, kidneys, cholesterol and ensure that you are not anaemic or diabetic) and height, weight and blood pressure measurements will also be taken. You will also have an electrocardiogram (ECG). This is a non-invasive test to look at the health of your heart. All women of child bearing age will have a pregnancy test.

If you do decide to participate, you will be asked to undergo one 4-Day and three 3-Day visits in-patient assessments. There will be at least 3 days between Visits 1 and 2. There will be at least 7 days between visits 2-3 and 3-4.

Study Visit 1

Day 1

On the day before the study visit we will ask you to refrain from strenuous exercise, caffeine and alcohol. You will then be requested to fast overnight from 10 pm (you are allowed to drink water).

On the study day, you will be asked to arrive at the NIHR/Wellcome Trust Imperial Clinical Research Facility at Hammersmith Hospital at approximately 8:00am. You will stay at the Clinical Research Facility for a 4 day visit (three nights).

Two thin, bendy plastic tubes will be placed through your nose and into your stomach and small intestine. The tubes will be placed by a trained medical professional in our team. We will put some lubricant on the end of each tube to make it slippery and place them through your nose and down into your stomach and small intestine. You will be sat upright as the tubes are placed and asked to drink water through a straw as this will help the tubes to go down. It will feel a bit uncomfortable whilst the tubes are being put in, however, any discomfort should subside once the tubes have been positioned. These tubes will allow us to

take samples from your stomach and small intestines after you have eaten to see how different foods are digested. These tubes will remain in place for the duration of the 4 day visit.

Day 2-4

For each 4-Day study visit, you will stay at the Clinical Research Facility at Hammersmith Hospital for three nights and throughout each study visit you will be provided with a diet containing different chickpeas with tissue-structures. You will receive the different chickpeas in a random order. The amounts of dietary fat and protein will be the same at each of the 3 study visits. You will be provided with a bed, all of your meals and will have access to toilet/showering facilities while staying at the Clinical Research Facility. You are welcome to wear your normal clothes but the researchers can provide you with hospital scrubs if you wish. While you are an inpatient at the Clinical Research Facility you will also have access to the internet and will be able to read, watch DVDs or do some work. iPads/laptops will be available during your stay upon request. There is also a lounge area with television, PCs and games consoles for entertainment in the evenings. More information about the facility including photographs can be found on the Clinical Research Facility website (www.imperial.crf.nihr.ac.uk).

On each of the 3 study mornings you will consume a chickpea-based breakfast in different structures.. Blood samples will be taken at certain time points for 3 hours after you eat the breakfast. A total of 100 ml of blood (5 tablespoons of blood) will be taken each morning. These will be taken through the plastic cannula. Following each test breakfast, samples from your stomach and small intestines will be taken every 15 minutes for 3 hours. After each sample is collected you will be asked to fill in a chart describing how hungry you feel. We will also measure your breath hydrogen levels by a real-time handheld monitor every hour for 3 hours after your breakfast. You need to blow into the sample mouthpiece (single use only). Then we can get the instant results.

Your urine will be collected throughout the three days to measure metabolite concentrations. We will provide an appropriate measurement container to collect urine.

Following the 3 hour measurement period, you will be able to read or watch DVDs at the Clinical Research Facility. We will provide all of the food you require for the duration of the 4 day study visit. You will be requested to fast every evening of the visit from 10 pm (you are allowed to drink water).

Following the final samples on the fourth study day, the tubes in your stomach and small intestines and the plastic cannula will be removed and you will be able to go home.

Visit 2, 3, 4

For each 3-Day study visit, you will stay at the Clinical Research Facility at Hammersmith Hospital for two nights and throughout each study visit you will be provided with a diet containing different chickpea tissue-structures. You will receive the different chickpeas in a random order. The amounts of dietary fat and protein will be the same at each of the 3 study visits. You will be provided with a bed, all of your meals and will have access to toilet/showering facilities while staying at the Clinical Research Facility. You are welcome to wear your normal clothes but the researchers can provide you with hospital scrubs if you wish. While you are an inpatient at the Clinical Research Facility you will also have access to the internet and will be able to read, watch DVDs or do some work. iPads/laptops will be available during your stay upon request. There is also a lounge area with television, PCs and games consoles for entertainment in the evenings. More information about the facility including photographs can be found on the Clinical Research Facility website (www.imperial.crf.nihr.ac.uk).

Day 1

On the day before each study visit we will ask you to refrain from strenuous exercise, caffeine and alcohol. You will then be requested to fast overnight (you are allowed to drink water).

On Day 1 of the study visit, you will be asked to arrive at the **Department of Imaging at Charing Cross Hospital** around 8:00am. You will have a tube placed through your nose by a trained medical professional. The end of this tube will lie within the small intestine (ileum) allowing us to collect and measure the contents of the gut. The tube will be placed whilst you are awake. It is not painful, but can result in transient discomfort which can be minimized with sips of water or sucking on an ice cube. Fluoroscopy is a type of medical imaging that shows a continuous X-ray image on a monitor, much like an X-ray movie. The tubes will remain in place for the duration of the 3-Day study visit. Following insertion of

the tubes at Charing Cross Hospital, you will be provided with a teal meal at approximately 09:00. Then you will be transported in a taxi with a member of our research team to the Clinical Research Facility at Hammersmith Hospital for the remainder of the study visit.

Days 2-3:

On the morning of Day 2, you will be provided with a test meal at approximately 09:00. Before the breakfast and for 8 hours afterwards samples will be collected from the tube placed in your nose to measure the gut contents. You will also be asked to breathe into a breath analyser every hour so that we can measure your breath hydrogen levels. This will give us information about the time it takes for the food you have eaten to reach your large bowel.

On the morning of day 3, you will have a small plastic cannula tube inserted into a vein in one arm. A vein is the type of blood vessel commonly used for taking blood samples. You may feel minor discomfort whilst the cannula is being inserted. After the cannula tube has been inserted this will be used to take blood samples to measure the levels of hormones which control hunger in your body. During each study visit approximately 100 ml of blood (5 tablespoons of blood) will be collected. At approximately 09:00 a test meal will be provided and gut content samples and blood samples will be collected throughout an 8 hour study period. After each sample is collected you will be asked to fill in a chart describing how hungry you feel. We will also measure your breath hydrogen levels every hour as on day 3. At approximately 17:00, the nasal tube and cannula tube will be removed and you will be free to go home. It is expected that the majority of participants will have the naso-enteric tubes removed through the nose at the Clinical Research Facility at Hammersmith Hospital. If more than mild discomfort seems likely to be caused by the removal of the tube, we will transport you in a taxi to Charing Cross Hospital for removal of the tube under fluoroscopy. Alternatively, the nasal end of the tube will be cut and the rest of the tube will be allowed to pass rectally.

In addition, you will also be asked to collect a stool sample on each day of the 3-Day study visit. We will explain to you in detail how to do this and you will be given an appropriate container.
After you have entered the study the clinicians may give you alternative treatment (such as painkillers for headaches) to that specified in the protocol at any stage if he/she feels it is in the participant's best interest, but the reasons for doing so will be recorded. In such cases, you would need to remain within the study for the purposes of follow-up and data analyses. You are free to withdraw at any time from the study without giving reasons and without prejudicing further treatment.

WHAT ARE WE TESTING?

We are measuring levels of hormones which influence appetite, other markers of appetite and metabolism, levels of nutrients in the bloodstream, nutrient molecules, as well as other routine blood tests. Food samples will be removed from your small intestine to look at the molecules we are interested in that may play a role in regulating how hungry you feel.

WHAT ARE THE SIDE EFFECTS OF TAKING PART?

The diets consumed over the course of the study are common food items and dietary supplements. They are generally not found to be linked to any serious side effects.

WHAT ARE THE POSSIBLE DISADVANTAGES AND RISKS OF TAKING PART?

Insertion of the cannula into your arm on each of the study visits may cause minor discomfort or superficial bruising. Serious risks associated with the insertion of the tubes are very rare and almost negligible. These risks include bleeding, perforation or damage to the base of the skull. Minor discomfort of the back of the throat does occur in the majority of patients and may result transiently in a sore mouth, thirst, swallowing difficulties or hoarseness. The fluoroscopy procedure will expose you to a small dose of radiation. The mean effective dose from each nasogastric tube procedure is equivalent to 2.8 months of natural background radiation (the same amount as you would be exposed to walking around outside) and would increase the risk of inducing cancer by 0.0025% (or 1 in 40,000). The minimum number of fluoroscopy

procedures that will be conducted is 3. The maximum number of fluoroscopy procedures that will be conducted is 6.

It should be noted that the health screenings performed as part of this study cannot be viewed as a comprehensive health check. However, vary rarely, unexpected observations may be detected which may need further investigation. In this event, you will be informed and a report will be sent to your GP, who will arrange further tests and coordinate your further care.

WHAT ARE THE POSSIBLE BENEFITS OF TAKING PART?

Taking part in the study will provide no direct benefit for you. The information that we get from this study will help us to better understand normal appetite regulation and may help us to better treat future patients who suffer from obesity. If any of the screening questionnaires or blood tests reveal any medical problems (e.g. diabetes, kidney or liver problems), your GP will be informed so that they can coordinate your further care, arrange any further tests, and refer you on to Hospital Doctors if necessary.

WILL MY TAKING PART IN THIS STUDY BE KEPT CONFIDENTIAL?

All information which is collected about you during the course of the research will be kept strictly confidential. The fluoroscopy procedures will be carried out at the Department of Imaging at Charing Cross Hospital and information regarding these procedures will be stored on NHS systems.

Any information about you which leaves the hospital will be kept in a secure location at Imperial College London. All personal data will be stored in locked filing cabinets in the Section of Investigative Medicine, Imperial College London. Only members of the Section of Investigative Medicine will have access to this. Personal data will only be stored on computers that can only be accessed from within the Section of Investigative Medicine, Imperial College London. All staff involved in the study are aware of the requirements of the Data Protection Act and adherence to Good Clinical Practice (GCP). Subjects will be given a personal study code number which will be used throughout the study and in the analysis of data. The anonymised samples and data will be sent to Food Innovation and Health Programme at Quadram Institute Bioscience at Norwich for analysis after non-disclosure agreement is signed.

Collected tissue samples may also be used in future ethically approved studies. Your GP will also be informed regarding your participation in the study.

Imperial College London is the sponsor for this study based in the United Kingdom. Imperial College London will be using information from you and your medical records in order to undertake this study and will act as the data controller for this study. This means that we are responsible for looking after your information and using it properly. Imperial College London will keep identifiable information about you 10 years after the study has finished in relation to data subject consent forms and primary research data.

Further information on Imperial College London's retention periods may be found at https://www.imperial.ac.uk/media/imperial-college/administration-and-support-services/records-and-archives/public/RetentionSchedule.pdf.

Your rights to access, change or move your information are limited, as we need to manage your information in specific ways in order for the research to be reliable and accurate. If you withdraw from the study, we will keep the information about you that we have already obtained. To safeguard your rights, we will use the minimum personally-identifiable information possible.
You can find out more about how we use your information [Professor Gary Frost, email: g.frost@imperial.ac.uk; Tel: 0208 383 8037.

LEGAL BASIS

As a university we use personally-identifiable information to conduct research to improve health, care and services. As a publicly-funded organisation, we have to ensure that it is in the public interest when we use personally-identifiable information from people who have agreed to take part in research. This means that

when you agree to take part in a research study, we will use your data in the ways needed to conduct and analyse the research study.
Health and care research should serve the public interest, which means that we have to demonstrate that our research serves the interests of society as a whole. We do this by following the UK Policy Framework for Health and Social Care Research.

INTERNATIONAL TRANSFERS

There may be a requirement to transfer information to countries outside the European Economic Area (for example, to a research partner). Where this information contains your personal data, Imperial College London will ensure that it is transferred in accordance with data protection legislation. If the data is transferred to a country which is not subject to a European Commission (EC) adequacy decision in respect of its data protection standards, Imperial College London will enter into a data sharing agreement with the recipient organisation that incorporates EC approved standard contractual clauses that safeguard how your personal data is processed.

CONTACT US

If you wish to raise a complaint on how we have handled your personal data or if you want to find out more about how we use your information, please contact Imperial College London's Data Protection Officer via email at dpo@imperial.ac.uk, via telephone on 020 7594 3502 and via post at Imperial College London, Data Protection Officer, Faculty Building Level 4, London SW7 2AZ.
If you are not satisfied with our response or believe we are processing your personal data in a way that is not lawful you can complain to the Information Commissioner's Office (ICO). The ICO does recommend that you seek to resolve matters with the data controller (us) first before involving the regulator.
Imperial College London and Imperial College Healthcare NHS Trust will collect information from you and your medical records for this research study in accordance with our instructions.

Imperial College London and Imperial College Healthcare NHS Trust will keep your name, and contact details including age confidential. Imperial College Healthcare NHS Trust will use this information as needed, to contact you about the research study, and make sure that relevant information about the study is recorded for your care, and to oversee the quality of the study. Certain individuals from Imperial College London and regulatory organisations may look at your medical and research records to check the accuracy of the research study. The people who analyse the information will not be able to identify you and will not be able to find out your name, age or contact details.

Imperial College London will keep identifiable information about you from this study for 10 years after the study has finished.

When you agree to take part in a research study, the information about your health and care may be provided to researchers running other research studies in this organisation and in other organisations. These organisations may be universities, NHS organisations or companies involved in health and care research in this country or abroad. Your information will only be used by organisations and researchers to conduct research in accordance with the UK Policy Framework for Health and Social Care Research.

This information will not identify you and will not be combined with other information in a way that could identify you. The information will only be used for the purpose of health and care research, and cannot be used to contact you or to affect your care. It will not be used to make decisions about future services available to you, such as insurance.

WHAT IF NEW INFORMATION BECOMES AVAILABLE?

Sometimes during the course of a research project, new information becomes available about the study. If this happens, your research doctor will tell you about it and discuss with you whether you want to continue in the study. If you decide to continue in the study you will be asked to sign an updated consent form. Also,

on receiving new information your research doctor might consider it to be in your best interests to withdraw you from the study.

WHAT HAPPENS WHEN THE RESEARCH STUDY STOPS?

Once the study has finished, the results of the study can be made available to you and/or your GP should you wish. If you have any problems immediately following the study, then you should contact one of the research doctors on the numbers provided below.

WHAT WILL HAPPEN TO THE RESULTS OF THE RESEARCH STUDY?

The results are likely to be published in the year following the study. Your confidentiality will be ensured at all times and you will not be identified in any publication. At the end of the study, the results of the study can be made available to you and/or your GP should you wish.

WHO IS ORGANISING AND FUNDING THE RESEARCH?

This study is being organised by the Section of Investigative Medicine, Imperial College London and is being funded by the Biotechnology and Biological Sciences Research Council (BBSRC).

WHO HAS REVIEWED THE STUDY?

This study was reviewed by HRA. This study was given a favourable ethical opinion for conduct in the NHS by the London-Camden and Kings Cross Research Ethics Committee

WILL I BE REIMBURSED FOR MY TRAVEL EXPENSES/TIME?

You will receive a fixed payment to cover expenses including travel costs of £10 for the screening visit, £500 for study visit 1, £350 for study visit 2,3,4 respectively.

WHAT IF SOMETHING GOES WRONG?

Imperial College London holds insurance policies which apply to this study. If you experience harm or injury as a result of taking part in this study, you will be eligible to claim compensation without having to prove that Imperial College is at fault. This does not affect your legal rights to seek compensation.
If you are harmed due to someone's negligence, then you may have grounds for a legal action. Regardless of this, if you wish to complain, or have any concerns about any aspect of the way you have been treated during the course of this study then you should immediately inform the Investigator (Professor Gary Frost, Section of Investigative Medicine, 6th Floor Commonwealth Building, Hammersmith Hospital, Imperial College London, Du Cane Road, London, W12 0NN, U.K. Tel: 020 8383 2820). The normal National Health Service mechanisms are also available to you such as contacting the local Patient Advice Liaison Services (PALS; pals@imperial.nhs.uk, 020 3313 0088). A member of the team will be able to give you their contact information upon request. If you are still not satisfied with the response, you may contact the Imperial College, Joint Research Compliance Office.

CONTACT FOR FURTHER INFORMATION

If you have any questions regarding the study please contact the researcher (Mingzhu Cai) on 07395757128 during working hours. The hospital switchboard (020 8383 1000) has home and mobile phone numbers for all the researchers involved in the study and can contact them at any time outside normal working hours. If you agree to take part in the study, you will also be given the contact details of the researchers.

If you experience any problems during this study, you may withdraw at any stage.

Thank you for taking the time to read this.

Appendix 2

Determining the effect of chickpea tissue-structures on metabolic responses, satiety regulation and gut content along the entire gastrointestinal tract

Professor Gary Frost

Please initial the box if you agree with each statement.

1. I confirm that I have read and understand the participant information sheet dated 01/07/2019 version 7 for the above study and had the opportunity to ask questions which have been answered fully.

2. I understand that my participation is voluntary and that I am free to withdraw at any time, without giving any reason, without my medical care or legal rights being affected.

3. I understand that sections of any of my research notes may be looked at by responsible individuals from Imperial College, from NHS Trust or from regulatory authorities where it is relevant to my taking part in this research.

4. I give permission for these individuals to have access to my records.

5. I give/do not give (delete as applicable) consent for information collected about me to be used to support other research in the future, including those outside of the EEA.

6. I give / do not give (delete as applicable) consent for samples collected during this study to be used in future ethically approved studies.

7. I give permission for my samples to be sent to other organizations, including these outsides of the EEA.

8. I consent to take part in the above study.

9. I give/do not give (delete as applicable) consent to being contacted to potentially taking part in other research studies.

_____	_____	_____
Name of Subject	Signature	Date
_____	_____	_____
Name of Person taking consent (if different from Principal Investigator)	Signature	Date
_____	_____	_____
Principal Investigator	Date	Signature

1 copy for subject; 1 copy for Principal Investigator; 1copy to be kept with hospital notes

Appendix 3 Phase 1 study (Chapter 4) dietary intervention SOP

Meal Preparation Instruction Sheet
Phase 1 Treatment [A]

You will need:

- 1 L Measuring jug
- 1.5 L Bowl
- Aluminium foil
- Thermomix w/Mixing bowl and Lid
- Balance
- Sieve/Colander (approx. 15 cm or 0.5 L)
- Serving bowl (>0.3 L capacity)
- Serving spoon
- Glass (~0.5 L volume)
- Drinking water
- Seasoning: 1 x Hartley's Sugar free Blackcurrant Jelly pot 115 g + 15 g Stute no added sugar Blackcurrant jam

DAY BEFORE THE STUDY

Put 75 g dry chickpeas in a colander, rinse until the starchy water runs clear, then put in a bowl and **add 1L** tap water. Cover with foil and leave overnight.

MORNING OF THE STUDY VISIT (start ~ 2h before test meal is due to be served)

1. DRAIN: Drain the water from the soaked chickpeas in a colander/sieve over the sink, rinse once with clean water and drain thoroughly.
2. WEIGH IN WATER: Place the empty Thermomix mixing bowl (without the lid) on the balance and press TARE then tip the drained chickpeas into the Thermomix mixing bowl and add **water (approx. 225 g)** until the total (tared) weight is **375 g**
3. COOK: Secure the lid. Use the Thermomix display screen to set **Timer (mm:ss) to 80:00 Temperature to 95°C** and **Stirrer in REVERSE** direction and **Speed setting 1**.
4. BLEND: When the audible alarm sounds (after 94 min) set the **Timer (mm:ss) to 09:00 (9 min**), **temperature to 95°C,** and the stirrer to **Speed setting 5 in REVERSE** direction.
5. WEIGH THE COOKED PORTION: Tare the Balance, then put the Thermomix mixing bowl without the lid on the balance and Record the weight of mixing bowl with cooked portion
6. LOOK UP SERVING SIZE: Use the 'Look-up table' to determine the weight of cooked meal and drink of water to serve to the participant.
7. WEIGH OUT SERVINGS:

Food: Place the serving bowl on the balance and tare, then use a serving spoon to add the cooked food to the bowl until target serving weight (from look-up table) is achieved. *The serving size for this meal is usually around* 280 g.
FLAVOURING: Stirring the chickpea with 1 x 115 g pot of jelly and 15 g of sugar-free jam.
Drink: Next, tare the balance to drinking glass and add drinking water until the target drink weight is achieved. Serve immediately and do not let the temperature of the meal fall below 60 degrees!

1. Serve immediately and do not let the temperature of the meal fall below 60 degrees!

**Take a sample from the portion that was not served into a freezer bag, flatten and freeze -20˚C.*

Meal Preparation Instruction Sheet
Phase 1 Treatment [B]

You will need:

- 1 L Measuring jug
- 1.5 L Bowl
- Aluminium foil
- Thermomix w/Mixing bowl and Lid
- Balance
- Fine-mesh Sieve/Colander (approx. 15cm or 0.5L)
- Serving bowl (>0.3 L capacity)
- Serving spoon
- Glass (~0.5 L volume)
- Drinking water
- Seasoning: 1 x Hartley's Sugar free Blackcurrant Jelly pot 115 g + 15 g Stute no added sugar Blackcurrant jam

DAY BEFORE THE STUDY

Put 75 g dry milled (1.6 - 2.0 mm) chickpeas in a colander, rinse until the water runs clear (approx. 4 L), then put in a bowl and add 1 L tap water. Cover with foil and leave overnight.

MORNING OF THE STUDY VISIT (start ~ 1h before test meal is due to be served)

1. DRAIN: Drain the water from the soaked chickpeas in a colander/sieve over the sink.
2. WEIGH IN WATER: Place the empty Thermomix mixing bowl (without the lid) on the balance and press TARE then tip the drained chickpeas into the Thermomix mixing bowl and add **water (approx. 150 g)** until the total (tared) weight is **300 g**
3. COOK: Secure the lid. Use the Thermomix display screen to set **Timer (mm:ss) to 50:00**; **Temperature to 95°C** and **Stirrer in REVERSE** direction and **Speed setting 1**.
4. WEIGH THE COOKED PORTION: Tare the Balance, then put the Thermomix mixing bowl without the lid on the balance and Record the weight of mixing bowl with cooked portion
5. LOOK UP SERVING SIZE: Use the 'Look-up table' to determine the weight of cooked meal and drink of water to serve to the participant.
6. WEIGH OUT SERVINGS:

   Food: Place the serving bowl on the balance and tare, then use a serving spoon to add the cooked food to the bowl **until target serving weight (from look-up table)** is achieved. The serving size for this meal is usually around 230 g.

   FLAVOURING: Stirring the chickpea with 1 x 115 g pot of jelly and 15 g of sugar-free jam.

Drink: Next, tare the balance to drinking glass and add drinking water until the target drink weight is achieved.

7. Serve immediately and do not let the temperature of the meal fall below 60 degrees
   * *Take a sample from the portion that was not served into a freezer bag, flatten and freeze -20˚C.*

Meal Preparation Instruction Sheet
Phase I Treatment [C]

You will need:

- 1 L Measuring jug
- 1.5 L Bowl
- Aluminium foil
- Thermomix w/Mixing bowl and Lid
- Balance
- Sieve/Colander (approx. 15 cm or 0.5 L)
- Serving bowl (>0.6 L capacity)
- Serving spoon
- Glass (~0.15 L volume)
- Drinking water
- Seasoning: 1 x Hartley's Sugar free Blackcurrant Jelly pot 115 g + 15 g Stute no added sugar blackcurrant jam

DAY BEFORE THE STUDY

Put 75 g dry de-hulled chickpeas in a colander, rinse until the water runs clear (approx. 4 L), then put in a bowl and add 1 L tap water. Cover with foil and leave overnight.

MORNING OF THE STUDY VISIT (start ~ 50 min before test meal is due to be served)

2. DRAIN: Drain the water from the soaked chickpeas in a colander/sieve over the sink, rinse once with clean water and drain thoroughly.
3. WEIGH IN WATER: Place the empty Thermomix mixing bowl (without the lid) on the balance and press TARE then tip the drained chickpeas into the Thermomix mixing bowl and add **water (approx. 487 g)** until the total (tared) weight is **637.5 g.**
4. BLEND: Secure the lid. Use the Thermomix display screen to set (in the following order): **Timer (mm:ss) to 03:00 (3 min)**; **Temperature to 37C** and **Blender to FORWARD X** direction and **Speed setting 10**.
5. COOK: When the audible alarm sounds after 3 min, Set the **Timer to (28 min) (mm:ss) 28:00; Temperature to 95°C**, and the **Blender to REVERSE** direction **and Speed setting 4**
6. LOOK UP SERVING SIZE: Use the 'Look-up table' to determine the weight of cooked meal and drink of water to serve to the participant.
7. WEIGH OUT SERVINGS:
   Food: Place the serving bowl on the balance and tare, then use a serving spoon to add the cooked food to the bowl **until target serving weight (from the look-up table)** is achieved. *The serving size for this meal is usually around 490 g.*
   FLAVOURING: Stirring the chickpea with 1 x 115 g pot of jelly and 15 g of sugar-free jam.
   Drink: Next, tare the balance to drinking glass and add drinking water until the target drink weight is achieved.
8. Serve immediately and do not let the temperature of the meal fall below 60 degrees!

**Take a sample from the portion that was not served into a freezer bag, flatten and freeze -20˚C.*

LOOK UP TABLE: to serve 30g Total Starch from chickpea per meal				
			FOOD	DRINK
Thermomix Jug empty weight (g)	If the thermomix jug with the cooked meal weighs … g	If the cooked meal weighs…g	You need to serve (g cooked)	with this amount of water in a glass (g)
1120	1757.5	637.5	**510.0**	***250.0***
1120	1750	630	**504.0**	***256.0***
1120	1730	610	**488.0**	***272.0***
1120	1710	590	**472.0**	***288.0***
1120	1690	570	**456.0**	***304.0***
1120	1670	550	**440.0**	***320.0***
1120	1650	530	**424.0**	***336.0***
1120	1630	510	**408.0**	***352.0***
1120	1610	490	**392.0**	***368.0***
1120	1590	470	**376.0**	***384.0***
1120	1570	450	**360.0**	***400.0***
1120	1550	430	**344.0**	***416.0***
1120	1530	410	**328.0**	***432.0***
1120	1510	390	**312.0**	***448.0***
1120	1495	375	**300.0**	***460.0***
1120	1470	350	**280.0**	***480.0***
1120	1445	325	**260.0**	***500.0***
1120	1420	300	**240.0**	***520.0***
1120	1420	300	**240.0**	***370.0***
1120	1395	275	**220.0**	***390.0***
1120	1370	250	**200.0**	***410.0***

Appendix 4 Phase 2 study (Chapter 5) dietary information

Meal Preparation Instruction Sheet
Phase 2 Treatment [X]

You will need:

- 1L Measuring jug
- 1.5L Bowl
- Aluminium foil
- Thermomix w/Mixing bowl and Lid
- Balance
- Sieve/Colander (approx. 15cm or 0.5L)
- Serving bowl (>0.3L capacity)
- Serving spoon
- Glass (~0.5L volume)
- Drinking water

Breakfast: 1 x Hartley's Sugar free Blackcurrant Jelly pot 115g + 15g Stute no added sugar Blackcurrant jam;
Lunch: 90g curry paste, 100g chicken breast chunks, 10g olive oil, and 150g baby carrots;
Dinner: 10g lemon juice, 2g parsley, 2g mint, 5g olive oil, 3g black pepper, 2g salt, 1 x Penne Bolognese Ready Meal.

DAY BEFORE THE STUDY

Put 160 g dry chickpeas in a colander, rinse until the starchy water runs clear, then put in a bowl and **add 1L** tap water. Cover with foil and leave overnight.

MORNING OF THE STUDY VISIT (start ~ 2h before test meal is due to be served)

9. DRAIN: Drain the water from the soaked chickpeas in a colander/sieve over the sink, rinse once with clean water and drain thoroughly.
10. WEIGH IN WATER: Place the empty Thermomix mixing bowl (without the lid) on the balance and press TARE then tip the drained chickpeas into the Thermomix mixing bowl and add **water (approx. 480 g)** until the total (tared) weight is **800 g**
11. COOK: Secure the lid. Use the Thermomix display screen to set **Timer (mm:ss) to 80:00 (80 min) Temperature to 95C** and **Stirrer in REVERSE** direction and **Speed setting 1**.
12. BLEND: When the audible alarm sounds (after 94 min) set the **Timer (mm:ss) to 09:00 (9 min**), **temperature to 95C°C,** and the stirrer to **Speed setting 5 in REVERSE** direction.
13. WEIGH THE COOKED PORTION: Tare the Balance, then put the Thermomix mixing bowl without the lid on the balance and Record the weight of mixing bowl with cooked portion
14. LOOK UP SERVING SIZE: Use the 'Look-up table' to determine the weight of cooked meal and drink of water to serve to the participant.
15. WEIGH OUT SERVINGS for breakfast, lunch, and dinner immediately. Place the serving bowl on the balance and tare, then use a serving spoon to add the cooked food to the

bowl **until target serving weight (from look-up table)** is achieved. *The serving size for breakfast, lunch, dinner is usually around 280g, 187g, and 187g.*

16. **FLAVOUR BREAKFAST**: **Stir** the chickpea with 1 x 115g pot of jelly and 15g of sugar-free jam

    Drink: Next, tare the balance to drinking glass and add water to reach target drink weight.

    Serve breakfast immediately and do not let the temperature of the meal fall below 60 ˚C!
17. **REFRIGERATE LUNCH and DINNER portions**: Use plastic wrap to seal the foods for lunch and dinner and then keep them at 4 ˚C until use.

**Take a sample from the portion that was not served into a freezer bag, flatten and freeze -20˚C.*

LUNCH OF THE STUDY VISIT (start ~ 30 min before test meal is due to be served)

1. WEIGHT CHICKEN WITH CURRY: weight 90g curry pasta, 10g olive oil, 100g tikka chicken breast chunks and mix them thoroughly.
2. HEATING CHICKEN WITH CURRY: Transfer the mixture into a saucepan with a lid and place it on a hob. Turn on the hub and set it on the setting of 3.
3. STIRRING: Start a timer for 5mins. Stirring occasionally to avoid the pasta sticking at the bottom of the pan.
4. KEEP THEM WARM: After 5 mins, switch the setting to 1 to keep them warm.
5. WEIGHT AND PREPARE CARROTS: During the 5-min cooking of curry and chicken, prepare the carrots. Drain and weight 150g carrots into a non-metallic bowl. Cover and microwave on 850W for 2 mins. Keep it in the microwave until serve.
6. REHEATING CHICKPEAS: take the chickpeas out of the fridge. Tap the cling film to knock the condensation on the underside into the chickpeas. Microwave the chickpeas for 2 min at 900 W. Measure the temperature and check if it has reached 83°C.
7. MAKE THE COMBO: Transfer chickpeas to a big dish. Pour the chicken with curry pasta on the top of chickpeas. Serve carrots on the side.
8. TURN OF THE HOB: remember to turn off the hob once finish.

DINNER OF THE STUDY VISIT (start ~ 30 min before test meal is due to be served)

1. MICROWAVE READY MEAL: take the Penne Bolognese Ready Meal out of the freezer. Pierce film lid before cooking. Microwave it at 750W for 9 minutes.
2. REHEATING CHICKPEAS: when the ready meal is cooking, take the chickpeas out of the fridge. Tap the cling film to knock the condensation on the underside into the chickpeas. Microwave the chickpeas for 2 min at 900 W. Measure the temperature and check if it has reached 83°C.
3. FLAVOURING: mix 10g lemon juice, 2g parsley, 2g mint, 5g olive oil, 3g black pepper, 2g salt in a bowl and pour over chickpeas as a dressing.
9. MAKE THE COMBO: Transfer the seasoned chickpeas to a big dish. Serve the Penne Bolognese (the whole things) on the side.

Meal Preparation Instruction Sheet
Phase 2 Treatment [Y]

You will need:

- 1L Measuring jug
- 1.5L Bowl
- Aluminium foil
- Thermomix w/Mixing bowl and Lid
- Balance
- Fine-mesh Sieve (approx. 15cm or 0.5L)
- Serving bowl (>0.3L capacity)
- Serving spoon
- Glass (~0.5L volume)
- Drinking water
- Flavouring:
  Breakfast: 1 x Hartley's Sugar free Blackcurrant Jelly pot 115g + 15g Stute no added sugar Blackcurrant jam;
  Lunch: 90g curry paste, 100g chicken breast chunks, 10g olive oil, and 150g baby carrots;
  Dinner: 10g lemon juice, 2g parsley, 2g mint, 5g olive oil, 3g black pepper, 2g salt, 1 x Penne Bolognese Ready Meal;

DAY BEFORE THE STUDY

Put 160 g dry milled (1.6 – 2.0 mm) chickpeas in a colander, rinse until the water runs clear (approx. 4L), then put in a bowl and add 1L tap water. Cover with foil and leave overnight.

MORNING OF THE STUDY VISIT (start ~ 2h before test meal is due to be served)

1. DRAIN: Drain the water from the soaked chickpeas in a colander/sieve over the sink.
2. WEIGH IN WATER: Place the empty Thermomix mixing bowl (without the lid) on the balance and press TARE then tip the drained chickpeas into the Thermomix mixing bowl and add **water (approx. 320 g)** until the total (tared) weight is **640 g**
3. COOK: Secure the lid. Use the Thermomix display screen to set **Timer (mm:ss) to 50:00 (50 min)**; **Temperature to 95°C** and **Stirrer in REVERSE** direction and **Speed setting 1**.
4. WEIGH THE COOKED PORTION: Tare the Balance, then put the Thermomix mixing bowl without the lid on the balance and Record the weight of mixing bowl with cooked portion
5. LOOK UP SERVING SIZE: Use the 'Look-up table' to determine the weight of cooked meal and drink of water to serve to the participant.

6. WEIGH OUT SERVINGS for breakfast, lunch, and dinner immediately. Place the serving bowl on the balance and tare, then use a serving spoon to add the cooked food to the bowl **until target serving weight (from look-up table)** is achieved. *The serving size for breakfast, lunch, dinner is usually around 230g, 153g, and 153g.* Then **DRAIN the Chickpeas and <u>SERVE ONLY THE SOLIDS</u>.**
7. **FLAVOUR BREAKFAST:** Stirring the chickpea with 1 x 115 g pot of jelly and 15 g of sugar-free jam.

   Drink: Next, tare the balance to drinking glass and add water to reach target drink weight.

   Serve breakfast immediately and do not let the temperature of the meal fall below 60˚C.
8. **REFRIGERATE LUNCH and DINNER portions**: Use plastic wrap to seal the foods for lunch and dinner and then keep them at 4 ˚C until use.

   * *Take a sample from the portion that was not served into a freezer bag, flatten and freeze -20˚C.*

LUNCH OF THE STUDY VISIT (start ~ 30 min before test meal is due to be served)

1. WEIGHT CHICKEN WITH CURRY: weight 90g curry pasta, 10g olive oil, 100g tikka chicken breast chunks and mix them in a bowl thoroughly.
2. HEATING CHICKEN WITH CURRY: Transfer the mixture into a saucepan with a lid and place it on a hob. Turn on the hub and set it on the setting of 3.
3. STIRRING: Start a timer for 5mins. Stirring occasionally to avoid the pasta sticking at the bottom of the pan.
4. KEEP THEM WARM: After 5 mins, switch the setting to 1 to keep them warm.
5. WEIGHT AND PREPARE CARROTS: During the 5-min cooking of curry and chicken, prepare the carrots. Drain and weight 150g carrots into a non-metallic bowl. Cover and microwave on 850W for 2 mins. Keep it in the microwave until serve.
6. REHEATING CHICKPEAS: take the chickpeas out of the fridge. Tap the cling film to knock the condensation on the underside into the chickpeas. Microwave the chickpeas for 2 min at 900 W. Measure the temperature and check if it has reached 83°C.
7. MAKE THE COMBO: Transfer chickpeas to a big dish. Pour the chicken with curry pasta on the top of chickpeas. Serve carrots on the side.
8. TURN OF THE HOB: remember to turn off the hob once finish.

DINNER OF THE STUDY VISIT (start ~ 30 min before test meal is due to be served)

1. MICROWAVE READY MEAL: take the Penne Bolognese Ready Meal out of the freezer. Pierce film lid before cooking. Microwave it at 750W for 9 minutes.
2. REHEATING CHICKPEAS: when the ready meal is cooking, take the chickpeas out of the fridge. Tap the cling film to knock the condensation on the underside into the chickpeas. Microwave the chickpeas for 2 min at 900 W. Measure the temperature and check if it has reached 83°C.
3. FLAVOURING: mix 10g lemon juice, 2g parsley, 2g mint, 5g olive oil, 3g black pepper, 2g salt in a bowl and pour over chickpeas as a dressing.
4. MAKE THE COMBO: Transfer the seasoned chickpeas to a big dish. Serve the Penne Bolognese (the whole things) on the side.

Meal Preparation Instruction Sheet
Phase 2 Treatment [Z]

You will need:

- 1L Measuring jug
- 1.5L Bowl
- Aluminium foil
- Thermomix w/Mixing bowl and Lid
- Balance
- Sieve/Colander (approx. 15cm or 0.5L)
- Serving bowl (>0.6L capacity)
- Serving spoon
- Glass (~0.15L volume)
- Drinking water
- Flavouring:
  Breakfast: 1 x Hartley's Sugar free Blackcurrant Jelly pot 115g + 15g Stute no added sugar Blackcurrant jam;
  Lunch: 90g curry paste, 100g chicken breast chunks, 10g olive oil, and 150g baby carrots;
  Dinner: 10g lemon juice, 2g parsley, 2g mint, 5g olive oil, 3g black pepper, 2g salt, 1 x Penne Bolognese Ready Meal;

DAY BEFORE THE STUDY

Put 160 g dry de-hulled chickpeas in a colander, rinse until the water runs clear (approx. 4L), then put in a bowl and add 1L tap water. Cover with foil and leave overnight.

MORNING OF THE STUDY VISIT (start ~ 50 min before test meal is due to be served)

1. DRAIN: Drain the water from the soaked chickpeas in a colander/sieve over the sink, rinse once with clean water and drain thoroughly.
2. WEIGH IN WATER: Place the empty Thermomix mixing bowl (without the lid) on the balance and press TARE then tip the drained chickpeas into the Thermomix mixing bowl and add **water (approx. 1040 g)** until the total (tared) weight is **1360 g.**
3. BLEND: Secure the lid. Use the Thermomix display screen to set (in the following order): **Timer (mm:ss) to 03:00 (3 min)**; **Temperature to 37C** and **Blender to FORWARD X** direction and **Speed setting 10**.
4. COOK: When the audible alarm sounds after 3 min, Set the **Timer to (28 min) (mm:ss) 28:00; Temperature to 95C**, and the **Blender to REVERSE** direction **and Speed setting 4**
5. LOOK UP SERVING SIZE: Use the 'Look-up table' to determine the weight of cooked meal and drink of water to serve to the participant for breakfast, lunch, and dinner.
6. WEIGH OUT SERVINGS for breakfast, lunch, and dinner immediately. Place the serving bowl on the balance and tare, then use a serving spoon to add the cooked food to the

bowl **until target serving weight (from the look-up table)** is achieved. *The serving size for breakfast, lunch, dinner is usually around 490g, 327g, and 327g.*

7. **FLAVOUR the BREAKFAST:** Stir the chickpea with 1 x 115g pot of jelly and 15g of sugar-free jam **Drink:** Next, tare the balance to drinking glass and add water to reach target drink weight.
   Serve breakfast immediately and do not let the temperature of the meal fall below 60 ˚C
8. **REFRIGERATE LUNCH and DINNER portions**: Use plastic wrap to seal the foods for lunch and dinner and then keep them at 4 ˚C until use.

** Take a sample from the portion that was not served into a freezer bag, flatten and freeze -20˚C.*

LUNCH OF THE STUDY VISIT (start ~ 30 min before test meal is due to be served)

1. WEIGHT CHICKEN WITH CURRY: weight 90g curry pasta, 10g olive oil, 100g tikka chicken breast chunks and mix them in a bowl thoroughly.
2. HEATING CHICKEN WITH CURRY: Transfer the mixture into a saucepan with a lid and place it on a hob. Turn on the hub and set it on the setting of 3.
3. STIRRING: Start a timer for 5mins. Stirring occasionally to avoid the pasta sticking at the bottom of the pan.
4. KEEP THEM WARM: After 5 mins, switch the setting to 1 to keep them warm.
5. WEIGHT AND PREPARE CARROTS: During the 5-min cooking of curry and chicken, prepare the carrots. Drain and weight 150g carrots into a non-metallic bowl. Cover and microwave on 850W for 2 mins. Keep it in the microwave until serve.
6. REHEATING CHICKPEAS: take the chickpeas out of the fridge. Tap the cling film to knock the condensation on the underside into the chickpeas. Microwave the chickpeas for 2 min at 900 W. Measure the temperature and check if it has reached 83°C.
7. MAKE THE COMBO: Transfer chickpeas to a big dish. Pour the chicken with curry pasta on the top of chickpeas. Serve carrots on the side.
8. TURN OF THE HOB: remember to turn off the hob once finish.

DINNER OF THE STUDY VISIT (start ~ 30 min before test meal is due to be served)

1. MICROWAVE READY MEAL: take the Penne Bolognese Ready Meal out of the freezer. Pierce film lid before cooking. Microwave it at 750W for 9 minutes.
2. REHEATING CHICKPEAS: when the ready meal is cooking, take the chickpeas out of the fridge. Tap the cling film to knock the condensation on the underside into the chickpeas. Microwave the chickpeas for 2 min at 900 W. Measure the temperature and check if it has reached 83°C.
3. FLAVOURING: mix 10g lemon juice, 2g parsley, 2g mint, 5g olive oil, 3g black pepper, 2g salt in a bowl and pour over chickpeas as a dressing.
4. MAKE THE COMBO: Transfer the seasoned chickpeas to a big dish. Serve the Penne Bolognese (the whole things) on the side.

Look-up Table Phase 2. Shows serving sizes needed to give 30g starch from chickpea at Breakfast, and 20g starch at lunch and dinner. The volume of water is adjusted so that the food+drink is standardised at 760g.

			BREAKFAST		LUNCH		DINNER	
			FOOD	DRINK	FOOD	DRINK	FOOD	DRINK
Thermomix Jug empty weight (g)	If the thermomix jug with the cooked meal weighs … g	If the cooked meal weighs…	You need to serve (g cooked)	with this amount of water in a glass (g)	Weigh out this amount (g) and refrigerate	with this amount of water in a glass (g)	Weigh out this amount (g) and refrigerate	with this amount of water in a glass (g)
1120	1920	800	300	460	200	560	200	560
1120	1916	796	299	462	199	561	199	561
1120	1912	792	297	463	198	562	198	562
1120	1908	788	296	465	197	563	197	563
1120	1904	784	294	466	196	564	196	564
1120	1900	780	293	468	195	565	195	565
1120	1896	776	291	469	194	566	194	566
1120	1892	772	290	471	193	567	193	567
1120	1888	768	288	472	192	568	192	568
1120	1884	764	287	474	191	569	191	569
1120	1880	760	285	475	190	570	190	570
1120	1876	756	284	477	189	571	189	571
1120	1872	752	282	478	188	572	188	572
1120	1868	748	281	480	187	573	187	573
1120	1864	744	279	481	186	574	186	574
1120	1860	740	278	483	185	575	185	575
1120	1856	736	276	484	184	576	184	576
1120	1852	732	275	486	183	577	183	577
1120	1848	728	273	487	182	578	182	578
1120	1844	724	272	489	181	579	181	579
1120	1840	720	270	490	180	580	180	580
1120	1836	716	269	492	179	581	179	581
1120	1832	712	267	493	178	582	178	582
1120	1828	708	266	495	177	583	177	583
1120	1824	704	264	496	176	584	176	584
1120	1820	700	263	498	175	585	175	585
1120	1816	696	261	499	174	586	174	586
1120	1812	692	260	501	173	587	173	587
1120	1808	688	258	502	172	588	172	588
1120	1804	684	257	504	171	589	171	589
1120	1800	680	255	505	170	590	170	590
1120	1796	676	254	507	169	591	169	591
1120	1792	672	252	508	168	592	168	592
1120	1788	668	251	510	167	593	167	593
1120	1784	664	249	511	166	594	166	594
1120	1780	660	248	513	165	595	165	595
1120	1776	656	246	514	164	596	164	596
1120	1772	652	245	516	163	597	163	597
1120	1768	648	243	517	162	598	162	598
1120	1764	644	242	519	161	599	161	599
1120	1760	640	240	520	160	600	160	600
1120	1756	636	239	522	159	601	159	601
1120	1752	632	237	523	158	602	158	602
1120	1748	628	236	525	157	603	157	603

Phase 2 study (Chapter 5) chickpeas with background diets

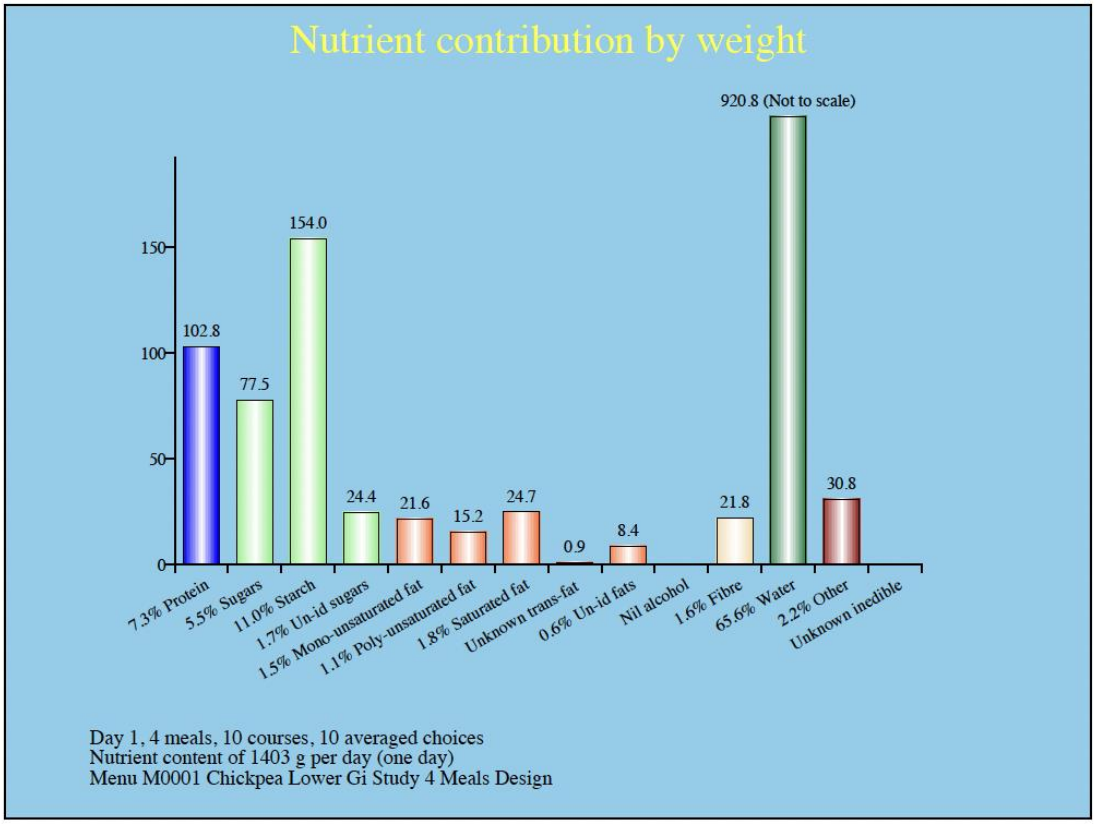
Meals	Ingredient	Quantity
Breakfast (0 min)		
	Chickpeas	60g material
	Harleys raspberry no added sugar jelly	1 pot
	Stute no added sugar blackcurrant Jam	15g
Lunch (240 min)		
	Chickpeas	50g material
	Patak's Tikka Masala Paste	70g
	Carrots	120g
	Tikka Chicken Breast Chunks	120g
Dinner (480min)		
	Chickpeas	50g material
	Harleys raspberry no added sugar jelly	1 pot
	Stute no added sugar blackcurrant Jam	5g
	Sainsbury's Beef Lasagne	1 serve
Evening snacks (720min)	Warburtons Toastie Thick Sliced White Bread	2 slices
	Flora original spread	18g
	Activia Strawberry Yogurt	115g

Phase 2 study (Chapter 5) DietPlan menu analysis

Nutrient	Unit	Total		per day	per meal	per course
Water	g	920.8	m	920.8	230.2	92.1
Total Nitrogen	g	16.54	e	16.54	4.13	1.65
Protein	g	102.8		102.8	25.7	10.3
Fat	g	70.8		70.8	17.7	7.1
Available Carbohydrate (mse)	g	256.0	+	256.0	64.0	25.6
Energy (kcal)	kcal	2029	+	2029	507	203
Energy (kJ)	kJ	8551	+	8551	2138	855
Starch (mse)	g	162.4	m	162.4	40.6	16.2
Total Sugars (mse)	g	81.4	m	81.4	20.4	8.1
Glucose	g	20.5	m	20.5	5.1	2.1
Fructose	g	18.3	m	18.3	4.6	1.8
Sucrose (mse)	g	22.4	m	22.4	5.6	2.2
Maltose (mse)	g	3.9	m	3.9	1.0	0.4
Lactose (mse)	g	9.2	m	9.2	2.3	0.9
Non-starch polysaccharides	g	21.8	m	21.8	5.5	2.2
Total dietary fibre (AOAC method)	g	30.9	m	30.9	7.7	3.1
Saturated fatty acids	g	24.7		24.7	6.2	2.5
Mono-unsaturated fatty acids	g	21.6	m	21.6	5.4	2.2
Poly-unsaturated fatty acids	g	15.2		15.2	3.8	1.5
Total trans fatty acids	g	0.9	m	0.9	0.23	0.09
Cholesterol	mg	156.6	m	156.6	39.1	15.7
Sodium (Na)	mg	6564	m	6564	1641	656
Potassium (K)	mg	2953	m	2953	738	295
Calcium (Ca)	mg	614	m	614	153	61
Magnesium (Mg)	mg	210	m	210	52	21
Phosphorus (P)	mg	1059	m	1059	265	106
Iron (Fe)	mg	8.53	m	8.53	2.13	0.85
Copper (Cu)	mg	0.69	m	0.69	0.17	0.07
Zinc (Zn)	mg	8.61	m	8.61	2.15	0.86
Chloride (Cl)	mg	3321	m	3321	830	332
Manganese (Mn)	mg	1.99	m	1.99	0.50	0.20
Selenium (Se)	ug	19.1	m	19.1	4.8	1.9
Iodine (I)	ug	85.5	m	85.5	21.4	8.6
Retinol	ug	214	m	214	53	21
Carotene	ug	12172	m	12172	3043	1217
Vitamin D	ug	0.7	m	0.7	0.17	0.07

Nutrient	Unit	Total		per day	per meal	per course
Vitamin E	mg	4.57	m	4.57	1.14	0.46
Thiamin	mg	1.30	m	1.30	0.32	0.13
Riboflavin	mg	1.09	m	1.09	0.27	0.11
Niacin	mg	18.50	m	18.50	4.63	1.85
Tryptophan divided by 60	mg	14.71	m	14.71	3.678	1.471
Vitamin B6	mg	1.61	m	1.61	0.40	0.16
Vitamin B12	ug	2.9	m	2.9	0.7	0.3
Total Folate	ug	173	m	173	43	17
Pantothenic acid, Pantothenate	mg	4.82	m	4.82	1.21	0.48
Biotin	ug	13.8	m	13.8	3.5	1.4
Vitamin C	mg	42	m	42	11	4

Key. For one or more contributory foods :
d: nutrient value derived or deduced
e: value estimated
+: present in significant, unknown amounts
m: missing value



Sources of energy :

Calories from	Total	per meal	per 100g	Percent	UK Food	UK Total
Protein	413 e	103	29	19.8	15%	15%
Carbohydrate	975 +	244	70	46.7	50%	47%
Fat	637	159	45	30.5	35%	33%
Alcohol	0	0	0	0.0		5%
Fibre	62 m	15	4	3.0		
Total	2088 m	522	149	100.0	100%	100%

Appendix 5 Standardised meal SOP for measuring ab libitum food intake

INGREDIENTS

50 grams Oil Sainsbury's

2 bags of Pasta shapes Basic Sainsbury's

2 pots of Tomato Basic Sainsbury's



1. Pour hot water from the hot water source in the kitchen into the big cooking pot (cover half of the pot).
2. Put it on the hob at maximum temperature. It will take 15 min to boil approx. with lid on so account for that time.
3. When boiling, put in the 2 pack of pasta and wait for the water to boil again. Cover it with the lid it will help the process go faster.

4. When the water starts boiling again, start a timer for 15 min. Make sure you stir every now and then to avoid pasta sticking at the bottom of the cooking pot.
5. While the pasta is cooking, measure 50 grams of oil and combine with the 2 pots of tomato sauce in the mixing bowl. Leave it resting.
6. When the pasta is ready, pour the content of the cooking pot steadily and with care through a colander on the sink.
7. Pour the pasta in the colander and back to the empty cooking pot.
8. Now pour the mix of tomato sauce and 50g of oil into the cooking pot.
9. Combine the sauce in the pasta with help of a tall spoon. Give it a short mix.
10. Serve ALL the mix in a big bowl.
11. Measure the weight of the bowl with pasta on the same scale before and after being consumed and jot down the value.
12. Bring the food to the participant using the wheelie pusher. Serve in a bowl with a lid and a fork

.

Appendix 6 PLS-DA analysis for gastric and duodenal samples

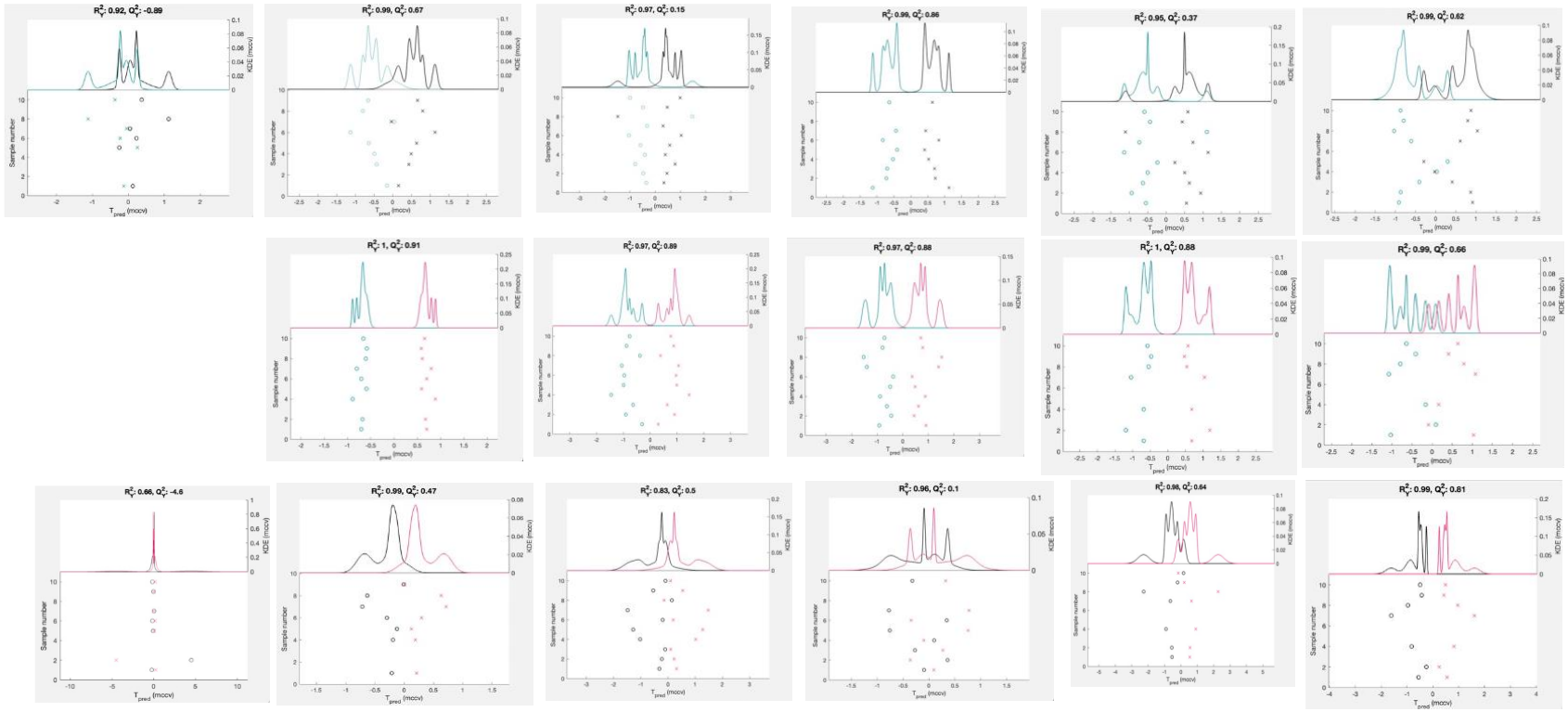


Figure 1. PLS-DA analysis for gastric samples between food structure interventions throughout the time. Each dot represents the metabolic profile of one subject containing 18,600 spectra variables. R^2 and Q^2 indicate the fit and predictability of the models. The comparison between Intact-C and Broken at T=0 was not available due to insufficient paired samples. intact single cells. Intact-S, intact single cells; Intact-C, intact cell clusters; Broken, Broken cells.

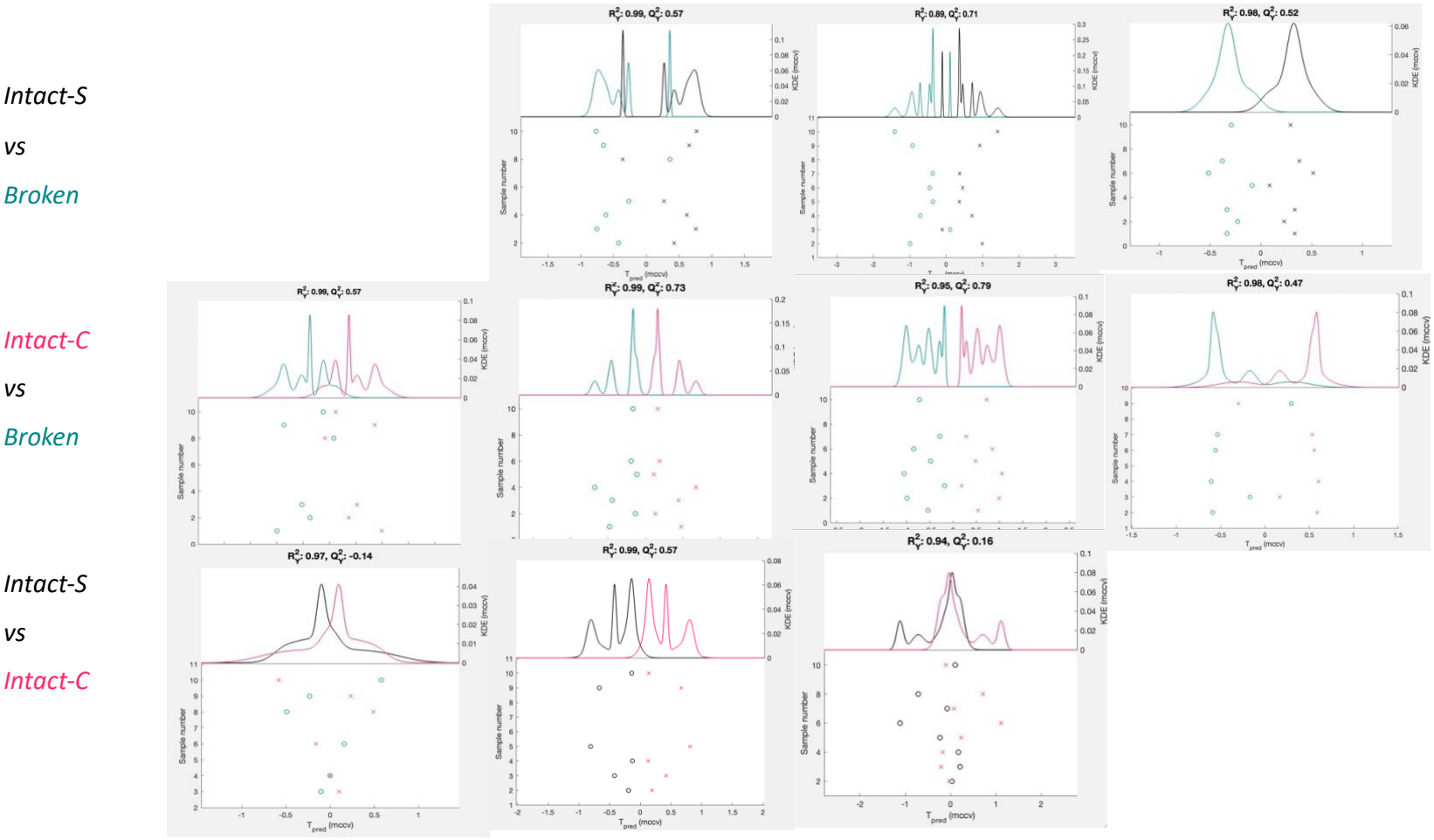


Figure 2. PLS-DA analysis for duodenal samples between food structure interventions throughout the time. Each dot represents the metabolic profile of one subject containing 18,600 spectra variables. R^2 and Q^2 indicate the fit and predictability of the models. Some comparisons were not available due to insufficient paired samples. intact single cells. Intact-S, intact single cells; Intact-C, intact cell clusters; Broken, Broken cells.

Appendix 7 Gastric pH change before and after meals.

Table 1. pH changes in gastric aspirations in 5 human subjects

Timepoint (min)	Subject 1	Subject 2	Subject 3	Subject 4	Subject 5
T=0	1.5	1.5	2.0	1.0	1.5
T=15	4.0	4.5	4.5	4.0	4.5
T=30	4.0	4.0	4.0	4.0	4.5
T=45	4.0	4.0	3.5	4.5	4.0
T=60	3.5	3.5	3.5	3.5	4.0
T=75	3.0	3.0	2.5	3.0	3.5
T=90	2.5	2.5	3.5	3.0	3.0

Appendix 8 VAS of hunger, desire to eat, and appetite for a meal after meals

Table 2 Incremental Area Under Curve (iAUC) for appetite measurment

	Intact-S	Intact-C	Broken	P value
Hunger iAUC $_{0\text{-}480min}$	17826.8±1515.3	14225.2±2684.9	13363.5±1947.9	0.30
Hunger iAUC $_{0\text{-}240min}$	9956.6±828.5	8281.8±1474.4	7223.6±1360.8	0.32
Hunger iAUC $_{240\text{-}480min}$	7870.1±865.7	5943.4±1332.6	6139.9±827.0	0.37
Desire to eat iAUC $_{0\text{-}480min}$	17273.4±2302.3	15506.1±3403.9	13354.7±2348.0	0.60
Desire to eat iAUC $_{0\text{-}240min}$	9715.7±1201.9	8392.0±1815.8	7084.3±1493.1	0.49
Desire to eat iAUC $_{240\text{-}480min}$	7557.8±1216.2	7114.1±1661.6	6270.4±1087.0	0.79
Appetite for a meal iAUC $_{0\text{-}480min}$	18742.9±2349.1	16015.7±2859.6	13894.9±2084.6	0.38
Appetite for a meal iAUC $_{0\text{-}240min}$	10487.2±1047.0	8938.7±1694.1	7243.1±1488.4	0.28
Appetite for a meal iAUC $_{240\text{-}480min}$	8255.6±1494.1	7077.0±1292.2	6651.8±1058.4	0.67

Data presented as mean ± SEM (n=8). Repeated measure one-way ANOVA was performed to test the difference between treatments. Intact-S, intact single cells; Intact-C, intact cell clusters; Broken, Broken cells

Appendix 9 Time profile of ileal glucose estimating foods retention time in the ileum

Table 3 Graphic representative parameters of ileal glucose

	Entry time/ First X (min)	Peak time/ Peak X (min)	Exit time/ Last X (min)	Peak value/ Peak Y (mmol/L)
Intact-S	36.3 ± 18.8	157.5 ± 29.9	343.7 ± 53.6	8.0 ± 2.1 [a]
Intact-C	30.6 ± 20.0	247.5 ± 48.7	451.7 ± 28.3	4.1 ± 0.9 [a]
Broken	17.5 ± 7.5	142.5 ± 50.6	299.3 ± 49.7	0.9 ± 0.2 [b]
Group mean	28.1 ±9.4	182.5 ±26.2	364.9 ±28.3	4.4 ±0.9
P value[1]	0.35	0.25	0.05	0.035
P trend[2]	0.67	0.56	0.03	0.032

Data presented as mean ± SEM (n=8). First X (min), when ileal glucose above the baseline levels; peak X (min) , when ileal glucose reached the maximum levels; last X (min), when ileal glucose returned the baselines; Peak Y; the maximum ileal glucose (mmol/L). [1] Repeated measure ANOVA; [abc] different letters demonstrated significant differences between treatments [2]P value of linear trend analysis following one way ANOVA

Appendix 10 Permission rights to publish Chapter 2 by The American Journal of Clinical Nutrition



RightsLink

Help | Live Chat

OXFORD UNIVERSITY PRESS

The impact of starchy food structure on postprandial glycemic response and appetite: a systematic review with meta-analysis of randomized crossover trials

Author: Cai, Mingzhu; Dou, Bowen

Publication: The American Journal of Clinical Nutrition

Publisher: Oxford University Press

Date: 2021-05-28

Copyright © 2021, Oxford University Press

Creative Commons

This is an open access article distributed under the terms of the Creative Commons CC BY license, which permits unrestricted use, distribution, and reproduction in any medium, provided the original work is properly cited.

You are not required to obtain permission to reuse this article.

© 2022 Copyright - All Rights Reserved | Copyright Clearance Center, Inc. | Privacy statement | Data Security and Privacy | For California Residents | Terms and ConditionsComments? We would like to hear from you. E-mail us at customercare@copyright.com